SMITHSONIAN CONTRIBUTIONS TO BOTANY • NUMBER 10

Fine Structure of the Cortex in the Lichen Family Parmeliaceae Viewed with the Scanning-electron Microscope

Mason E. Hale, Jr.

SMITHSONIAN INSTITUTION PRESS
City of Washington
1973

ABSTRACT

Hale, Mason E., Jr. Fine Structure of the Cortex in the Lichen Family Parmeliaceae Viewed with the Scanning-electron Microscope. *Smithsonian Contributions to Botany,* number 10, 92 pages, 150 figures, 1973.—The scanning-electron microscope was used to examine the cortical surface of 123 species of lichens in 12 genera of the lichen family Parmeliaceae. Two general types of cortex were found, one consisting of exposed hyphae and one with the hyphae covered by a thin polysaccharide epicortex. The epicorticate species fell into two groups, one with a tightly appressed continuous epicortex and one with a more loosely associated pored epicortex. Type of epicortex is a constant character at the genus and section level and appears to have considerable usefulness in the taxonomy of the family.

OFFICIAL PUBLICATION DATE is handstamped in a limited number of initial copies and is recorded in the Institution's annual report, *Smithsonian Year*. SI PRESS NUMBER 4781. SERIES COVER DESIGN: Leaf clearing from the katsura tree *Cercidiphyllum japonicum* Siebold and Zuccarini.

Library of Congress Cataloging in Publication Data
Hale, Mason E.
Fine structure of the cortex in the lichen family Parmeliaceae viewed with the scanning-electron microscope.
(Smithsonian contributions to botany, no. 10)
Bibliography: p.
1. Parmeliaceae. 2. Lichens—Anatomy. Ultrastructure (Biology). I. Title. II. Series: Smithsonian Institution. Smithsonian contributions to botany, no. 10.
QK1.S2747 no. 10 [QK585.P2] 581'.08s [589'.1] 72-8039

For sale by the Superintendent of Documents, U.S. Government Printing Office
Washington, D.C. 20402 - Price $2 (paper cover)

Contents

Fine Structure of the Cortex in the Lichen Family Parmeliaceae Viewed with the Scanning-electron Microscope

Mason E. Hale, Jr.

Introduction

The scanning-electron microscope (SEM) is one of the newest tools available to biologists. Electron beams reflected from the surfaces of objects produce images with a remarkable three-dimensional quality because of the great depth of focus. The range of magnification, from 20 to 100,000 diameters, is very great, although photographs become fuzzy over 10,000 diameters. The electron microscope (EM), which is often used to study the internal structure of hyphal and algal cells, also magnifies at 10,000 diameters or more (see Jacobs and Ahmadjian, 1969), but the specimens can be examined only as two-dimensional sections. Thus the SEM bridges the gap between the EM and the low power light-reflecting stereomicroscope.

The first use of the SEM in lichen research, as far as I am aware, was reported briefly by Peveling and Vahl (1968). The next study (Peveling, 1970, a report of a symposium held in 1969) contained more detailed descriptions, showing, for example, crystal formations on hyphae and certain surface details. Hawksworth in the same year (1969) published the first comprehensive investigation of a lichen family (Alectoriaceae) with the intent of applying the information to taxonomic problems. He identified several orientations of cortical hyphae that were useful in delimiting genera. More recently, Tibell (1971) has shown the value of the SEM in studying ascospore structure in the Cypheliaceae. These first efforts have demonstrated convincingly that the SEM has real potential for opening up new and previously unexplored areas of study in lichen morphology and systematics.

The purpose of this report is to describe in detail the cortical surface of representative species in the Parmeliaceae and to ascertain the value of fine structure in the taxonomy of the family. Interpretation of some of these structures is at best tentative and may indeed prove erroneous on future more intensive studies using data from the SEM in conjunction with EM sections and chemical analyses. It is hoped, nevertheless, that the photographs presented here will enable other lichenologists to make their own interpretations.

ACKNOWLEDGMENTS.—I have a number of colleagues to thank for constructive discussions on the nature of cortical fine structure. They include Dr. Vernon Ahmadjian, Dr. William L. Culberson, Dr. D. L. Hawksworth, and Dr. Harold Robinson. Dr. Jerome Jacobs prepared EM sections of *Parmelia croceopustulata* and provided an interpretation of the micrograph that I have used. All of the photographs except for this one (Figure 14) were reproduced by the Smithsonian Photographic Services Division.

Mason E. Hale, Jr., Department of Botany, National Museum of Natural History, Smithsonian Institution, Washington, D.C. 20560.

The Scanning-electron Microscope

The samples were photographed by Mr. Walter Brown of the Smithsonian Scanning-electron Laboratory with a Cambridge Stereoscan Mark 2A. Voltage was uniformly 20KV since this was found to be most satisfactory with biological materials. The electron beams were perpendicular to the plane of the slide, giving the effect of viewing the specimens from directly above. In a few instances the samples were tilted as much as 69° to afford an oblique view. Separation of stereo pairs when two photographs were taken was 7°. Samples were plated with gold on a specially made biased rotating disk. The gold layer is estimated to be 200–400 angstroms thick.

Samples

All of the samples were taken from herbarium specimens preserved in the United States National Herbarium, unless otherwise stated. It would have been ideal to examine only type-specimens at first in order to establish a standard for the fine structure of each species. I did, in fact, use types whenever possible, but most specimens were recent collections identified by morphological and chemical comparisons with types. Older material from the 19th century, especially that collected in the tropics, was often so densely covered with fine hyphae of molding fungi or with debris and unidentified particles (Figure 1) that surface details could sometimes not be recognized. These artifacts are apparently caused by poor preservation.

Preparation of the samples is very simple compared with the EM or other techniques where fixing and sectioning are required. One can take a dried lichen thallus directly from the herbarium and cut out sections as large as 10 mm (the maximum size accommodated by the Stereoscan SEM), although 1–2 mm is adequate since, as will be shown below, the area of cortex examined will usually be less than 0.20 mm. The sample is affixed to a cover glass with glue (in my case water-soluble Elmer's glue), air dried, and plated with gold in a vacuum. The entire surface abutting the cover glass must be firmly grounded or electrical discharge will give streaked photographs. Tall specimens, 1 mm or more high, are also prone to discharge.

A dried herbarium specimen obviously has low water content, and the hyphae and algae are shriveled to some extent. Peveling and Vahl (1968) made a special study of possible distortion in dried thalli compared with thalli that had been wetted and freeze-dried. They found relatively little, and I did not pursue this problem myself. Without freeze-drying, incidentally, the water in a wet specimen would evaporate off in the vacuum used in gold plating and probably cause severe degassing and cracking. Freeze-drying would be the method of choice for certain kinds of studies where shrinkage must be avoided and there is no reason why it could not be used with lichens.

A specimen can be scanned rapidly at low power (20–100 diameters) in order to select a standard area for enlargement. I usually took an area in the center of a lobe tip 0.5–2.0 mm back from the margin, depending on lobe width. It is difficult at first to gain perspective in SEM photography because the range of magnification is so great. The best working magnification, used by both Peveling and Hawksworth, is between 500 and 2500 diameters. An example of how much of the thallus surface is included in such photographs is illustrated in Figure 2. At 500 diameters, for example, the standard 4×5 negative (print area about 10×11 cm) encompasses an area about 0.20 mm wide and 0.22 mm long. At 1000 diameters this would be reduced to 0.09×0.11 mm and at 2000 about 0.05×0.06 mm. For this study I used two standardized enlargements, 500 and 2000 diameters.

Structure of the Thallus

Vertical Structure

I prepared cross-sections of a few species to get a better idea of the general internal organization of the thallus and its relation to the surface layers. Vertical or oblique free-hand sections were made with a razor blade and thin strips about 0.5–1.0 mm wide mounted on their side. These were scanned and photographed at different magnifications. The following layers were easily identified (see Figures 3,4).

Lower Cortex.—This is a discrete layer consisting of densely conglutinated hyphae with lumina still intact. Medullary hyphae come off from the top of this layer. Rhizines originate as thick strands (Figure 5) which are composed of vertically arranged conglutinated hyphae in cross-section, not unlike those in the lower cortex (Figure 6).

MEDULLA.—The medulla occupies the bulk of the thallus and has an appearance little different from that in microscopic preparations. Degree of packing and conglutination differs widely from species to species (Figure 7) and even from lobe to lobe in the same plant (cf. Figures 3,4). Encrusting crystals of lichen substances may be conspicuous and dense to absent on the medullary hyphae (Figures 7,15,18).

ALGAL LAYER.—The algae are much more difficult to spot than in a stained cross-section. Viewed stereoscopically they stand out as round though shriveled cells scattered within a palisade-like layer (Figures 3,7,8) or lying just below the upper cortex (Figure 10). Some may break away when sections are cut with this technique. In any event the algae seem to have a very loose association with the hyphae.

UPPER CORTEX.—The lower part of the upper cortex is similar to the lower cortex in consisting of densely conglutinated hyphae, though with smaller more compressed lumina and perhaps not as clearly separated from the hyphae in the algal layer. The layer in total appears to be somewhat thinner, two to three cells thick (12μ–18μ), although this varies according to the species. The structure of the upper part of the cortex showed considerable differentiation. This is the layer viewed with the SEM and will be discussed in more detail below.

The Epicortex

The various species in the Parmeliaceae examined could be divided into two major groups depending on the presence or absence of a thin polysaccharide layer above the cortical hyphae. D. L. Hawksworth (in litt.) proposed the name "epicortex" for this layer, and it seems to be comparable in certain respects to Peveling's "Kittsubstanz" (cementing substance). One group of lichens lacks any epicortical layer, the cortical hyphae being exposed directly at the surface, and they will be called "nonepicorticate." The other major group has an epicortal layer covering the cortical hyphae; these, then, are epicorticate.

NONEPICORTICATE TYPE

The horizontally arranged hyphae in the lower part of the upper cortex turn upward to form a forest of loosely packed stubby hyphal tips (cf. Figures 146–150). These stand out especially well in a stereo view (Figure 9). This type of cortex is characteristic of the genus *Pseudevernia* and has been found in some species of the Graphidaceae and Thelotremataceae (see Figure 11 for *Graphina confluens*), but it is by no means typical of crustose lichens. This kind of structure is apparently the one called fastigiate by the morphologists of the 19th century. An interesting consequence of this type of organization is that gas exchange between the algal layer and the exterior is completely uninhibited since there are many gaps between the hyphae providing access to the algae below.

EPICORTICATE TYPE

The upper cortical hyphae in this type are completely or partially covered by a thin amorphous epicortex 0.6μ–1.0μ thick. This noncellular layer is secreted by the hyphae and is apparently similar in composition to the thick outer polysaccharide layer that has been found enveloping hyphae in lichens. There are two kinds of epicortex which may or may not be morphogenetically related, one without pores and one with pores.

THE NONPORED EPICORTEX.—Here the entire upper surface is covered by the thin epicortical membrane (Figure 12*a*). This layer, about 1μ thick, is so closely joined to the thick polysaccharide walls of underlying hyphae that outlines and convolutions of the hyphae are easily distinguished. As a result, the surface of nonpored epicorticate lichens viewed from above almost always appears nodular or mammilate (Figure 13*a,b*) and in an oblique view undulating or sinuous (Figure 13*c*).

A distinctive feature of the nonpored epicortex is its reaction to electron beams. Photographs of lichens with this structure tend to be fuzzy or blurred, even at 500 diameters but especially so at 2000 (see, for example, Figures 42, 49, 66, 144). It would appear that some of the electrons penetrate the gold and are reflected back from a lower layer. This double reflection would account for the fuzziness. Another feature is that nonpored epicorticate lichens tend to degass, shrink, and crack excessively when exposed to intense electron beams used in focusing at 10,000 to 50,000 diameters (cf. Figures 30, 64, 80). Cracking can actually be seen developing within a few seconds.

THE PORED EPICORTEX.—The basic structure here is a noncellular amorphous layer 0.6μ–0.8μ thick lying on and in part free from the hyphal layer below (Figure 12*b*). The three-dimensional nature of this layer stands out vividly in stereo photographs (cf. Figure 8) which show free edges of the layer as flaps curling up (also see Figures 53, 81, 88, 105). A section through the cortex of *Parmelia croceopustulata* viewed with an electron microscope (Figure 14) shows an electron-dense polysaccharide layer that stains only with lead, barely distinguishable from the hyphal cell walls below. The reaction of the polysaccharides in the pored epicortex to electron beams is also different on the average from that of the nonpored epicortex. Photographs are almost always sharper, indicating very little electron penetration below the epicortex. Degassing and cracking at high electron intensity are also encountered much less often than in the nonpored epicortex.

The underlying hyphae are basically arranged as in the nonepicorticate type with the outermost ones becoming short erect stubs (Figure 15; also Figures 91, 105), also seen more clearly in stereo photographs (Figure 16). This epicortex may be an extremely smooth and flat sheet, giving no hint of the presence of underlying hyphae (Figures 15, 18*a*, 78), or an undulating layer where contours of individual hyphae can be recognized (Figures 18*b*, 119, 130).

The most remarkable feature of this type of epicortex is the formation of pores, actual perforations of the polysaccharide layer exposing the underlying cortical hyphae (Figures 15, 91, 105) and providing passageways to the algal layer for gas exchange (Figures 3, 8). These pores cannot be distinquished with a stereo binocular even under highest magnification. They are produced more or less uniformly over the upper cortex (Figure 17) but in some groups, in particular *Parmelia* subgenus *Parmelia* section *Irregulares* and subgenus *Everniiformes*, they occur in groups (Figures 70, 71, 123).

The origin of these pores is quite unknown at this time. Their regularity would seem to rule out random tearing or imperfections in the epicortex. They form very early in thallus development if the example of *Parmelia gigas* may be considered typical. A series of panoramic photographs of the area from the lobe tip to a point 0.6 mm from the tip in this species shows a very narrow marginal zone at the growing point where no pores are present. This intergrades abruptly into a disorganized zone which may actually be nonepicorticate. An epicortex gradually forms and a mature zone of regularly formed pores become visible (Figure 19). These pores differ significantly from the better known pseudocyphellae in size and internal structure. Pseudocyphellae (Figures 68, 69, 138), much larger than epicortical pores, actually interrupt and penetrate both the epicortex and the underlying hyphal layer, and are closed off with a loosely packed irregular layer of shriveled, weakly conglutinated hyphae (Figure 69). The fine structural pores described here, rarely more than 25μ in diameter, are formed by perforations in the epicortex which do not disturb the cortical hyphae.

The epicortex acts as a site for deposition of lichen substances. This layer contains electron-light extracted profiles that apparently represent crystals of atranorin originating at its interface with the hyphae (Figure 14). Crystals of typical cortical substances, atranorin (Figures 19*a*, 85, 97, 107), lichexanthone (Figures 102, 111), and usnic acid (Figures 19*b*, *c*, 96, 103, 121, 135), are ultimately deposited on the surface of the epicortex as well as in it and are also abundant around and inside the pores (Figure 19*b*). They readily dissolve out in acetone leaving a polysaccharide skeleton bare of acids (Figure 19*b*). Although the crystals are secreted extracellularly by the cortical hyphae, they soon migrate through the polysaccharide epicortex intact.

FINE STRUCTURE OF THE LOWER SURFACE

The lower surface of three epicorticate species, two of them pored and one nonpored, was examined to compare them with the upper cortex. All were uniformly epicorticate and nonpored, even when the upper cortex was strongly pored (Figure 21). As one would surmise, gas exchange through the lower cortex is probably negligible.

Variation in Epicortical Structure

We must determine the constancy and range of variation in fine structure of the cortex before we can use it as a taxonomic character. The high cost of SEM work and the limited availability of the machine, however, easily discourage one from achieving this goal. Although I usually examined

only one specimen of each species, I prepared samples of two or more specimens or lobes of the same specimen for a number of species, especially when a discrepancy or point of interest was found.

In one instance I selected five specimens of the pan-temperate *Parmelia caperata* from several countries. All had distinct poring and three were virtually indistinguishable (Figures 22*a,b,* 91). The other two had fewer and smaller pores (Figure 22*c, d*). These differences were unrelated to geography. We should not rule out a correlation with ecological conditions, but this kind of information is only rarely given in sufficient detail on herbarium labels.

Other examples of multiple samples can be illustrated for *Parmelia conspersa* (Figures 53,54), *P. croceopustulata* (Figures 15, 105) *P. crozalsiana* (Figures 13, 93), *P. dissecta* (Figures 1, 83), *P. fissicarpa* (Figures 18*b*,110), *P. formosana* (Figures 17*c*,111), *P. imbricatula* (Figures 17*d*,113), *P. physcioides* Figures 1,118), *P. rigida* (Figures 132, 133), and *P. xanthina* (Figures 20*d*,135, lobes from the same specimen). I feel satisfied, in any event, that specimen-to-specimen variation for most species is quite small and that as exceptions are found they can be subjected to more exhaustive study as funding and machine time permit. Hawksworth (1969) had earlier found an acceptably small range of variation in the orientation of hyphae in *Alectoria.*

Another source of variation could be the age of the lobe (cf. Hawksworth, 1969). The center of the lobe where I took most samples is at most 2–3 years old, assuming growth rates of 1–4 mm per year from these primarily tropical foliose species. To make comparisons with older lobes, I examined one long linear lobe of *Parmelia gigas,* photographing the center of the tip (Figure 112), a point 5 cm back from the tip which I estimated to be about 10 years old, and a point 10 cm back from the same tip (Figure 23) which may be as much as 20 years old. Pores were best developed at the tip but were easily distinguished at 5 cm back and less so at 10 cm. Perhaps the pores in older areas gradually fill in as the need for gas exchange diminishes.

Value of Cortical Fine Structure in Systematics

The family Parmeliaceae was chosen for this study because it is a large, varied, and taxonomically well-known group of at least 11 genera, one of which (*Parmelia*) is divided into 13 major subgenera and sections. As I had hoped and as will be seen in the photographs, cortical fine structure proves to be a remarkably constant character at the generic and sectional levels. A summary of the results is given in Table 1 and details of individual groups are discussed more fully below. The most interesting discovery was that lichens with pseudocyphellae (or even nonpseudocyphellate lichens in genera that may produce them) never form a pored epicortex. Conversely, lichen species with a pored epicortex never produce pseudocyphellae.

I can cite several examples where epicortical structure has helped in assigning species to the correct section in a genus. *Parmelia vanderbylii* Zahlbruckner was described from South Africa as

Table 1.—*Numerical and structural survey of species in Parmeliaceae*

Taxa	Total species	Number Examined	Epicortex: Nonpored	Epicortex: Pored	Pseudocyphellae
Anzia	15	3		+?	
Asahinea	3	2	+		+
Cavernularia	2	2	+		
Cetraria	75	5	+		+
Cetrelia	14	2	+		+
Heterodea	1	1	+		
Hypogymnia	25	4	+	+?	
Menegazzia	15	2	+		
Pannoparmelia	2	2		+	
Parmelia					
Subgenus *Melanopharmelia*	80	8	+		(+)
Subgenus *Xanthoparmelia*	80	7		+	
Subgenus *Parmelia*					
Section *Parmelia*	25	6	+		+
Section *Simplices*	25	3	+		+
Section *Irregulares*	7	3		+	
Section *Relicinae*	25	6		+	
Section *Bicornutae*	30	4		+	
Section *Imbricaria*	38	8		+	
Section *Cyclocheila*	49	11	(+)	+	
Section *Hypotrachyna*	90	22		+	
Subgenus *Everniiformes*	14	4		+	
Subgenus *Amphigymnia*	125	9		+	
Parmeliopsis	5	2		+	
Platismatia	10	3	+		+
*Pseudevernia**	6	5			

*=Nonepicorticate, ?=Uncertain (?)=Rare occurrence.

a member of section *Melanoparmelia*. It is indeed a small dark species, superficially a typical brown *Parmelia*. The SEM photograph, however, shows a pored epicortex more typical of species in section *Cyclocheila* (Figure 99), not of *Melanoparmelia* which always has a nonpored epicortex. Another example is *Parmelia jamesii* Hale, a species from New Zealand which seemed to belong in section *Parmelia* (the *P. saxatilis* group) because of the faint white reticulation at the lobe tips. The epicortex is pored (Figure 85) and this species can therefore be tentatively placed in section *Imbricaria* since species in section *Parmelia* are nonpored.

A final example is the common *Parmelia ulophyllodes* (Vainio) Savicz, which appears to belong to section *Cyclocheila* but which, except for lack of distinct pseudocyphellae, also falls near *P. flaventior* and definitely does not belong in section *Cyclocheila*, although its ultimate disposition has not yet been decided.

While the structure of the epicortex is a valuable character at the sectional level, too few data are available to evaluate its use as a species character. I did find one case, *Parmelia formosana* Zahlbruckner vs. *P. pustulifera* Hale (Figures 111, 119), where pore size and evenness of the surface were sufficiently different to be used with other characters to distinguish two species (Hale, 1972). Preliminary study also suggests that pore size and density are correlated with chemistry in the isidiate species of the *P. laevigata* complex, including *P. addita* Hale (Figure 100), *P. dentella* (Figure 106), *P. orientalis* Hale (Figure 117), and *P. imbricatula* (Figure 113). Many more specimens will have to be examined, however, to make a conclusive judgment in this case.

The essential features of each genus are discussed briefly below. Further elaboration on the classification and characters used in the taxonomy may be found in Culberson and Culberson (1968a), Hale and Kurokawa (1964), and Hale (1965).

Anzia Stizenberger

FIGURES 24–26

SPECIES EXAMINED.—*Anzia colpodes, A. japonica,* and *A. ornata.*

While this genus is better placed in the Anziaceae (Culberson and Culberson, 1968a), it is included here because of its long association with the Parmeliaceae. The two characters that distinguish the genus are numerous spores in each ascus (rather than the normal eight) and a unique mesh of black hyphae on the lower surface. There is a well-developed epicortex which appears to be nonpored or irregularly pored. The unusual sculpturing in *A. colpodes* (Figure 24) is similar to that in *Heterodea muelleri* (Figure 36). The epicortical structure, then, seems to support the logic of a separate family, but a clearer definition of the cortex here will require examination of many more specimens.

Asahinea Culberson

FIGURES 27, 28

SPECIES EXAMINED.—*Asahinea chrysantha* and *A. scholanderi.*

This is one of the segregates of *Cetraria,* sensu lato, proposed by Culberson and Culberson (1968b). Both species investigated have a smooth to undulating nonpored epicortex similar to that in other cetrarioid species.

Cavernularia Degelius

(not illustrated)

This small genus of two species (*C. hultenii* Degelius and *C. lophyrea* (Acharius) Degelius) is superficially similar to *Hypogymnia* but has unique invaginations of the lower cortex into the medulla. Both species have a typical nonpored epicortex.

Cetraria Acharius

FIGURES 29–33

SPECIES EXAMINED.—*Cetraria commixta, C. halei, C. nivalis, C. oakesiana,* and *C. pinastri.*

This large temperate-boreal genus has great morphological diversity, ranging from tiny foliose species like *Cetraria fendleri* (Tuckerman) Nylander to the fruticose Iceland Moss (*C. islandica* (L.) Acharius). I examined five species and found all to have a nonpored epicortex and a nodular surface. This would seem to be the characteristic cortical structure for the genus.

Cetrelia Culberson and Culberson

FIGURES 34, 35

SPECIES EXAMINED.—*Cetrelia chicitae* and *C. olivetorum.*

This genus includes broad-lobed pseudocyphellate parmelioid species formerly classified in either *Parmelia* or *Cetraria* (Culberson and Culberson, 1968b). As one would expect, the epicortex is nonpored and the surface nodular.

Heterodea Müller-Argau

FIGURE 36

SPECIES EXAMINED.—*Heterodea muelleri.*

This genus is endemic to Australia and has been classified in the Parmeliaceae more for want of a more appropriate family than from any real affinity. The cortical structure is unusual, a nonpored epicortex with very deep sculpturing, much deeper than in *Anzia* or *Hypogymnia.* The genus should probably be removed from this family.

Hypogymnia (Nylander) W. Watson

FIGURES 37–42

SPECIES EXAMINED.—*Hypogymnia bitteriana, H. enteromorpha, H. metaphysodes,* and *H. physodes.*

This is a well-established segregate of *Parmelia* with hollow lobes and no rhizines. Nine specimens of four species were examined, but it is obvious that much more study will be needed to find a pattern in the genus. Most specimens appear to be typically nonpored and epicorticate. *Hypogymnia bitteriana* has very sparce pores while one specimen of *H. enteromorpha* had what seemed to be distinct pores. Eastern United States specimens of *H. enteromorpha,* long suspected of being specifically distinct from the western population, have greater or lesser development of the pecularly sculptured furrowing seen in *Anzia* and *Heterodea.*

Menegazzia Massalongo

FIGURES 43, 44

SPECIES EXAMINED.—*Menegazzia cincinnata* and *M. terebrata.*

This primary austral genus, a segregate of *Parmelia,* has hollow lobes as in *Hypogymnia,* large perforations in the upper cortex, and no rhizines. Both species examined have a distinctly epicorticate nonpored layer and a nodular surface, not unlike that in *Hypogymnia.*

Pannoparmelia Darbishire

FIGURES 45, 46

SPECIES EXAMINED.—*Pannoparmelia angustata* and *P. anzioides.*

This genus is very similar to *Anzia* in having a dense network of black hyphae below but differs in having eight spores and, in the two species seen, usnic acid. The upper layer of hyphae are arranged mostly horizontally in an irregular configuration and at least some pores appear to originate from gaps between hyphae, although the epicortex is clearly developed (Figure 8*b*). Interestingly it differs in this respect from *Anzia* (Figures 24–26) which is basically nonpored and nodular.

Parmelia Acharius

FIGURES 47–141

Subgenus *Melanoparmelia* Hue

FIGURES 47–52

SPECIES EXAMINED.—*Parmelia acetabulum, P. disjuncta, P. olivacea, P. ryssolea, P. septentrionalis,* and *P. subolivacea.*

The systematic position of this subgenus is not firmly established. The main character for the group is the brown color attributed to an unidentified apparently noncrystalline pigment, "Parmelia brown." The thallus morphology, short often rotund lobes, simple rhizines, and lack of cilia, places it superficially near section *Cyclocheila* of subgenus *Parmelia,* which has a pored epicortex. The infrequent occurence of small pseudocyphellae might even relate it to section *Simplices.* All six species (eight specimens) investigated have a nonpored epicortex and a more or less strongly nodular surface. Variation between species is very small. All evidence suggests that *Melanoparmelia* should have at least subgeneric status in *Parmelia.*

Subgenus *Xanthoparmelia* (Vainio) Hale

FIGURES 53–60

SPECIES EXAMINED.—*Parmelia conspersa, P. cumberlandia, P. hyporhytida, P. ioanis-simae, P. plittii, P. taractica,* and *P. tasmanica.*

All species in this subgenus are saxicolous (rarely on soil), contain usnic acid, and have simple rhizines without marginal cilia. Section *Cyclocheila,* except for lack of usnic acid in most species, is very close in morphology. Seven species and nine specimens in subgenus *Xanthoparmelia* were examined. All have a pored epicortex with abundant deposition of usnic acid crystals. The well-known *P. conspersa* (Figure 54) has very large pores but the largest occur in *P. hyporhytida* (Figure 56). Two closely related species, *P. taractica* (Figure 59) and *P. tasmanica* (Figure 60), which differ primarily in color of the lower surface, have sparse development of pores, a character that may well separate them from the "conspersa" group. The SEM may, indeed, prove to be a useful way to delineate the numerous otherwise poorly differentiated species in this subgenus.

Subgenus *Parmelia*

FIGURES 61–121

Section *Parmelia*

FIGURES 61–66

SPECIES EXAMINED.—*Parmelia cunninghamii, P. fraudans, P. omphalodes, P. saxatilis, P. squarrosa,* and *P. sulcata.*

The arctic-boreal to temperate species in this section have similar lobe configuration, pseudocyphellae or pseudocyphellae-like white reticulation, and simple chemistry (salacinic or rarely protocetraric acid). Six species and eight specimens studied consistently had a nonpored epicortex and nodular surface. The cortex is virtually indistinguishable from that in section *Simplices.*

Section *Simplices* (Hale and Kurokawa) Hale

FIGURES 67–69

SPECIES EXAMINED.—*Parmelia bolliana, P. borreri,* and *P. rudecta.*

This small group of temperate pseudocyphellate *Parmeliae* has a uniformly nonpored epicortex and a nodular surface. It is closely related to section *Parmelia* above in fine structure but the chemical characters are completely different, the chief lichen substances being gyrophoric and lecanoric acids.

Section *Irregulares* (Vainio) Vainio

FIGURES 70, 71

SPECIES EXAMINED.—*Parmelia cetrata, P. maura,* and *P. simulans* (not illustrated).

This small section is characterized by a finely reticulately cracked cortex. The cracks show up well in the SEM photographs (Figure 71). Three specimens and three species have a very similar pored epicortex and a smooth surface. The pores tend to be grouped with broad intervening areas of nonpored cortex. This section forms a link between subgenus *Amphigymnia* and the narrow-lobed subgenus *Parmelia* (especially section *Imbricaria*) but the epicortical structure does not help us decide to which group it is better assigned.

Section *Relicinae* (Hale and Kurokawa) Hale

FIGURES 72–76

SPECIES EXAMINED.—*P. fluorescens, P. malesiana, P. planiuscula, P. ramosissima,* and *P. subabstrusa.*

Species in this section have inflated marginal bulbate cilia and always produce usnic acid, although the crystals are not easily seen in the SEM photographs. All of the five species and eight specimens examined have a pored epicortex. The pores are generally small and relatively sparce, a correlation perhaps with the humid environment of the tropical rainforest where most of the species have evolved.

Section *Bicornuta* Lynge

FIGURES 77–80

SPECIES EXAMINED.—*P. confoederata, P. coronata, P. pigmentacea,* and *P. subinflata.*

This section has the same bulbate cilia as section *Relicinae* but lacks usnic acid. Few of the species occur in the humid lowland tropics; most are montane-tropical or temperate. Four species and

five specimens all have a distinct pored epicortex, the pores in *P. coronata* being unusually well developed (Figure 78).

Section *Imbricaria* (Schreber) Fries

FIGURES 81–88

SPECIES EXAMINED.—*Parmelia antillensis, P. aurulenta, P. dissecta, P. horrescens, P. jamesii, P. quercina, P. scortea,* and *P. wallichiana.*

There is a great range of morphological variation in this rather heterogeneous assemblage of marginally ciliate species. Eight species and ten specimens studied have a pored epicortex and a smooth to undulating surface. Pore variation was rather great in *P. dissecta.* The holotype from France has very large elongate pores (Figure 1*a,b,*) whereas two other specimens, one from the United States and one from Japan (Figure 83) have uniformly smaller round pores. The curly objects on the type of *P. dissecta* (Figure 1*a,b*) and on *P. wallichiana* (Figure 88) have not been identified.

Section *Cyclocheila* (Vainio) Räsänen

FIGURES 89–99

SPECIES EXAMINED.—*Parmelia aptata, P. baltimorensis, P. caperata, P. congruens, P. crozalsiana, P. cryptochlorophaea, P. malaccensis, P. rutidota, P. salacinifera, P. texana,* and *P. vanderbylii.*

This section is also rather heterogeneous and contains many narrow-lobed species with simple rhizines but lacking marginal cilia. Some of the species, e.g., *Parmelia caperata,* have rather broad rotund lobes, but the bare marginal zone below is much narrower than in subgenus *Amphigymnia.* Sixteen specimens of eleven species have a pored epicortex. *Parmelia crozalsiana* was represented by one specimen with small sparse pores (Figue 93) and two specimens with a typical, well-developed nonpored epicortex with a nodular surface, (Figure 13*a,b*), much as in section *Parmelia* although there is no other justification for placing it there. Three other species that are closely related in lobe configuration and chemistry, *P. aptata* (Figure 89), *P. cryptochlorophaea* (Figure 94), and *P. texana* (Figure 98), also tend to have a strongly nodular surface, but pores, though small and sparce, are developed in the epicortex.

Section *Hypotrachyna* Vainio

FIGURES 100–121

SPECIES EXAMINED.—*Parmelia addita, P. adjuncta, P. brasiliana, P. caraccensis, P. chicitae, P. croceopustulata, P. dentella, P. endochlora, P. erythrocardia, P. exsecta, P. fissicarpa, P. formosana, P. gigas, P. imbricatula, P. laevigata, P. livida, P. neodissecta, P. orientalis, P. physcioides, P. pustulifera, P. scytodes,* and *P. sinuosa.*

This is the largest single section in the subgenus. All species have dichotomously branched rhizines and sublinear lobes. Most have evolved in tropical montane regions. Chemical variation is very rich and indicates a high level of evolution. There was a considerable degree of uniformity in cortical structure among the 38 specimens of 22 species examined. All have a pored epicortex, and although variation in pore size and density between species may be great, specimen-to-specimen variation in the same species is not.

Subgenus *Everniiformes* (Hue) Hale and Wirth

FIGURES 122–125

SPECIES EXAMINED.—*Parmelia americana, P. neocirrhata, P. pseudonepalensis,* and *P. vexans.*

This small montane-tropical group has linear channeled lobes and long marginal cilia. Rhizines are either absent below or simple to branched. It seems most closely related to section *Hypotrachyna* although the rhizines are quite different. Four species (five specimens) examined all have a pored epicortex with some clumping of the pores.

Subgenus *Amphigymnia* Vainio

FIGURES 126–135

SPECIES EXAMINED.—*Parmelia cristifera, P. haitiensis, P. hypoleucina, P. hypotropa, P. louisianae, P. perforata, P. rigida, P. tinctorum,* and *P. xanthina.*

This subgenus is characterized by broad rotund lobes 10–30 mm wide and a zone at the margin below free of rhizines. Both chemical and morphological diversity are great. Nine species and eleven specimens were examined. All except *P. perforata* have a well-developed pored epicortex, and no significant difference could be found between the two major sections, *Amphigymnia* and *Perlatae.*

Parmelia perforata (Figure 131) is anamolous in that much of the cortex appears to be nonepicorticate as in *Pseudevernia*. It is of interest that its presumptive chemical counterpart, *P. rigida* (Figure 133) which contains alectoronic acid instead of norstictic acid, has a normal pored epicortex, as does the presumed sorediate counterpart of *P. perforata*, *P. hypotropa* (Figure 129).

Parmelia Species of Uncertain Position

FIGURES 136–141

Several species of *Parmelia* have not yet been assigned to any of the recognized sections because they are anomolous in one or more respects. *Parmelia flaventior*, for example, seems amphigymnioid but differs sharply from species in subgenus *Amphigymnia* in having pseudocyphellae. On the other hand, the chemistry (lecanoric acid and usnic acid) is totally different from that of *Cetrelia* where it might otherwise be placed. As would be expected with a pseudocyphellate species, the epicortex is nonpored and nodular. *Parmelia ulophyllodes* (Figure 141) appears to be related to *P. flaventior* but lacks obvious pseudocyphellae and is smaller, much as the species in subgenus *Parmelia* section *Cyclocheila*. It is, however, nonpored and very similar to *P. flaventior*. Another relative of *P. flaventior*, *P. praesignis* (Figure 138), lacks soredia but has identical epicortical structure. Another amphigymnioid species, *P. thomsonii* (Figure 140), has a normal pored epicortex but because of the conspicuous erect marginal pycnidia does not fit well into subgenus *Amphigymnia*.

Parmelia sphaerosporella has all of the characteristics of a species in section *Cyclocheila*, but it has a nonpored nodular epicortex (Figure 139). Finally, *P. meiophora*, an endemic Asian species, appears to be in section *Imbricaria* but the nonpored epicortex and probably pseudocyphellae place it closer to section *Parmelia* (Figure 137).

Parmeliopsis Nylander

FIGURES 2, 142

SPECIES EXAMINED.—*Parmeliopsis ambigua* and *P. placorodia*.

This small genus resembles *Parmelia* rather closely but always has a pale lower surface and a different type of conidiophore. The SEM photographs show a strongly pored epicortex similar to that in many sections of *Parmelia*, suggesting a close affinity.

Platismatia Culberson and Culberson

FIGURES 143–145

SPECIES EXAMINED.—*Platismatia glauca*, *P. stenophylla*, and *P. tuckermanii*.

This small segregate of *Cetraria* includes the widespread boreal *P. glauca*. The epicortical structure is quite uniform, nonpored and nodular. It falls very close to both *Cetrelia* and *Asahinea*.

Pseudevernia Zopf

FIGURES 146–149

SPECIES EXAMINED.—*Pseudevernia cladonia*, *P. consocians*, *P. furfuracea*, *P. olivetorina*, and *P. intensa*.

Although only recently generally accepted as a segregate of *Parmelia*, this genus is amply distinct in morphology (Hale, 1968). Rhizines are lacking and the lower surface is strongly channeled. The surface structure is unusual. There is no epicortex at all, the crowded erect hyphal tips forming a kind of pseudocortex with various degrees of conglutination.

Atlas of SEM Photographs

The following series of photographs (Figures 24–150) illustrates the cortical surface of 123 species taken at two standardized enlargements, 500 diameters (upper photograph, 1 mm = 2μ) and 2000 diameters (lower photograph, 2 mm = 1μ). See Figure 2 for the relative areas included in the original photographs. The final prints as shown here were trimmed to 9 × 9 cm. The × 2000 enlargement was usually taken at or near the center of the × 500 photograph and included in it, but in a few cases it was selected outside this area to avoid accumulations of debris. Many kinds of artifacts are to be seen on the cortical surface, including pollen grains (Figures 66, 108, 123), crystals of lichen substances (Figures 85, 121, 135), pruina caused by calcium oxalate crystals (Figure 93), hyphae of saprophytic fungi (Figures 61, 74, 89, 95, 97, 108), and unidentified debris (Figures 25, 87). White

areas in the photographs, especially around pores, are created by a thinner layer of gold.

The photographs are arranged alphabetically by genus and within each genus by species. In *Parmelia* the sections are phylogenetically arranged but within sections the species are alphabetic. Data to identify each specimen include collector, collector's number, and country or state of origin.

Literature Cited

Culberson, W. L., and C. F. Culberson.
1968a. A Phylogenetic View of Chemical Evolution in the Lichens. *Bryologist,* 73:1–33
1968b. The Lichen Genera *Cetrelia* and *Platismatia* (Parmeliaceae). *Contributions from the United States National Herbarium,* 34:449–558.

Hale, M. E.
1965. A Monograph of *Parmelia* Subgenus *Amphigymnia*. *Contributions from the United States National Herbarium,* 36:193–358.
1968. A Revision of the Lichen Genus *Pseudevernia*. *Bryologist,* 71:1–11.
1972. *Parmelia pustulifera,* a New Lichen from Southeastern United States. *Brittonia,* 24:22–27.

Hale, M. E., and S. Kurokawa.
1964. Studies on *Parmelia* Subgenus *Parmelia*. *Contributions from the United States National Herbarium,* 36:121–191.

Hawksworth, D. L.
1969. The Scanning Electron Microscope: An Aid to the Study of Cortical Hyphal Orientation in the Lichen Genera *Alectoria* and *Cornicularia*. *Journal Microscopie,* 8:753–760.

Jacobs, J. B., and V. Ahmadjian.
1969. The Ultrastructure of Lichens, I: A General Survey. *Journal of Phycology,* 5:227–240.

Peveling, E.
1970. Die Darstellung der Oberflachenstrukturen von Flechten mit dem Raster-Elektronenmikroskop. *Berichte der Deutschen Botanischen Gesellschaft,* neue folge 4:89–101.

Peveling, E., and J. Vahl.
1968. Die Anwendung der Gefrieratzmethode für Untersuchungen mit Raster-Elektronenmikroskop im Vergleich mit herkommlichen Untersuchungsmethoden. *Beitrag Elektronenmikroskopiche Direktabbildung von Oberflachen,* 1:205–212.

Tibell, L.
1971. The Genus *Cyphelium* in Europe. *Svensk Botanisk Tidskrift,* 65:138–164.

FIGURES 1–150

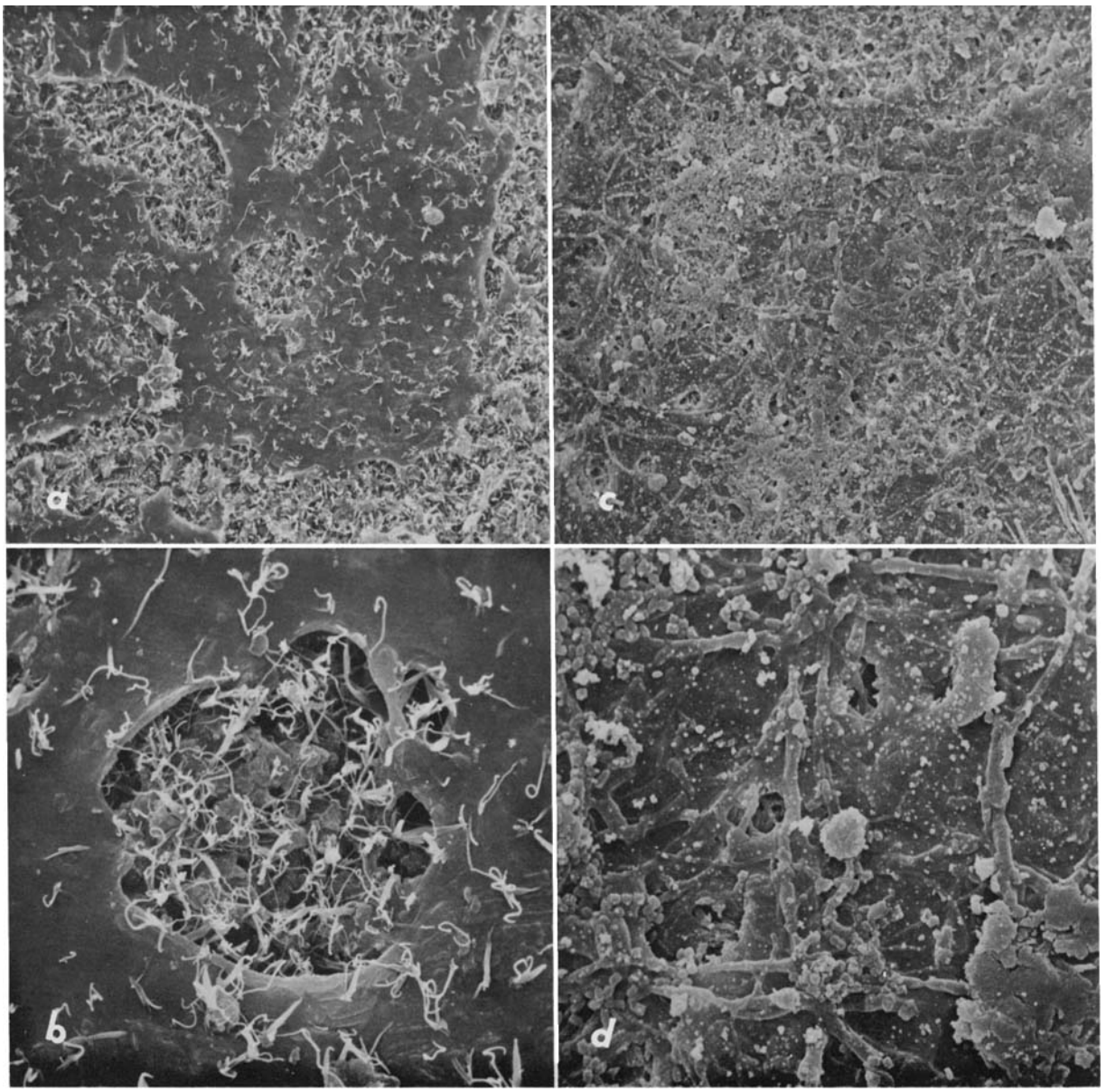

FIGURE 1.—Artifacts on the cortical surface: *a*, unidentified curled artifacts on *Parmelia dissecta* Nylander (*Nylander*, France, holotype, P) (×500); *b*, same specimen enlarged (×2000); *c*, presumed fungal infection of *P. physcioides* Nylander (*Humboldt and Bonpland* s.n., Venezuela, isotype, US) (×500); *d*, same specimen enlarged (×2000).

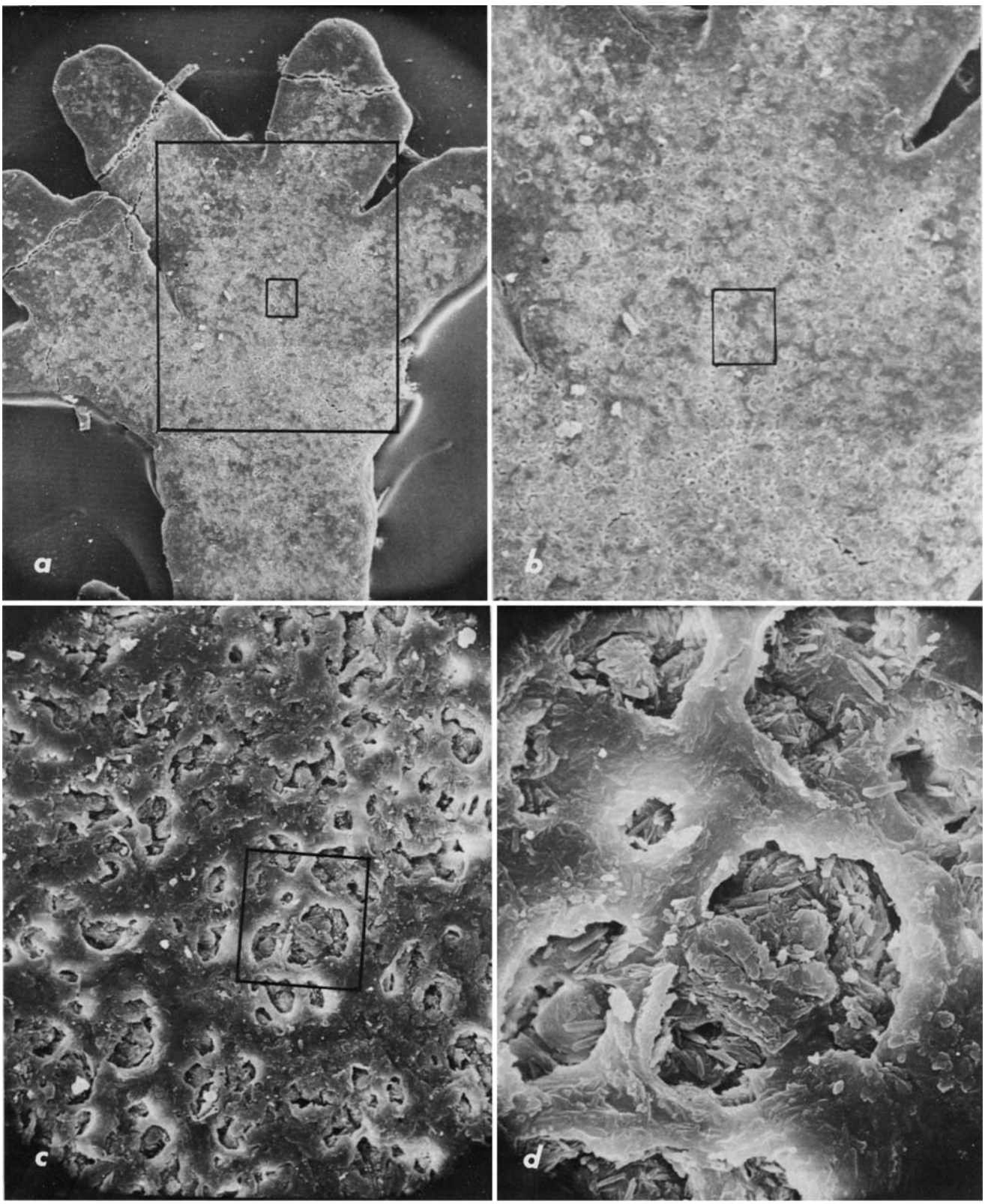
a
b
c
d

FIGURE 2.—Comparison of areas viewed with the SEM at different magnifications using *Parmeliopsis ambigua* (Acharius) Nylander (*Tuckerman*, New Hampshire): *a*, ×50, lobe about 2 mm long showing approximate areas viewed at ×100 (larger rectangular shown in *b*) and at ×500 (smaller rectangular equivalent to area viewed in *c*); *b*, ×100 (showing area equivalent to that in *c*); *c*, ×500, print area about 0.20 × 0.22 mm (rectangle indicating area enlarged in *d*); *d*, ×2000, print area about 0.05 × 0.06 mm.

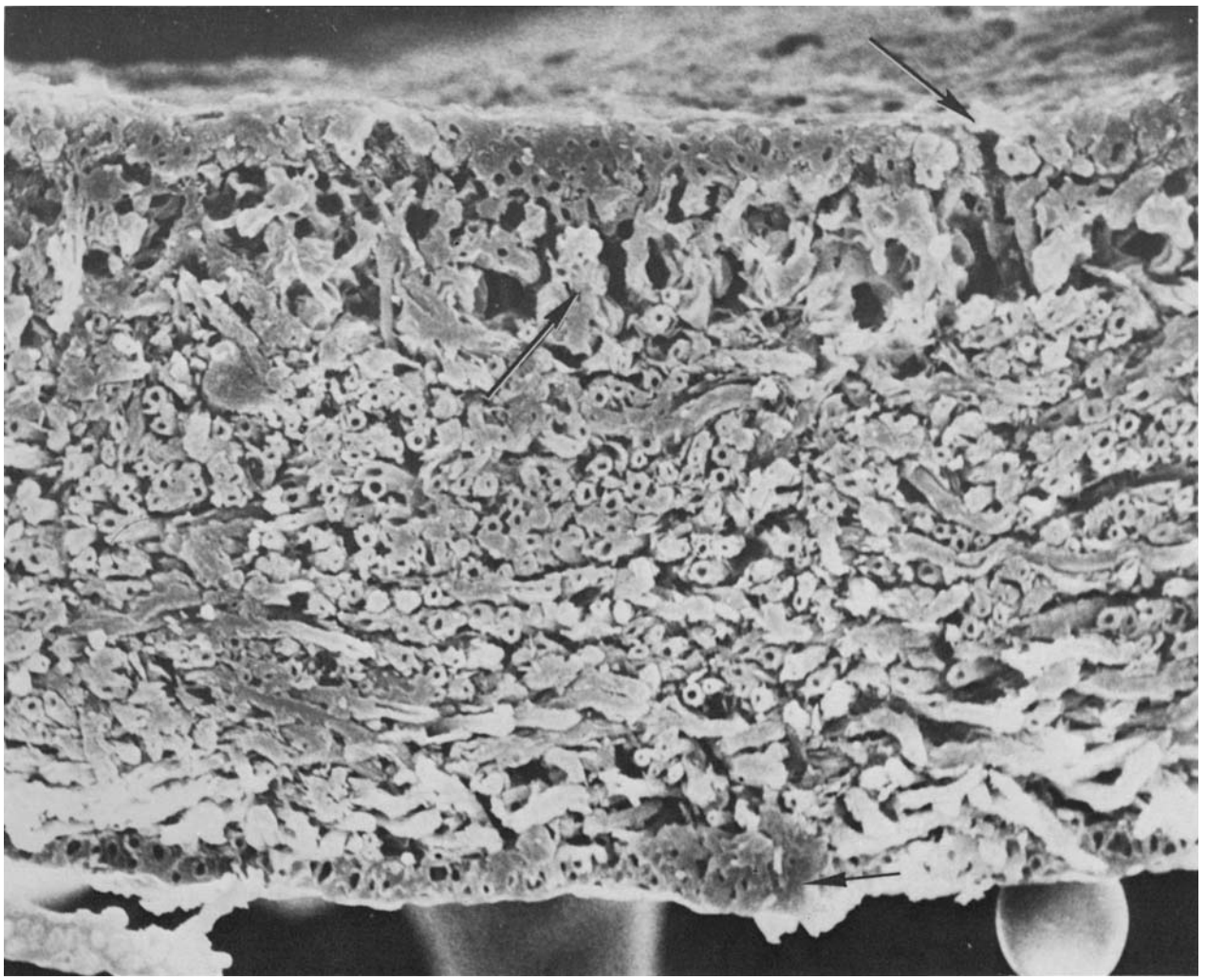

FIGURE 3.—Vertical cross-section of *Parmelia xanthina* (Müller-Argau) Vainio (same plant shown in Figure 135), showing the upper cortex (epicortex too thin to see), a pore (upper arrow), palisadelike algal layer (algal cell identified with arrow), medulla, and lower cortex (lower arrow) (about ×1000, 1 mm=about 1μ).

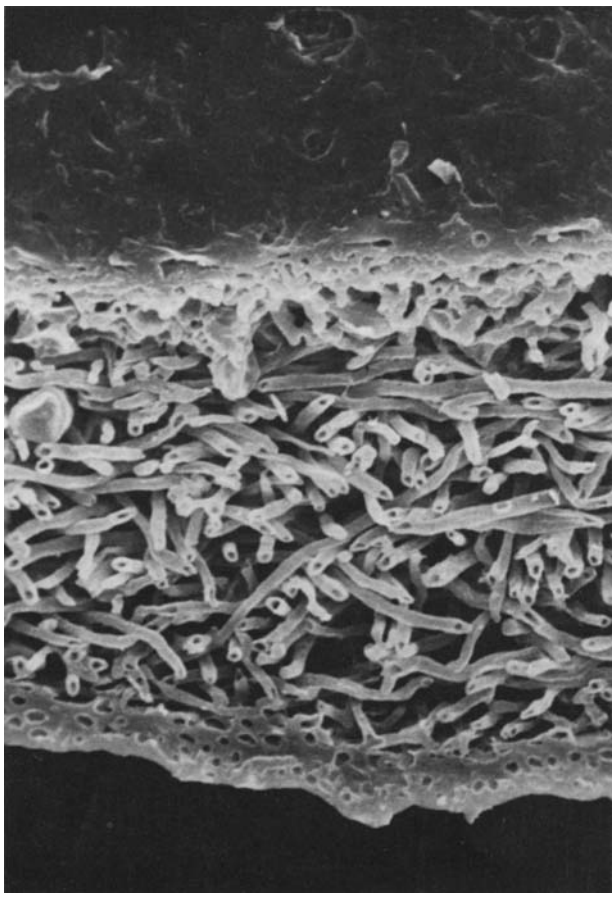

FIGURE 4.—Oblique cross-section of *Parmelia xanthina* (second lobe of plant shown in Figure 3) (about ×700).

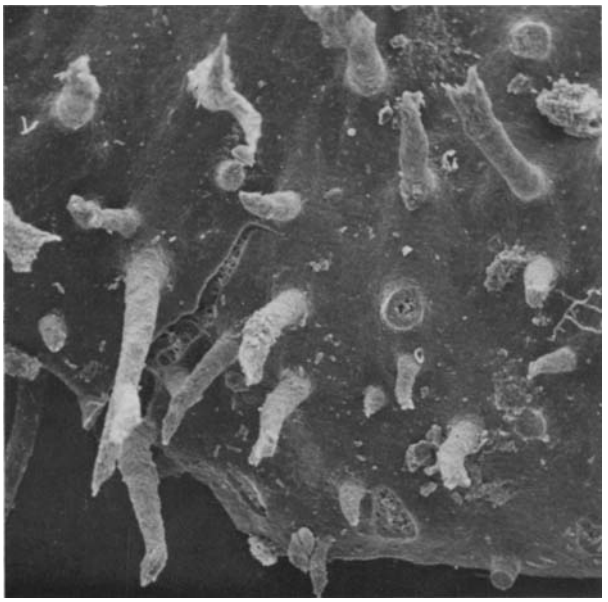

FIGURE 5.—Lower surface of *Parmelia saxatilis* (L.) Acharius (*Hale* 36387, Canada) (×100). (Stump of broken rhizine in right center enlarged in Figure 6.)

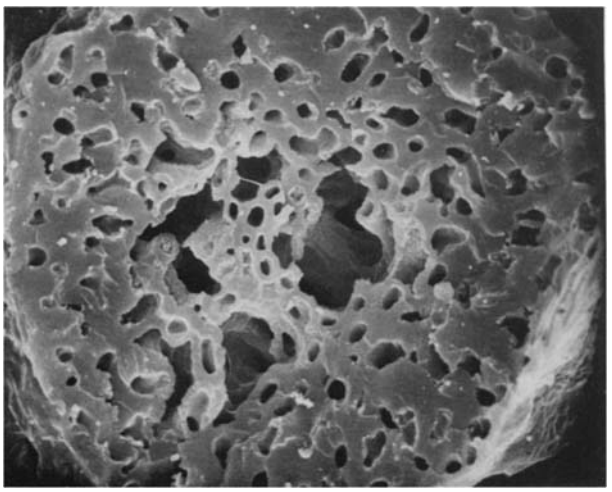

FIGURE 6.—Cross-section of a rhizine of *Parmelia saxatilis* (same specimen shown in Figure 5) (×2000).

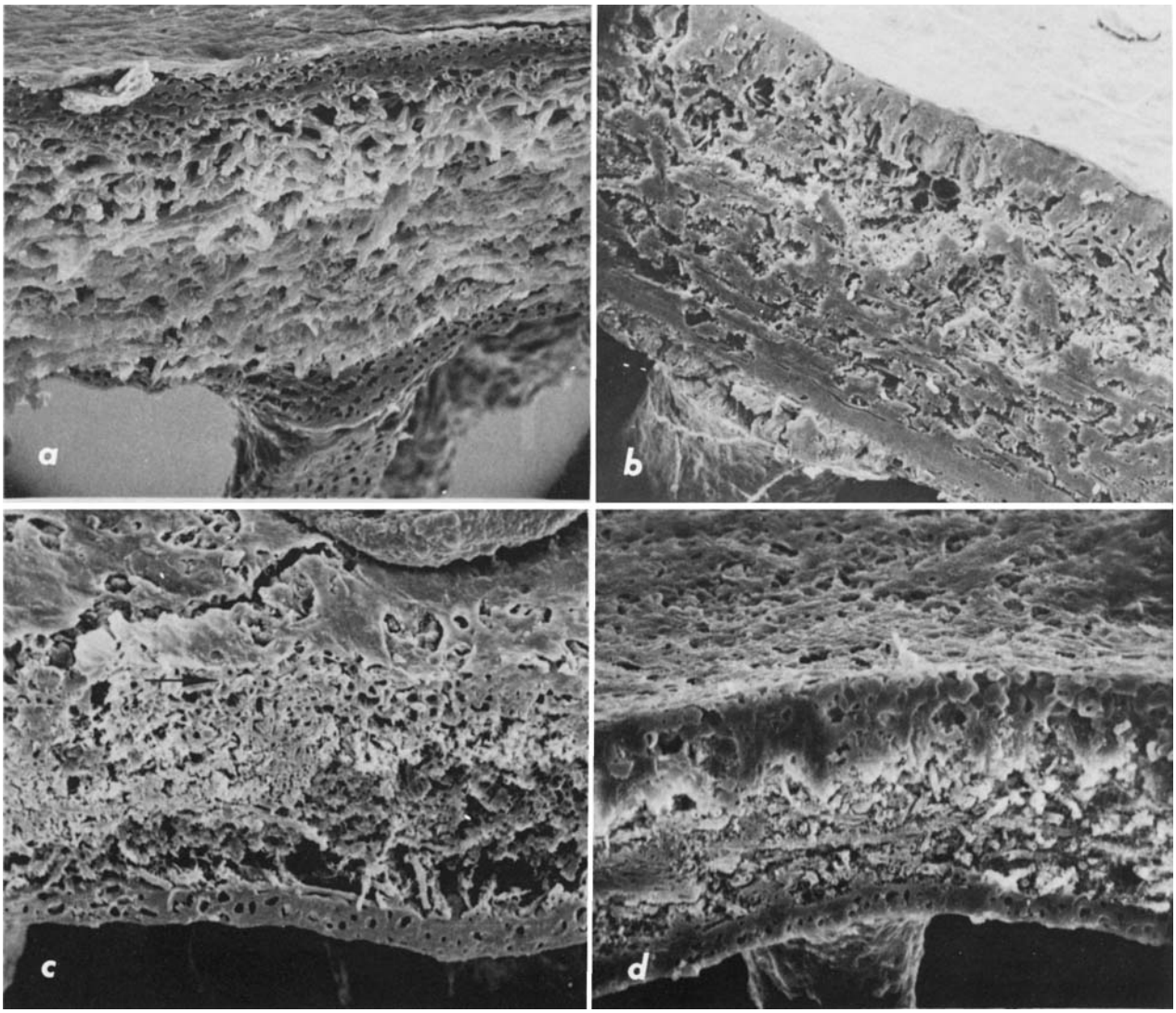

FIGURE 7.—Cross-sections of various species of *Parmelia*: *a*, *Parmelia saxatilis* (same plant shown in Figure 64); *b*, *P. fluorescens* Hale (same plant shown in Figure 72) (this species has an unusual arrangement of the cortical hyphae in columns); *c*, *P. neodissecta* Hale (same plant shown in Figure 116) (blob at the top right is glue; arrow points of top of cortex); *d*, *P. croceopustulata Kurokawa* (*Hale* 33269, North Carolina) *a*, *b*, and*d*, about ×500; *c* about ×600.

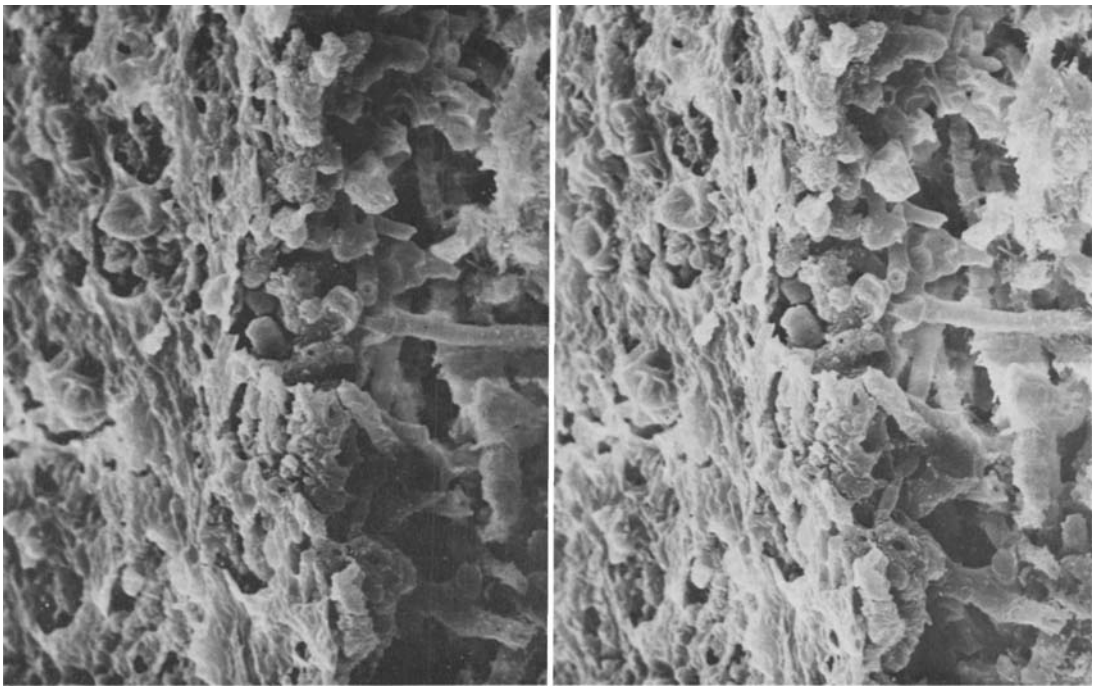

FIGURE 8.—Stereo photographs of a cross-section of *Parmelia croceopustulata* (same plant shown in Figure 105) (×1000). These can be viewed with a standard stereo map viewer at approximately 12 cm above the photograph.

FIGURE 9.—Stereo view of a cross-section of *Pseudevernia furfuracea* (L.) Hale and Culberson showing arrangement of cortical hyphae, the cortical layer, and the upper medullary area (same plant shown in Figure 148) (×1000). Compare Figure 148 for a perpendicular view of the same plant.

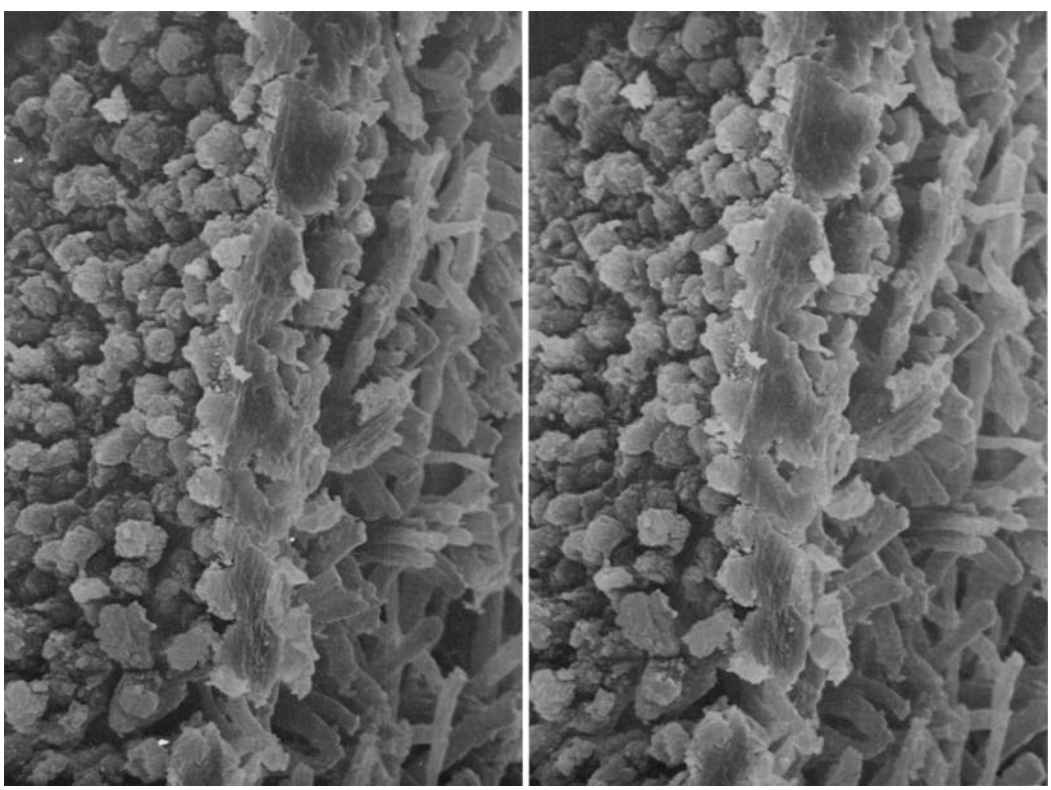

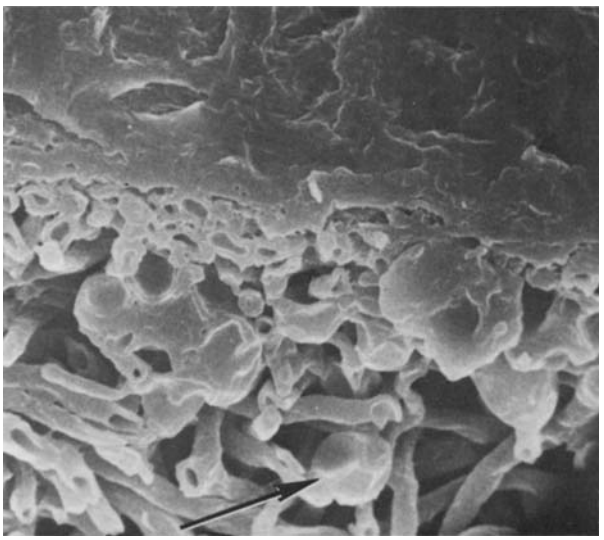

FIGURE 10.—Close-up of the algal layer in *Parmelia xanthina* (same plant shown in Figure 4) (×2000). Arrow points to an algal cell. Part of the upper surface of the cortex, the cortical layer, and part of the medulla are also shown.

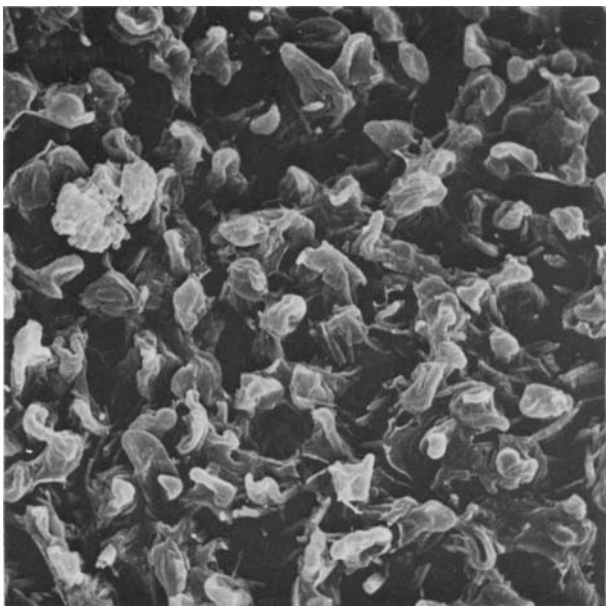

FIGURE 11.—Surface of *Graphina confluens* (Fée) Müller-Argau (*Hale* 20169, Mexico) (×2000).

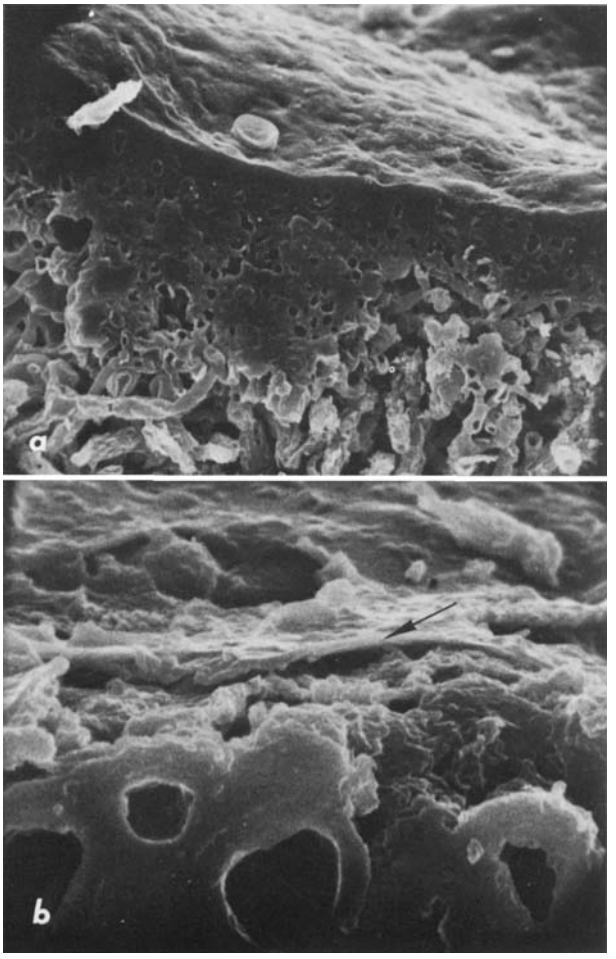

FIGURE 12.—Cross-sections of the cortical layer in (*a*) a non-pored epicorticate species, *Parmelia bolliana* Müller-Argau (*Adams* 34, Oklahoma) (×1000) and (*b*) a pored epicorticate species, *P. croceopustulata* Kurokawa (same plant shown in Figure 7*d*) (×5000). Arrow points to epicortex.

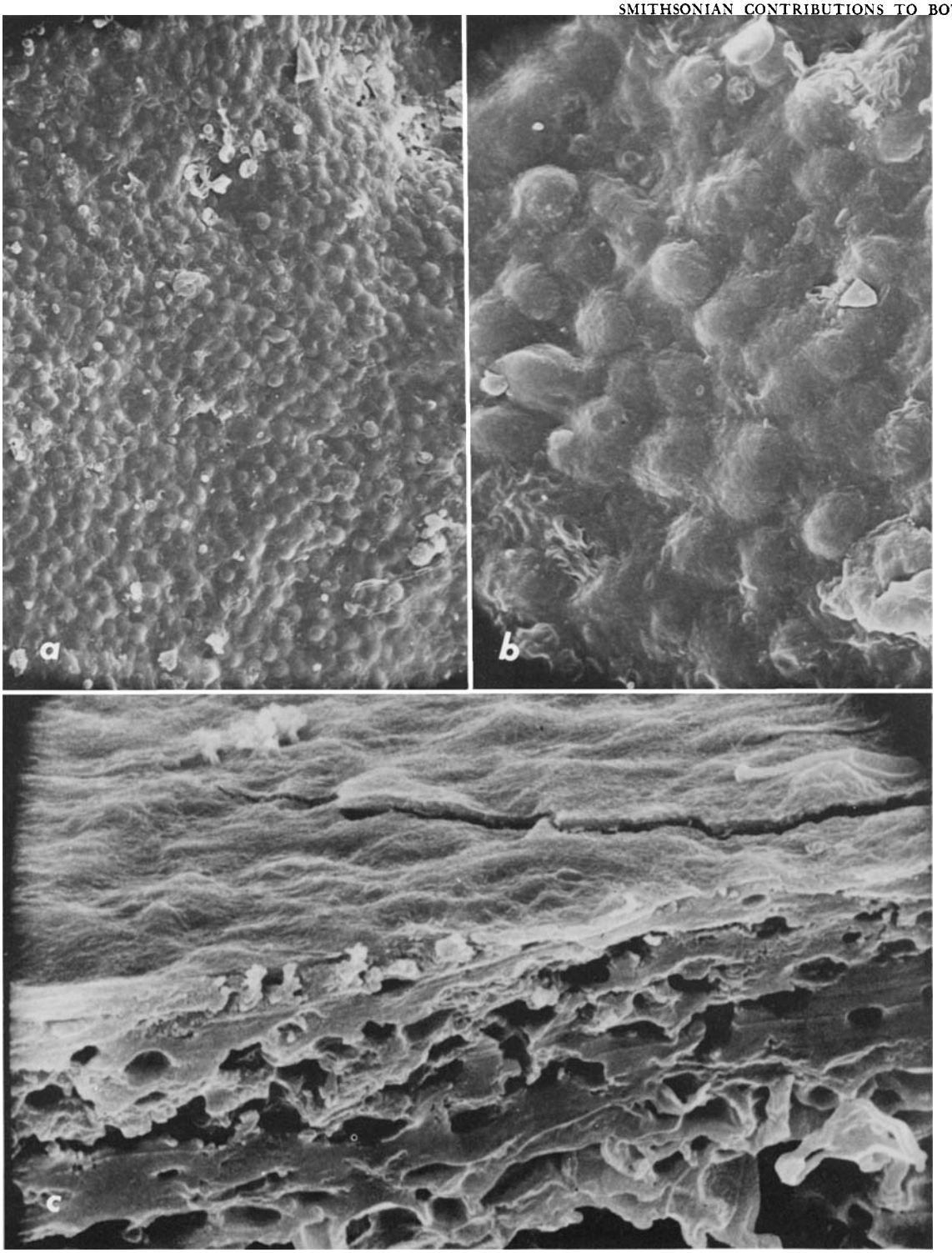

FIGURE 13.—Cortex surface of some nonpored epicorticate species: *a*, nodular surface of *Parmelia crozalsiana* Bouly de Lesdain (*Skorepa* 1757, Ilinois) (×500); *b*, same plant enlarged ×2000; *c*, oblique view of the nodular surface of *P. squarrosa* Hale (same plant shown in Figure 65) (About ×2500) (Compare Figure 65 for a perpendicular view of this specimen).

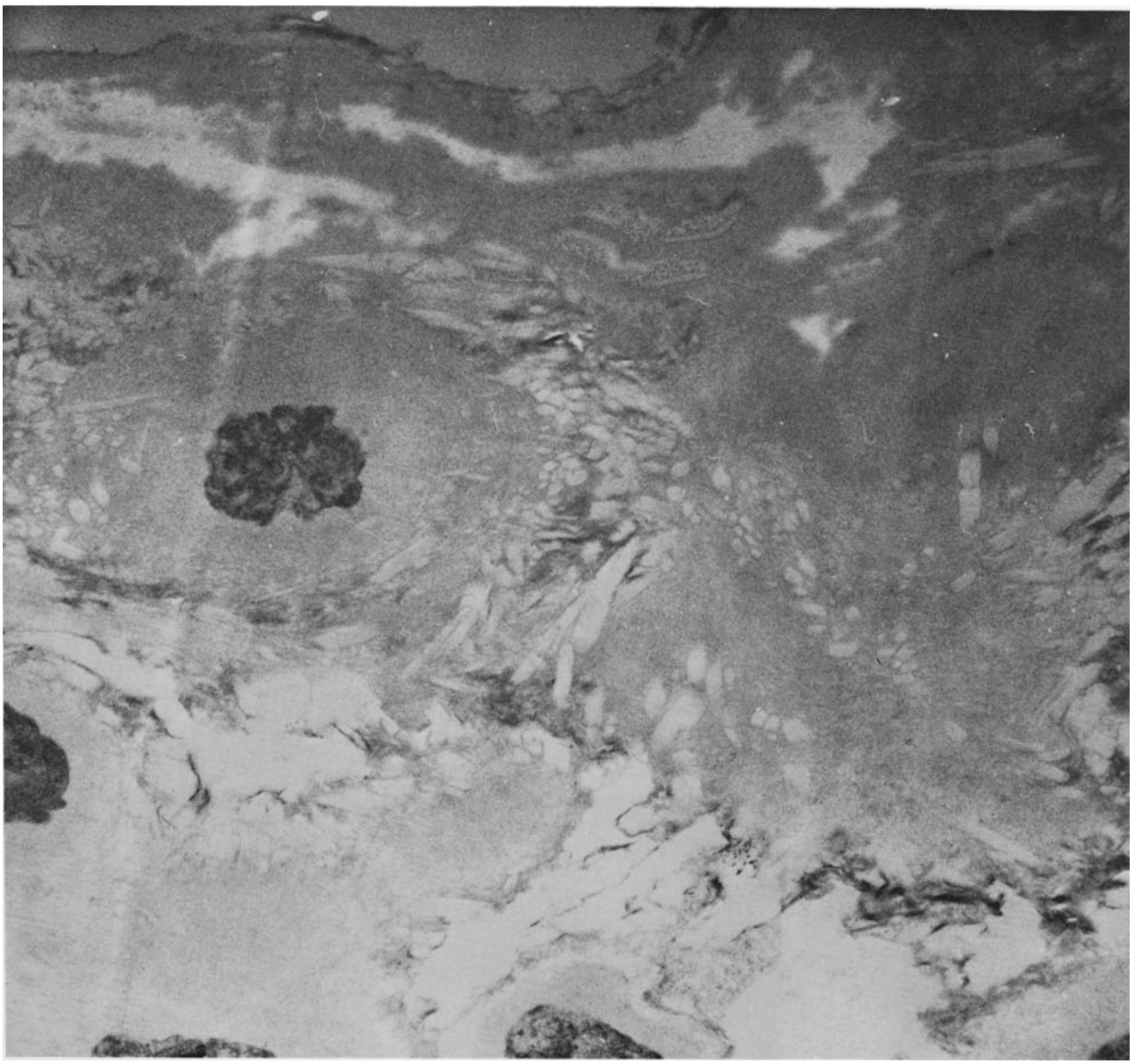

FIGURE 14.—Section of the cortex and epicortex of *Parmelia croceopustulata* Kurokawa (same plant as in Figure 105) viewed with electron microscope (×24,000). The electron-light extracted areas at periphery of the hyphae and below the epicortex are apparently sites of lichen acid deposition. Photograph by Dr. Jerome Jacobs.

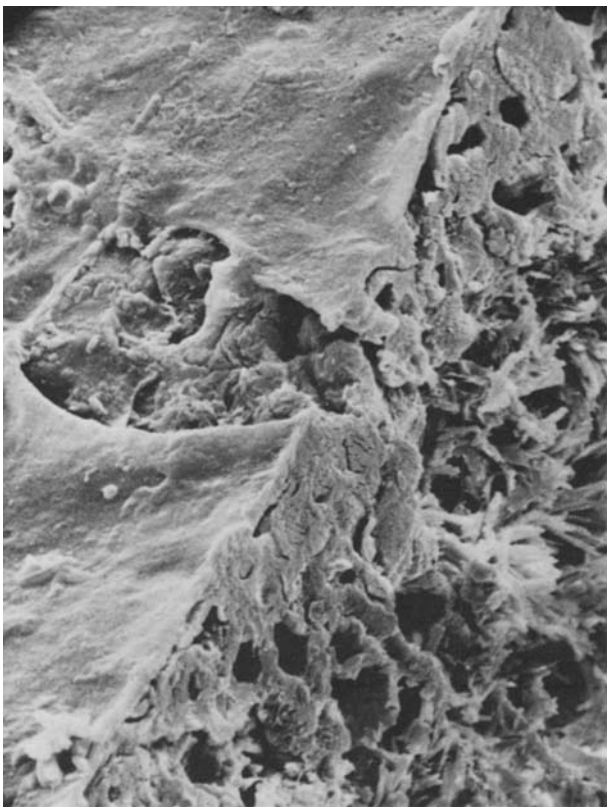

FIGURE 15.—Cross-section of *Parmelia croceopustulata* Kurokawa (same plant shown in Figure 105), showing the flat epicortex, one pore, hyphal stubs in the pore, cross-section of the cortical hyphae, and top of the medulla and crystal-encrusted hyphae (about ×2000).

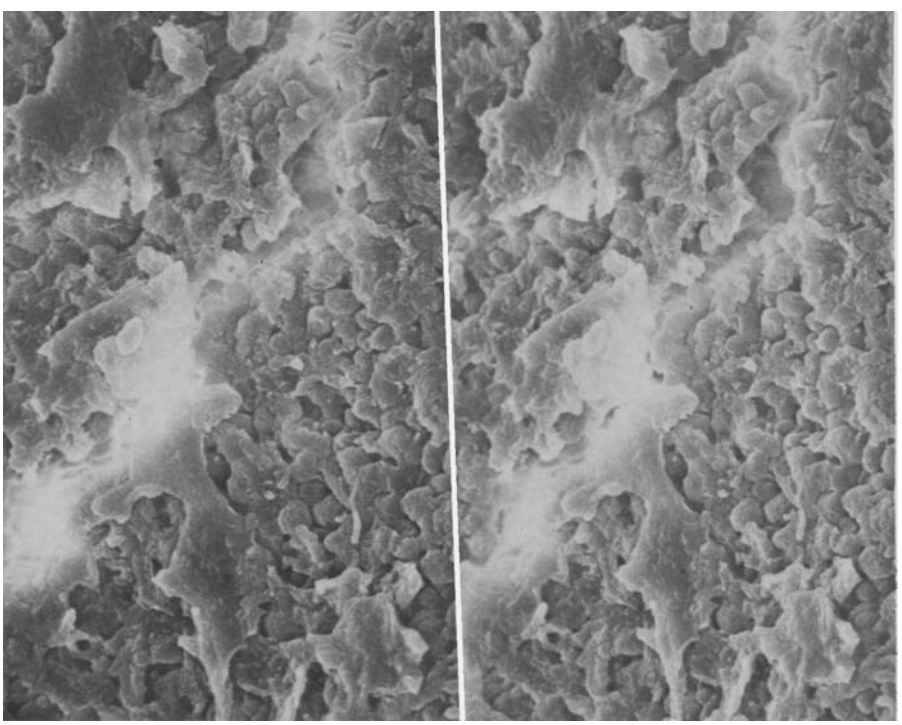

FIGURE 16.—Stereo view of the surface of *Parmelia croceopustulata* Kurokawa (same plant shown in Figure 7*d*) (×1000). For method of stereo viewing see Figure 8.

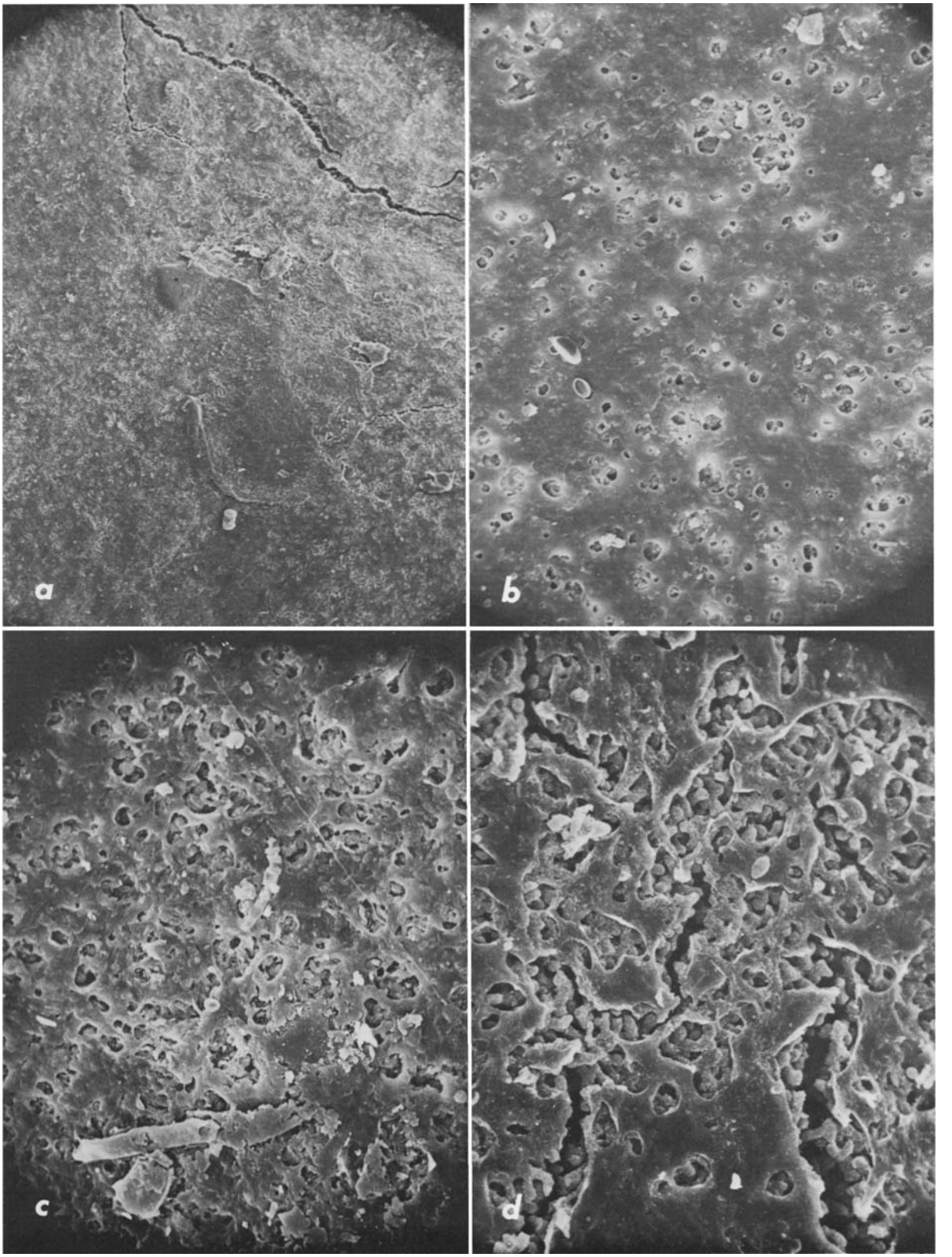

FIGURE 17.—Pore configuration in several species of *Parmelia: a,* general arrangement of pores in part of a lobe of *P. aurulenta* Tuckerman (same plant shown in Figure 82) (×50); ***b, P.*** *fissicarpa* Kurokawa (*Esterhuysen* 10115, Cape Province, South Africa) (×500); *c, P. formosana* Zahlbruckner (*Hale* 21883, Mexico) (×500); *d, P. imbricatula* Zahlbruckner (same plant shown in Figure 18*a*) (×500).

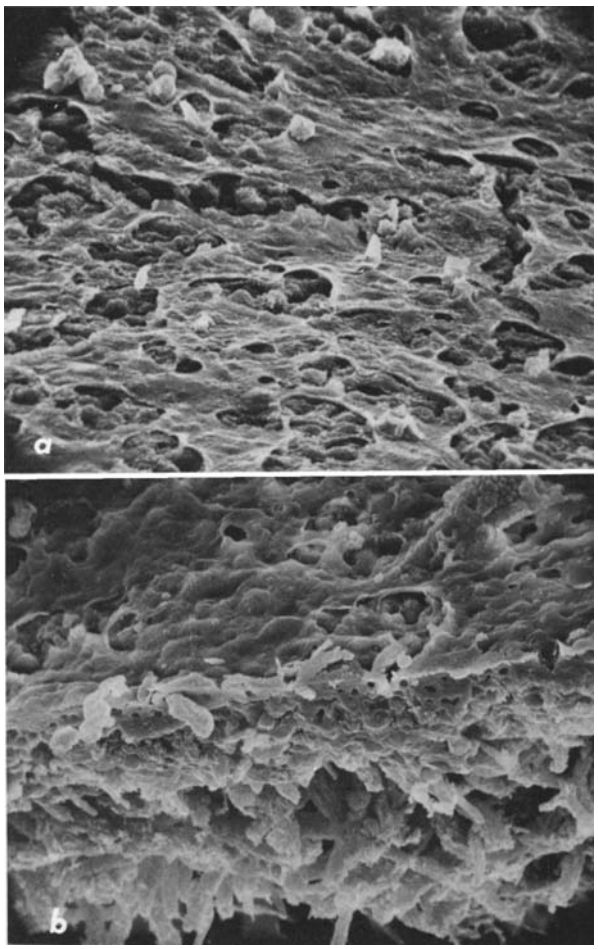

FIGURE 18.—Oblique views of the cortex surface of pored epicorticate species: *a*, smooth surface of *P. imbricatula* Zahlbruckner (*Kurokawa* 2181, Java) (×1000) (for perpendicular view of the same plant see Figure 18*d*); *b*, nodular surface of *P. aurulenta* Tuckerman (*Hale* 17391, Pennsylvania) (×1000) (for perpendicular view of a different specimen see Figure 82).

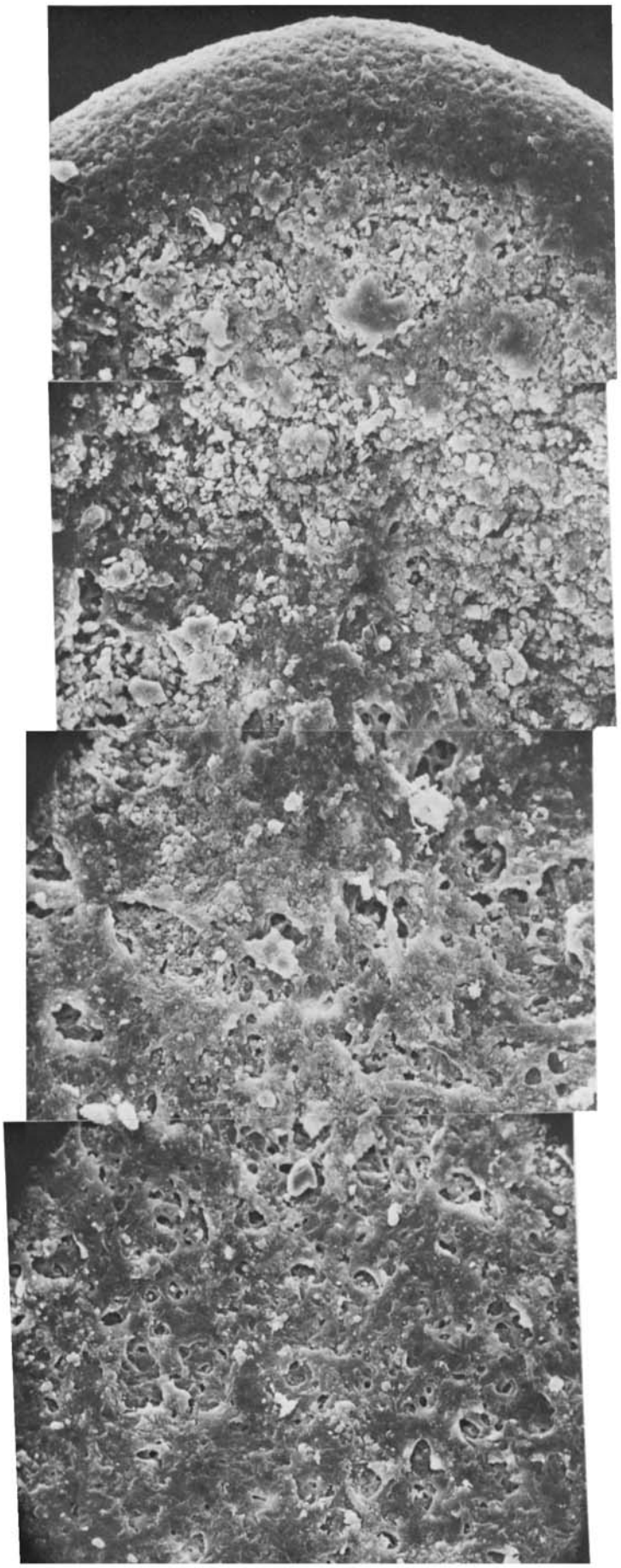

FIGURE 19.—Panorama of photographs taken from the lobe tip to about 0.60 mm from the tip of *Parmelia gigas* Kurokawa (*Killip* 18394, Columbia). Center of this lobe (about 1.5 mm from the tip) is illustrated in Figure 112.

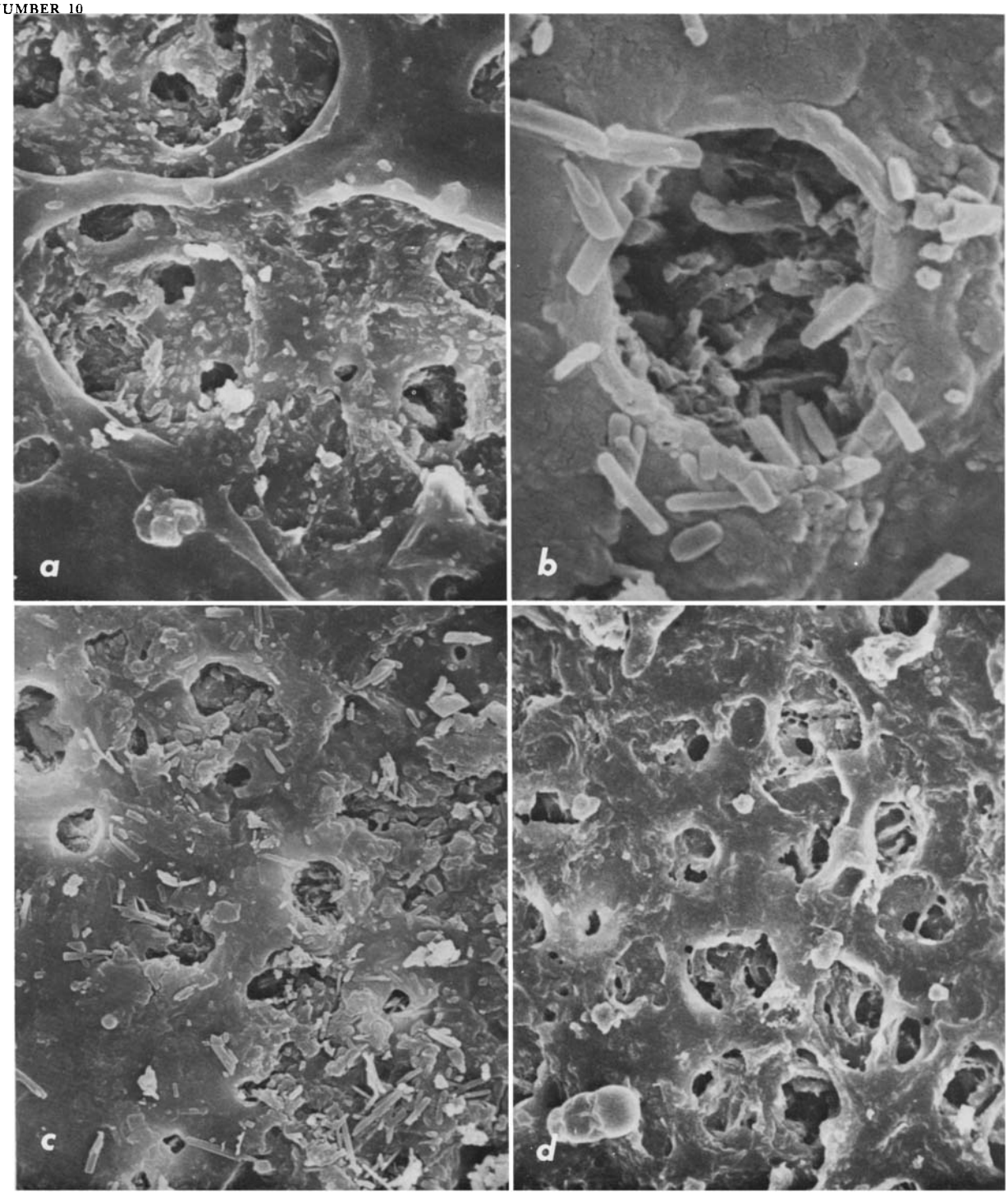

FIGURE 20.—Deposition of crystals of lichen substances in the epicortex: *a*, atranorin in *Parmelia gigas* Kurokawa (same plant shown in Figure 112) (×2000); *b*, usnic acid around a pore in *P. sinuosa* (Smith) Acharius (same plant shown in Figure 121) (×10,000); *c*, usnic acid in *P. xanthina* (Müller-Argau) Vainio (second lobe of plant shown in Figure 135) (×2000); *d*, sample from same lobe of specimen in *c* but extracted with acetone (×2000).

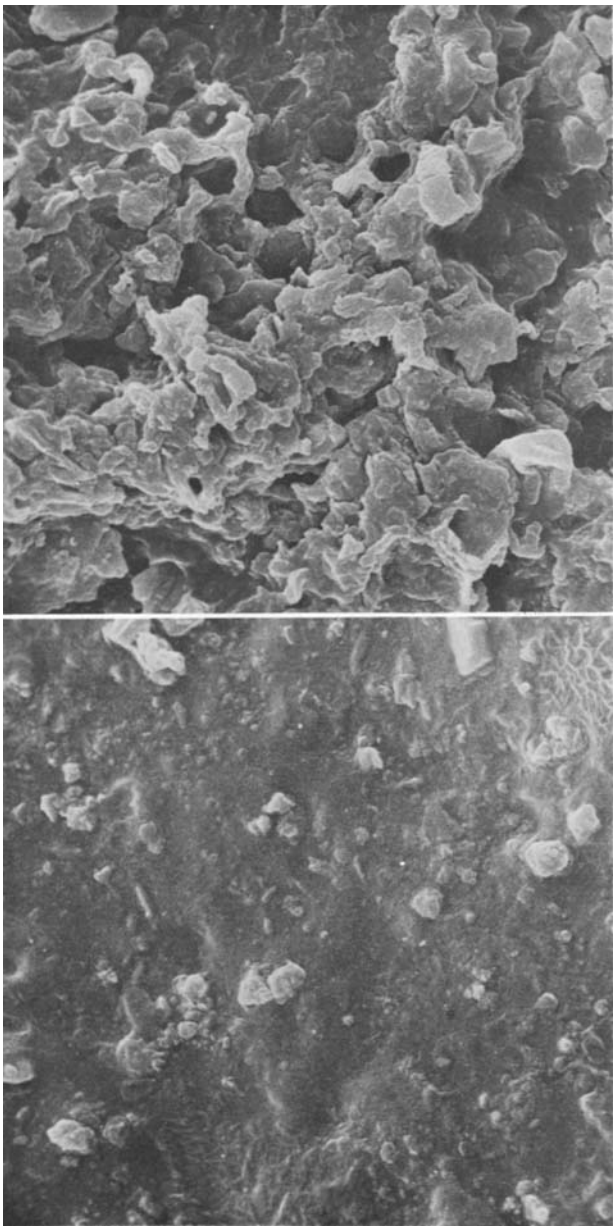

FIGURE 21.—Comparison of the upper and lower surfaces of *Parmelia perforata* (Jacquin) Acharius: upper surface (above; see also Figure 131) and lower surface from a lobe on the same specimen (*Hale* 16921, Florida) (both ×2000).

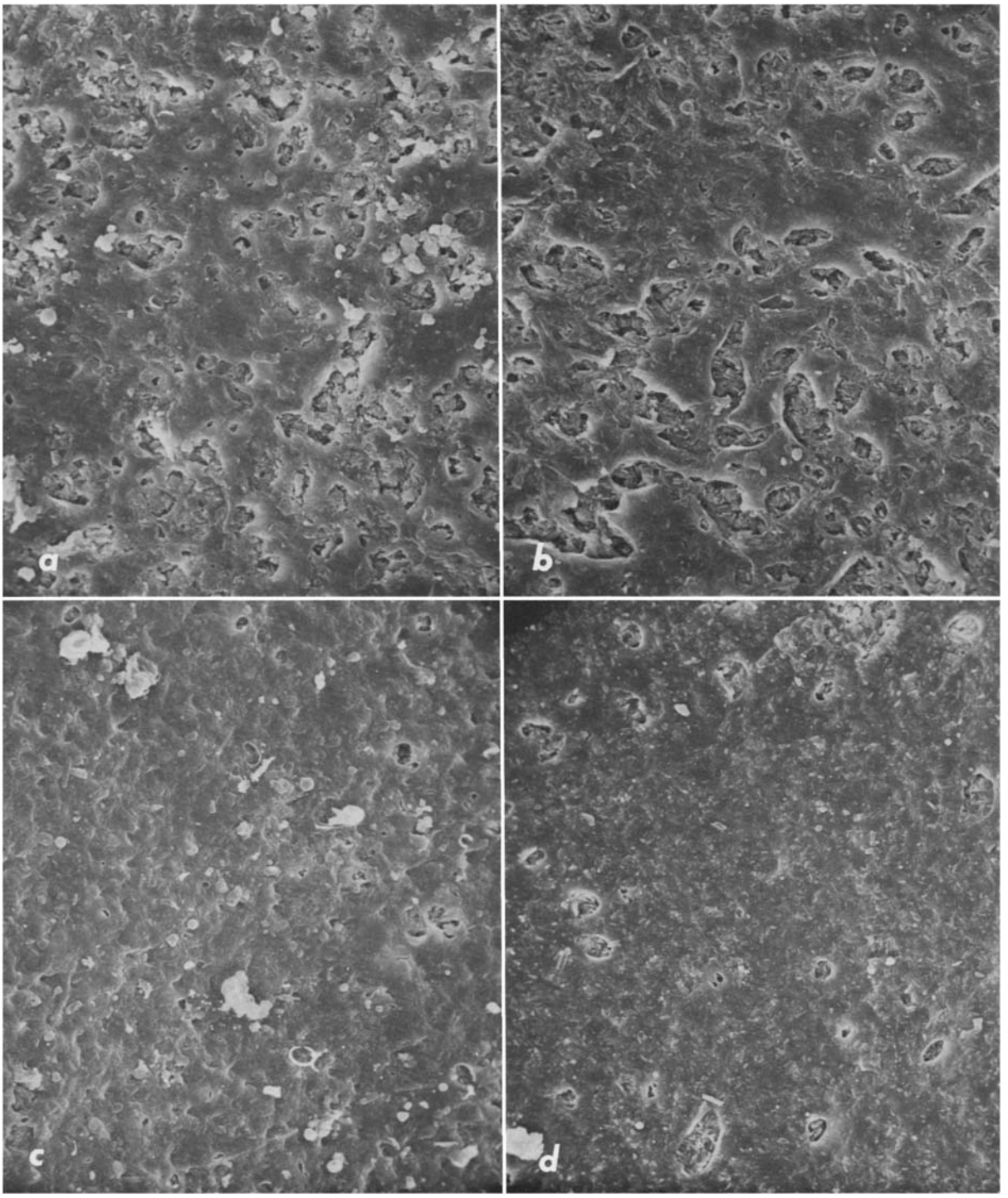

FIGURE 22.—Comparison of pore development in four different specimens of *Parmelia caperata* (L.) Acharius: *a, Hale* 20343, Mexico; *b, Maas Geesteranus* 14153, Netherlands; *c, Culberson* 12000, France; *d, Kurokawa* 64462, Japan (all ×500). See Figure 91 for another specimen of *Parmelia caperata*.

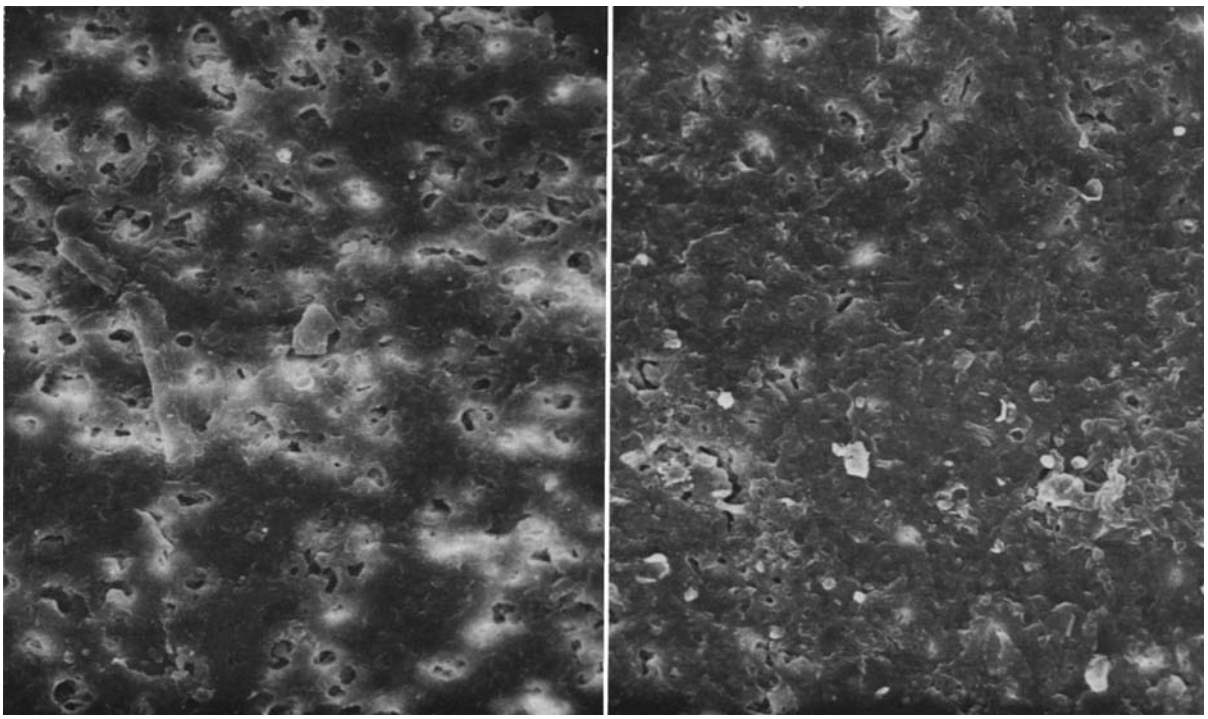

FIGURE 23.—Pore development in *Parmelia gigas* Kurokawa at an area 5 cm from the lobe tip (left) and 10 cm from the tip (right) (same plant illustrated in Figures 19 and 112) (×500).

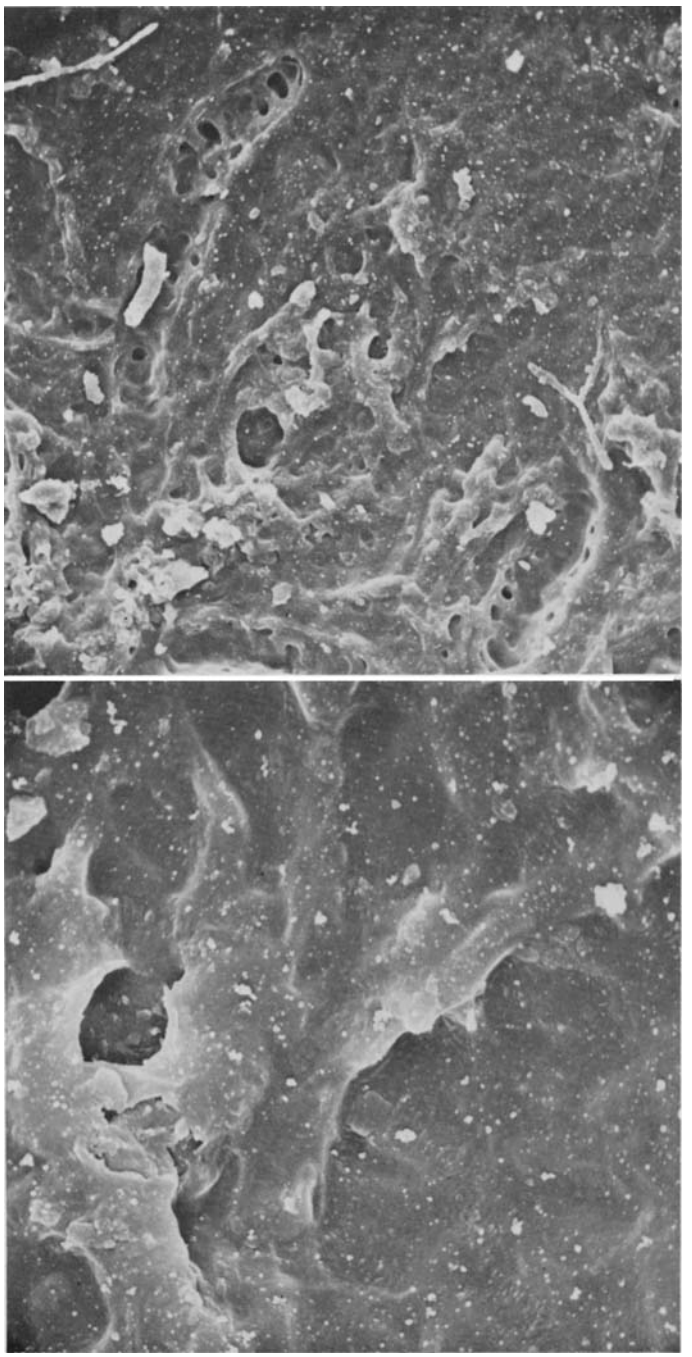

FIGURE 24.—*Anzia colpodes* (Acharius) Stizenberger (*Willey* 3, Massachusetts).

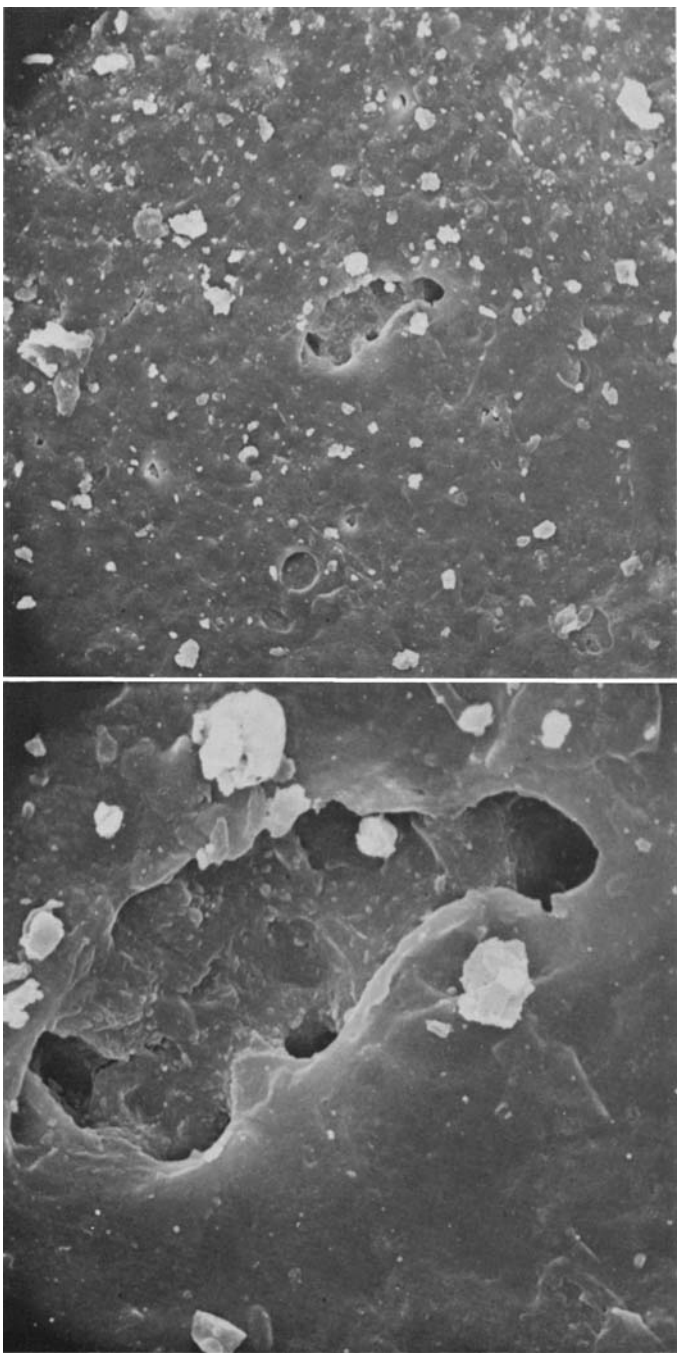

FIGURE 25.—*Anzia japonica* (Tuckerman) Müller-Argau (*Wright* s.n., Japan).

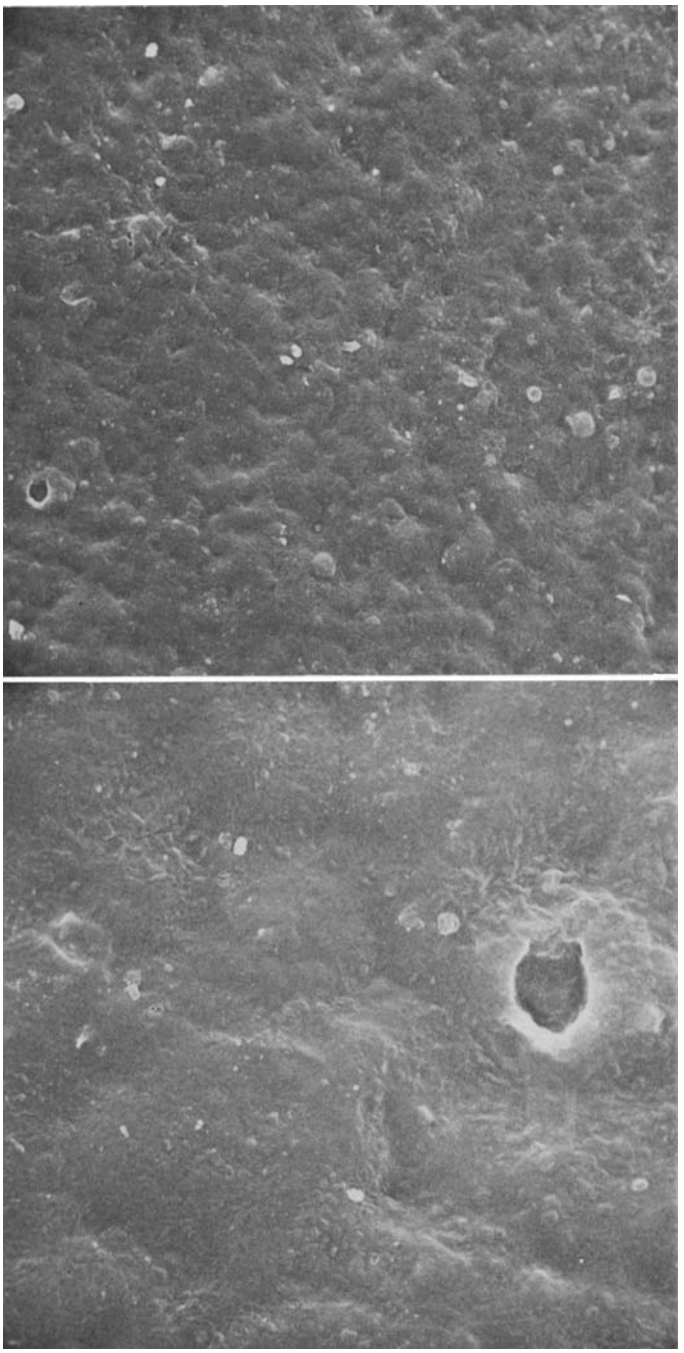

FIGURE 26.—*Anzia ornata* (Zahlbruckner) Asahina (*Kurokawa* 58239, Japan).

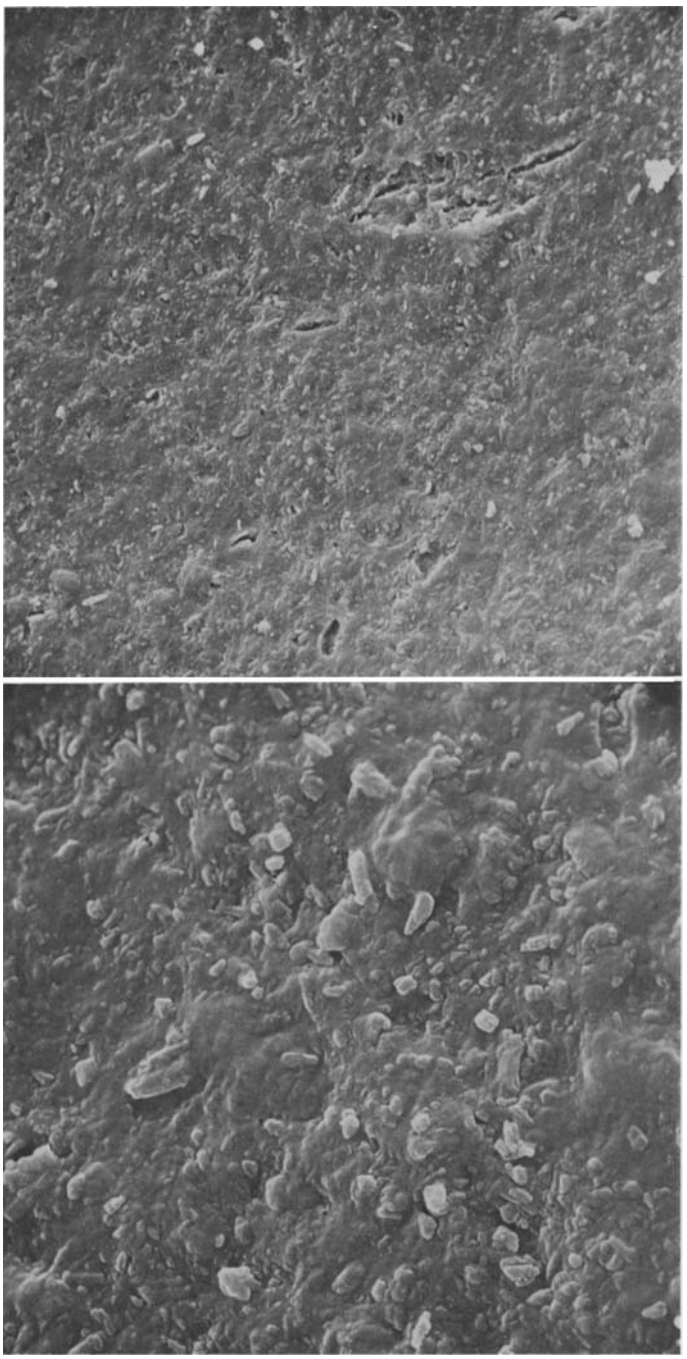

FIGURE 27.—*Asahinea chrysantha* (Tuckerman) Culberson and Culberson (*Potter* 6103, Alaska).

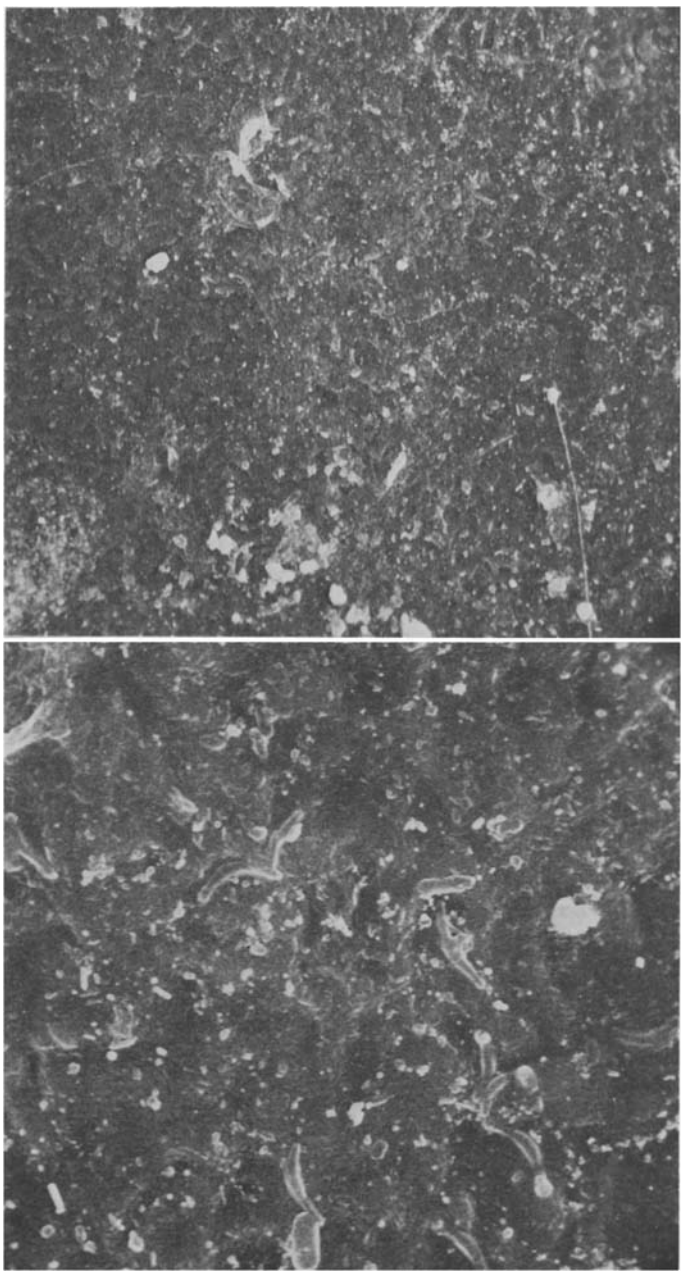

FIGURE 28.—*Asahinea scholanderi* (Llano) Culberson and Culberson (*Thomson* 15715, Canada).

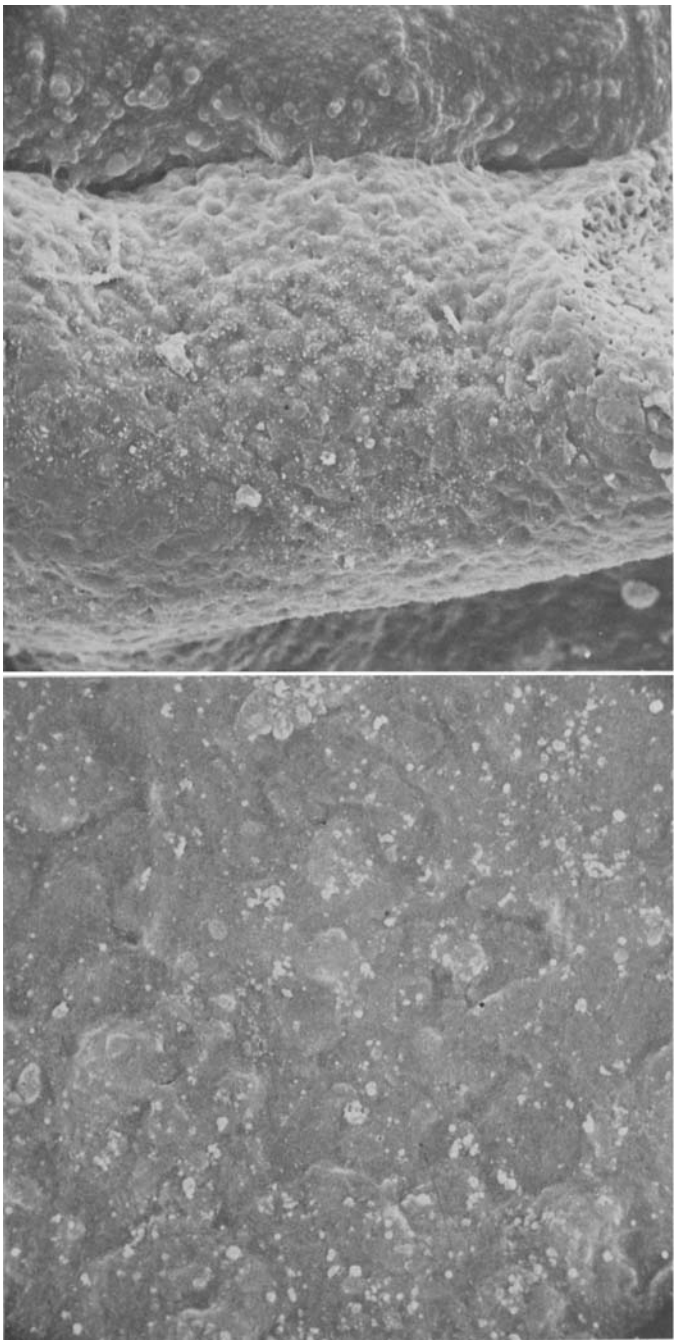

FIGURE 29.—*Cetraria commixta* (Nylander) T. Fries (*Crombie* s.n., England).

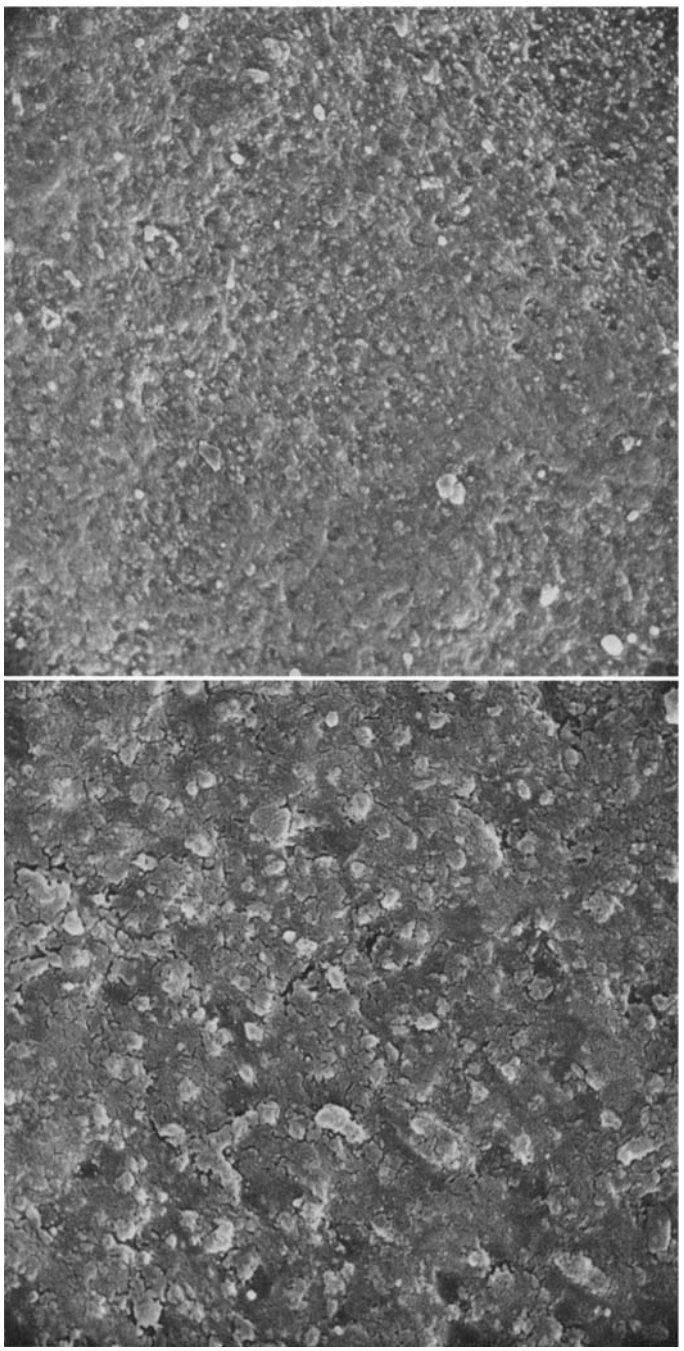

FIGURE 30.—*Cetraria halei* Culberson (*Hale* 34200, Michigan).

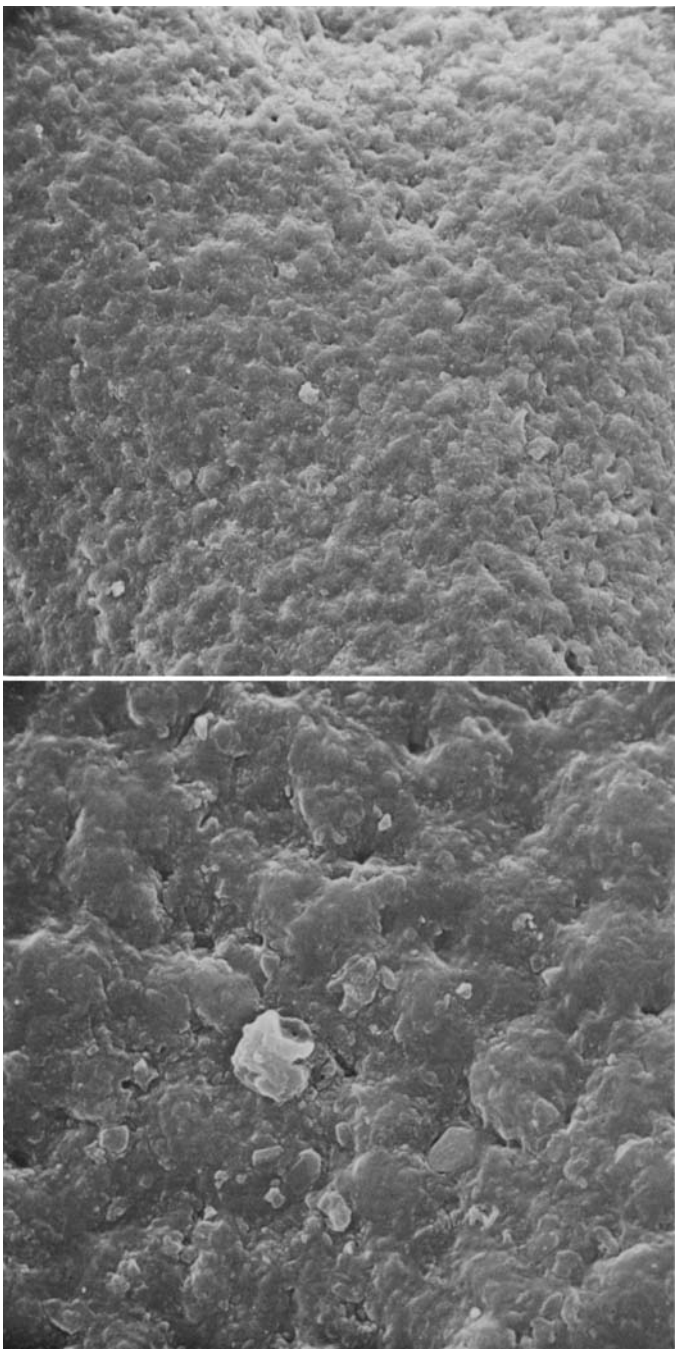

FIGURE 31.—*Cetraria nivalis* (L.) Acharius (*Bird* 17254, Canada).

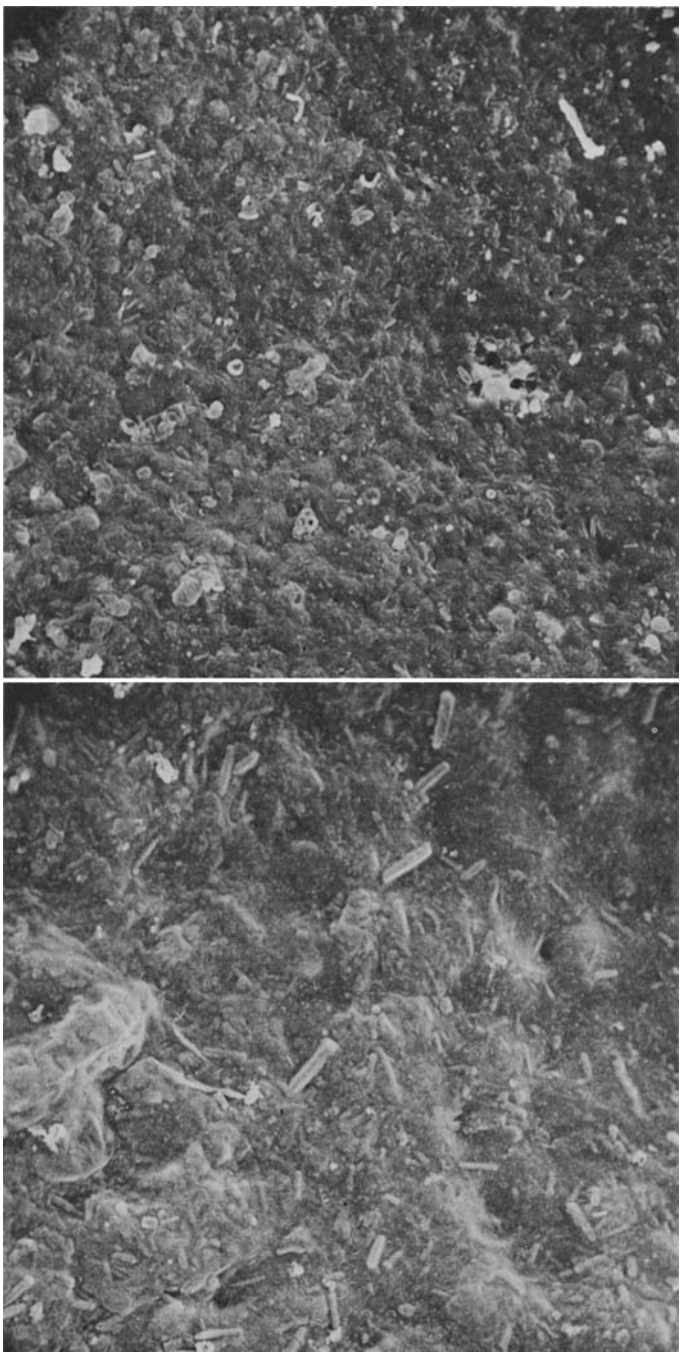

FIGURE 32.—*Cetraria oakesiana* Tuckerman (*Culberson* 4556, New Hampshire).

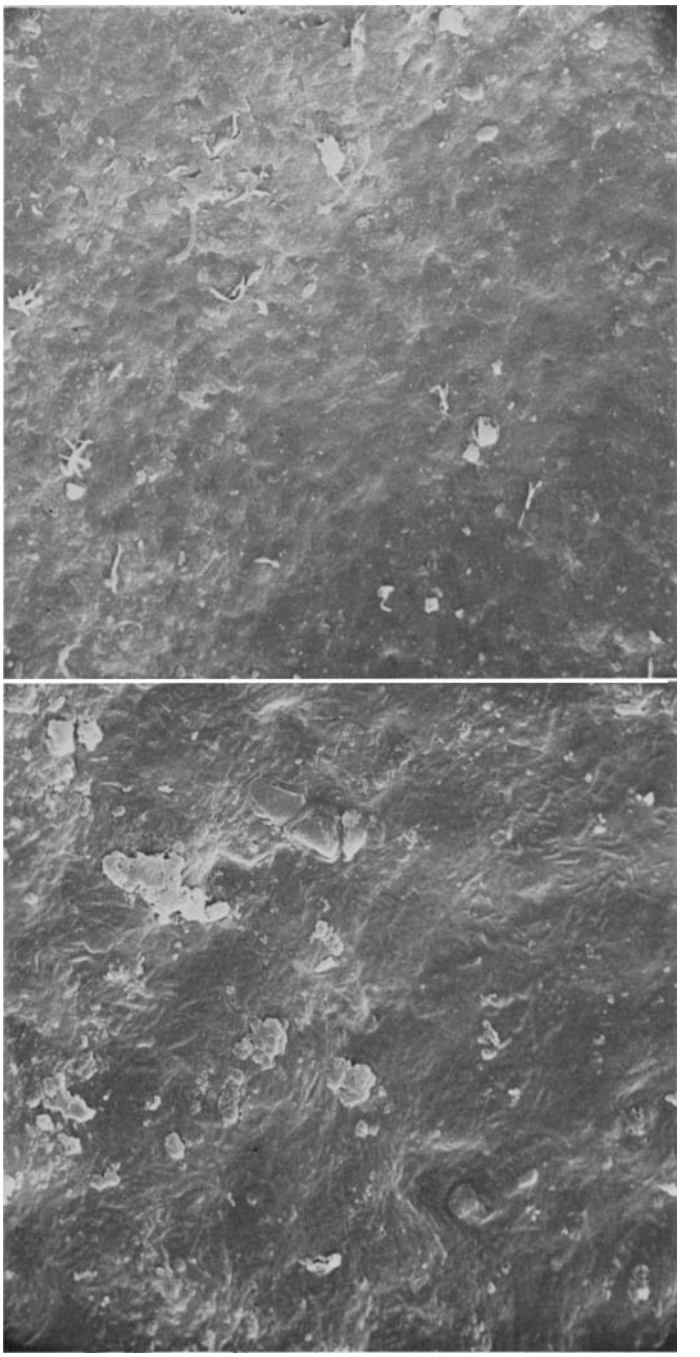

FIGURE 33.—*Cetraria pinastri* (Scopali) S. F. Gray (*Baumgartner* 874 in Kryptogamae Vindobonensis, Austria).

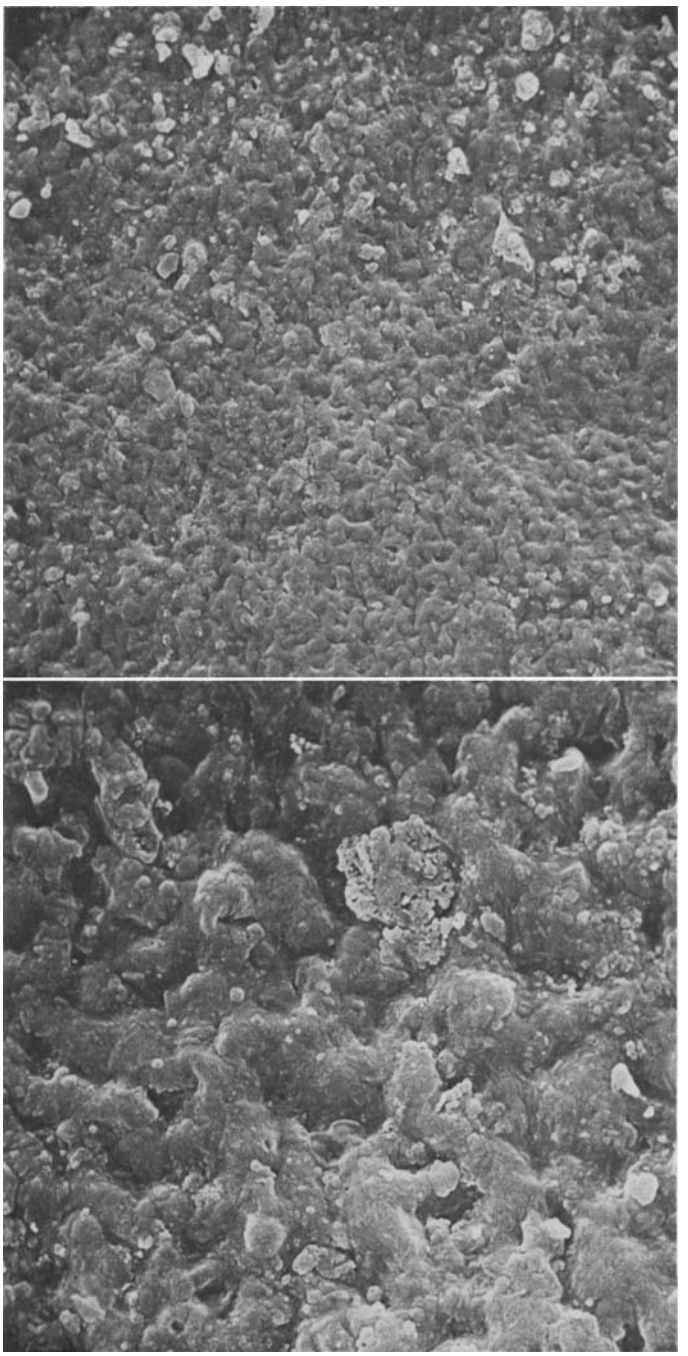

FIGURE 34.—*Cetrelia chicitae* (Culberson) Culberson and Culberson (*Hale* 19212, Virginia).

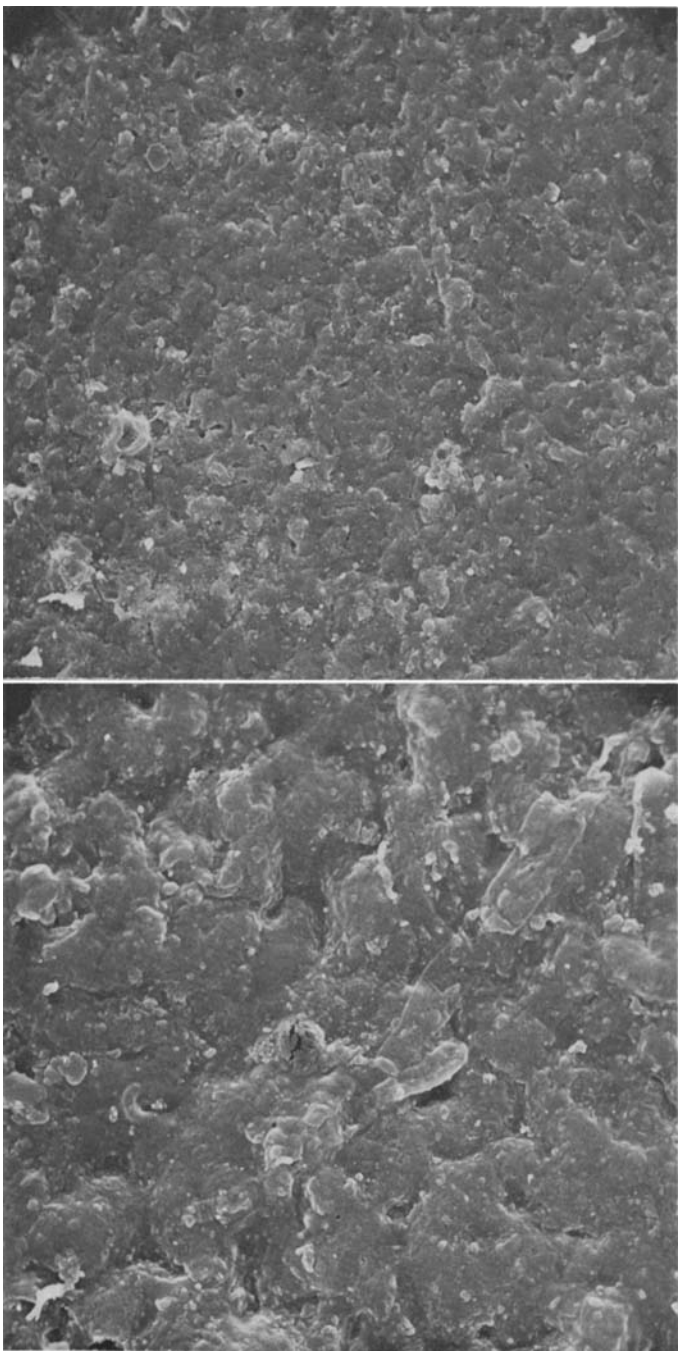

FIGURE 35.—*Cetrelia olivetorum* (Nylander) Culberson and Culberson (*Hale* 33411, Virginia).

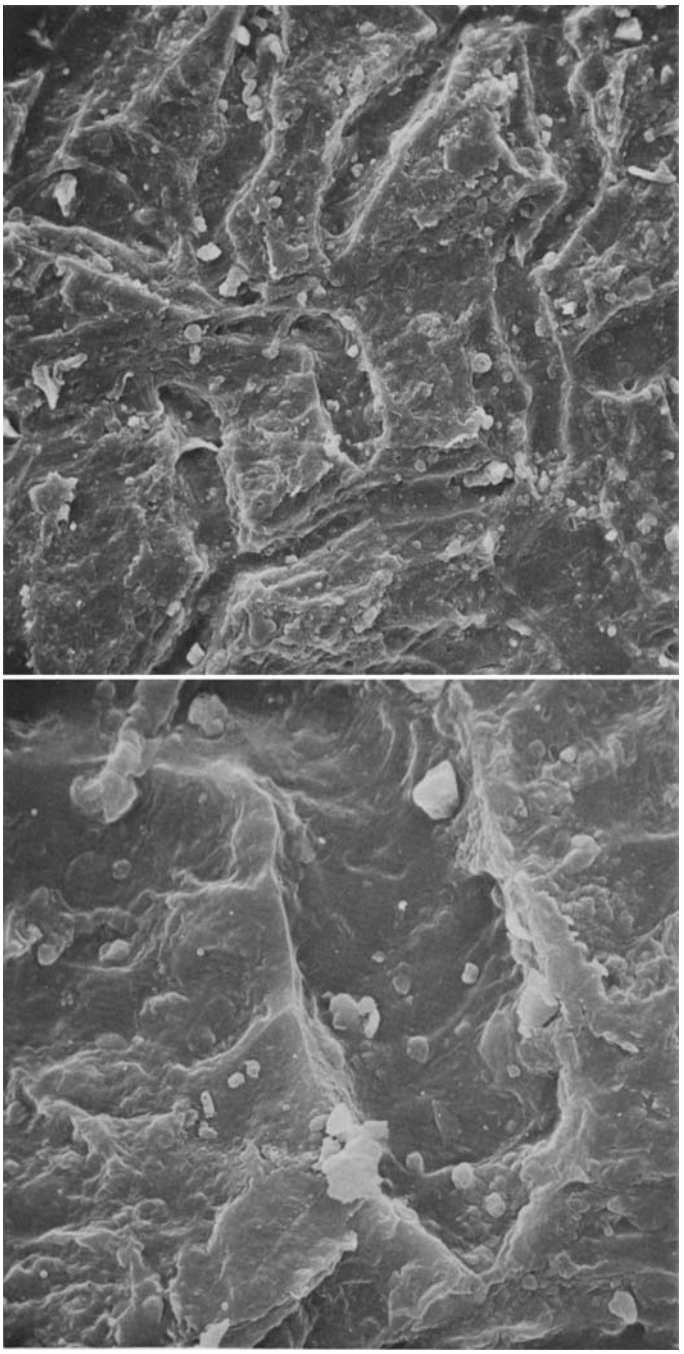

FIGURE 36.—*Heterodea muelleri* (Hampe) Nylander (*James* 2106a, Australia).

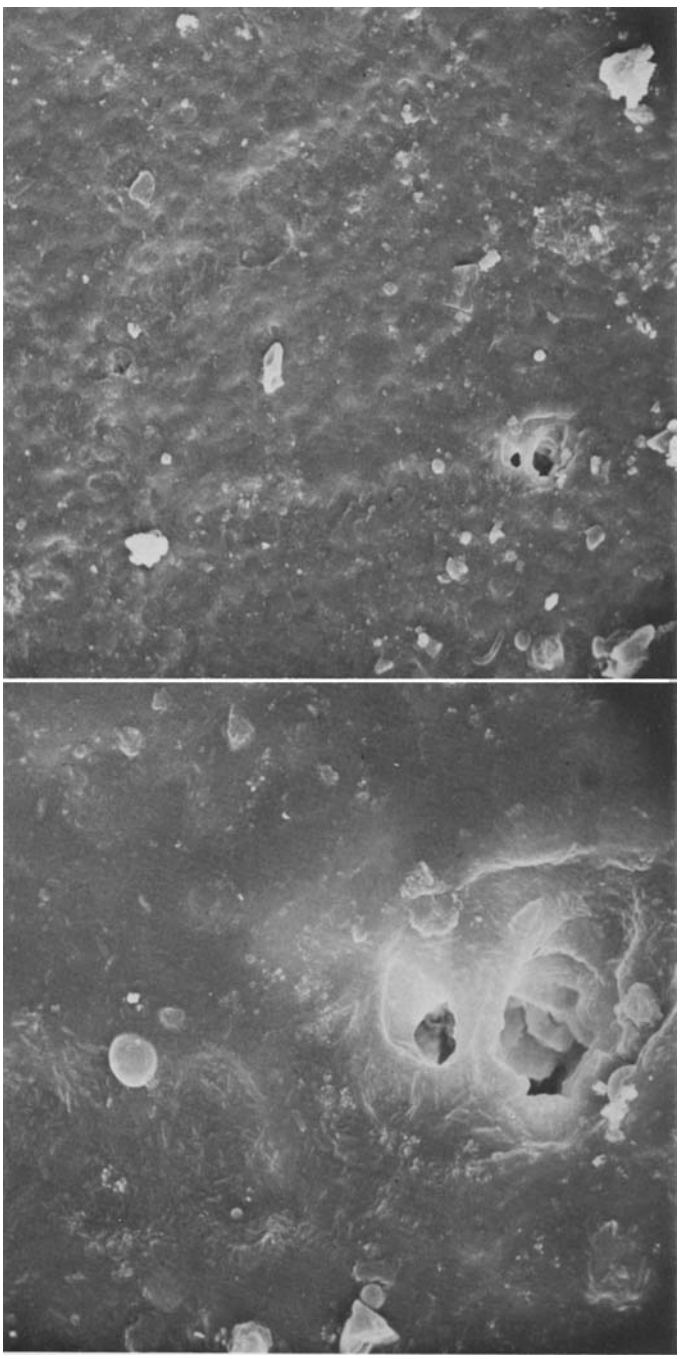

FIGURE 37.—*Hypogymnia bitteriana* (Zahlbruckner) Krog (*Kjellmert* s.n., Sweden).

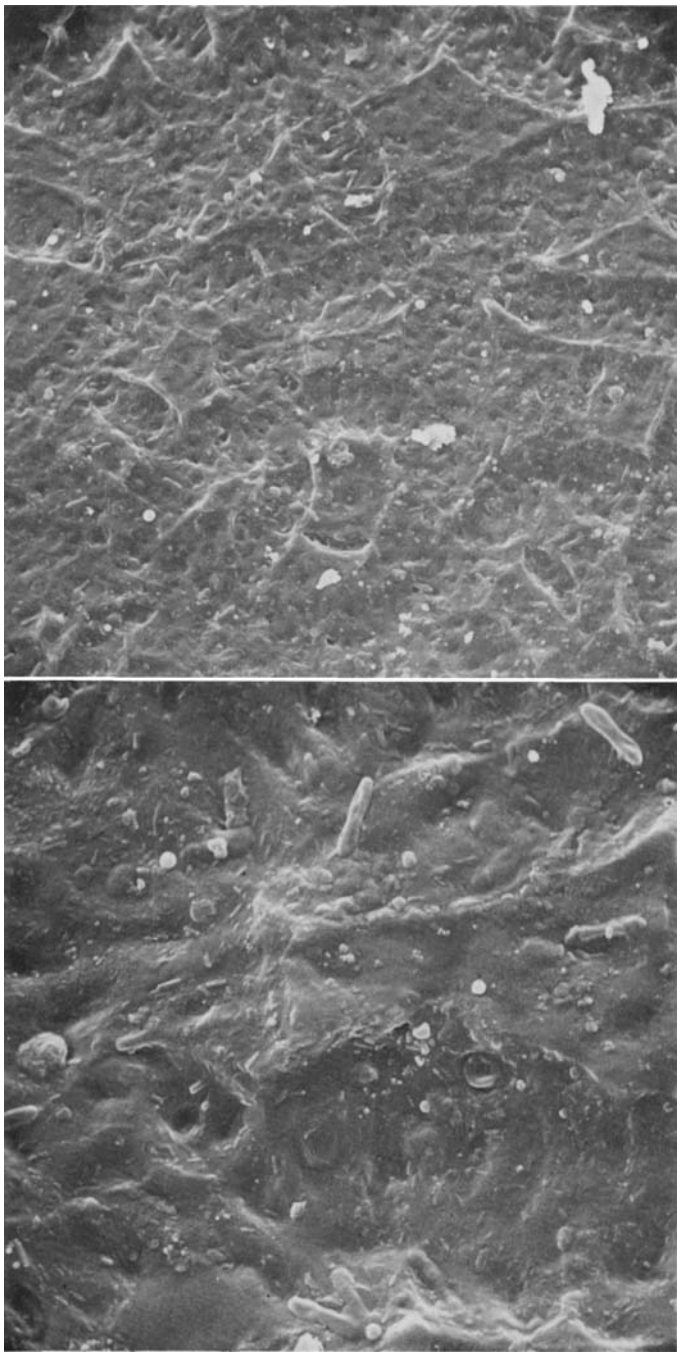

FIGURE 38.—*Hypogymnia enteromorpha* (Acharius) Nylander (*Hale* 10972, West Virginia).

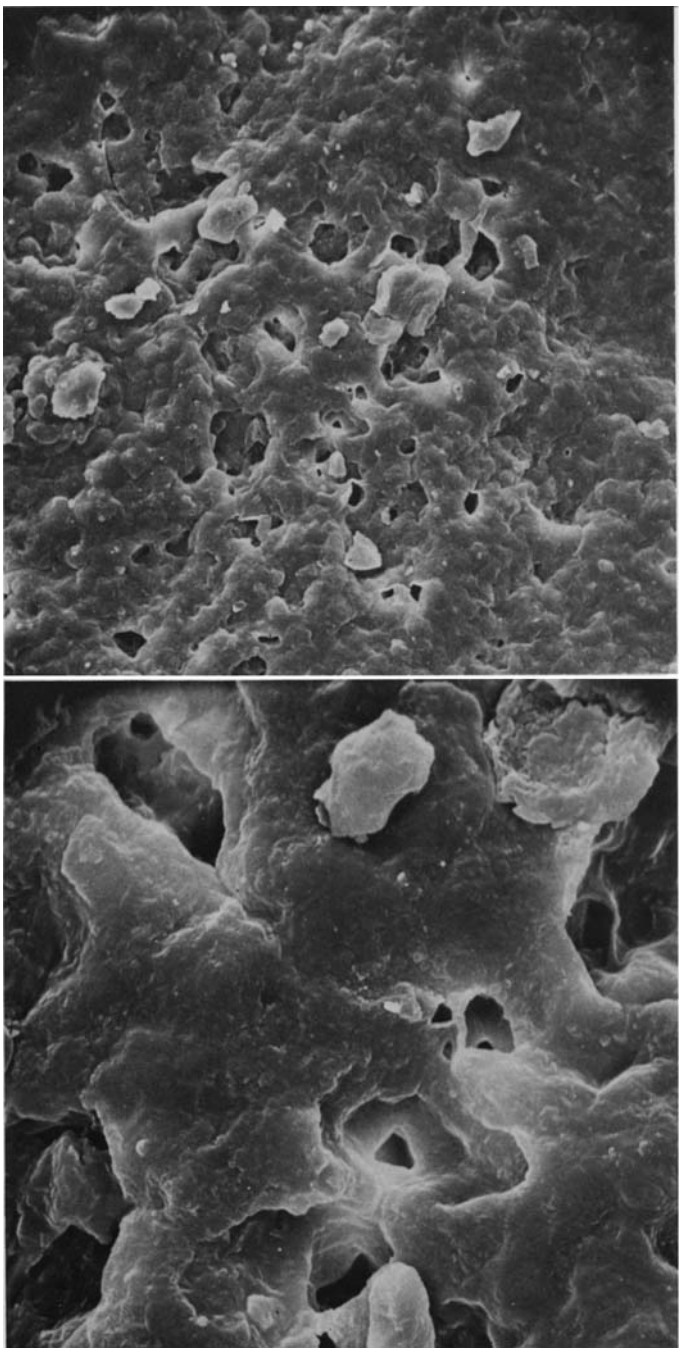

FIGURE 39.—*Hypogymnia enteromorpha* (Acharius) Nylander (*Hale* 33698, California).

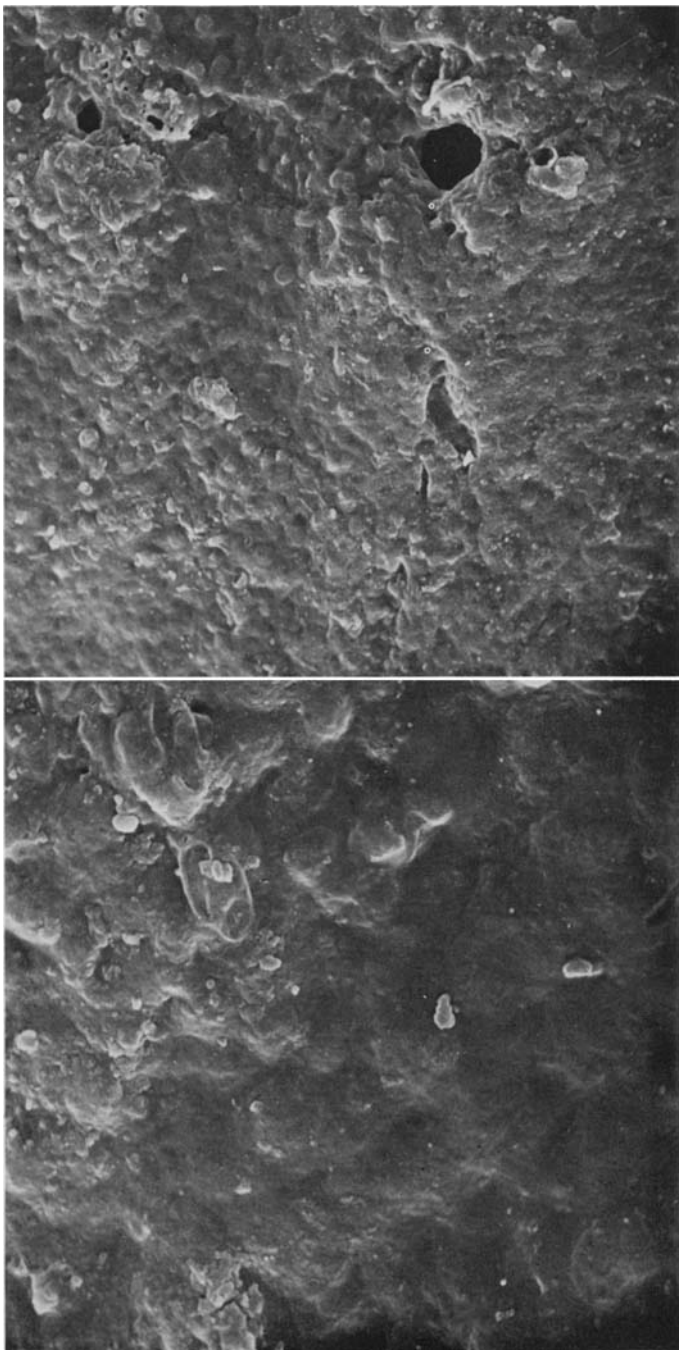

FIGURE 40.—*Hypogymnia enteromorpha* (Acharius) Nylander (*Hale* 21520, Oregon).

FIGURE 41.—*Hypogymnia metaphysodes* Asahina (*Fujikawa* s.n., Japan, isotype specimen).

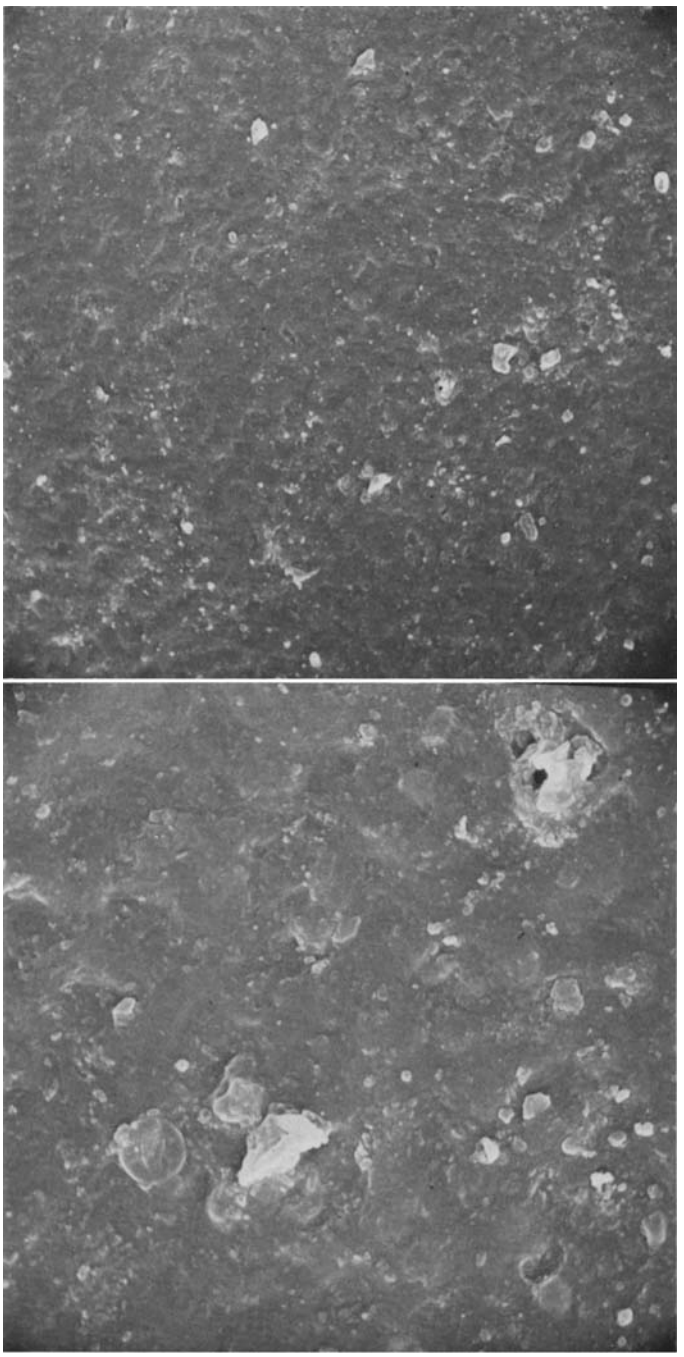

FIGURE 42.—*Hypogymnia physodes* (L.) Nylander (*Culberson* 11994, France).

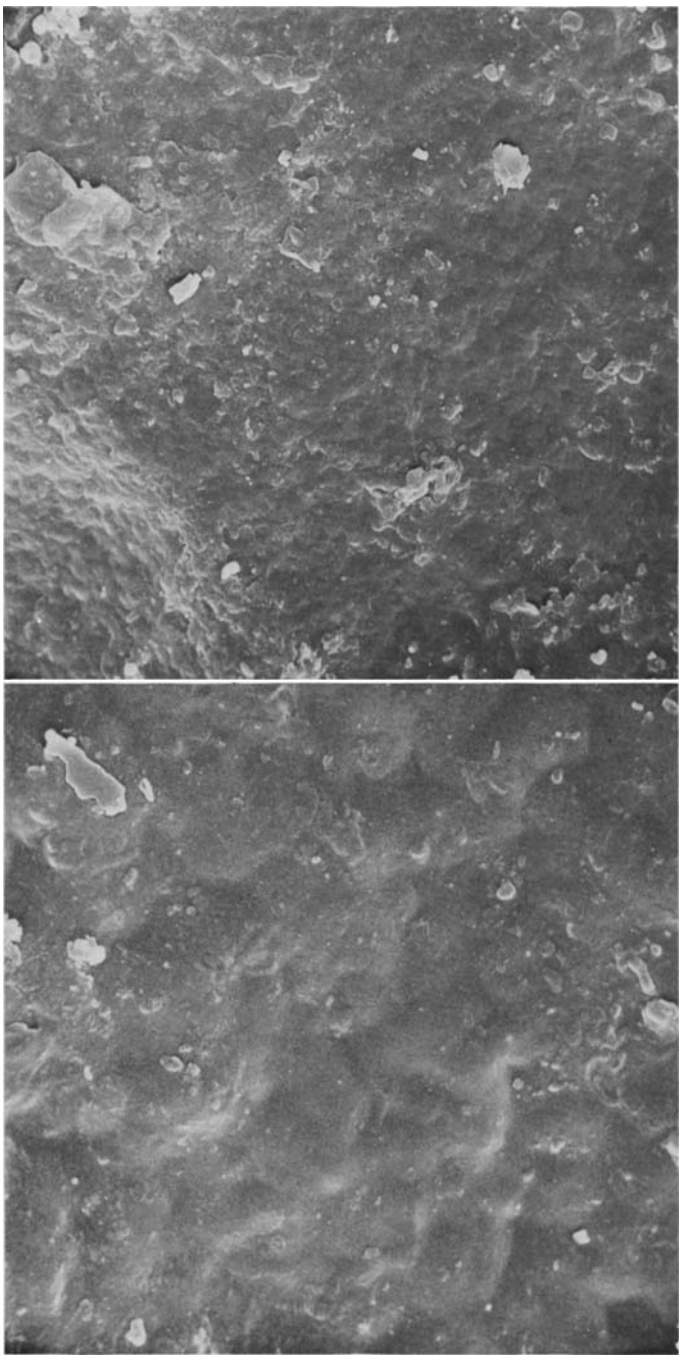

FIGURE 43.—*Menegazzia cincinnata* (Acharius) Bitter (*Mahu* 1642, Chile).

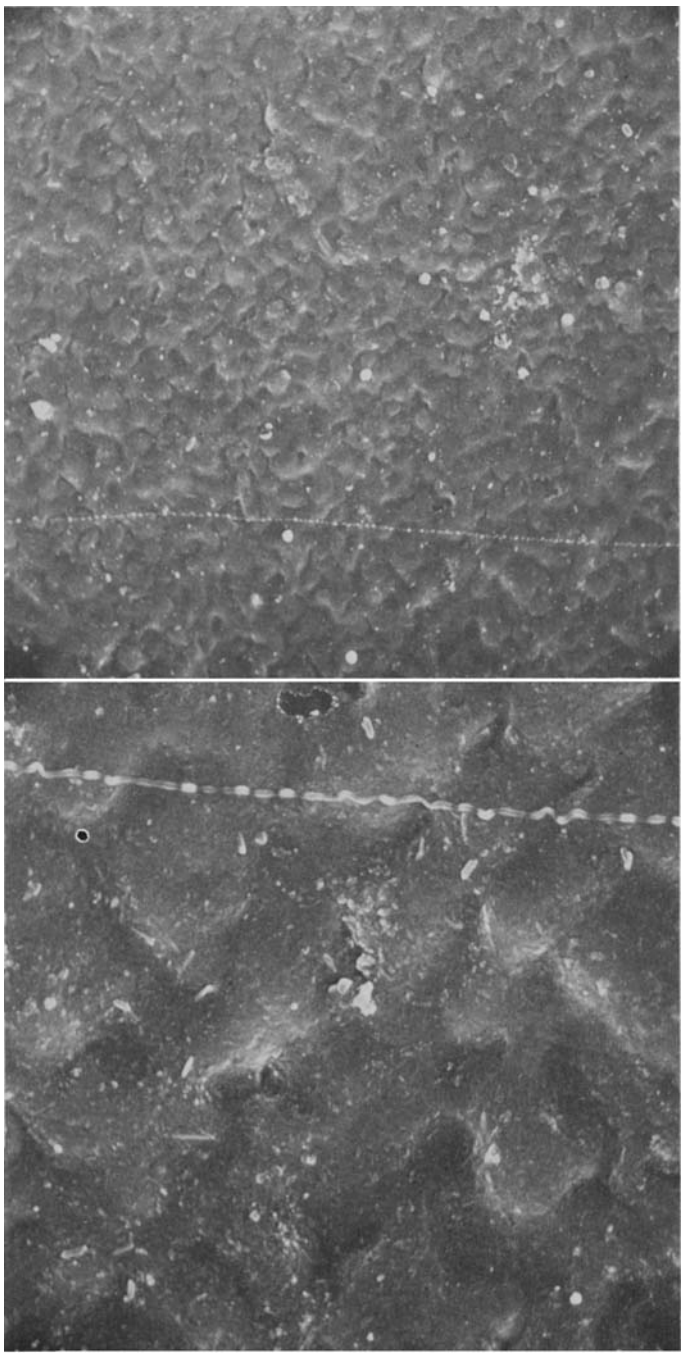

FIGURE 44.—*Menegazzia terebrata* (Hoffmann) Massalongo (*Denison* 836, Canada).

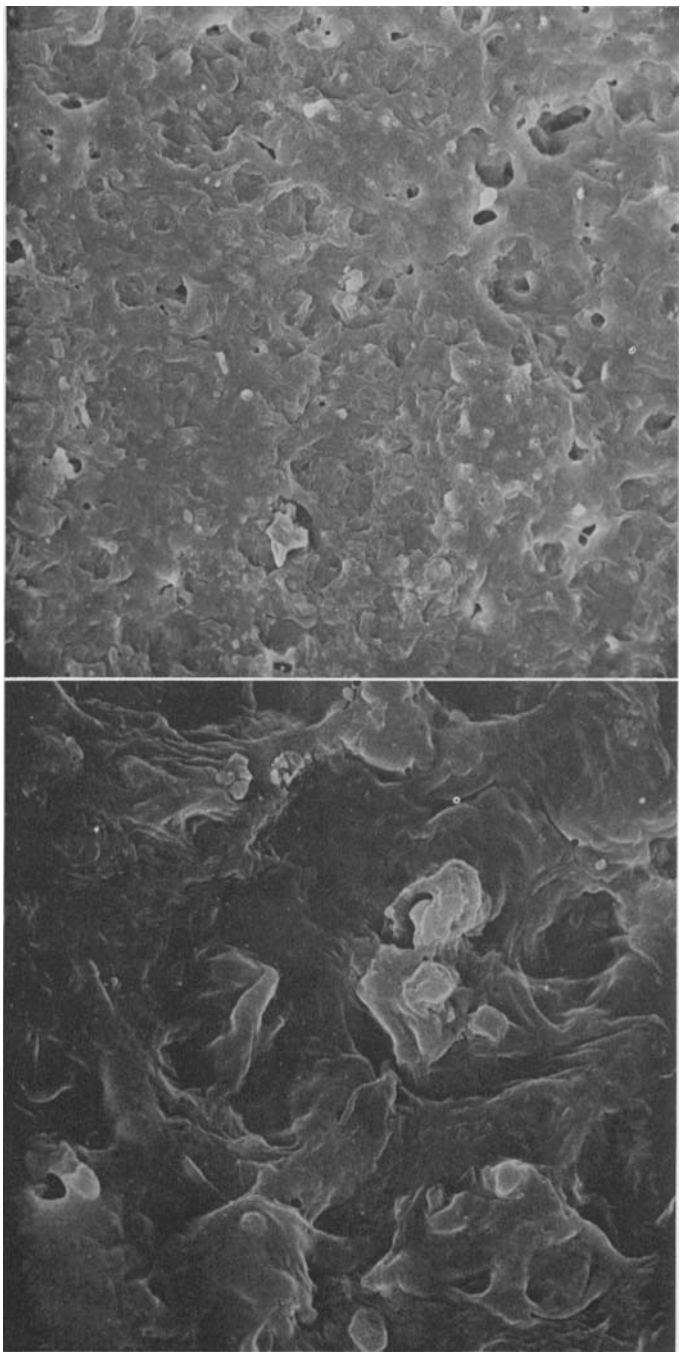

FIGURE 45.—*Pannoparmelia angustata* (Persoon) Zahlbruckner (*Imshaug* 47661, New Zealand).

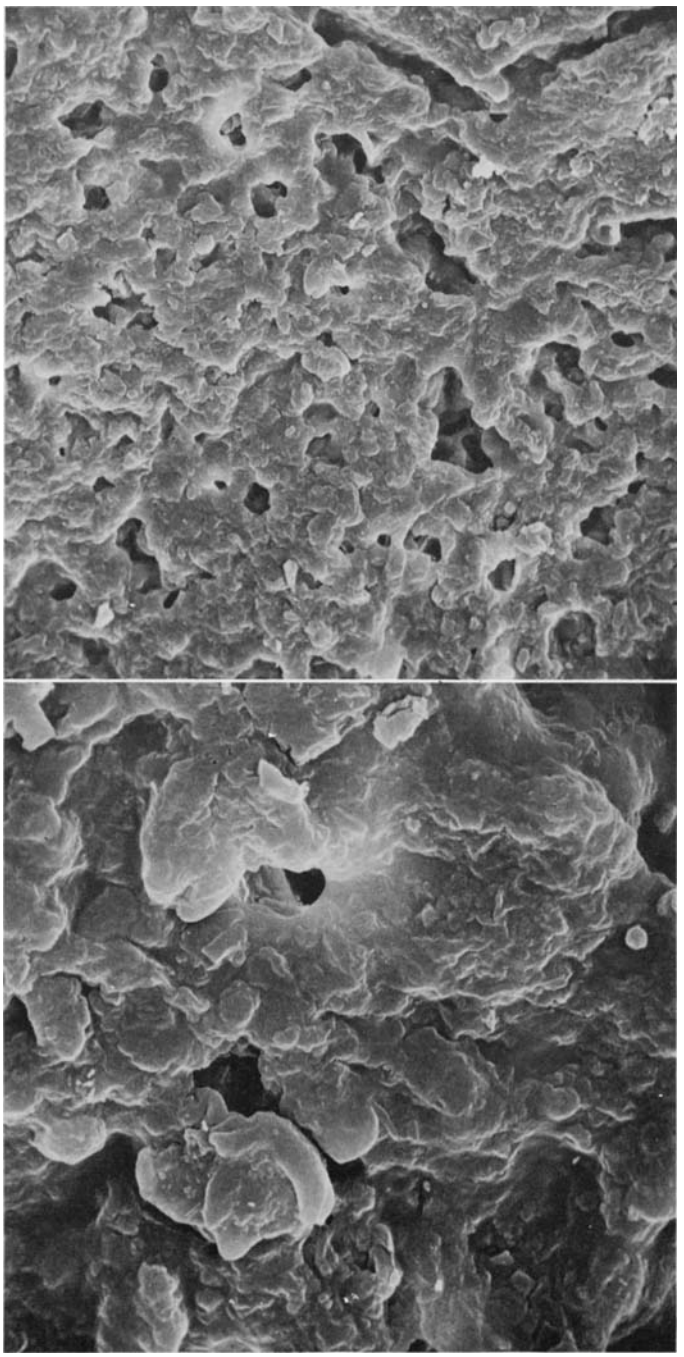

FIGURE 46.—*Pannoparmelia anzioides* Darbishire (*Imshaug* 45476, Chile).

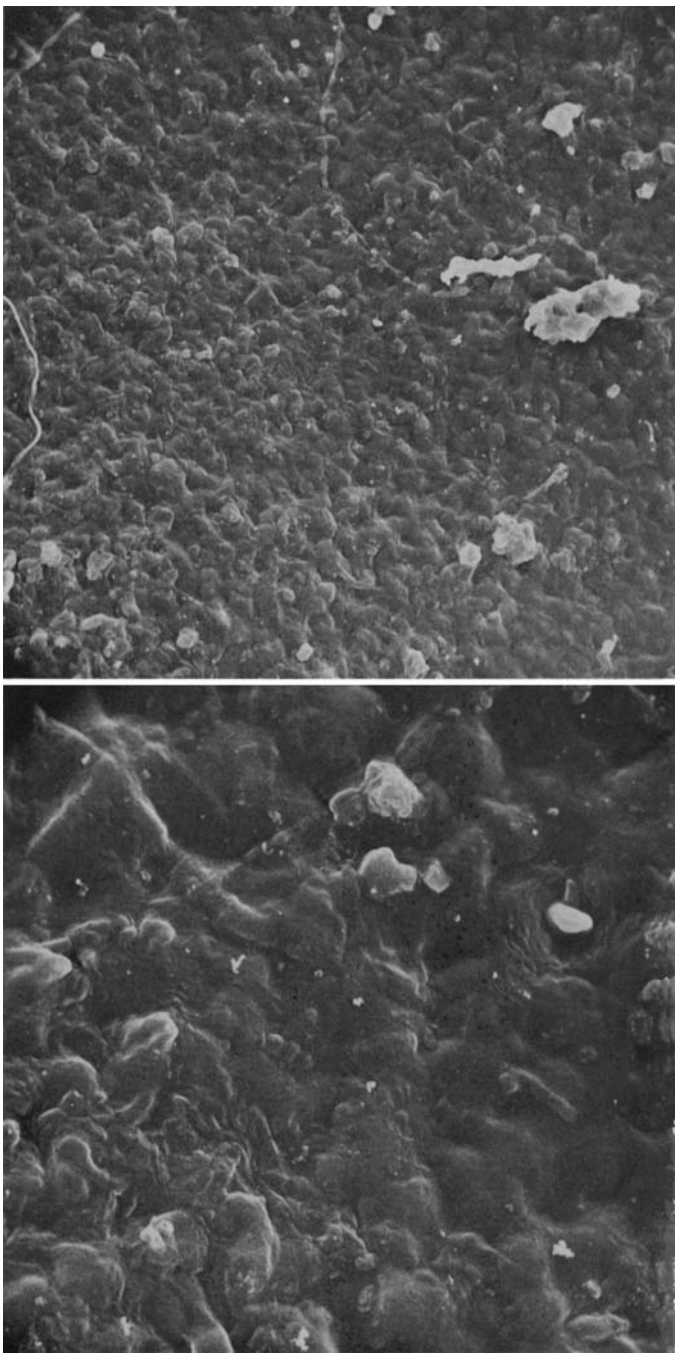

FIGURE 47.—*Parmelia acetabulum* Acharius (*Tomin* s.n., Russia).

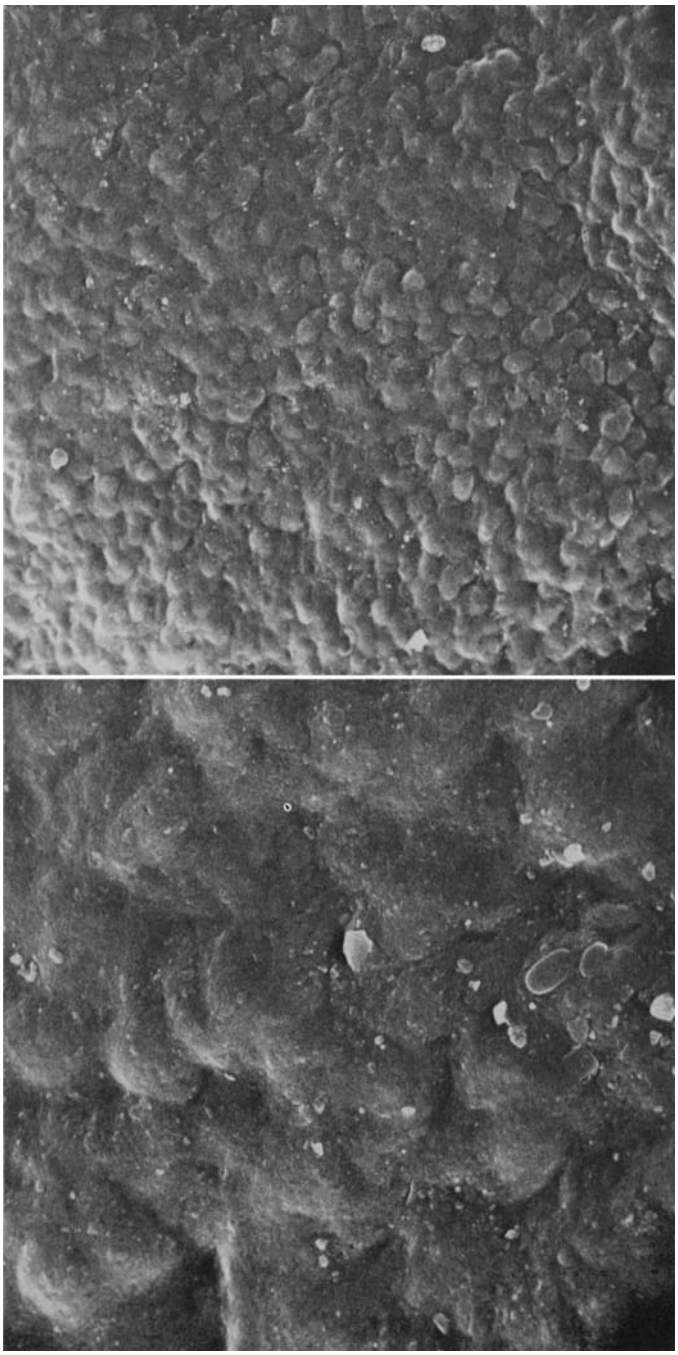

FIGURE 48.—*Parmelia disjuncta* Erichsen (*Thomson* 12466, Canada).

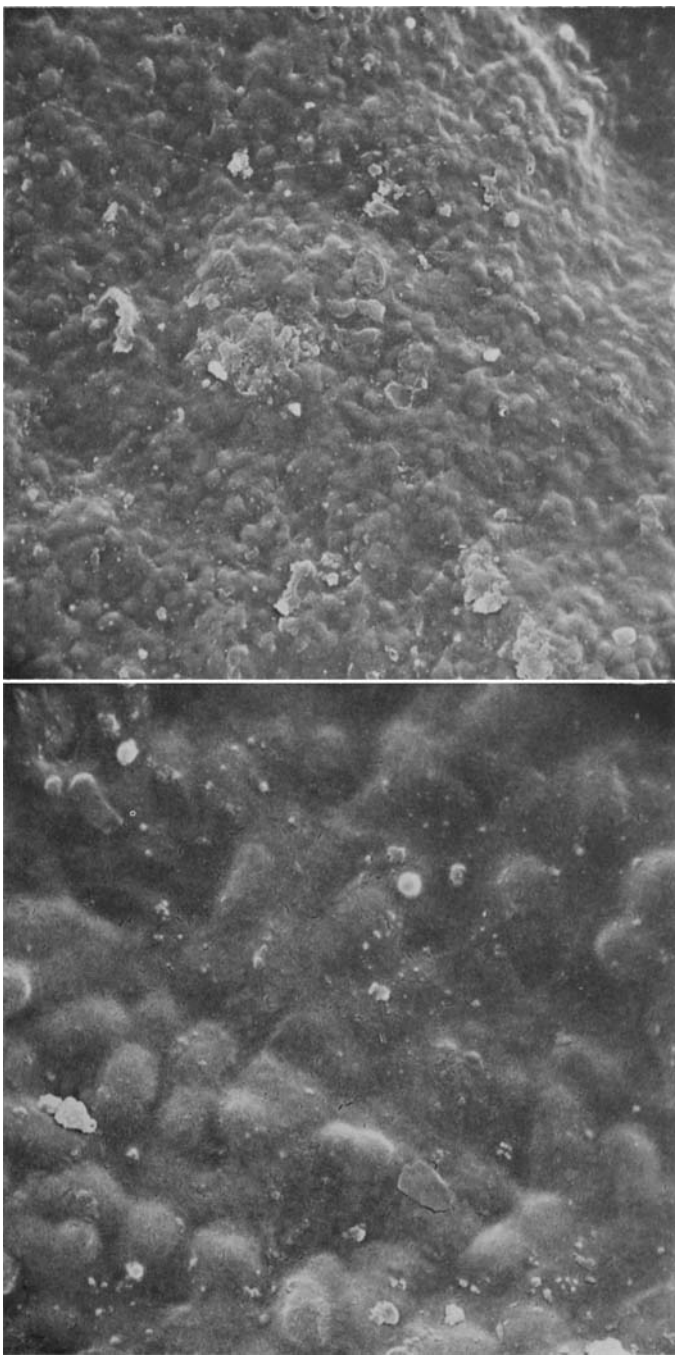

FIGURE 49.—*Parmelia olivacea* (L.) Acharius (*Hale* s.n., Canada).

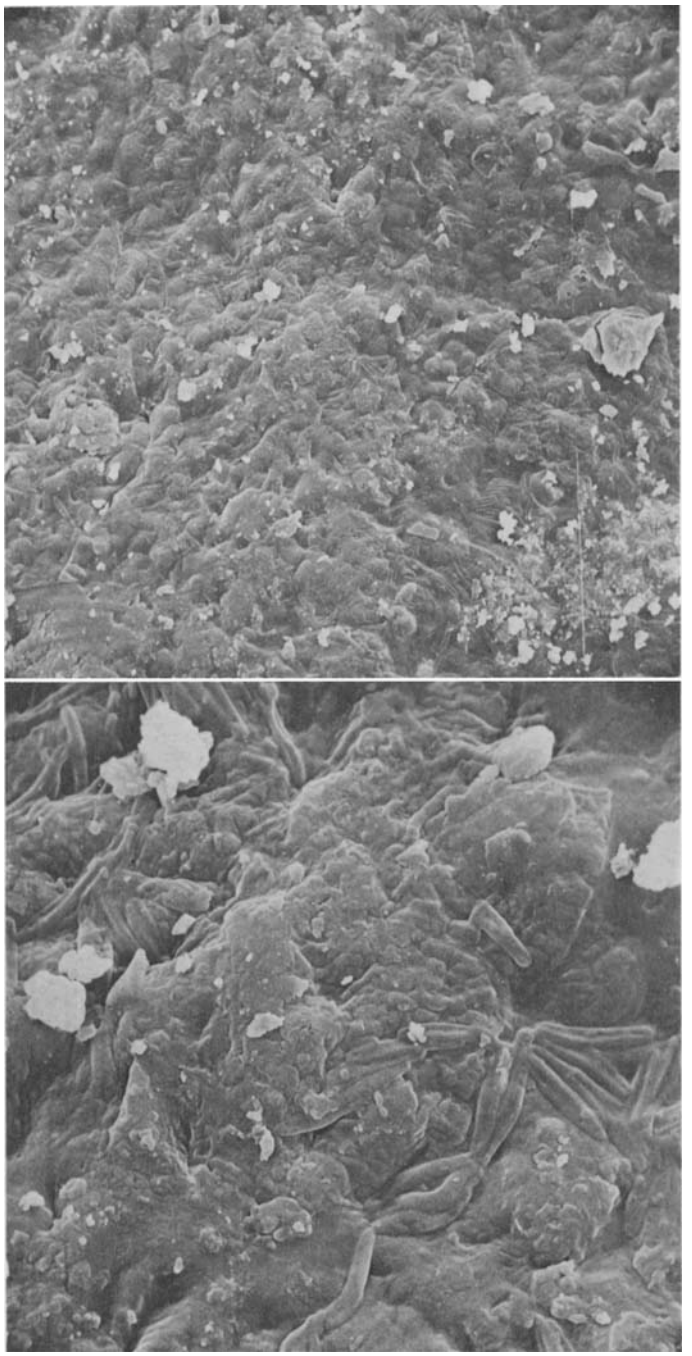

FIGURE 50.—*Parmelia ryssolea* Acharius (*Kraschennikov* s.n., Russia).

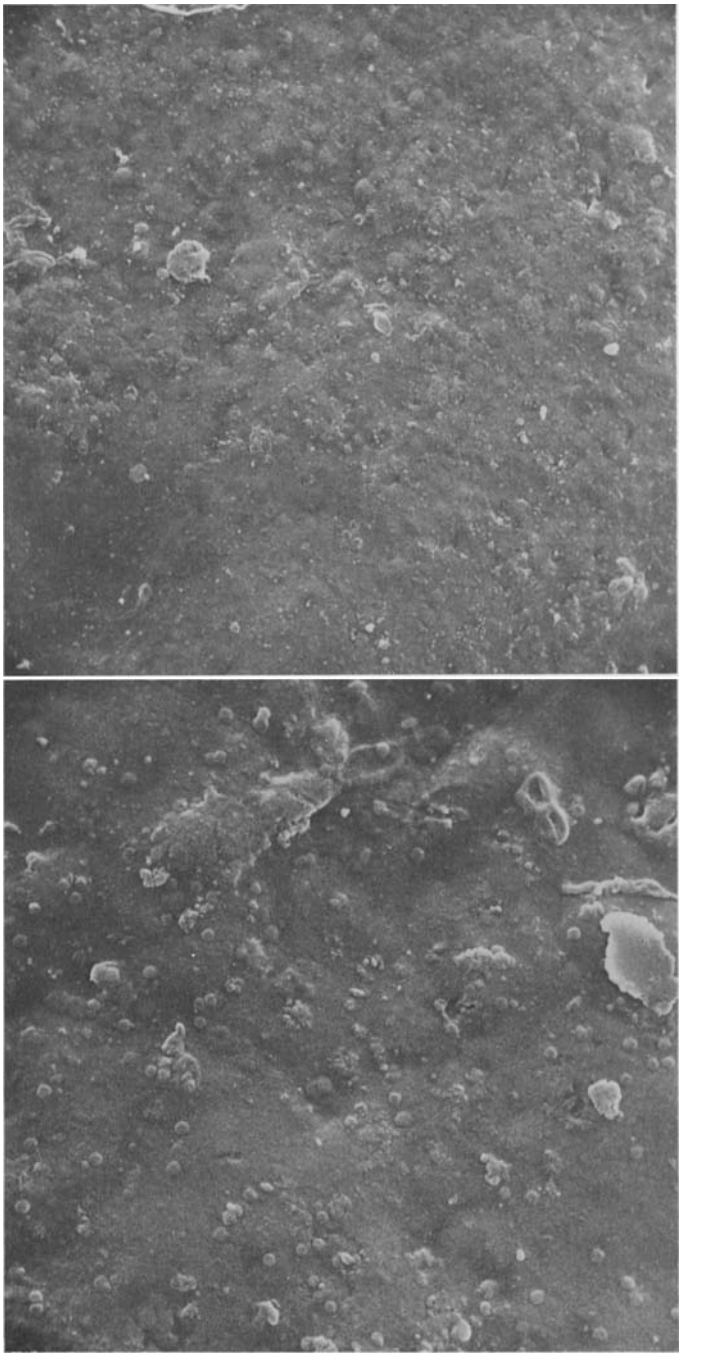

FIGURE 51.—*Parmelia septentrionalis* (Lynge) Ahti (*Hale* 33909, Canada).

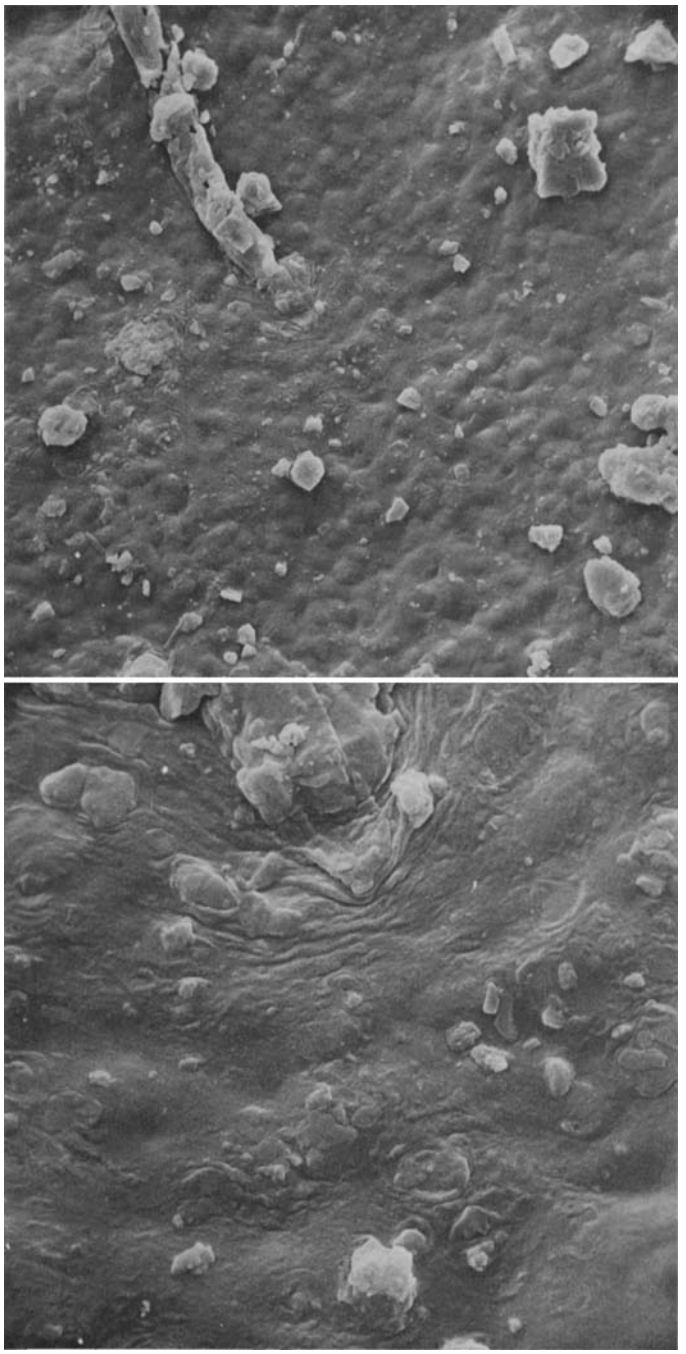

FIGURE 52.—*Parmelia subolivacea* Nylander (*Shushan* 15202, California).

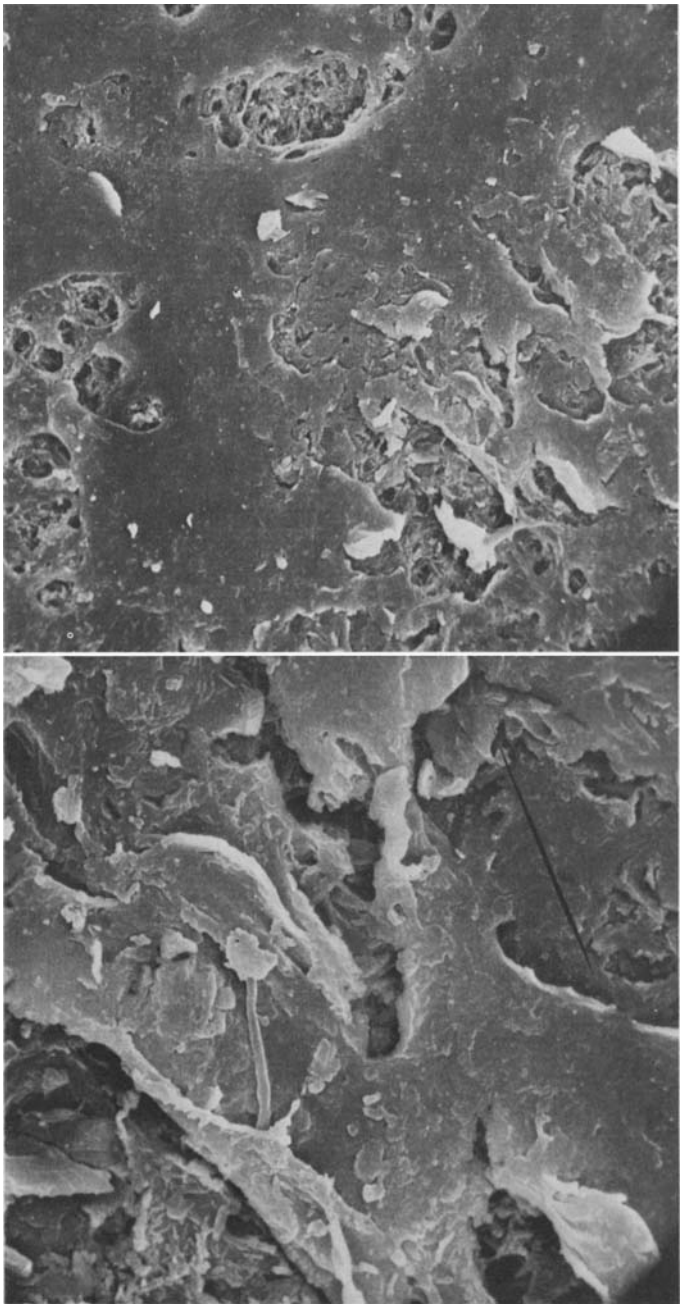

FIGURE 53.—***Parmelia conspersa*** (Acharius) Acharius (***Hale*** 34653, Canada).

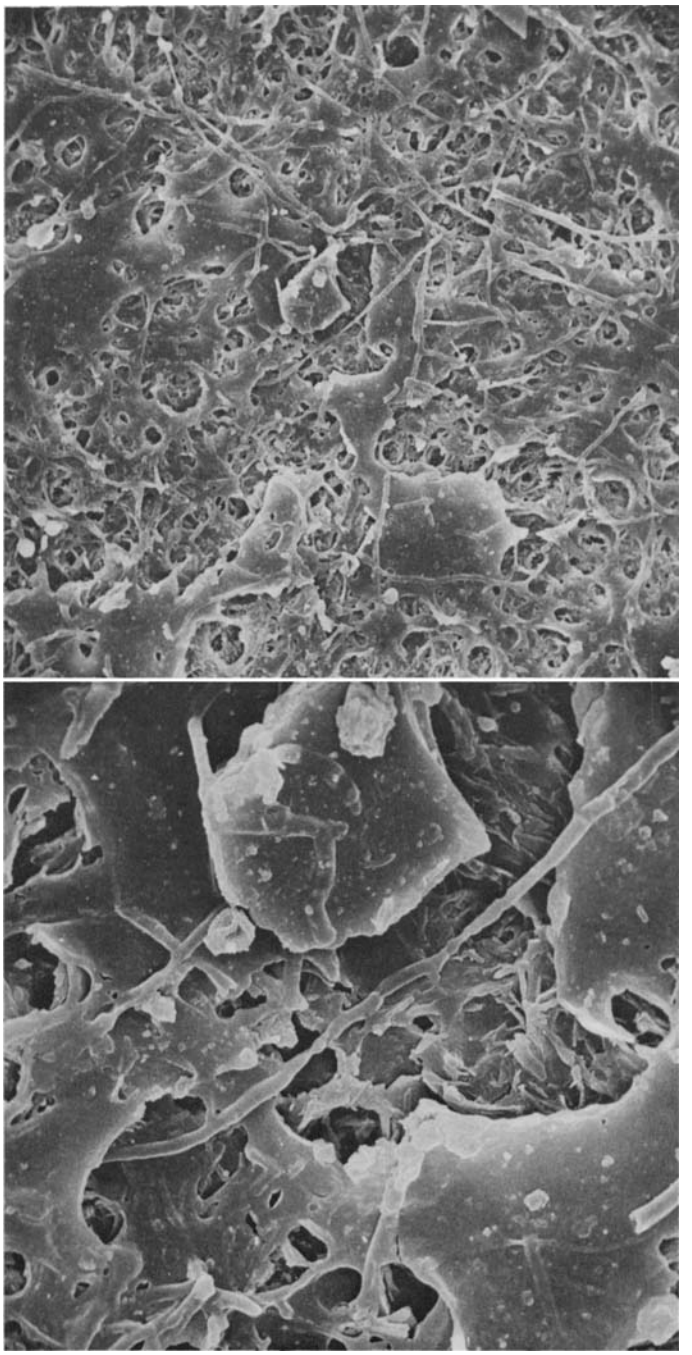

FIGURE 54.—*Parmelia conspersa* (Acharius) Acharius (*Sampaio* 246, Portugal).

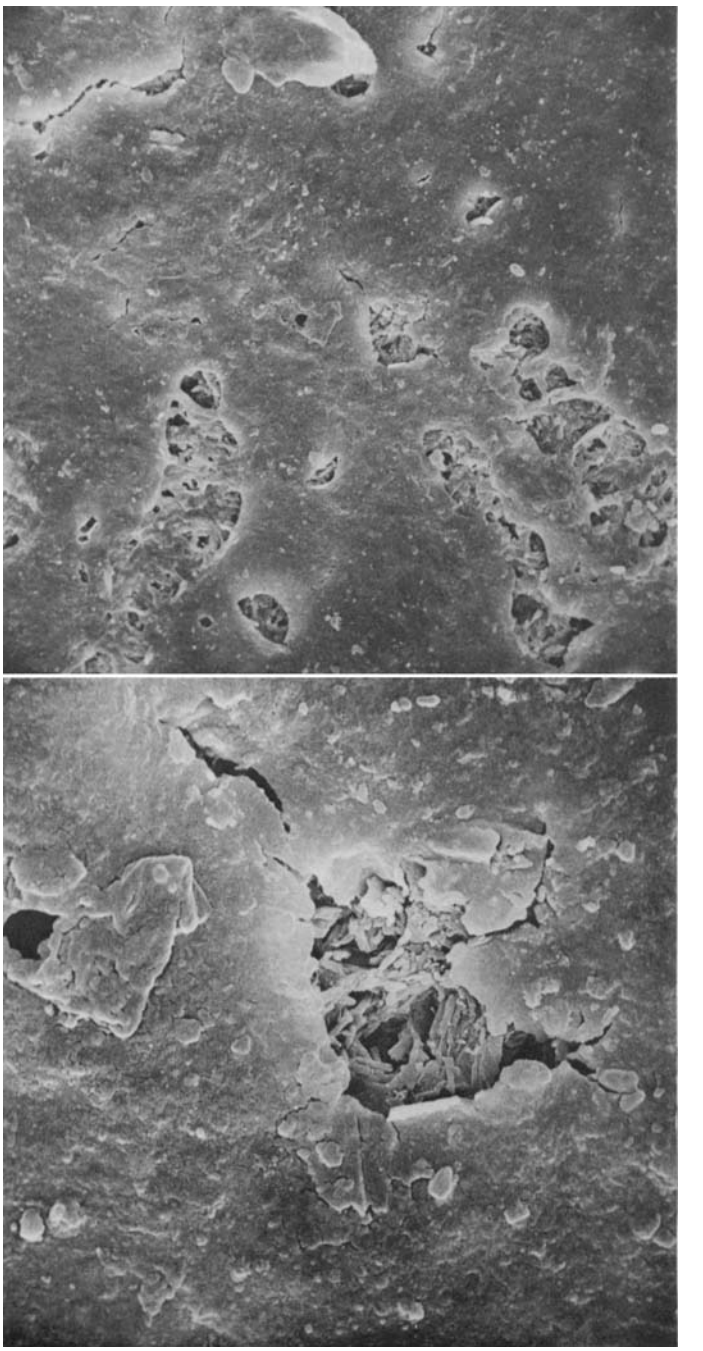

FIGURE 55.—*Parmelia cumberlandia* (Gyelnik) Hale (*Hale* 36560, Canada).

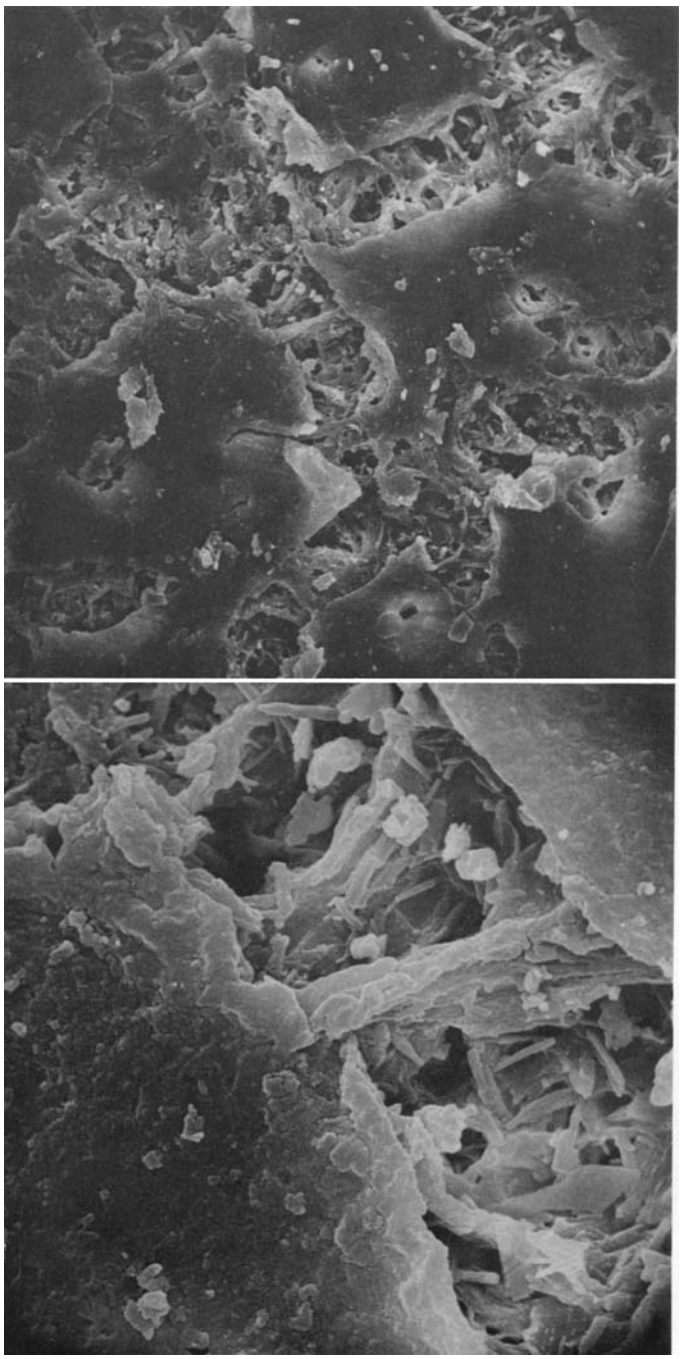

FIGURE 56.—*Parmelia hyporhytida* Hale (*Kofler* s.n., Basutoland, holotype in LD).

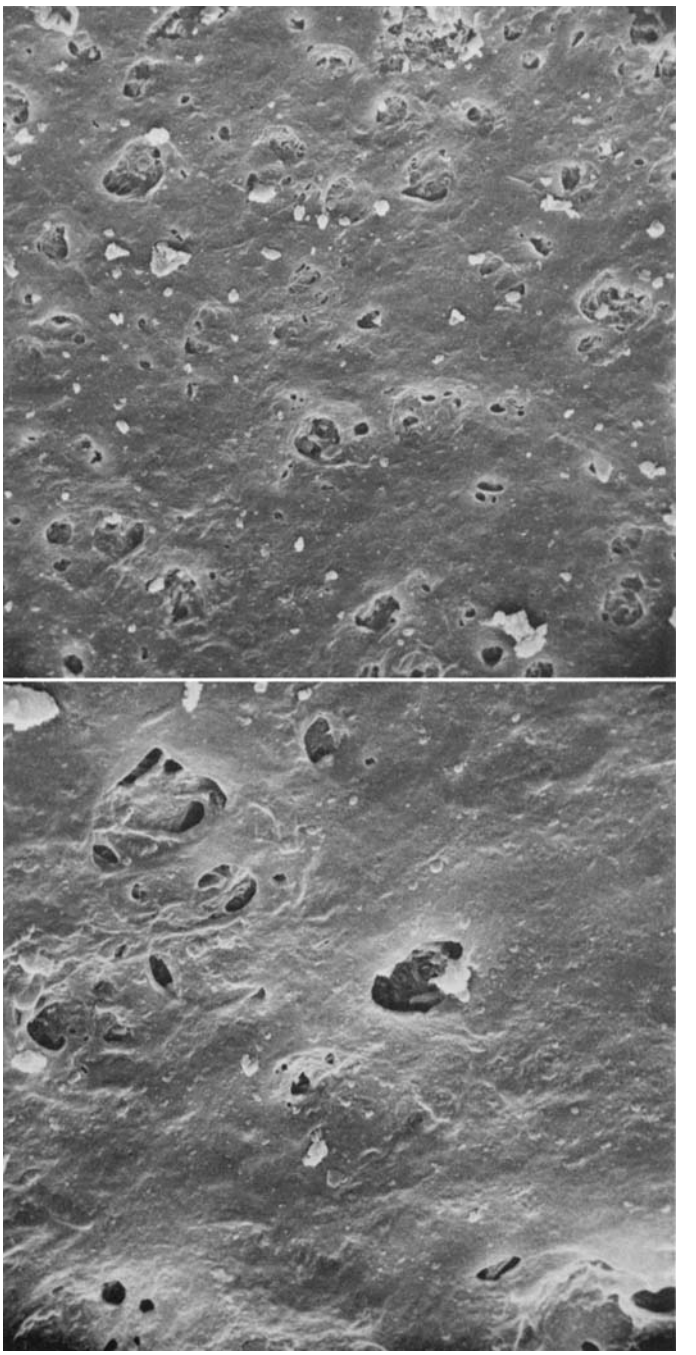

FIGURE 57.—*Parmelia ioanis-simae* Gyelnik (*Nicholas* 5982, Mexico, isotype specimen).

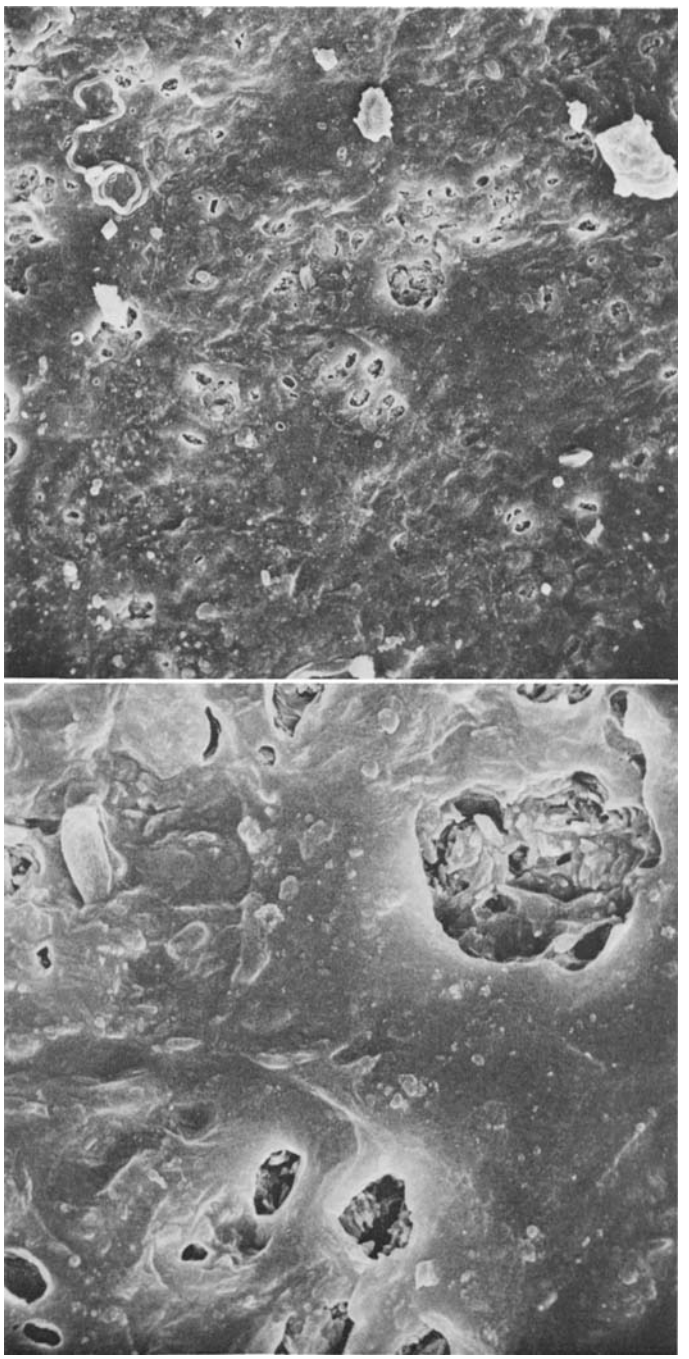

FIGURE 58.—*Parmelia plittii* Gyelnik (*Denison* 683, Canada).

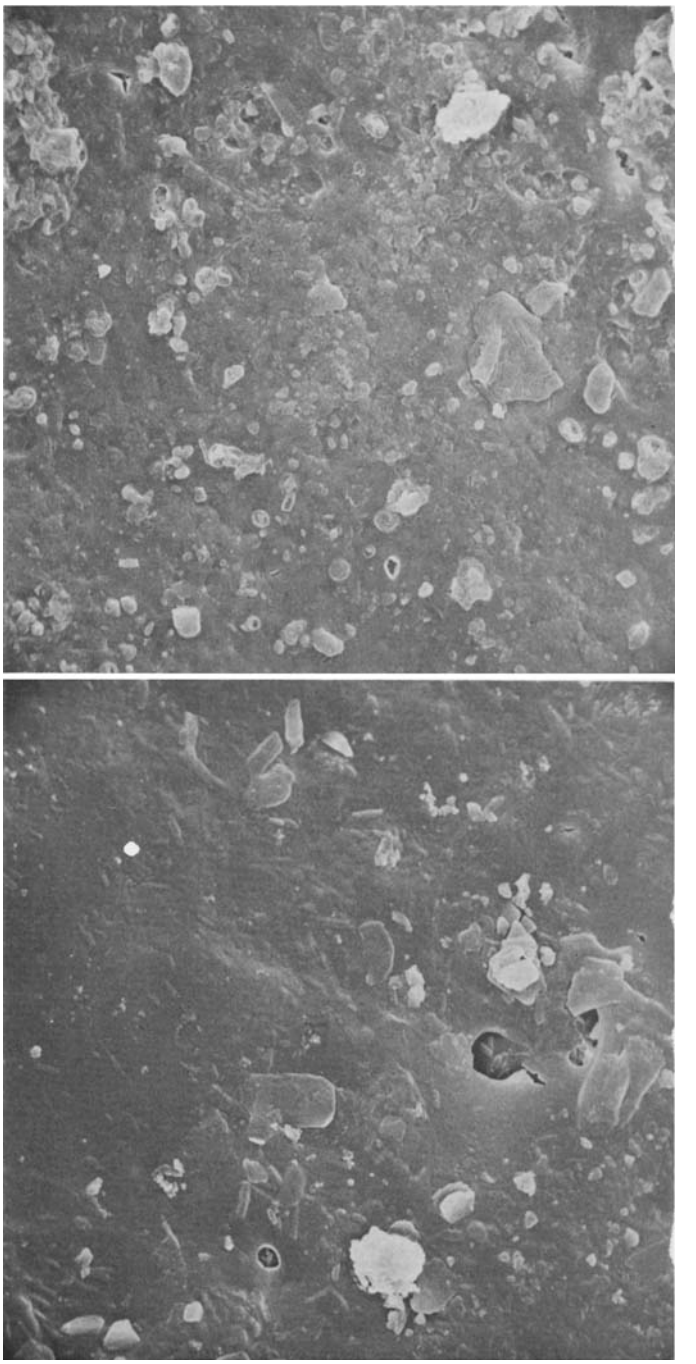

FIGURE 59.—*Parmelia taractica* Krempelhuber (*Hakulinen* s.n., Finland).

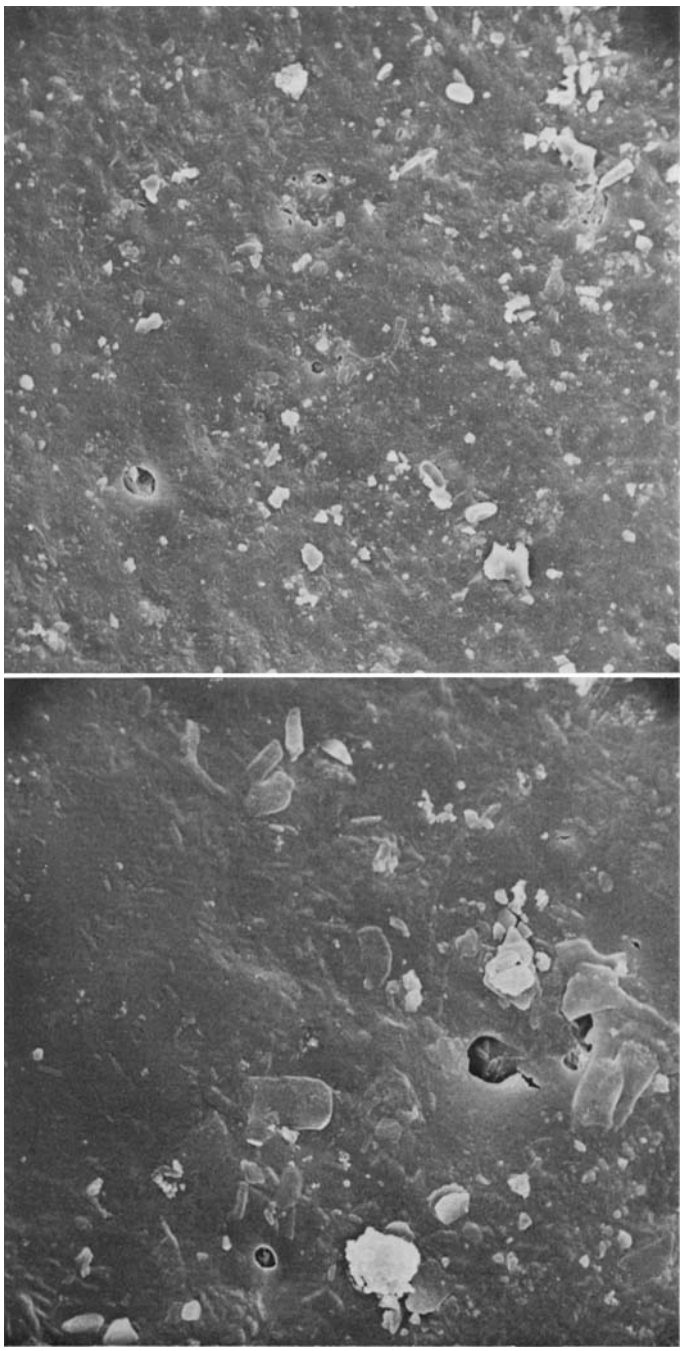

FIGURE 60.—*Parmelia tasmanica* Hooker and Taylor (*Hale* 23606, Minnesota).

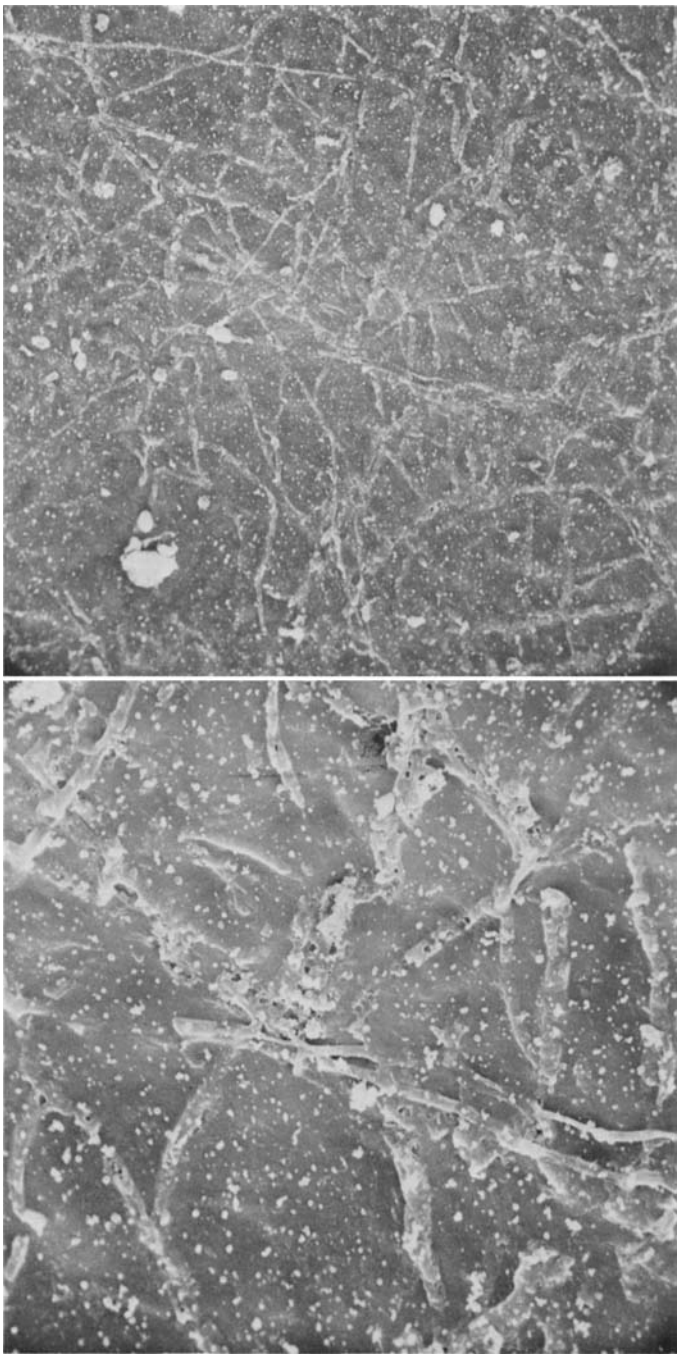

FIGURE 61.—*Parmelia cunninghamii* Crombie (*Cunningham* s.n., Falkland Islands, holotype in BM).

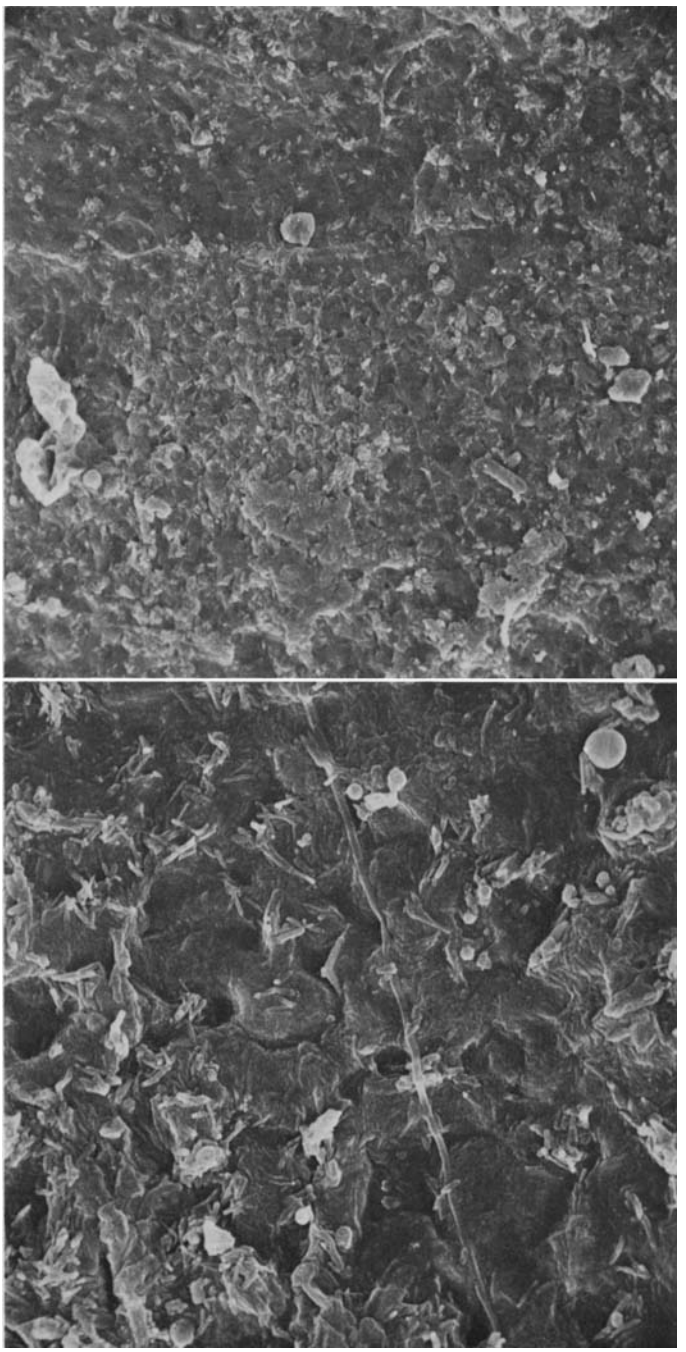

FIGURE 62.—*Parmelia fraudans* Nylander (*Hale* 36414, Canada).

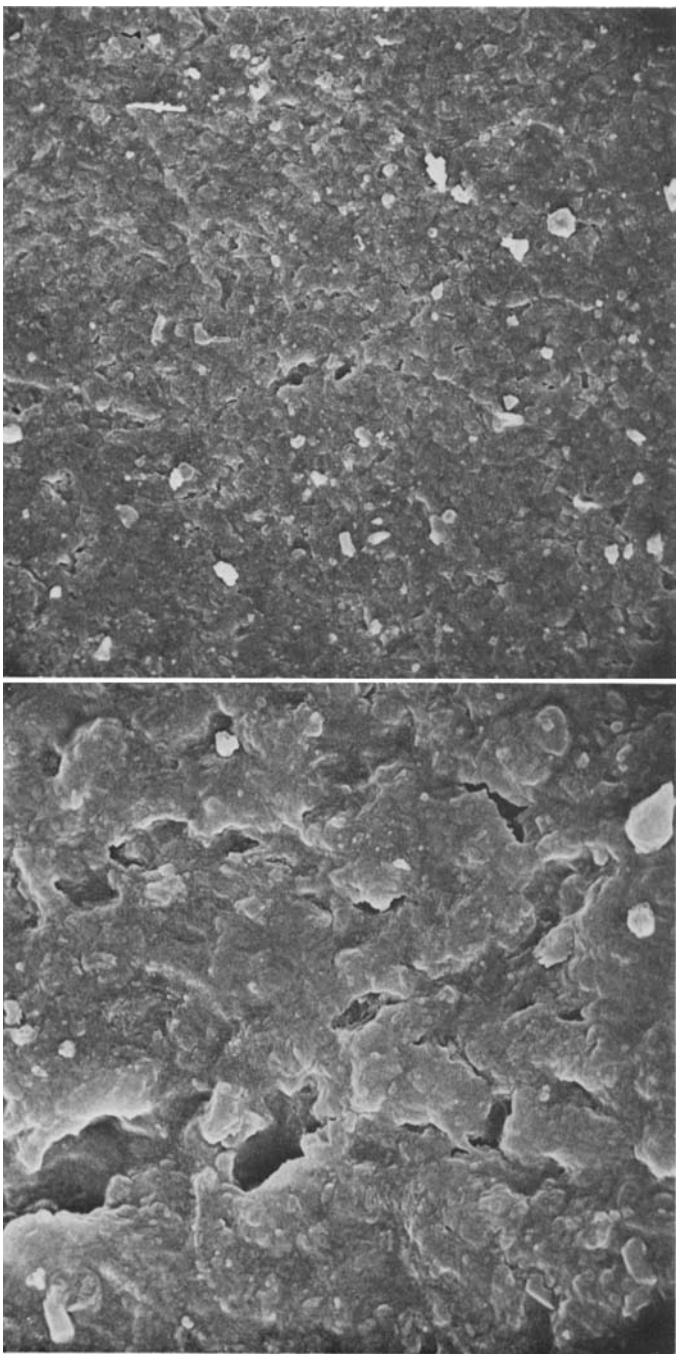

FIGURE 63.—*Parmelia omphalodes* (L.) Acharius (*Muller* 1355, Alaska).

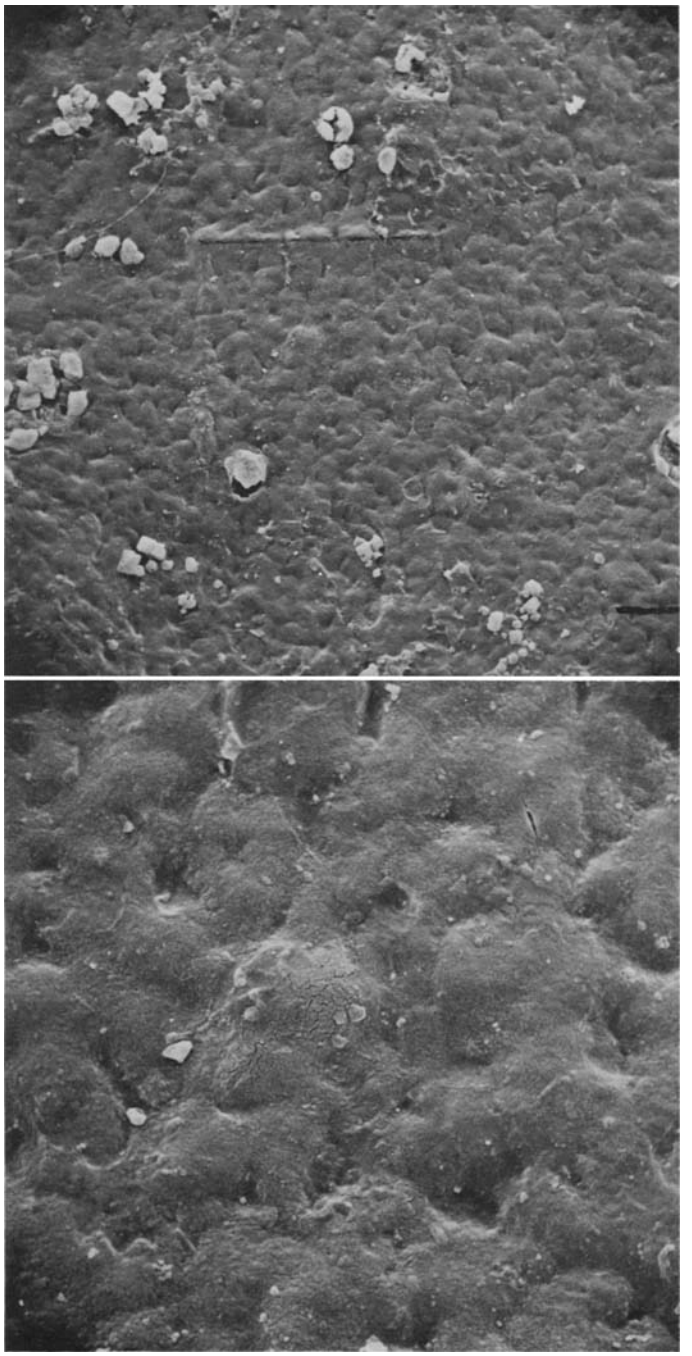

FIGURE 64.—*Parmelia saxatilis* (L.) Acharius (*Hale* s.n., Canada).

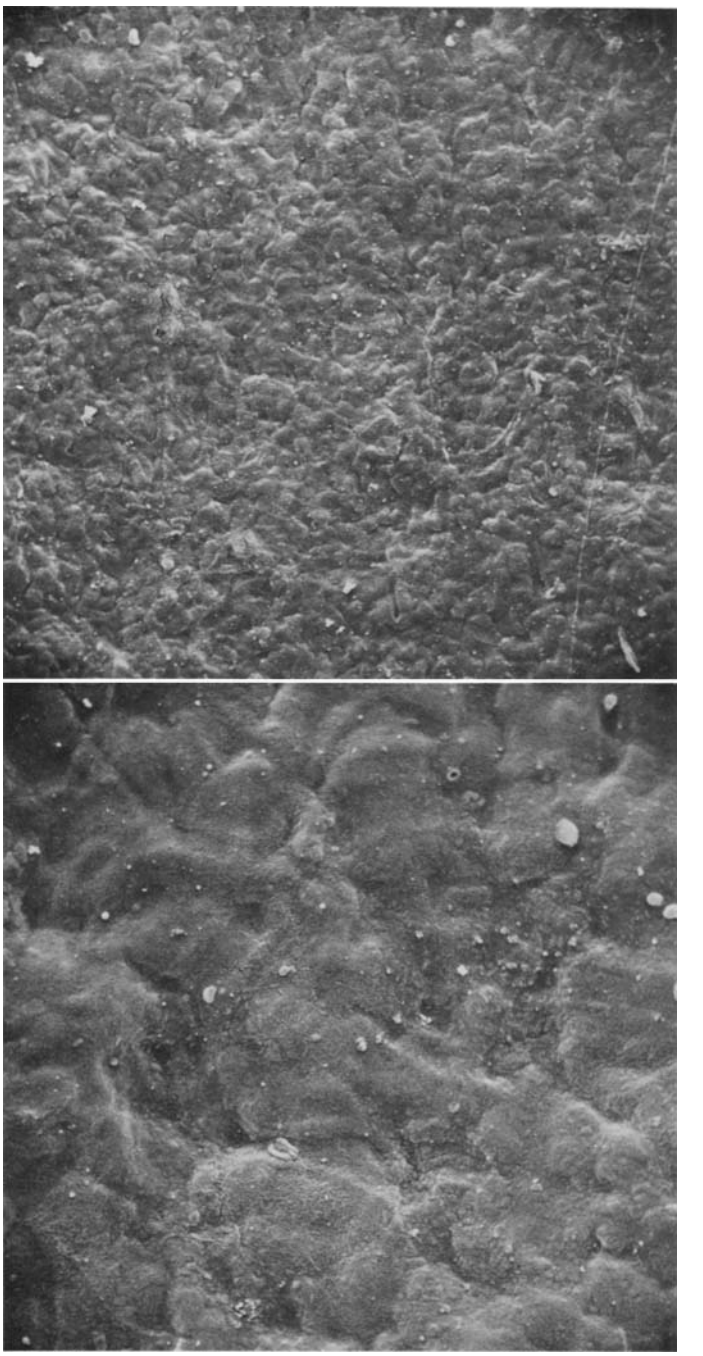

FIGURE 65.—*Parmelia squarrosa* Hale (*Hale* 18922, Virginia).

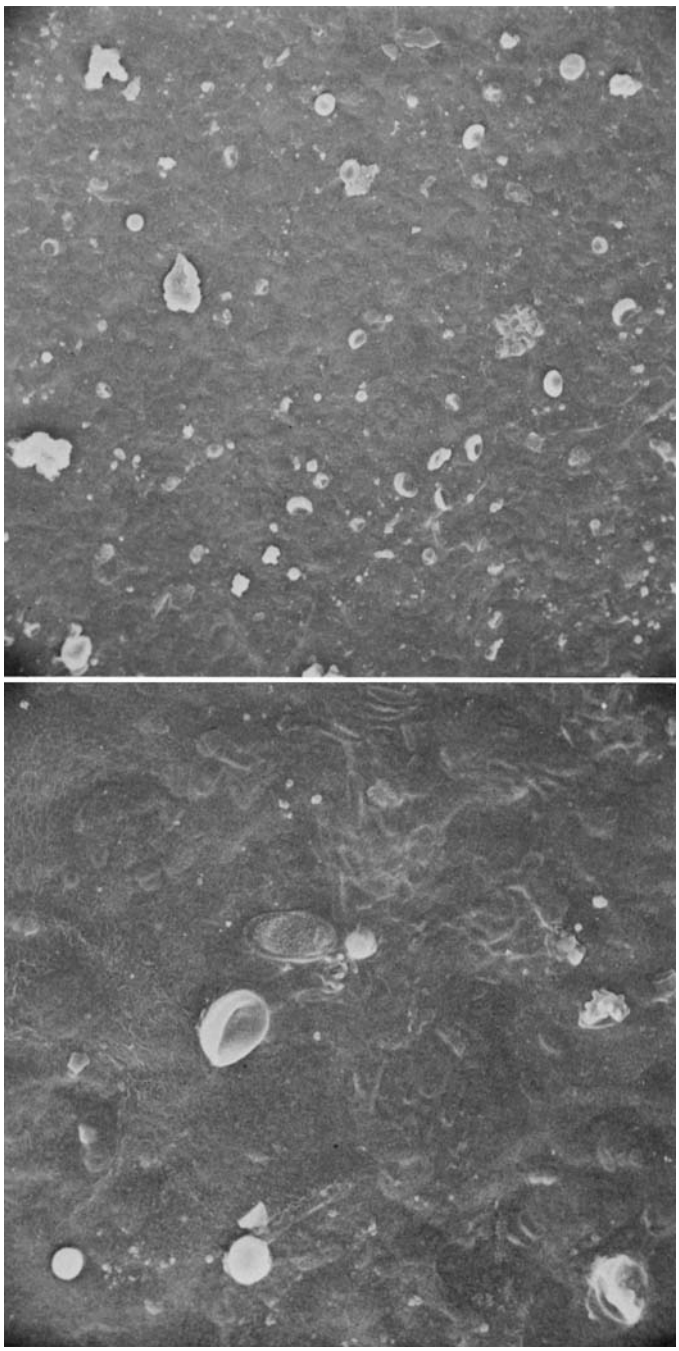

FIGURE 66.—*Parmelia sulcata* Taylor (*Hale* 14914, Connecticut).

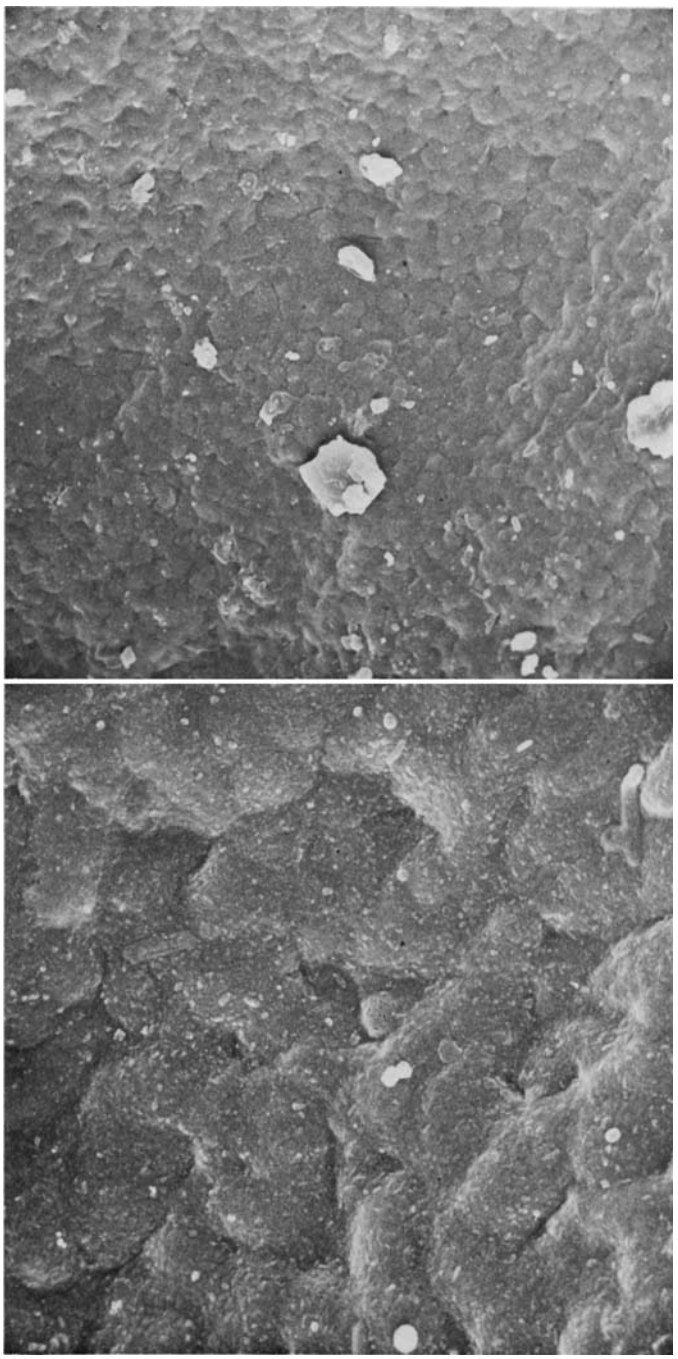

FIGURE 67.—*Parmelia bolliana* Müller-Argau (*Hale* 23691, Minnesota).

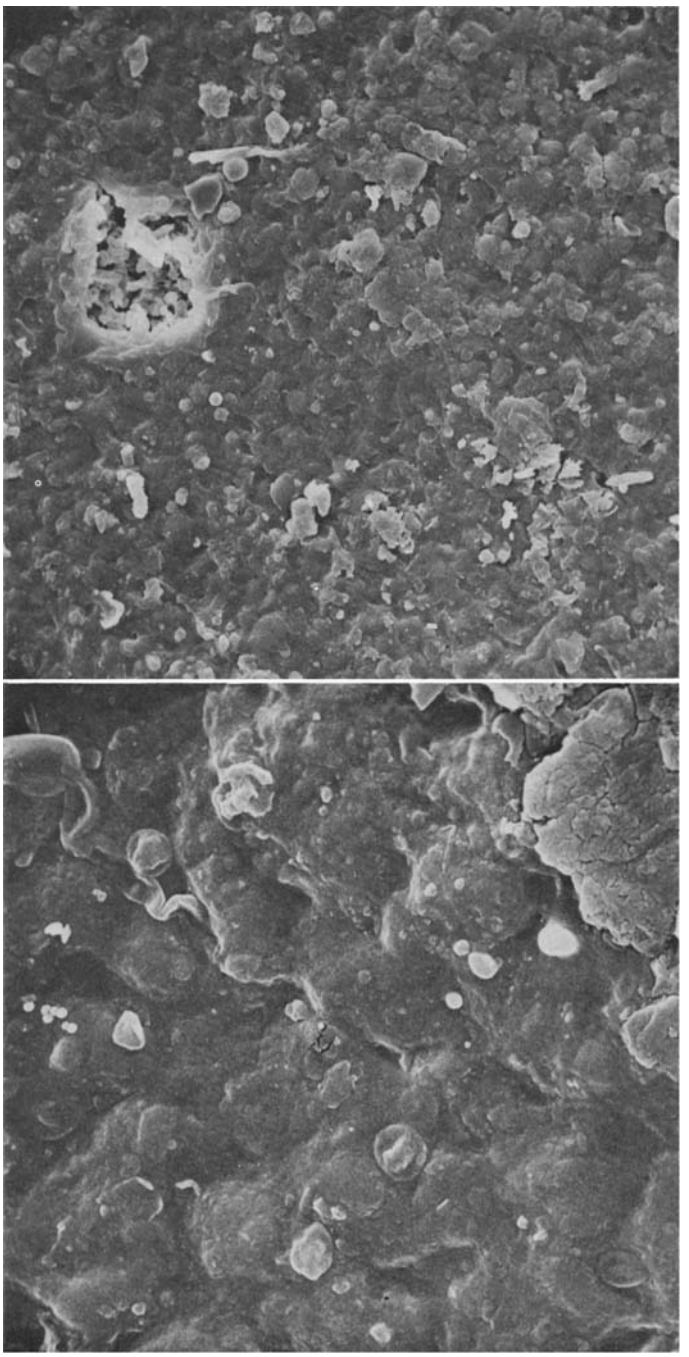

FIGURE 68.—*Parmelia borreri* (Smith) Turner (*Culberson* 10099, Ohio).

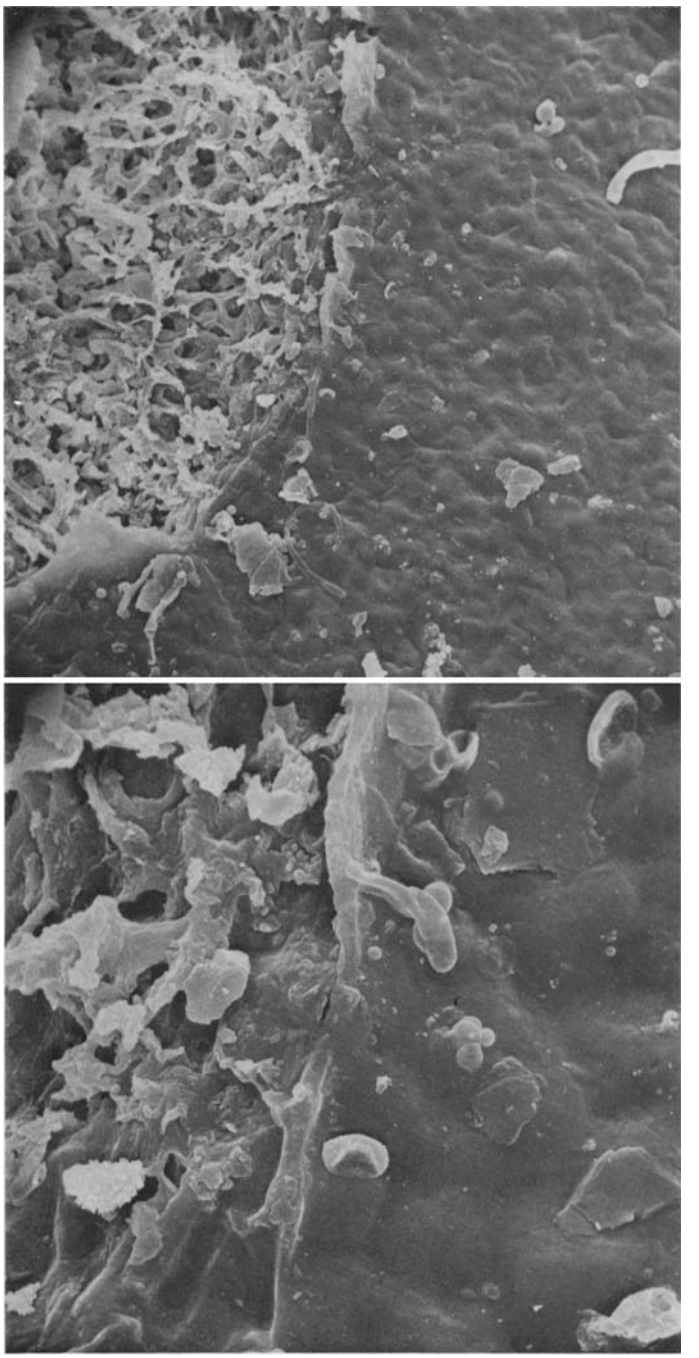

FIGURE 69.—*Parmelia rudecta* Acharius (*Hale* 14769, Conecticut). A large pseudocyphella is included in the photographs.

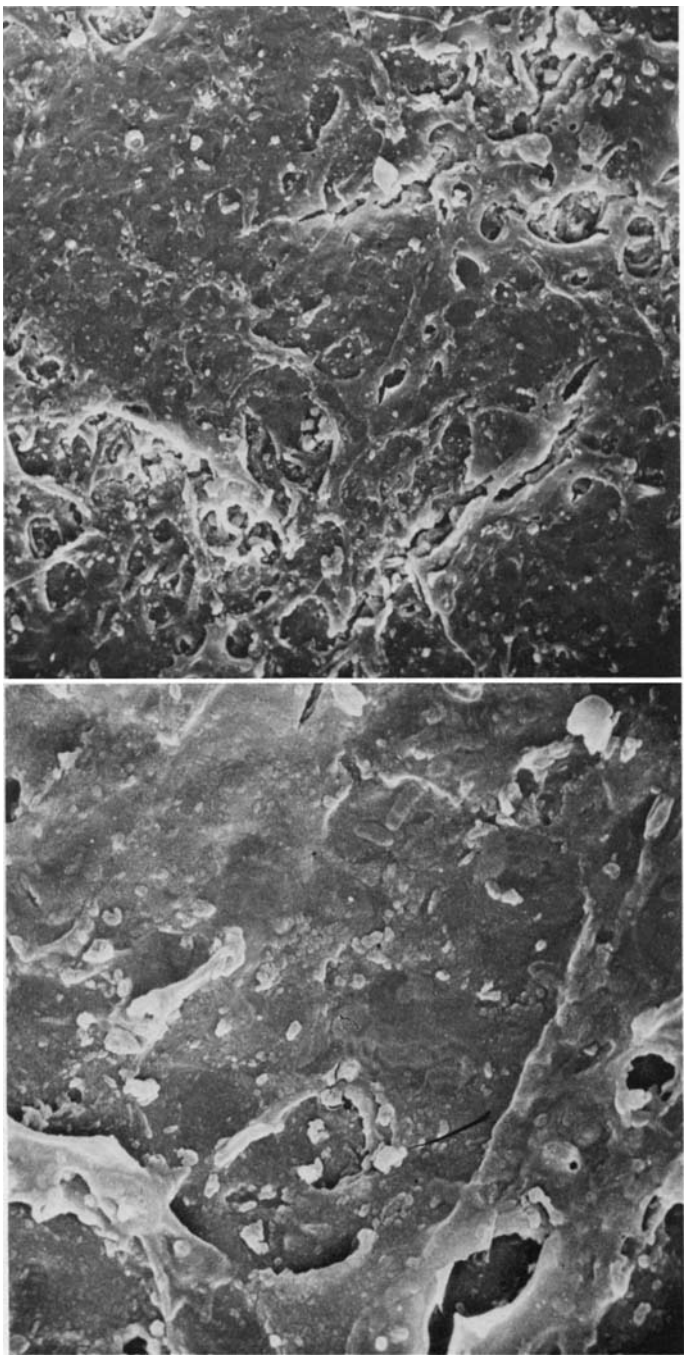

FIGURE 70.—*Parmelia cetrata* Acharius (*Hale* 30821, Georgia).

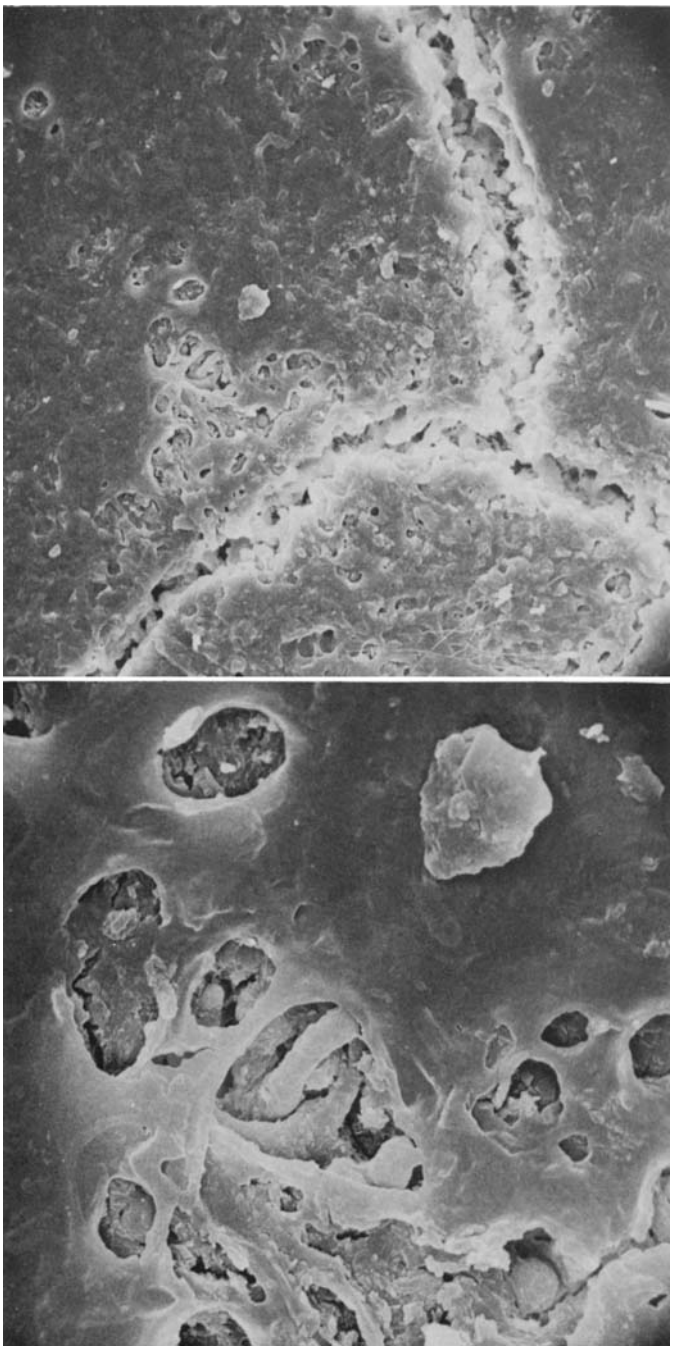

FIGURE 71.—*Parmelia maura* Persoon [=*P. reticulata* Taylor] (*Plitt* s.n., Jamaica).

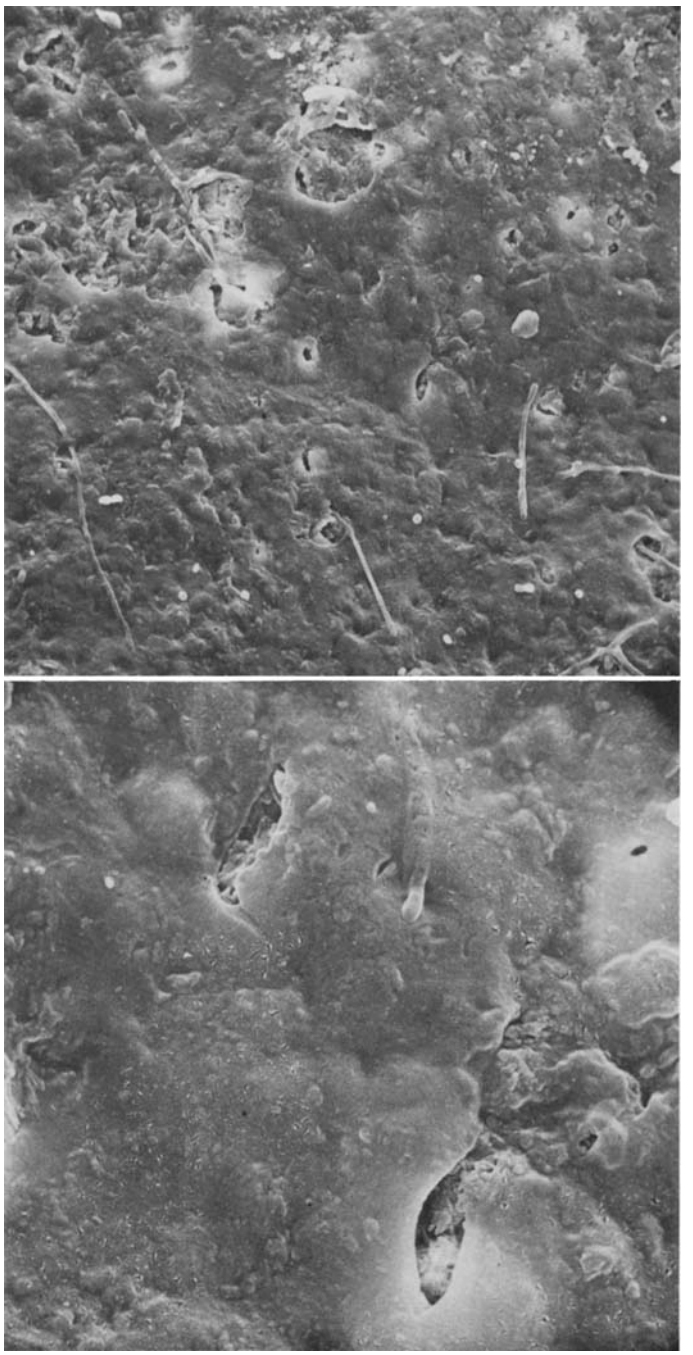

FIGURE 72.—*Parmelia fluorescens* Hale (*Hale* 28637, Sabah, holotype).

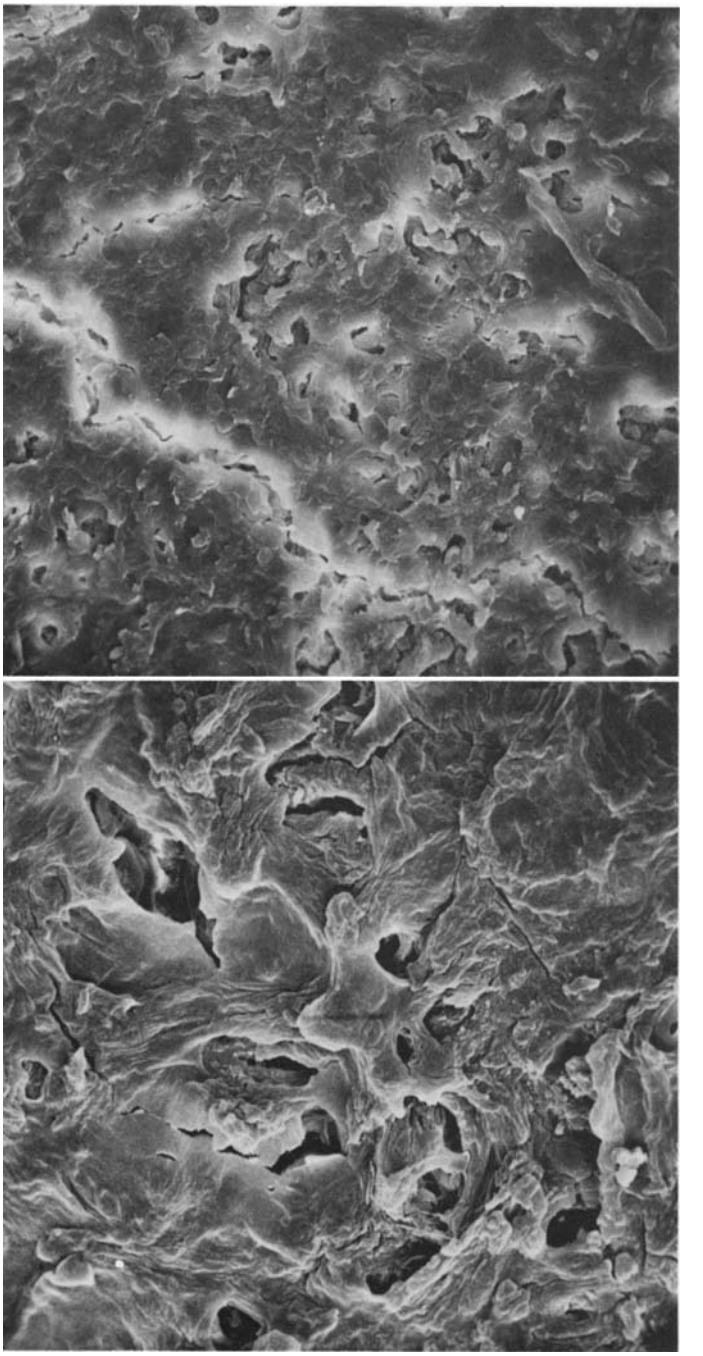

FIGURE 73.—*Parmelia malesiana* Hale (*Hale* 25178, Philippines).

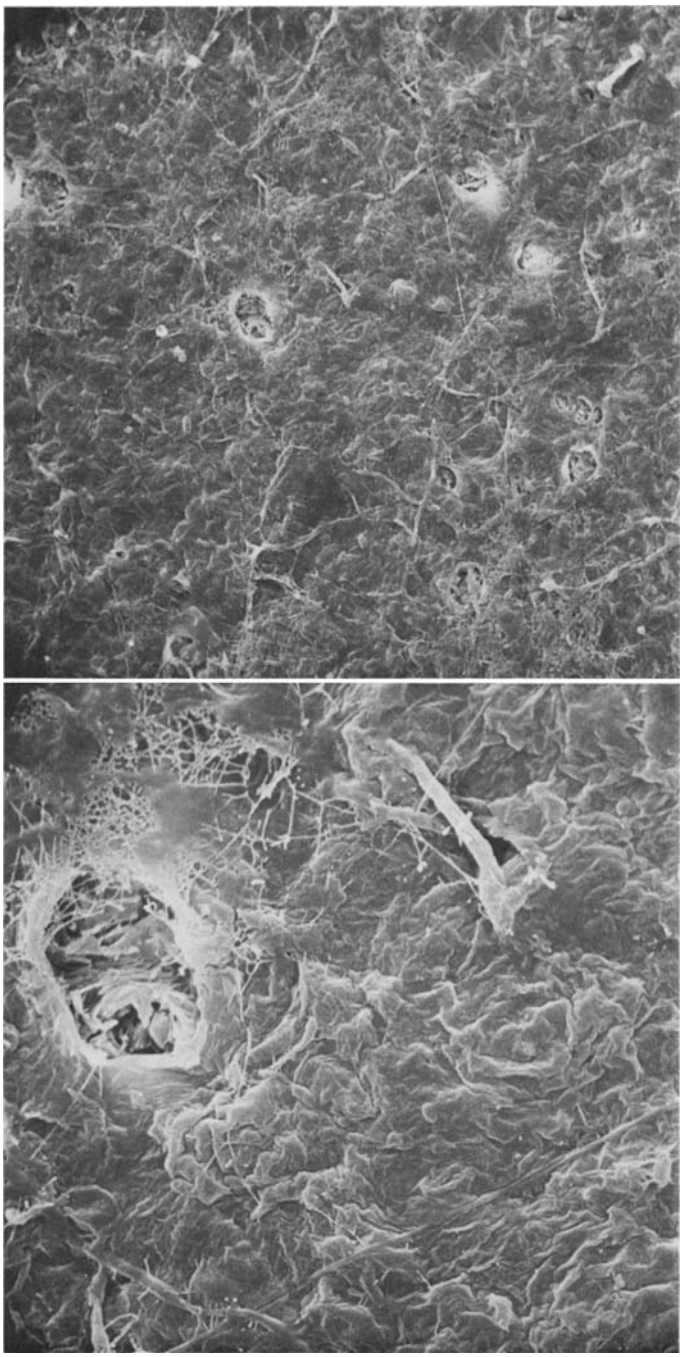

FIGURE 74.—*Parmelia planiuscula* Kurokawa (*Neervoort* 427, Java, holotype). Thallus infested by a fungus.

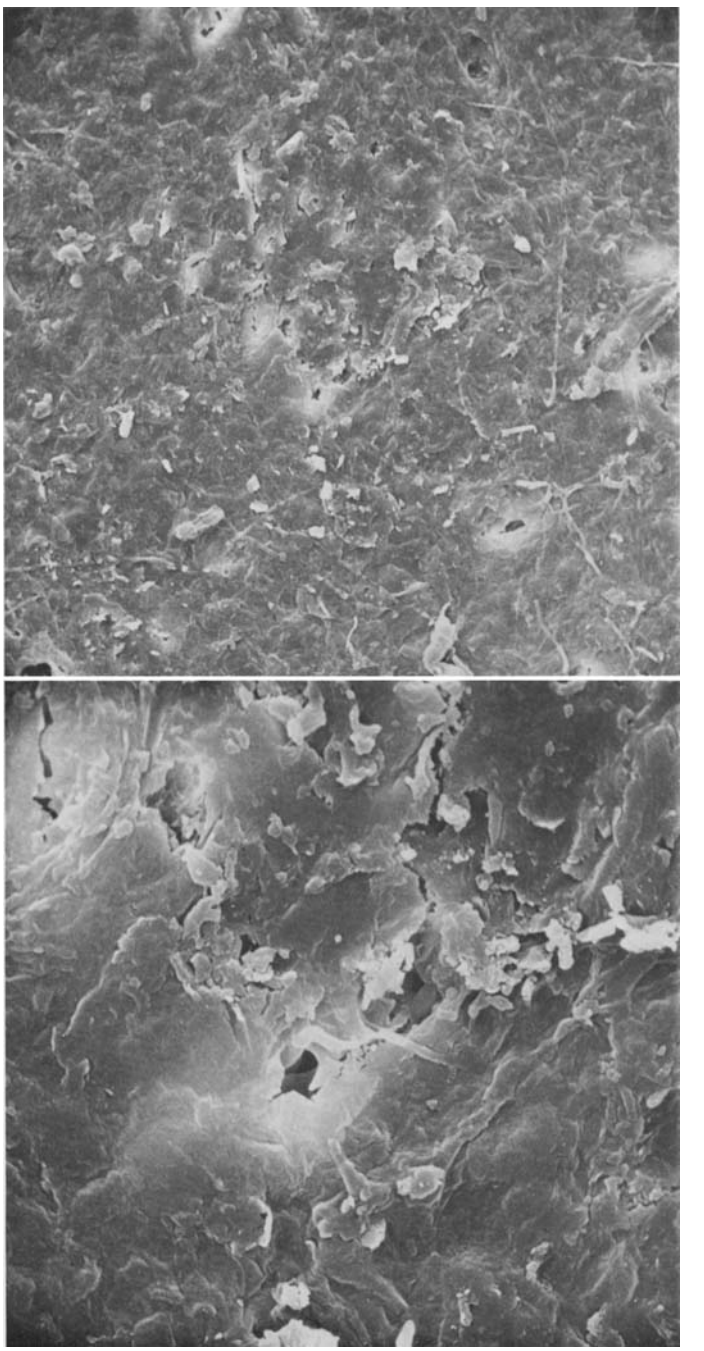

FIGURE 75.—*Parmelia ramosissima* Kurokawa (*Buwalda* 4583, Java, holotype).

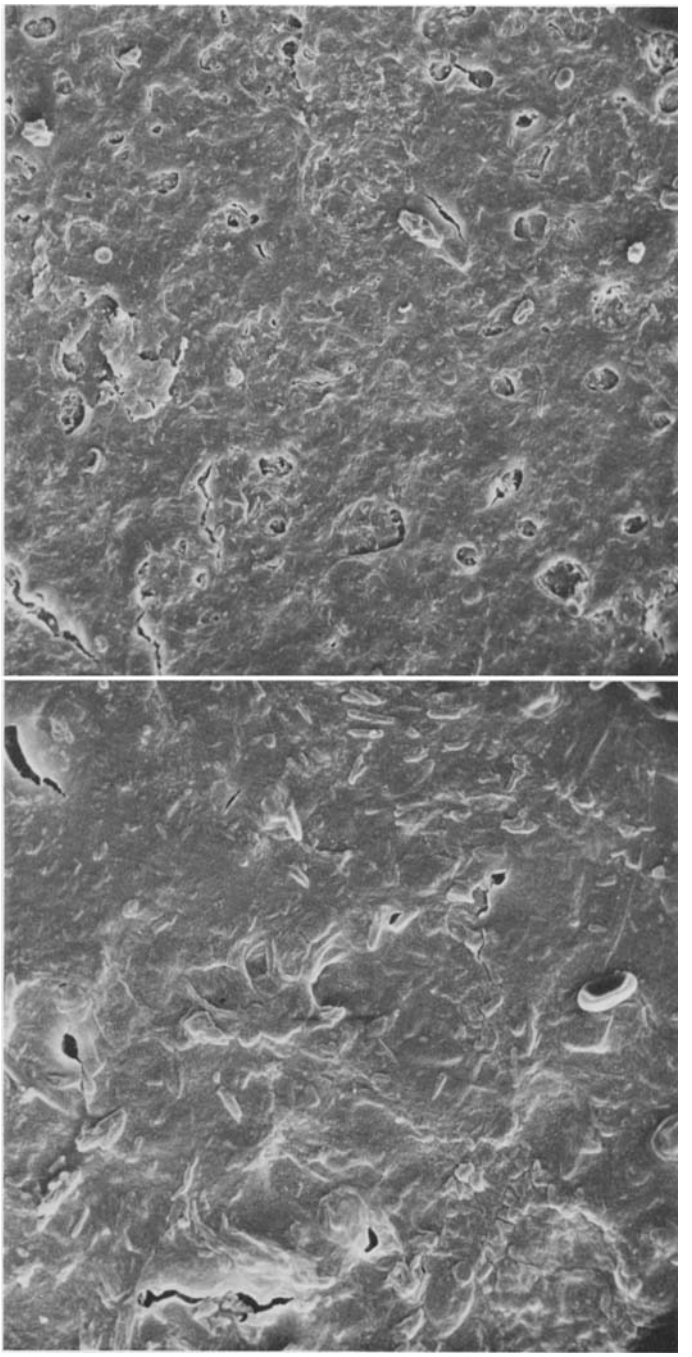

FIGURE 76.—*Parmelia subabstrusa* Gyelnik (*Hale* 25141, Philippines).

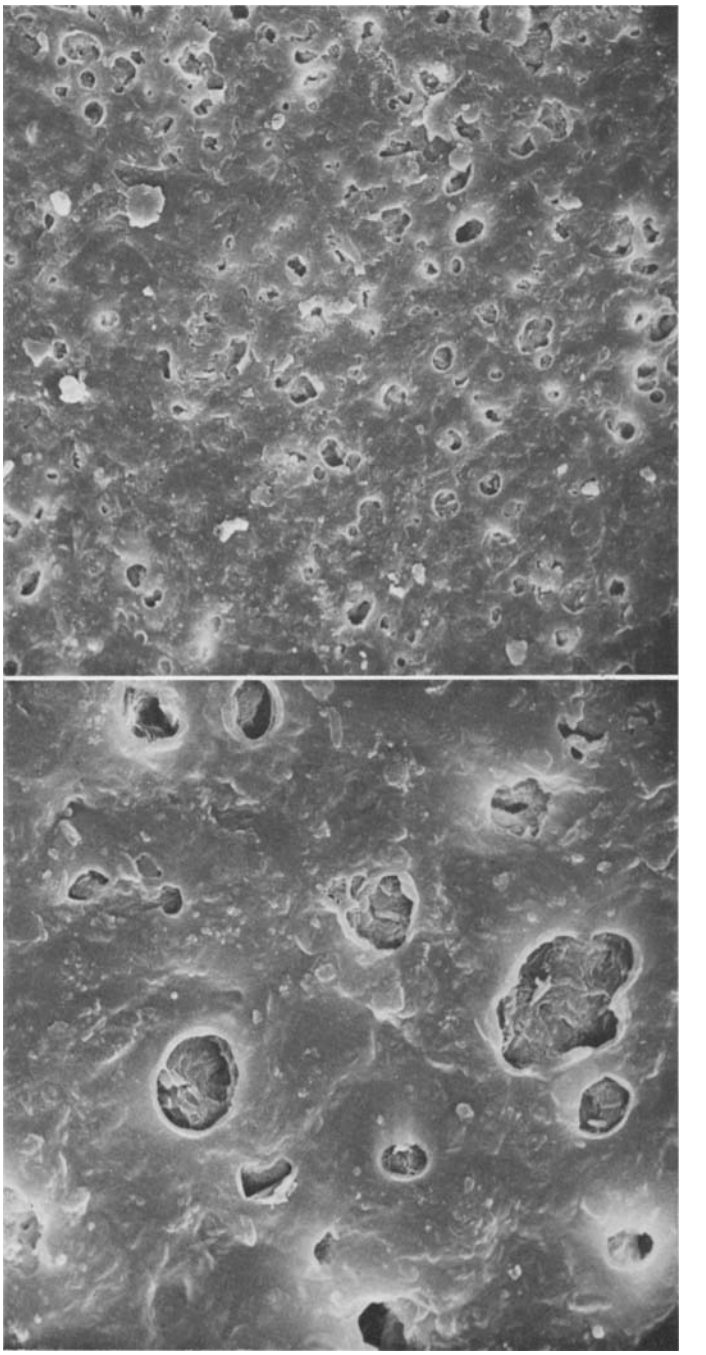

FIGURE 77.—*Parmelia confoederata* Culberson (*Culberson* 9010, North Carolina, isotype).

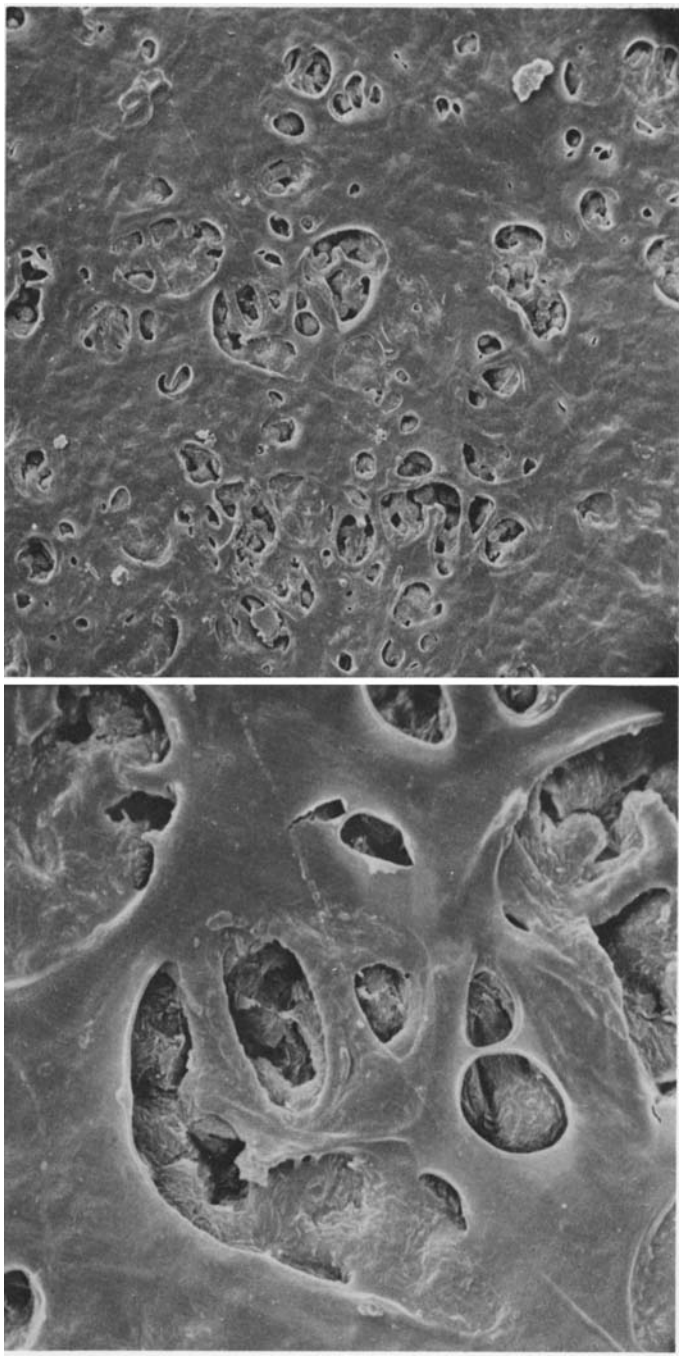

FIGURE 78.—*Parmelia coronata* Fée (*Hale* 20505, Mexico).

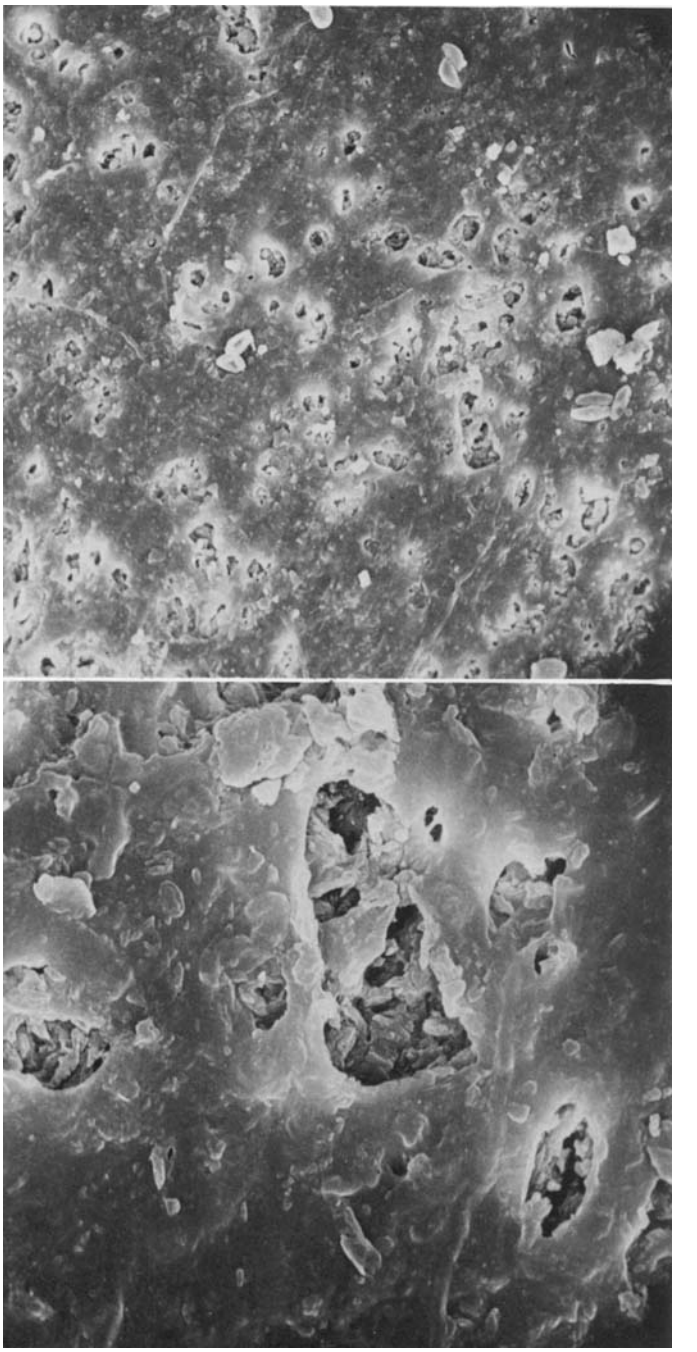

FIGURE 79.—*Parmelia pigmentacea* Hale (*Hale* 26895, Philippines, holotype).

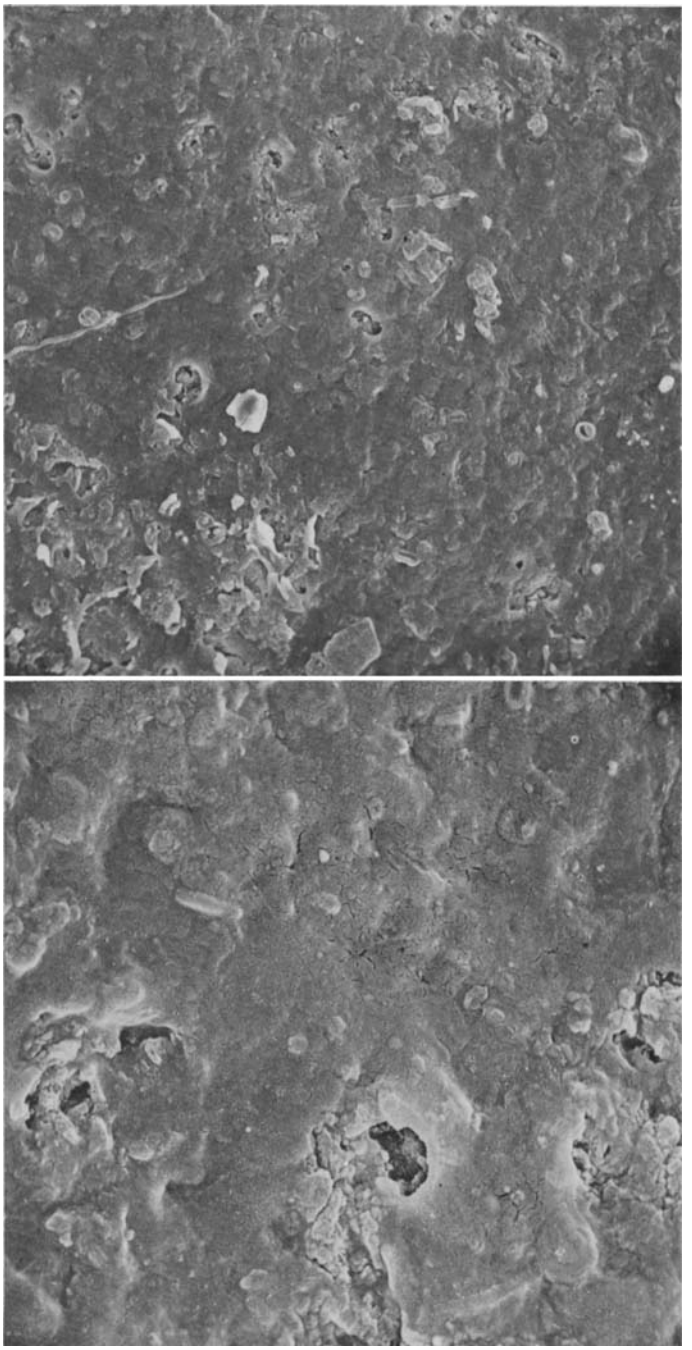

FIGURE 80.—*Parmelia subinflata* Hale (*Hale* 26641, Philippines, holotype).

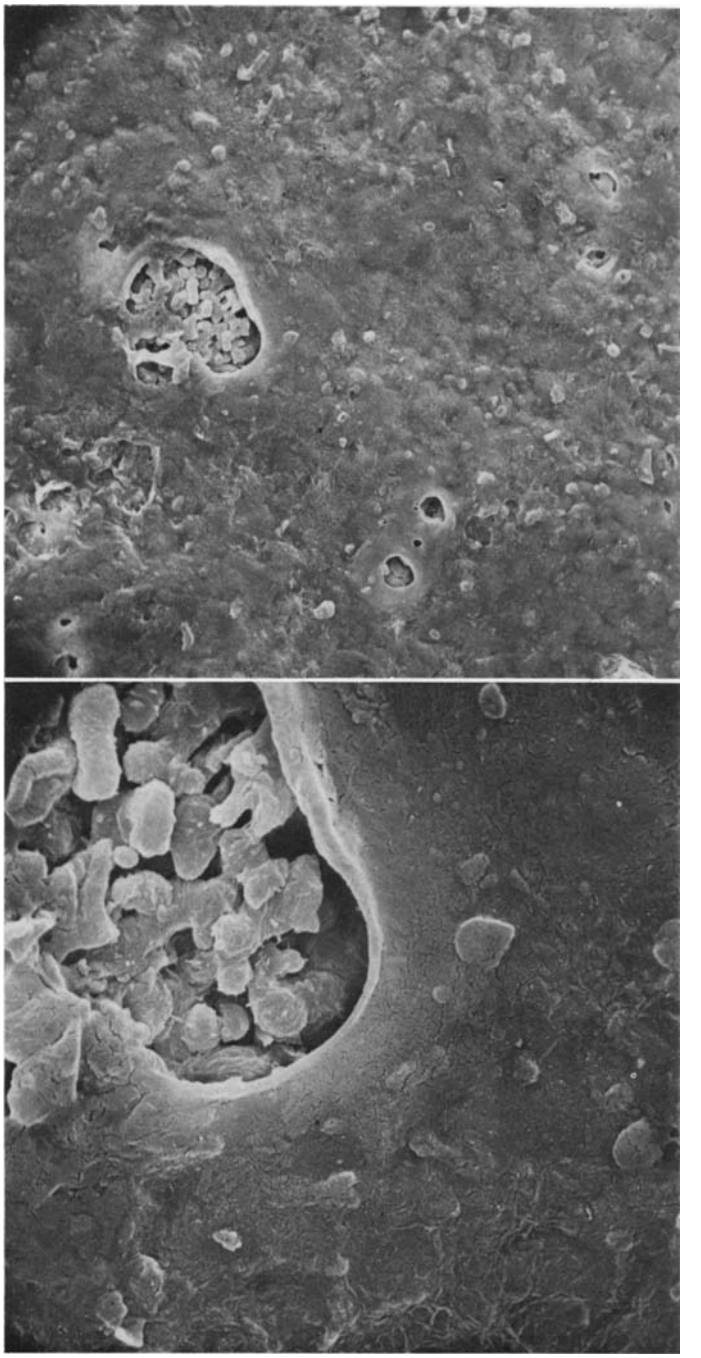

FIGURE 81.—*Parmelia antillensis* Nylander (*Hale*, 35504, Dominica).

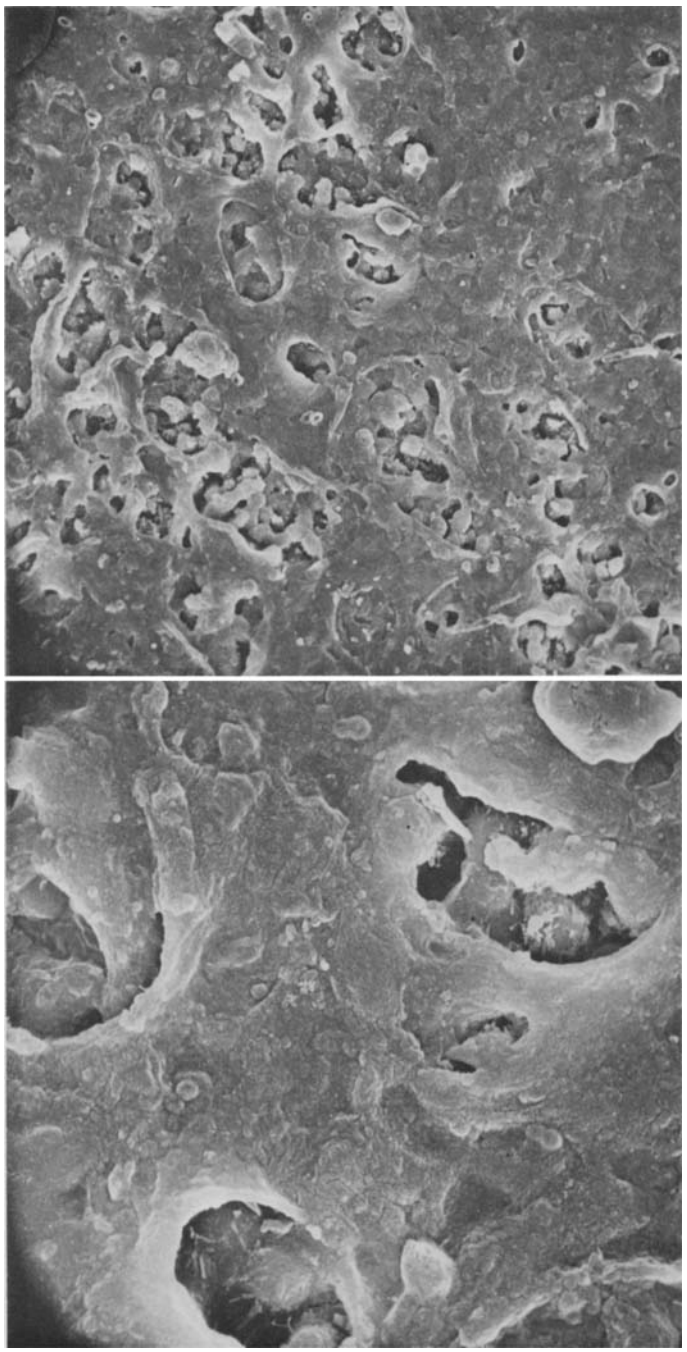

FIGURE 82.—*Parmelia aurulenta* Tuckerman (*Thieret* 24389. Louisiana).

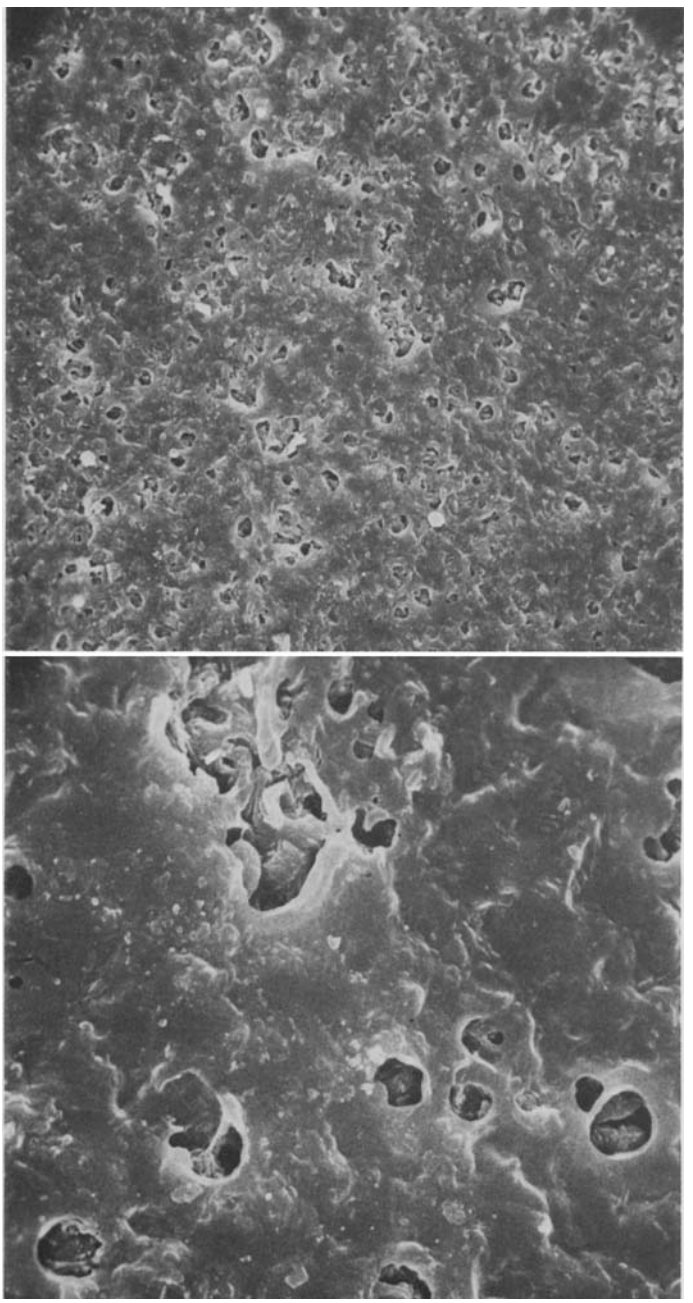

FIGURE 83.—*Parmelia dissecta* Nylander (*Hale* 29536, Japan).

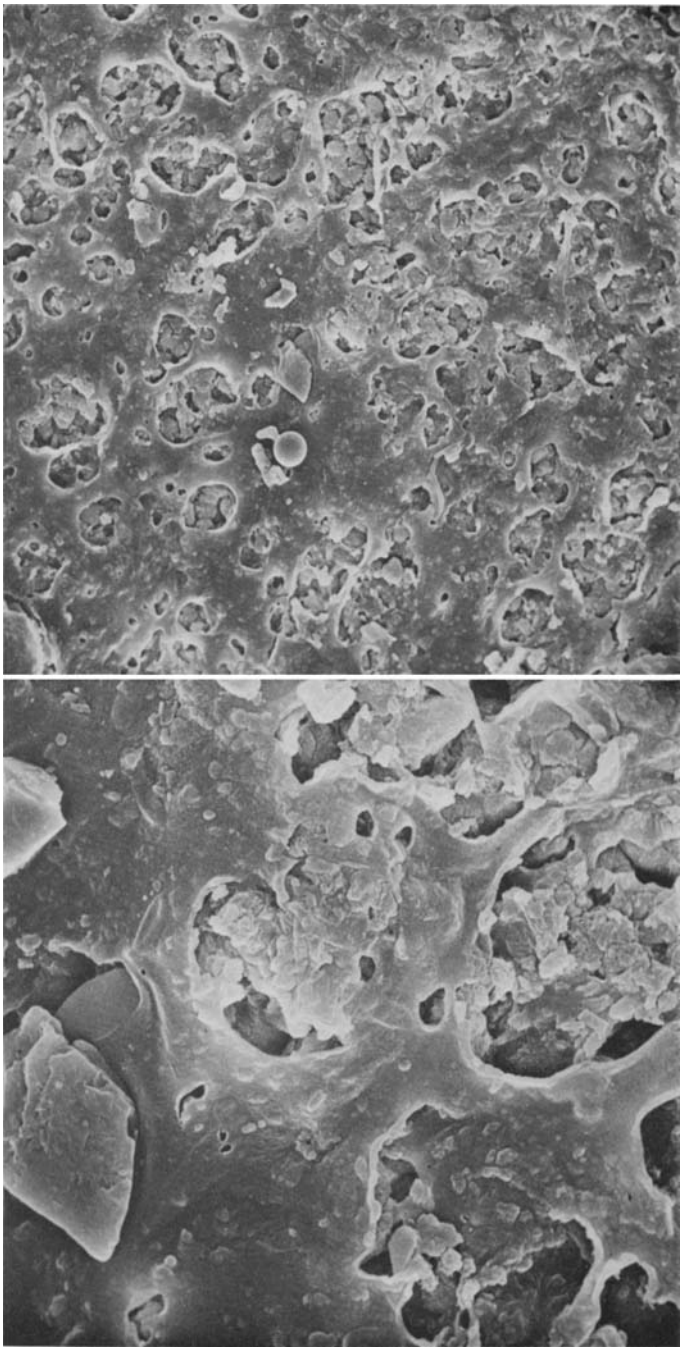

FIGURE 84.—*Parmelia horrescens* Taylor (*Hale* 36970, Tennessee).

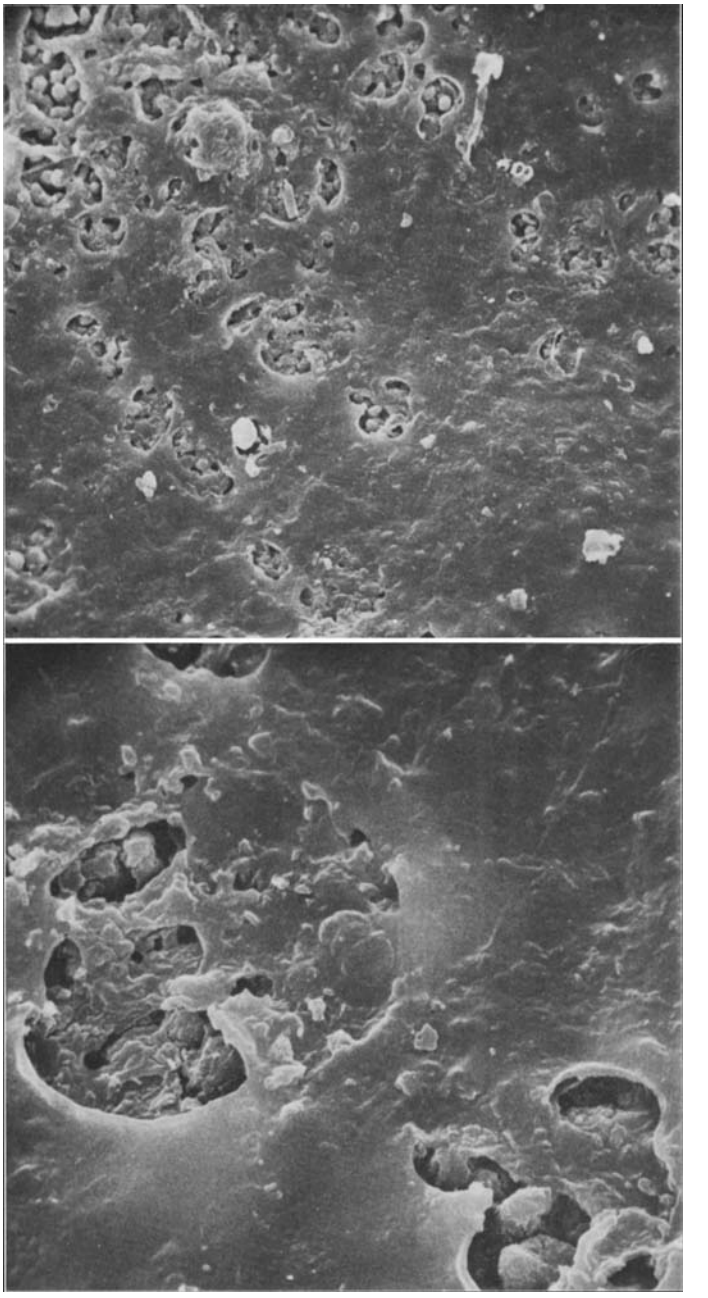

FIGURE 85.—*Parmelia jamesii* Hale (*James* 2118, New Zealand, holotype).

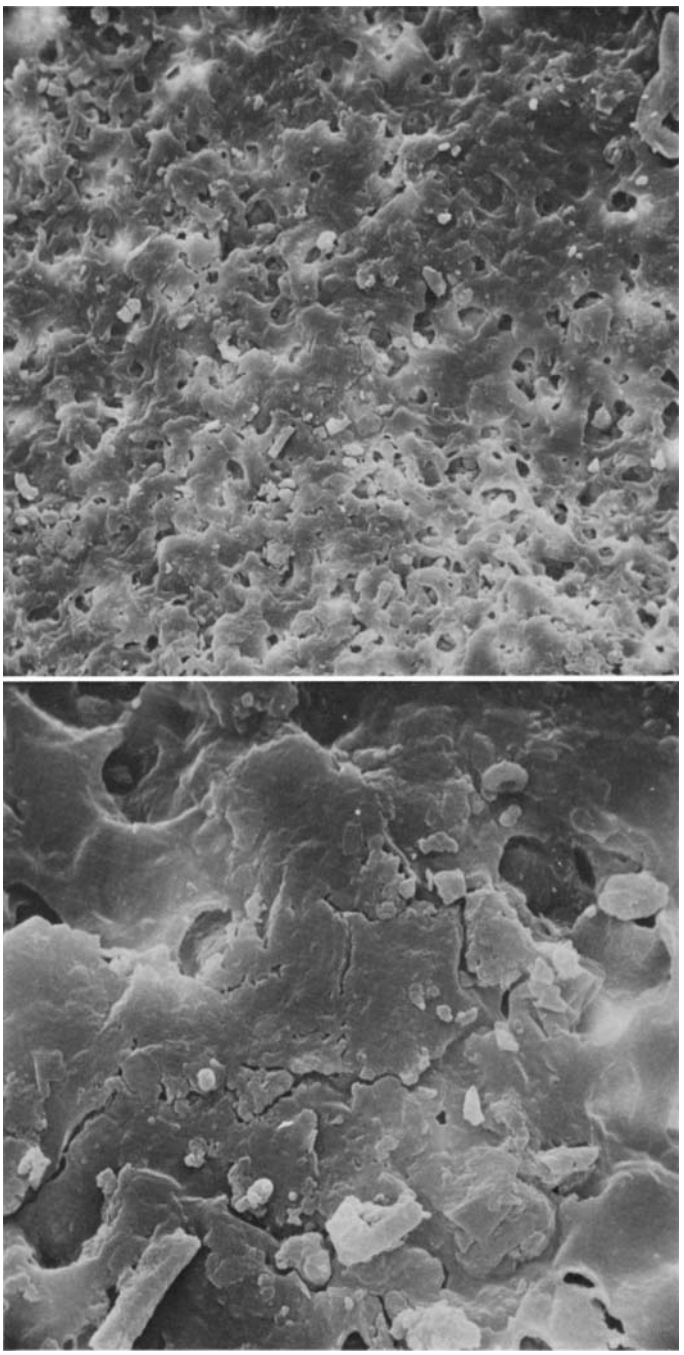

FIGURE 86.—*Parmelia quercina* (Willdenow) Vainio (*Tavares* 1082, Portugal).

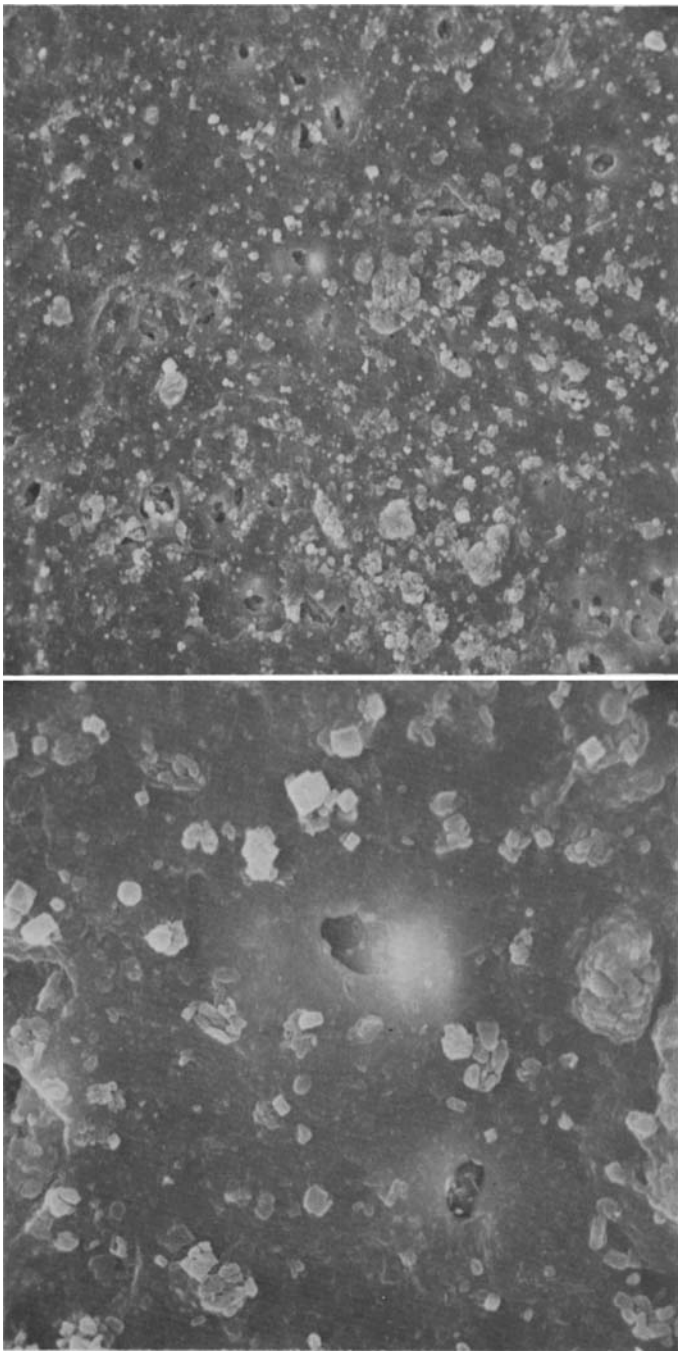

FIGURE 87.—*Parmelia scortea* Acharius (*Vězda* 762, Yugoslavia).

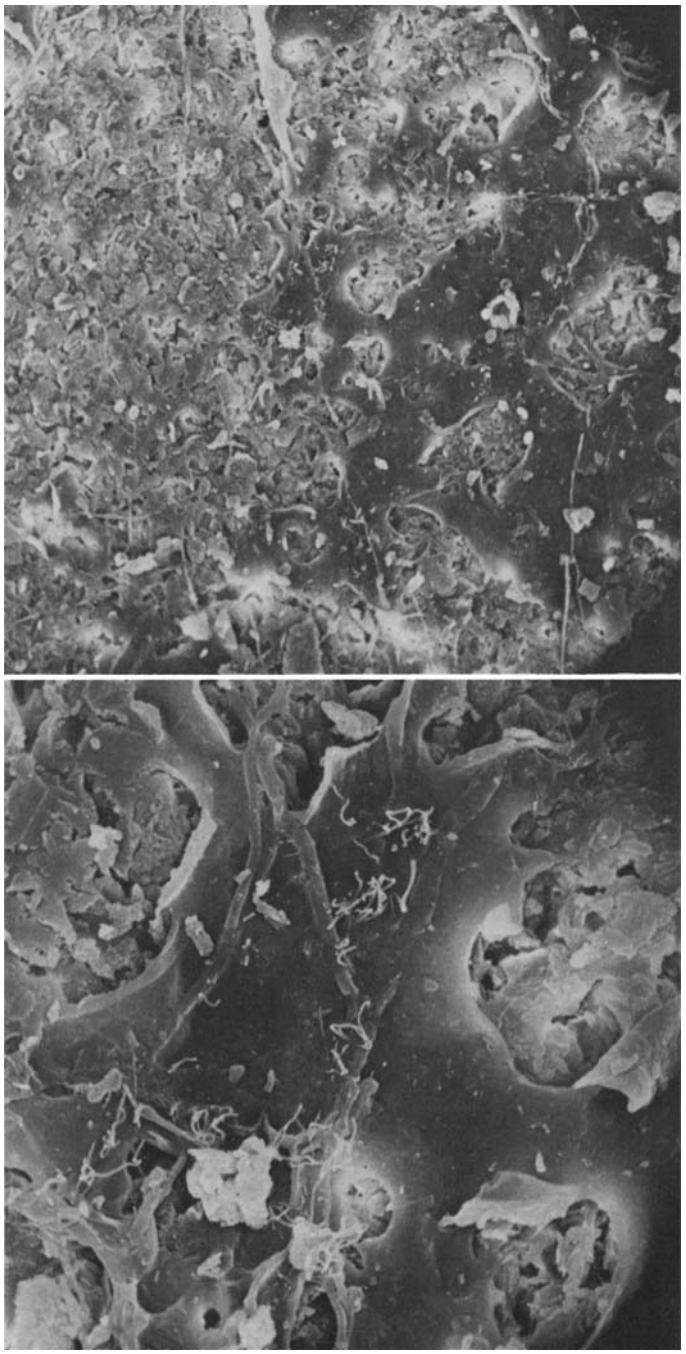

FIGURE 88.—*Parmelia wallichiana* Taylor (*Wallich* s.n., India, holotype in FH-Tayl).

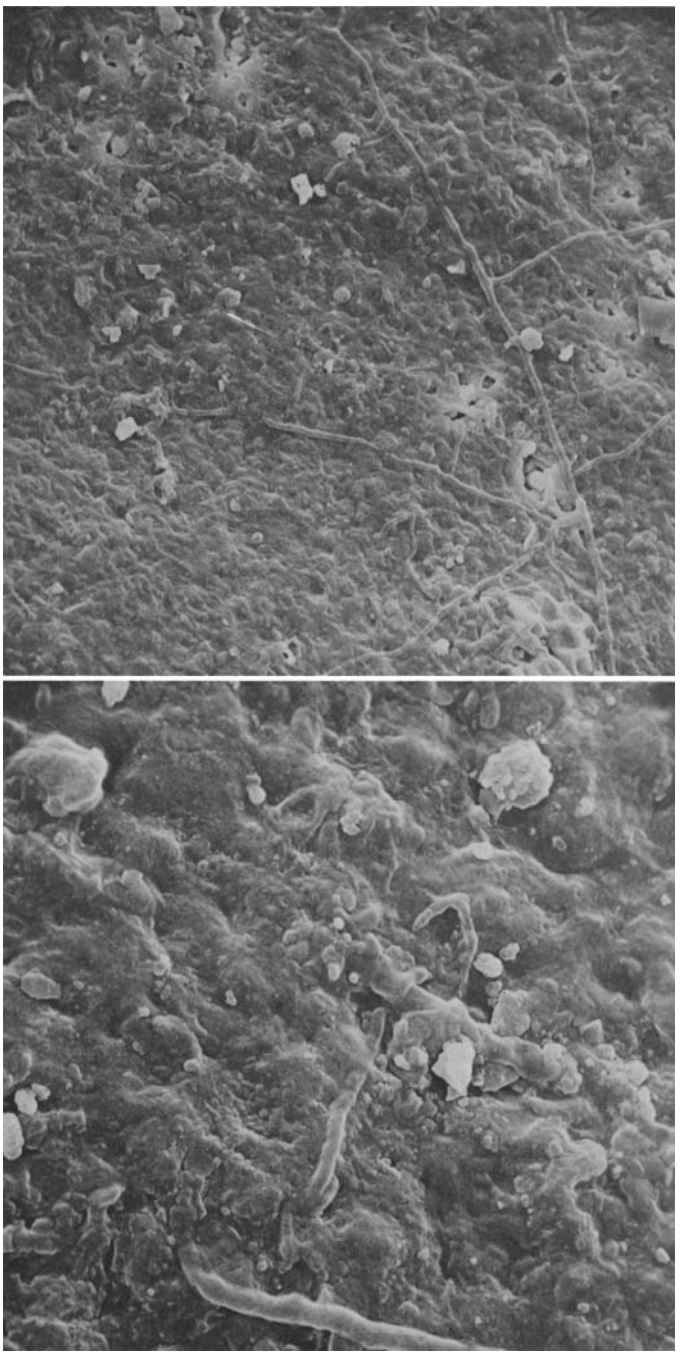

FIGURE 89.—*Parmelia aptata* Krempelhuber (*Togashi* s.n., Nepal).

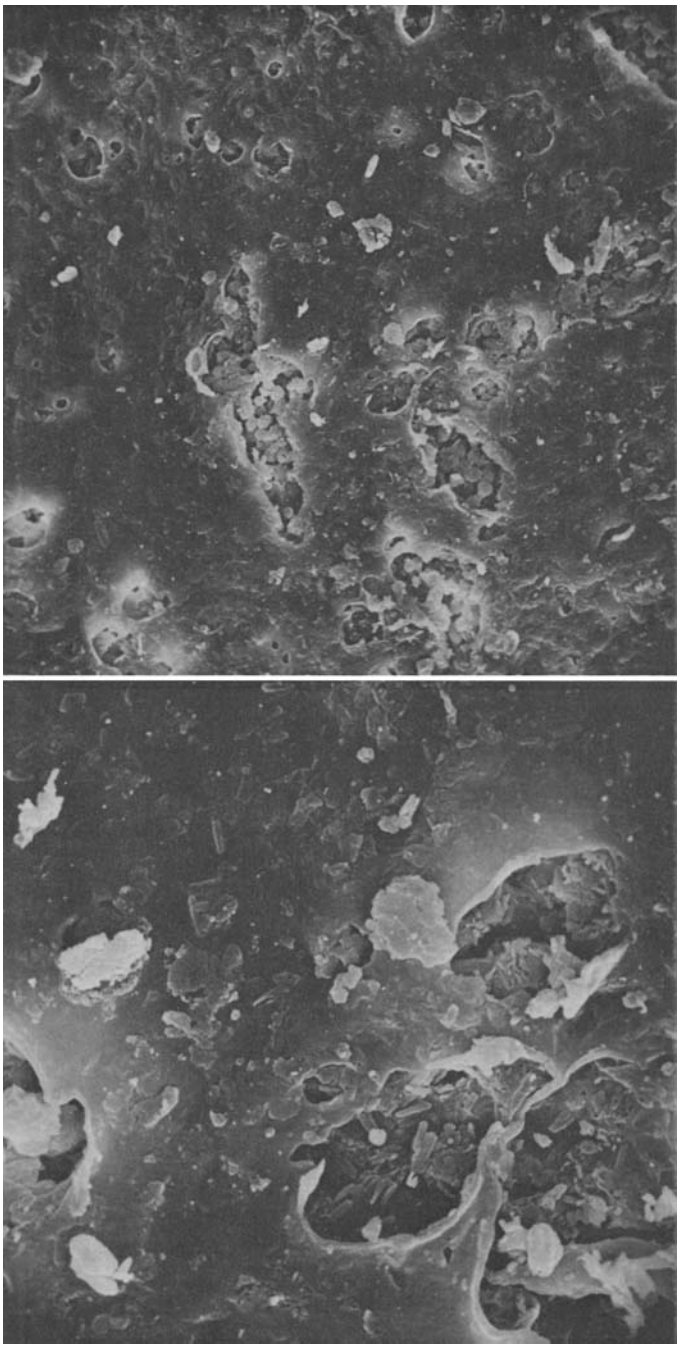

FIGURE 90.—*Parmelia baltimorensis* Foriss and Gyelnik (*Fink and Fuson* 340, Indiana).

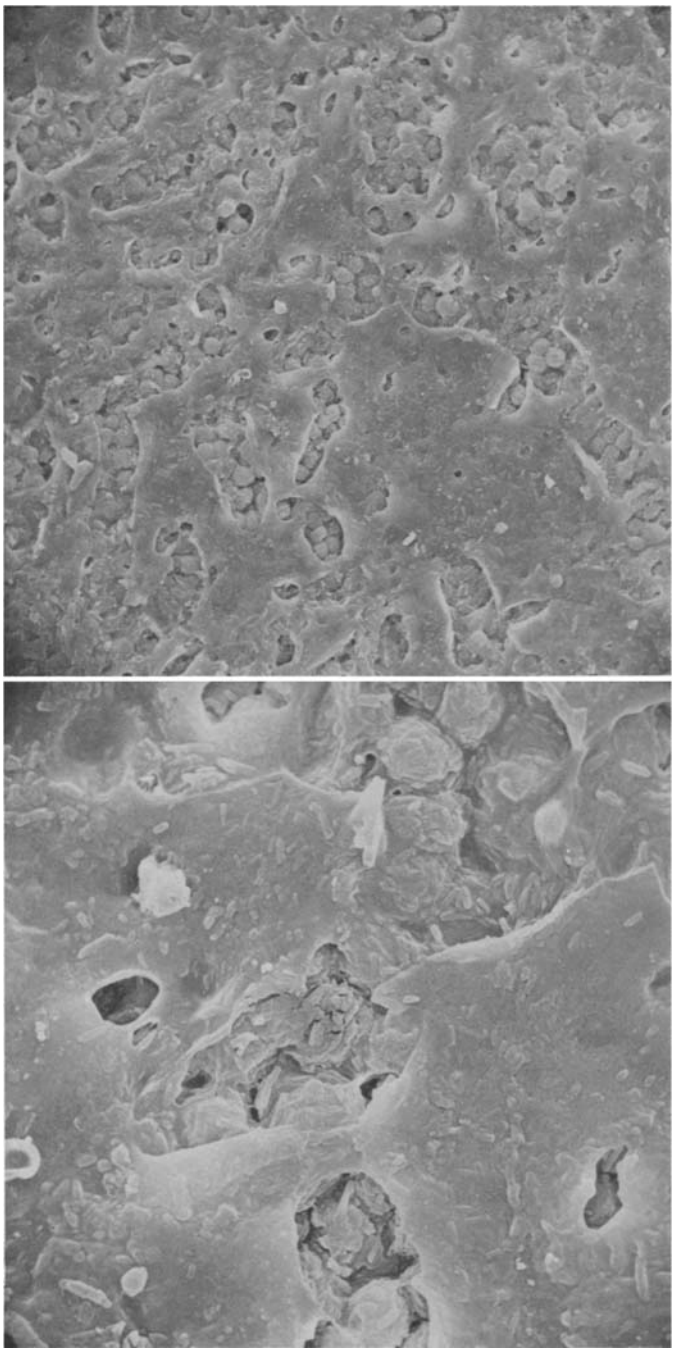

FIGURE 91.—*Parmelia caperata* (L.) Acharius (*Hale*, 22229, Virginia).

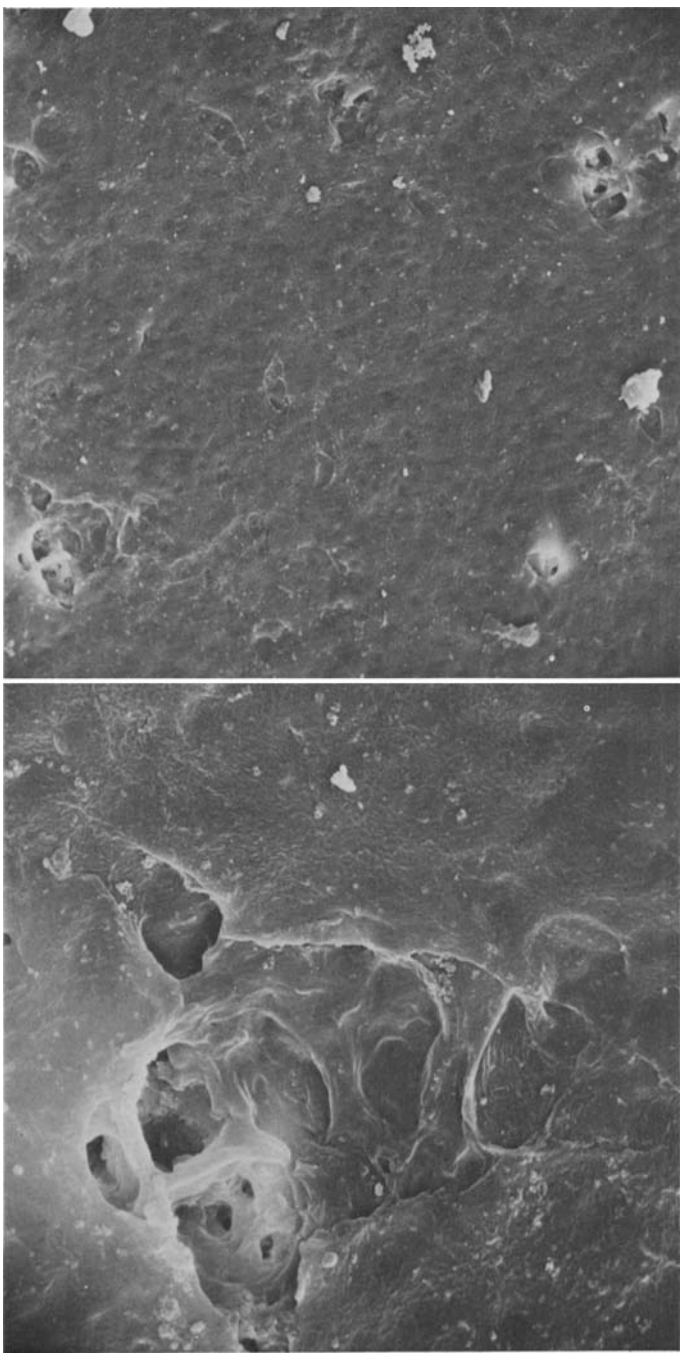

FIGURE 92.—*Parmelia congruens* Acharius (*Kelley* 5713, Florida).

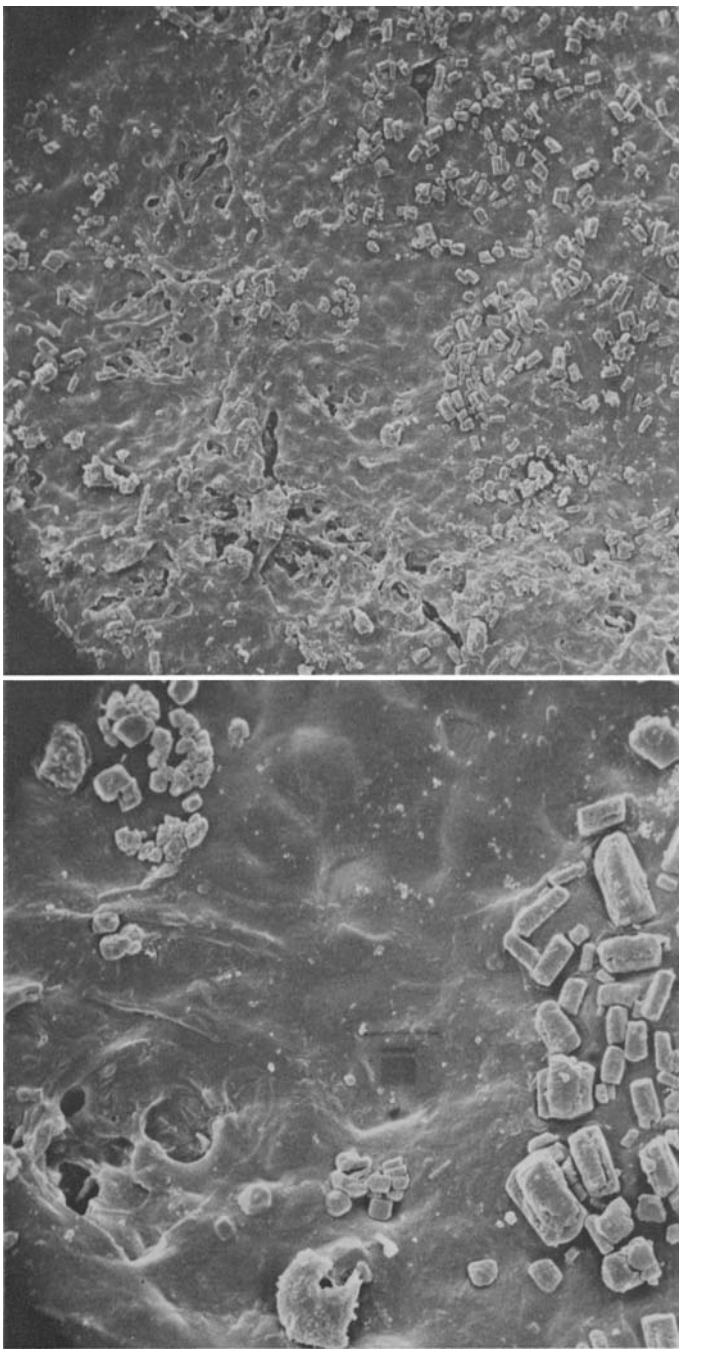

FIGURE 93.—*Parmelia crozalsiana* Bouly de Lesdain (*Sbarbaro* 96, Italy).

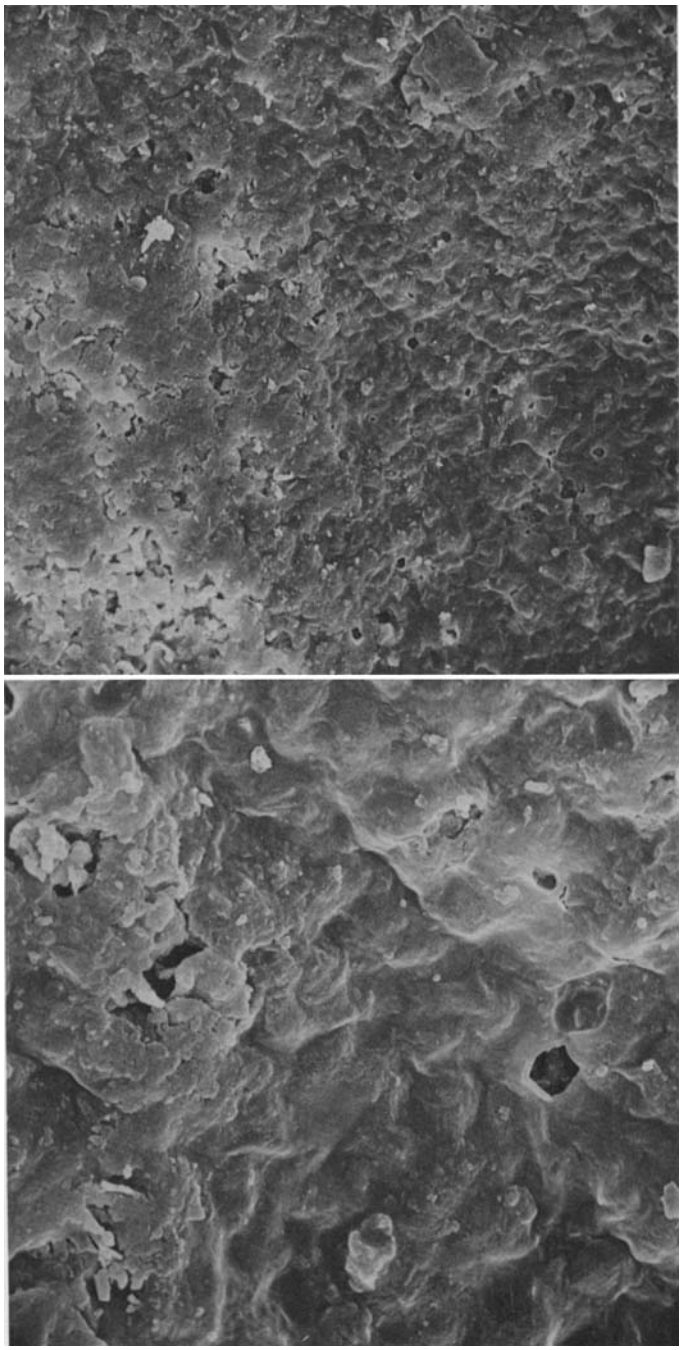

FIGURE 94.—*Parmelia cryptochlorophaea* Hale (*Allard* 15715a, Dominican Republic, holoype).

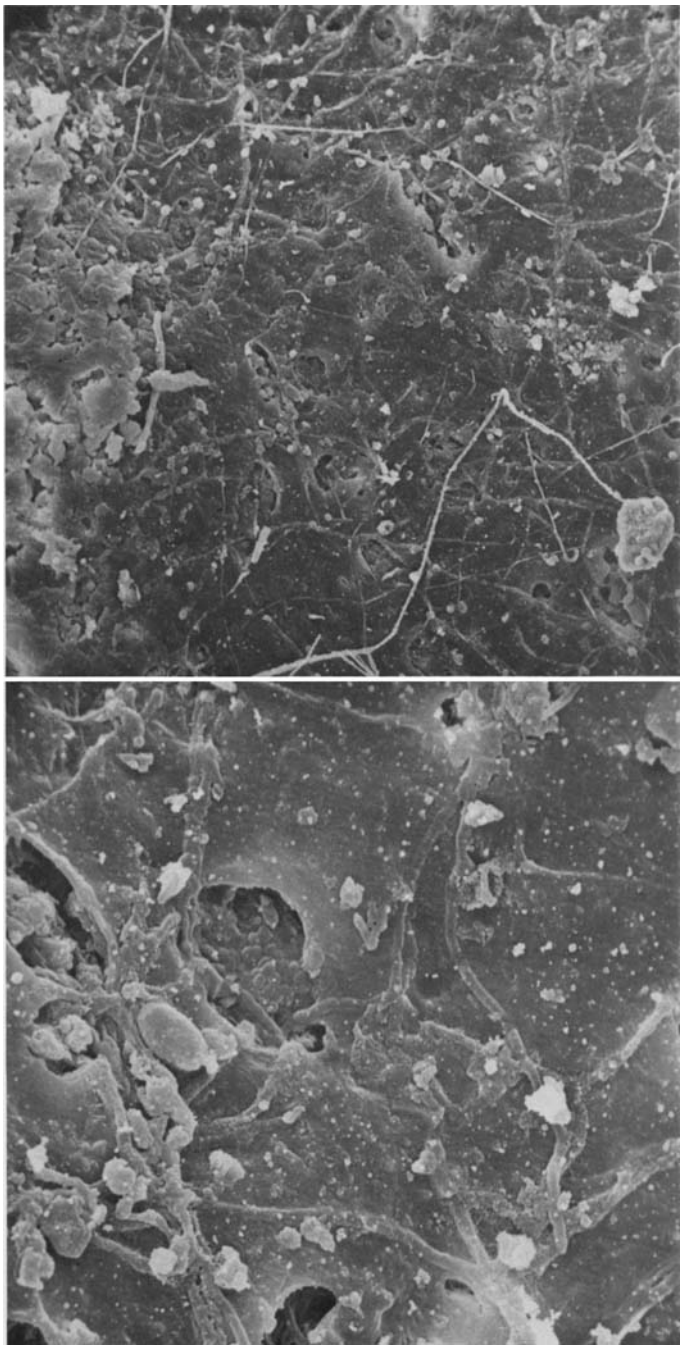

FIGURE 95.—*Parmelia malaccensis* Nylander (*Maingay* 21, Malaya, holotype in H).

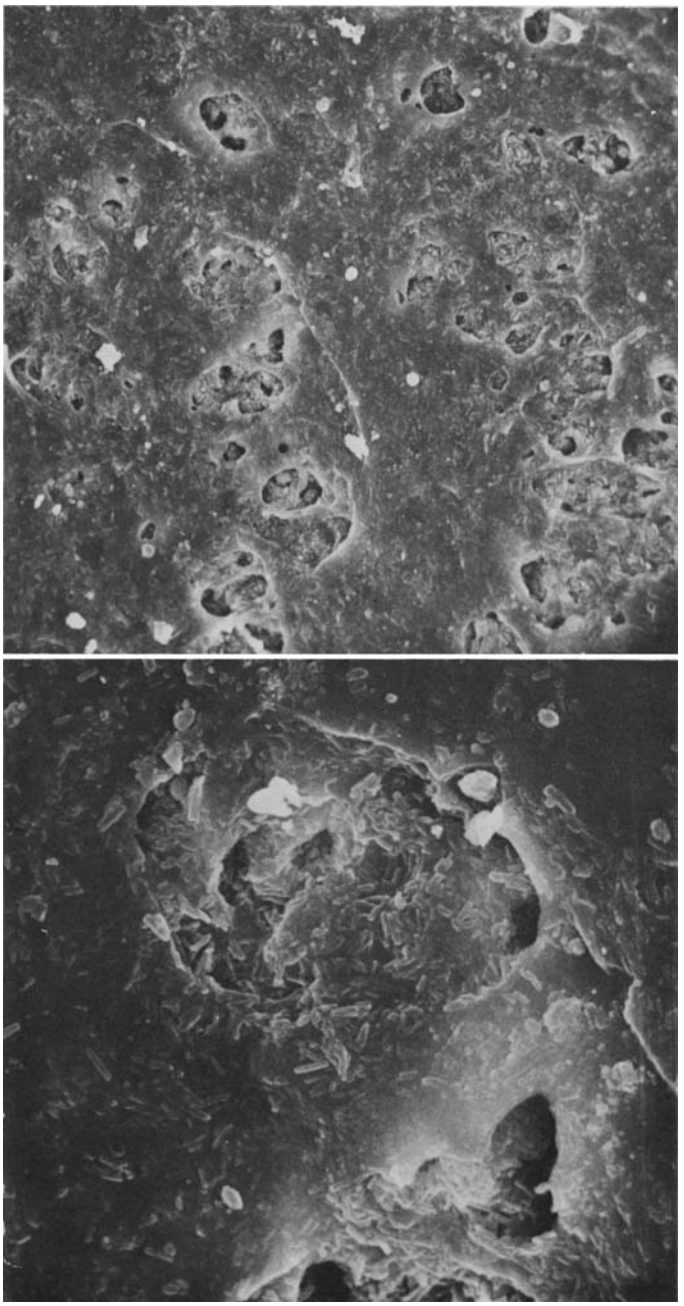

FIGURE 96.—*Parmelia rutidota* Hooker and Taylor (*Weber* 268 (Lichenes Exsiccati), Australia).

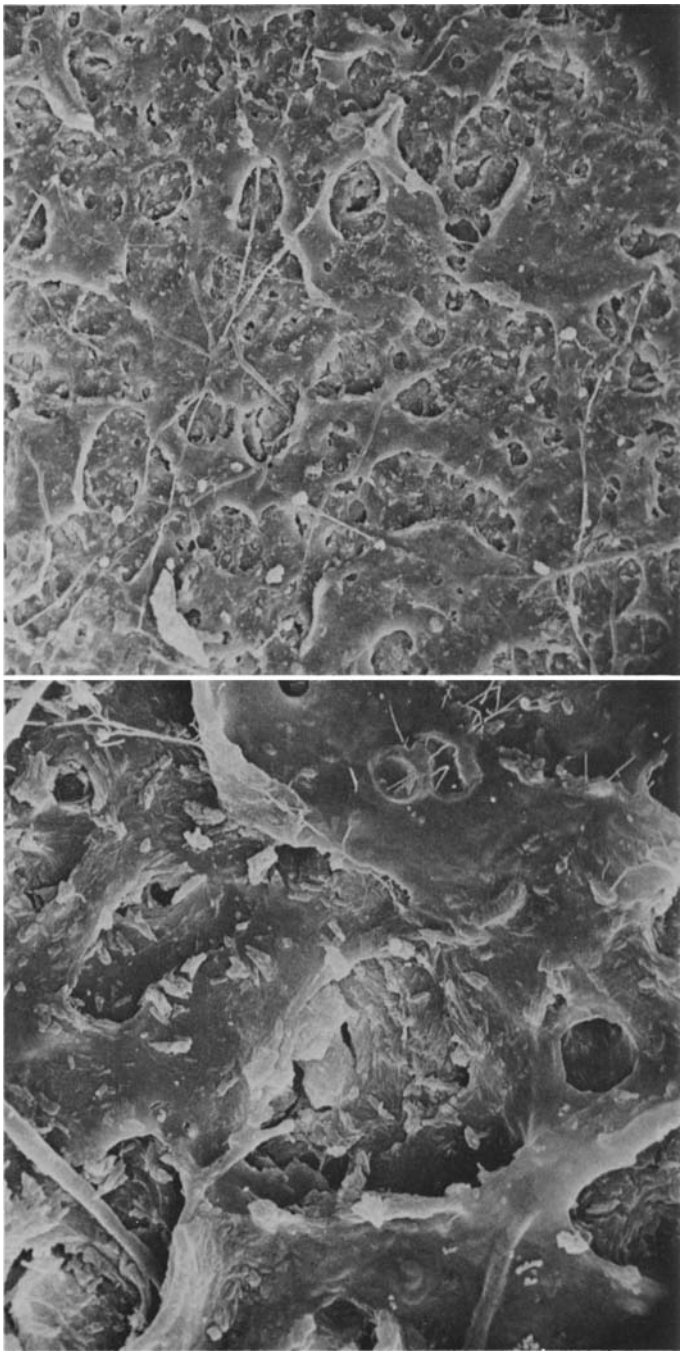

FIGURE 97.—*Parmelia salacinifera* Hale (*Rapp* s.n., Florida, holotype).

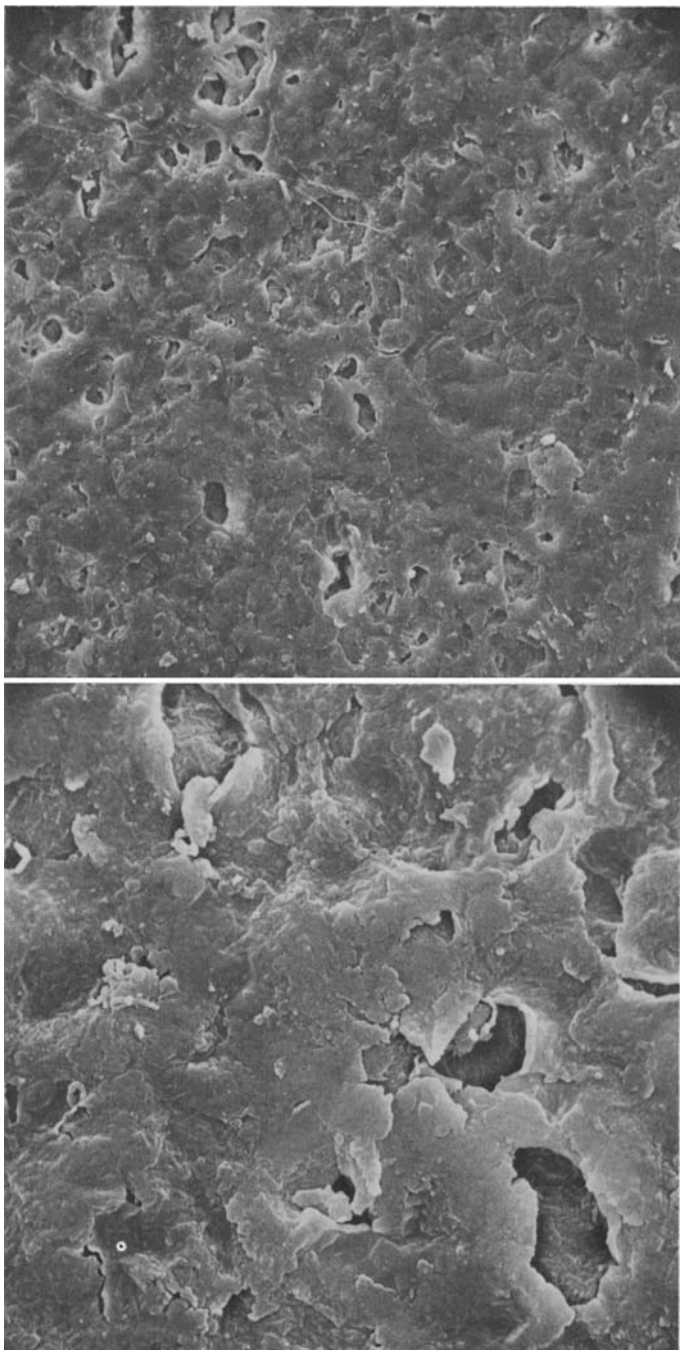

FIGURE 98.—*Parmelia texana* Tuckerman (*Wright*, Texas, isotype).

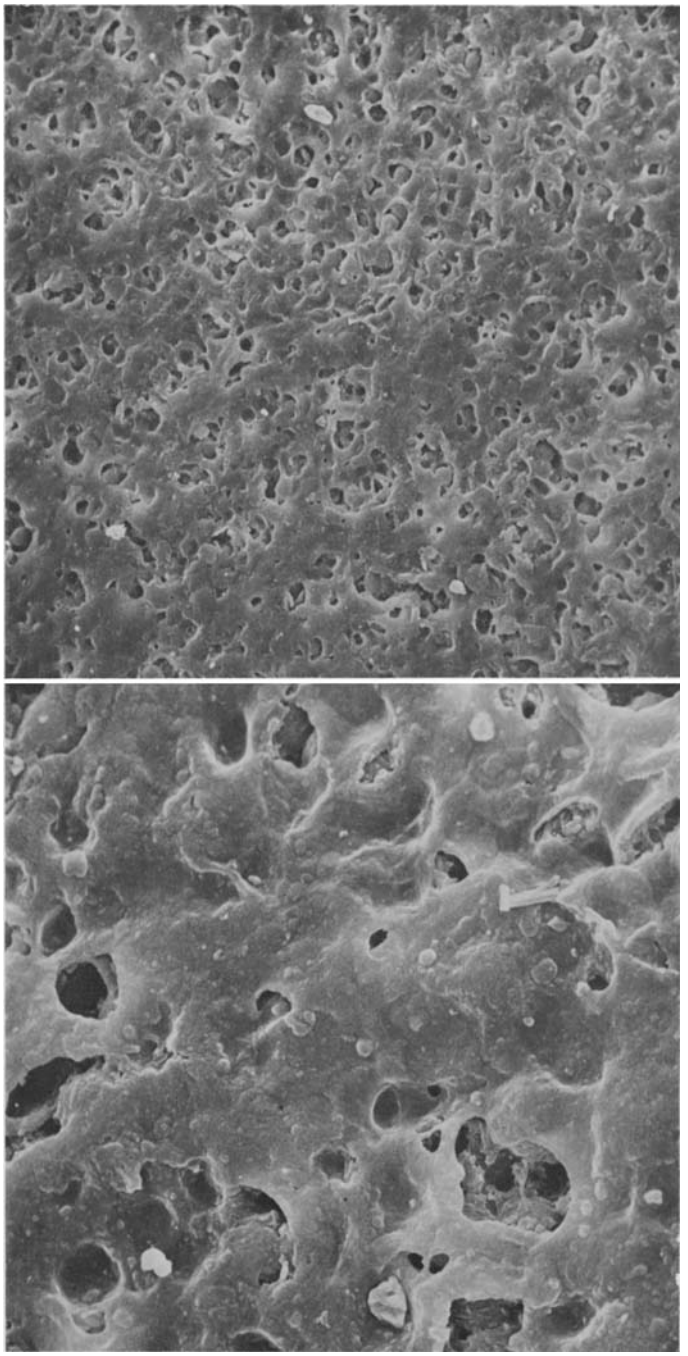

FIGURE 99.—*Parmelia vanderbylii* Zahlbruckner (*van der Byl* s.n., South Africa, holotype in W).

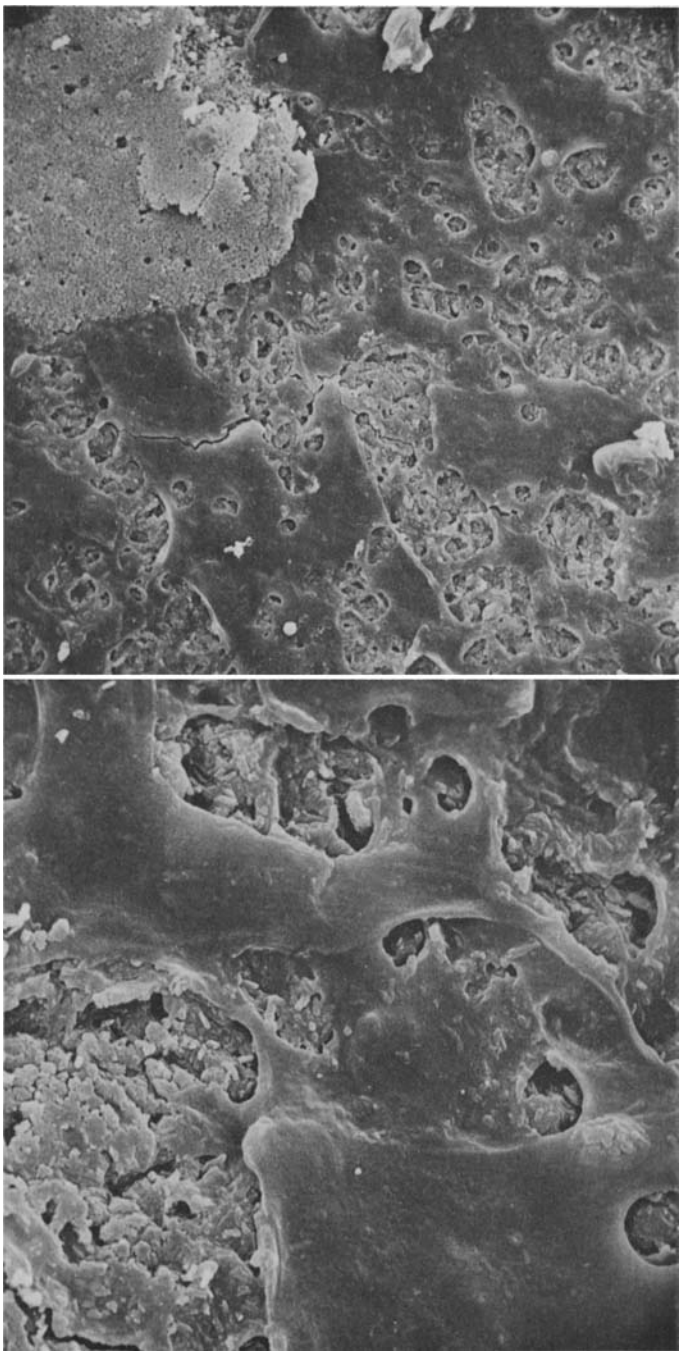

FIGURE 100.—*Parmelia addita* Hale (*Hale* 28342, Sabah, holotype).

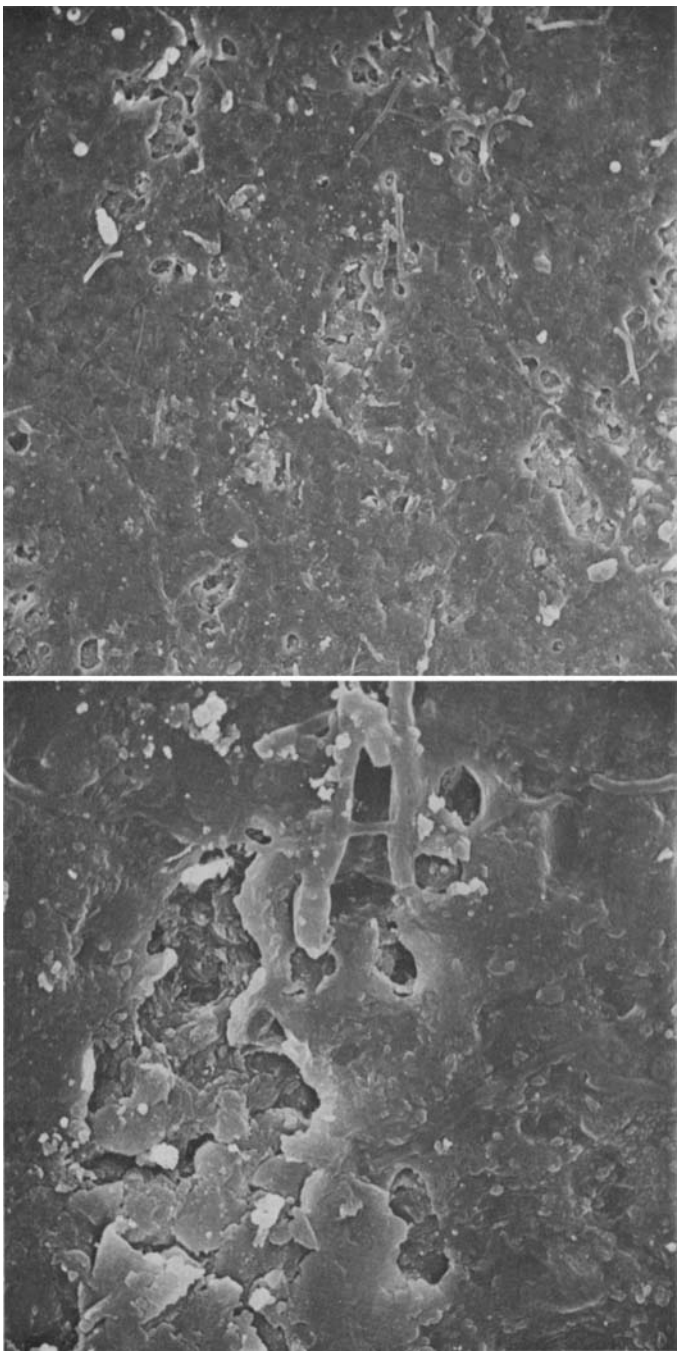

FIGURE 101.—*Parmelia adjuncta* Hale (*Kurokawa* 50110, Japan).

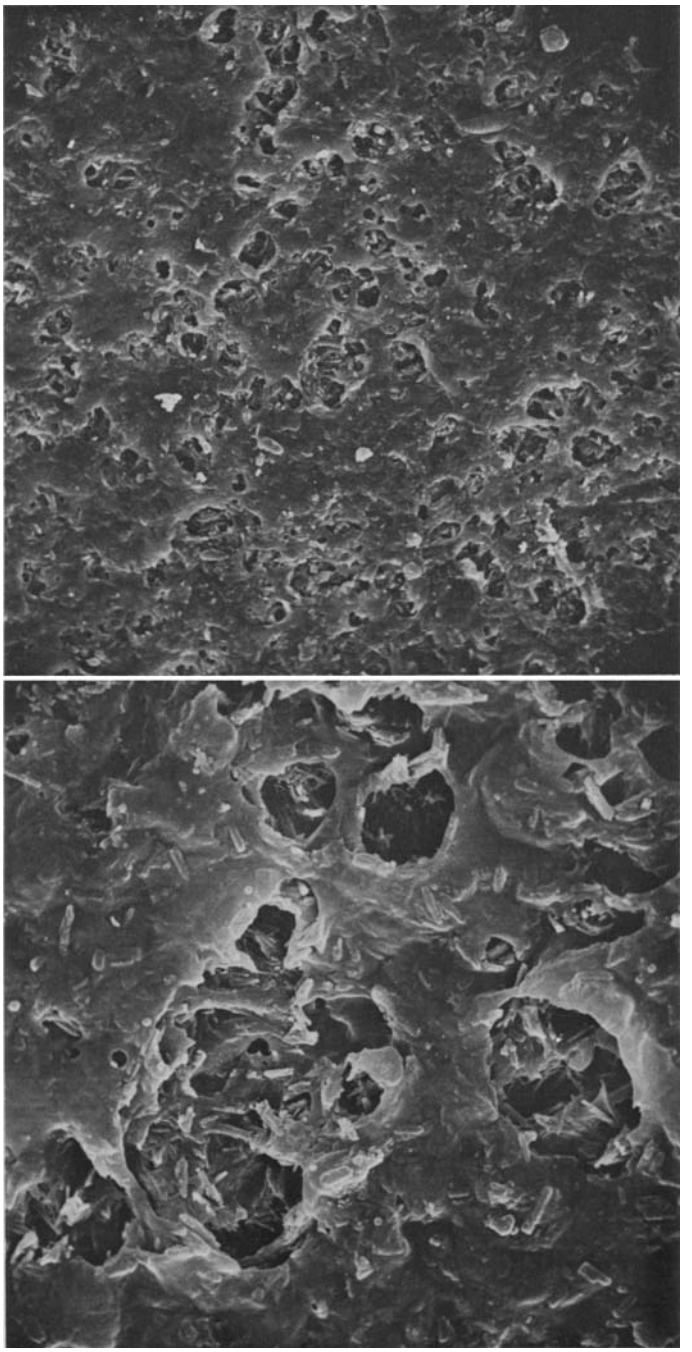

FIGURE 102.—*Parmelia brasiliana* Nylander (*Eiten* 2031, Brazil).

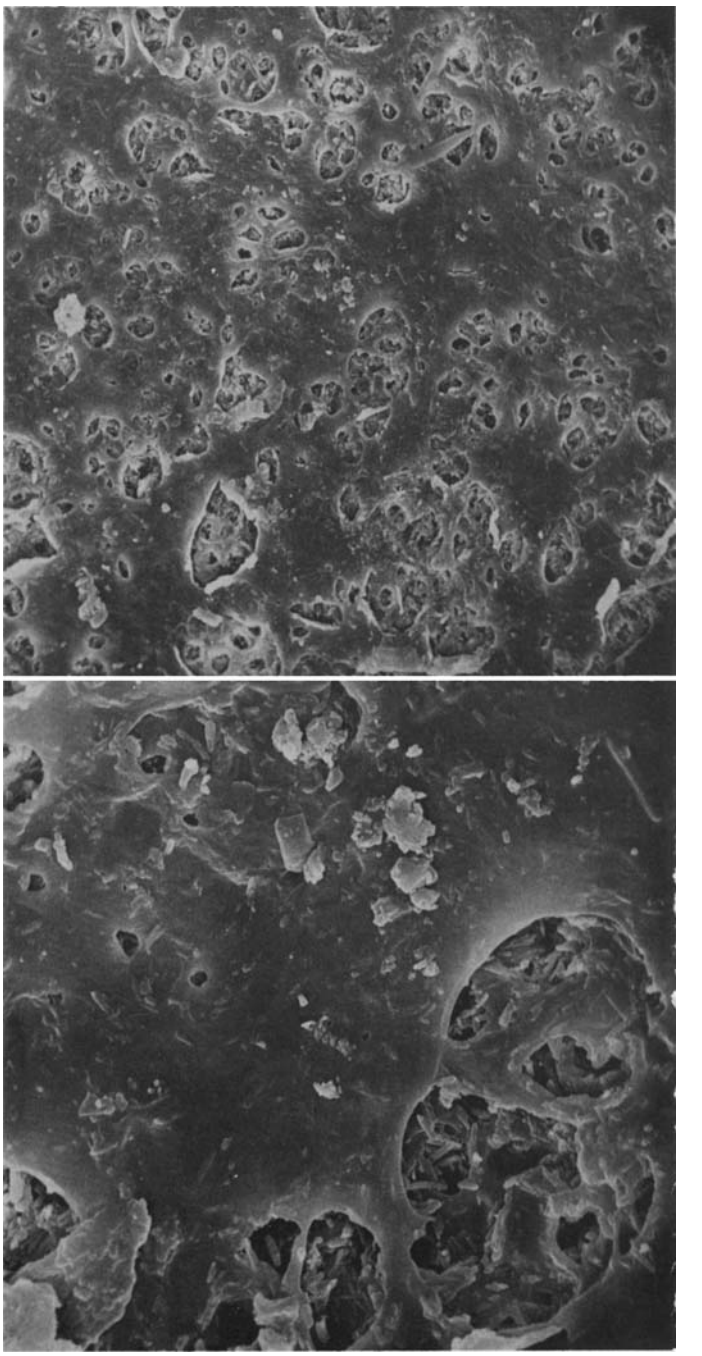

FIGURE 103.—*Parmelia caraccensis* Taylor (*Poelt* 7512, Venezuela).

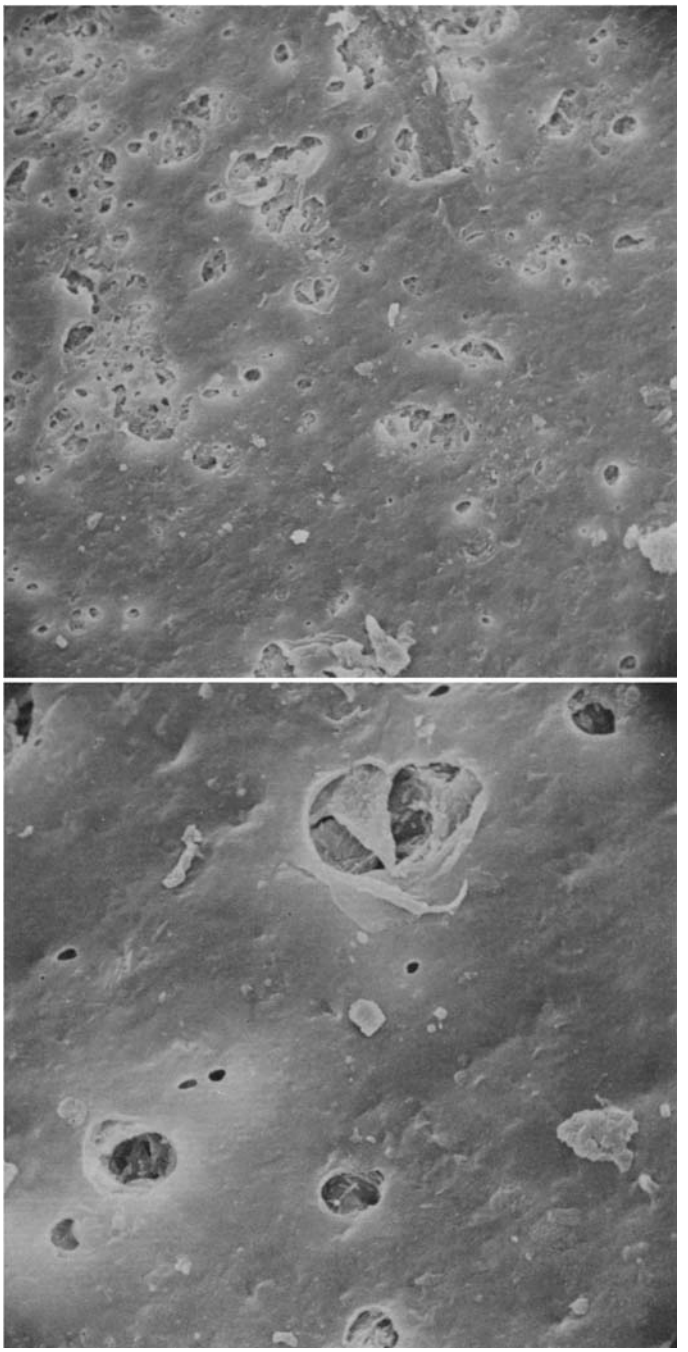

FIGURE 104.—*Parmelia chicitae* Hale (*Culberson* 13210, Costa Rica, holotype).

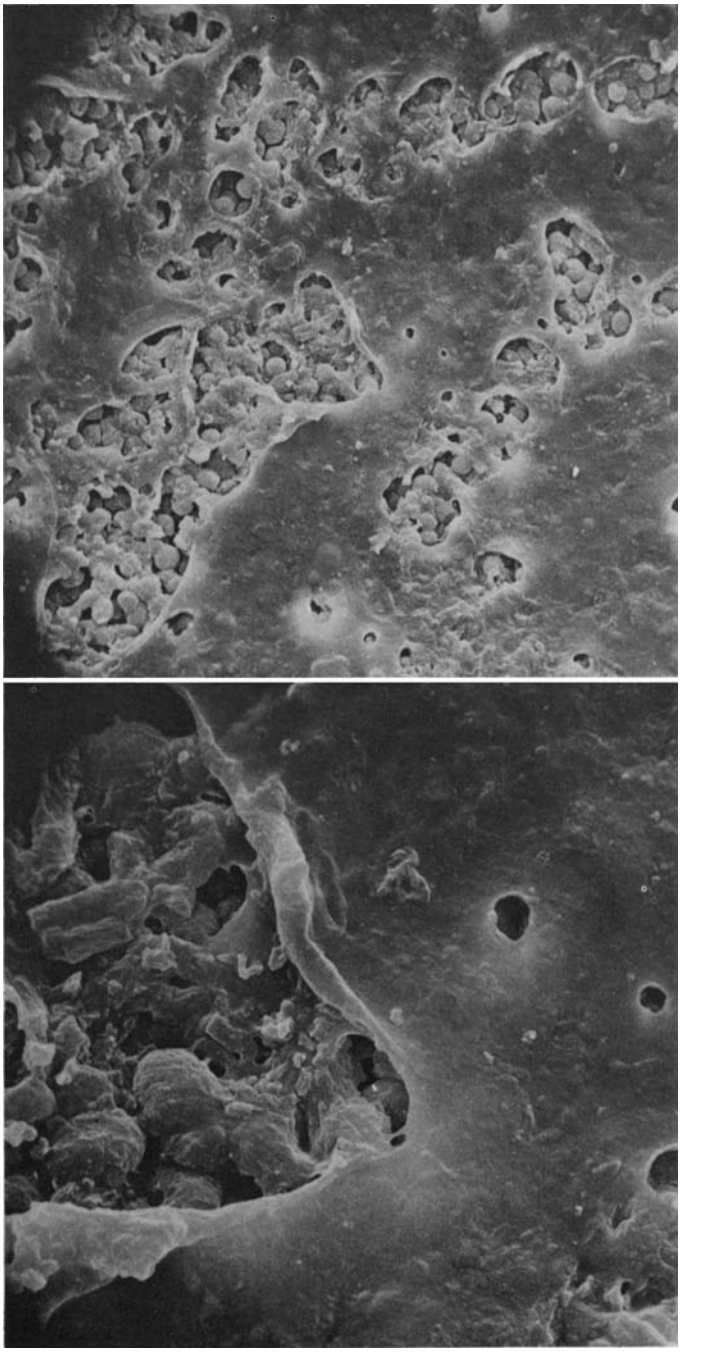

FIGURE 105.—*Parmelia croceopustulata* Kurokawa (*Imshaug* 22275, North Carolina).

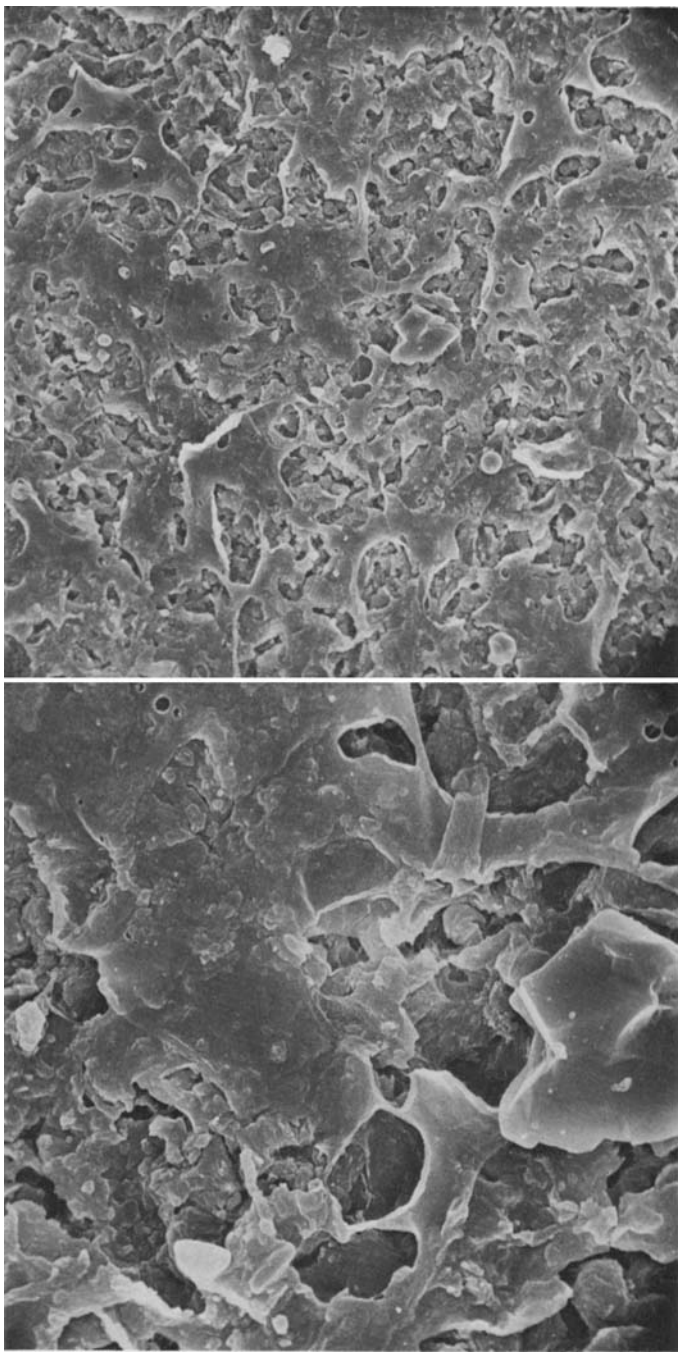

FIGURE 106.—*Parmelia dentella* Hale and Kurokawa (*Hale* 34176, Alabama, topotype).

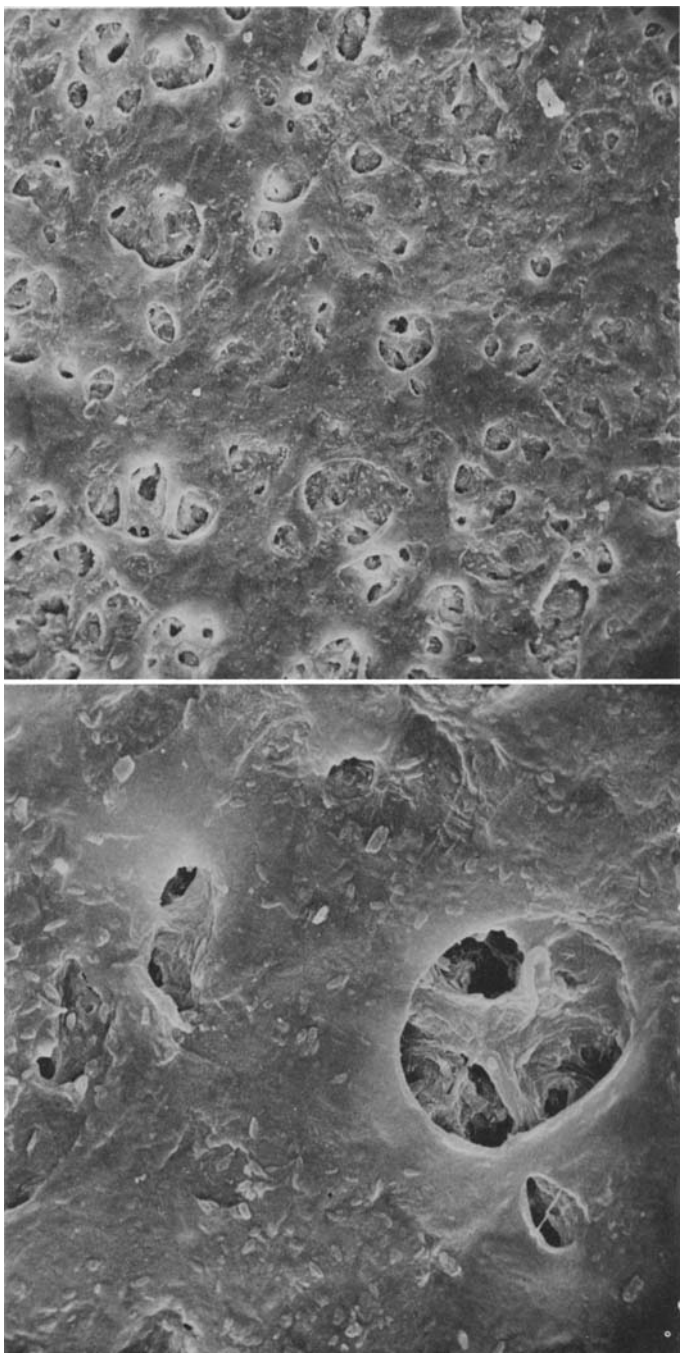

FIGURE 107.—*Parmelia endochlora* Leighton (*Hale* 31300, Hawaii).

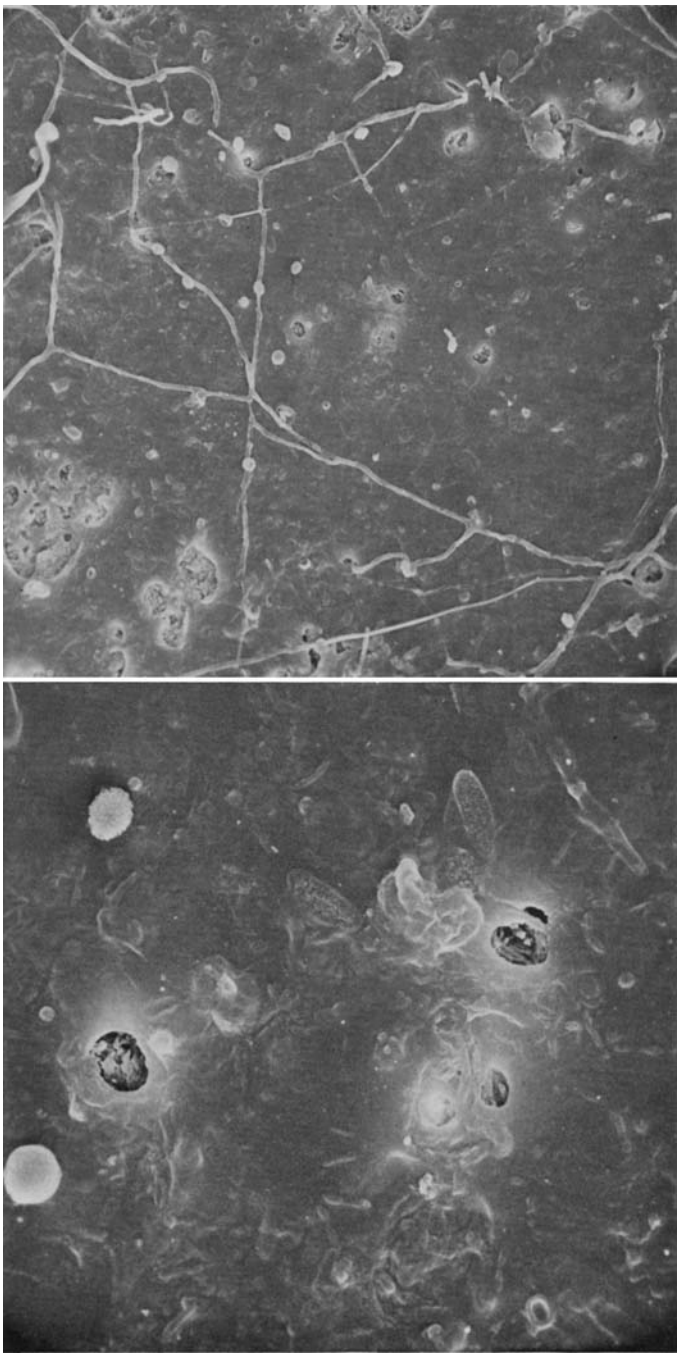

FIGURE 108.—*Parmelia erythrocardia* Zahlbruckner (*Damazio* 1761, Brazil, holotype in W).

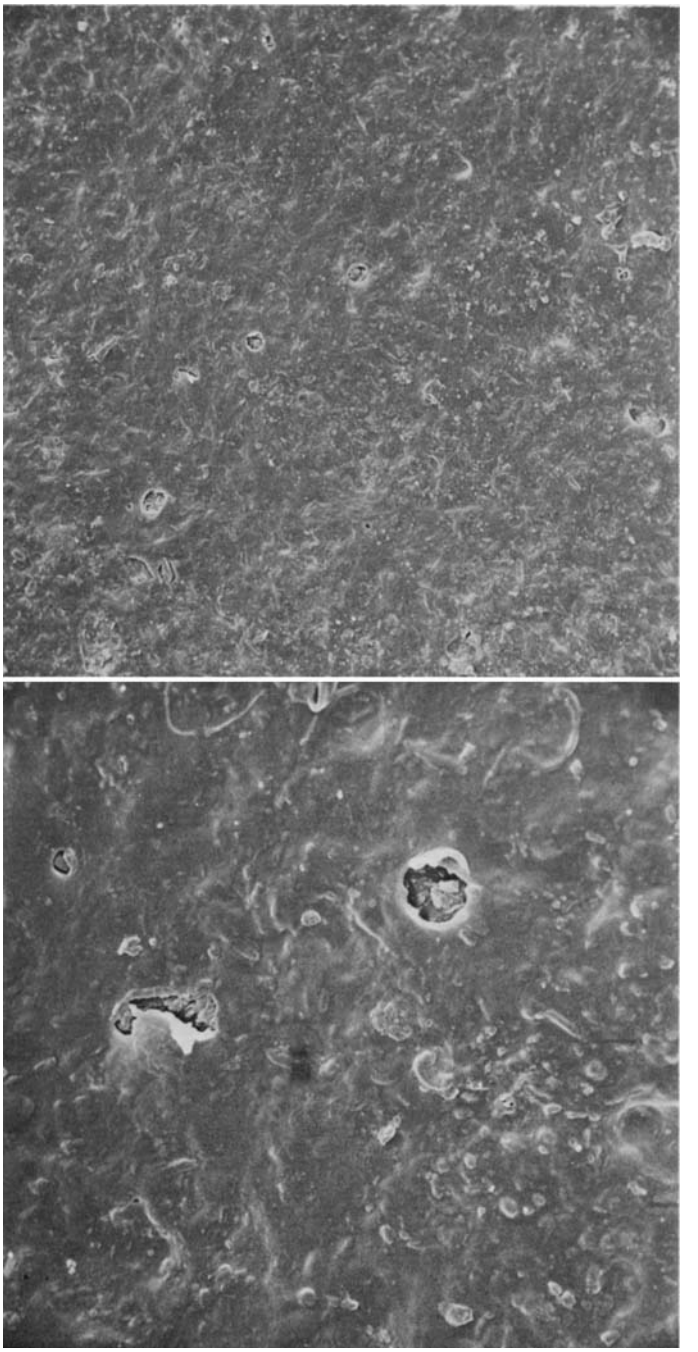

FIGURE 109.—*Parmelia exsecta* Taylor (*Hale* 26103, Philippines).

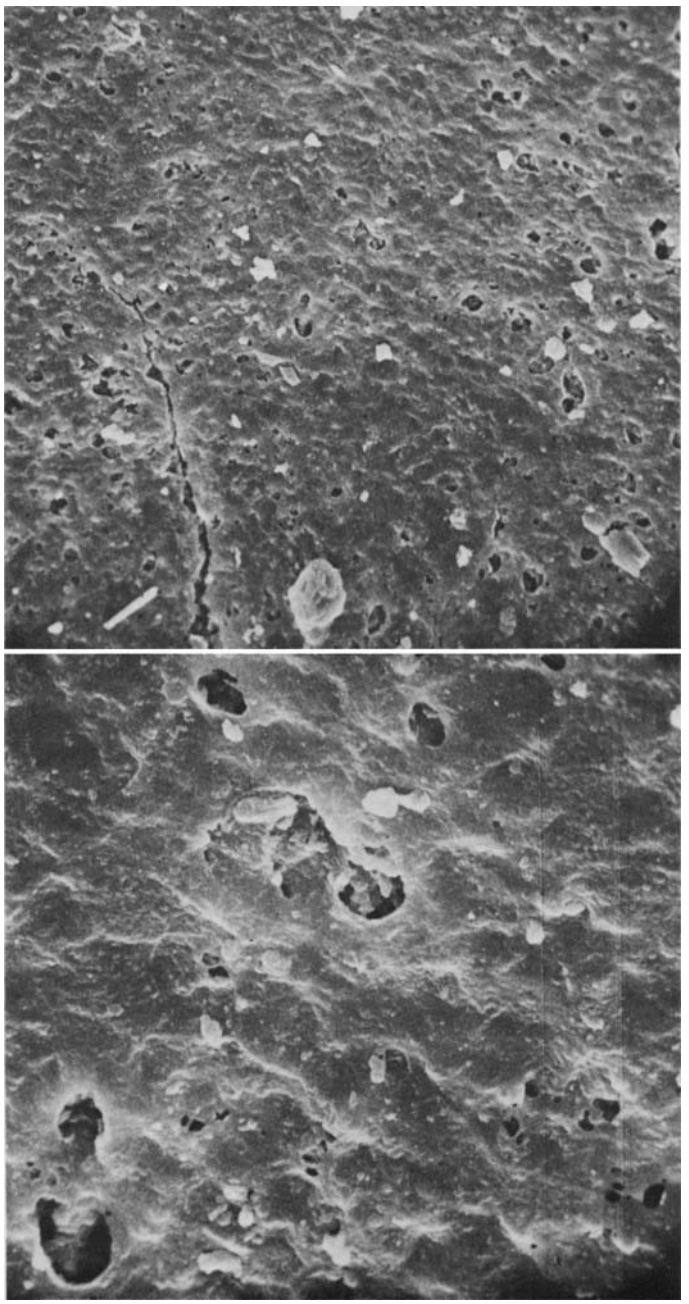

FIGURE 110.—*Parmelia fissicarpa* Kurokawa (*Almborn* 8374, South Africa, holotype).

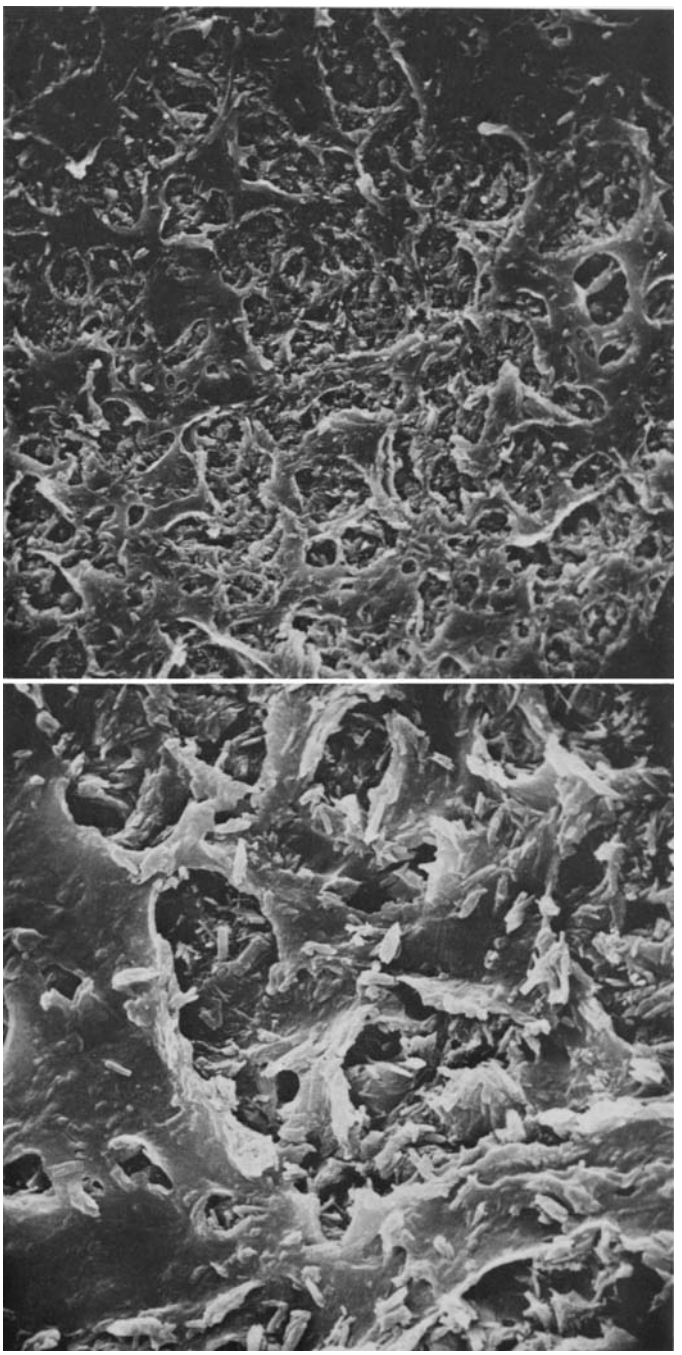

FIGURE 111.—*Parmelia formosana* Zahlbruckner (*Hale* 17503, Florida).

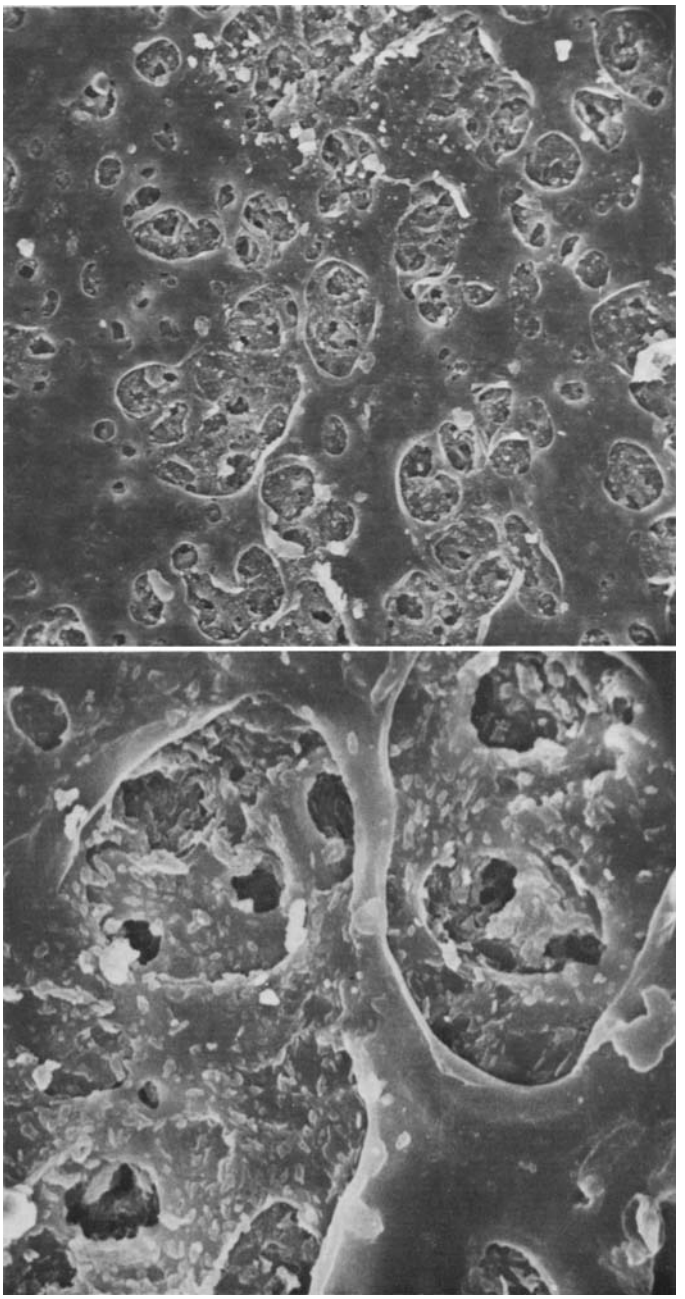

FIGURE 112.—*Parmelia gigas* Kurokawa (*Killip* 18394, Colombia).

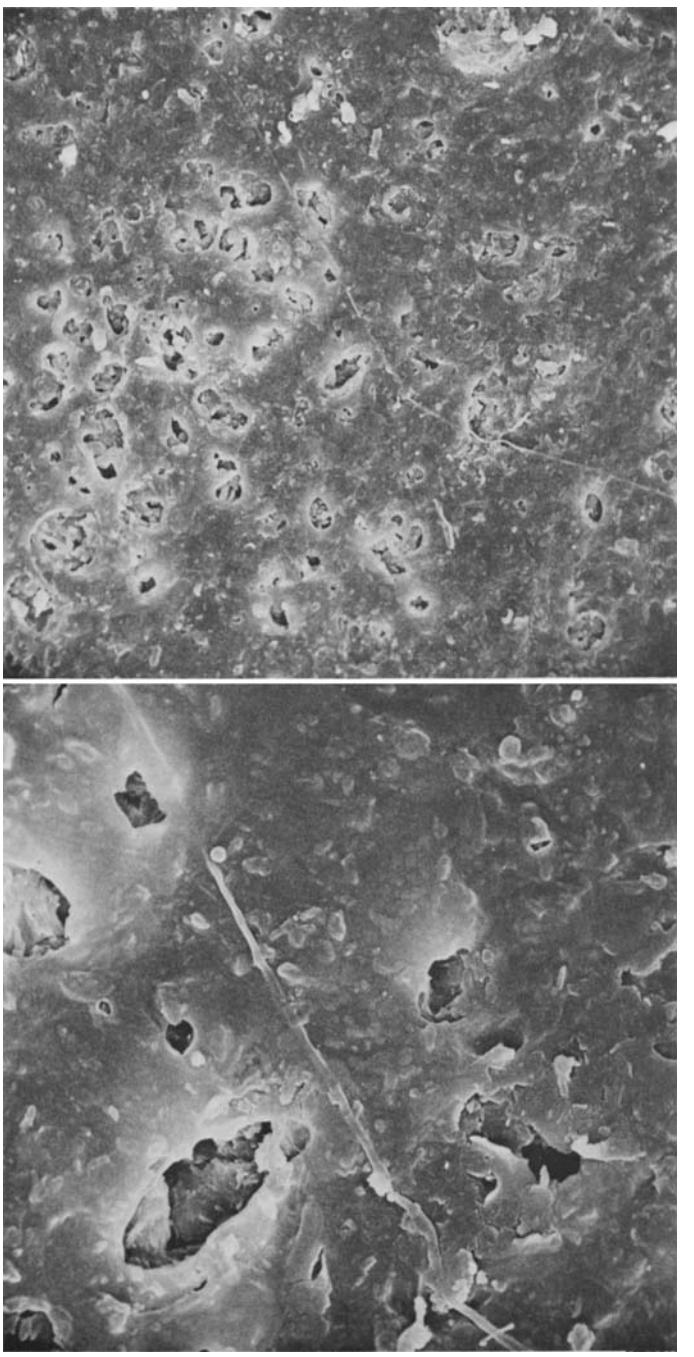

FIGURE 113.—*Parmelia imbricatula* Zahlbruckner (*Kurokawa* 2181, Java).

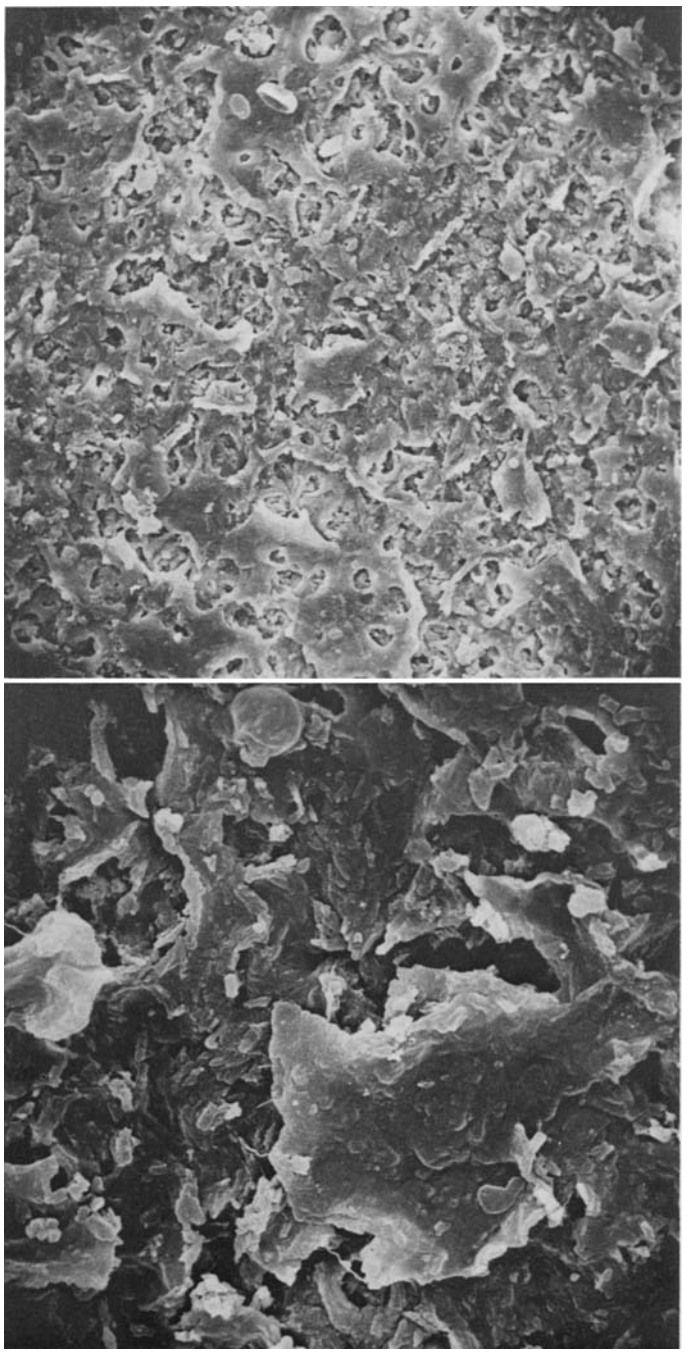

FIGURE 114.—*Parmelia laevigata* (Smith) Acharius (*Yoshimura* 650533, Mexico).

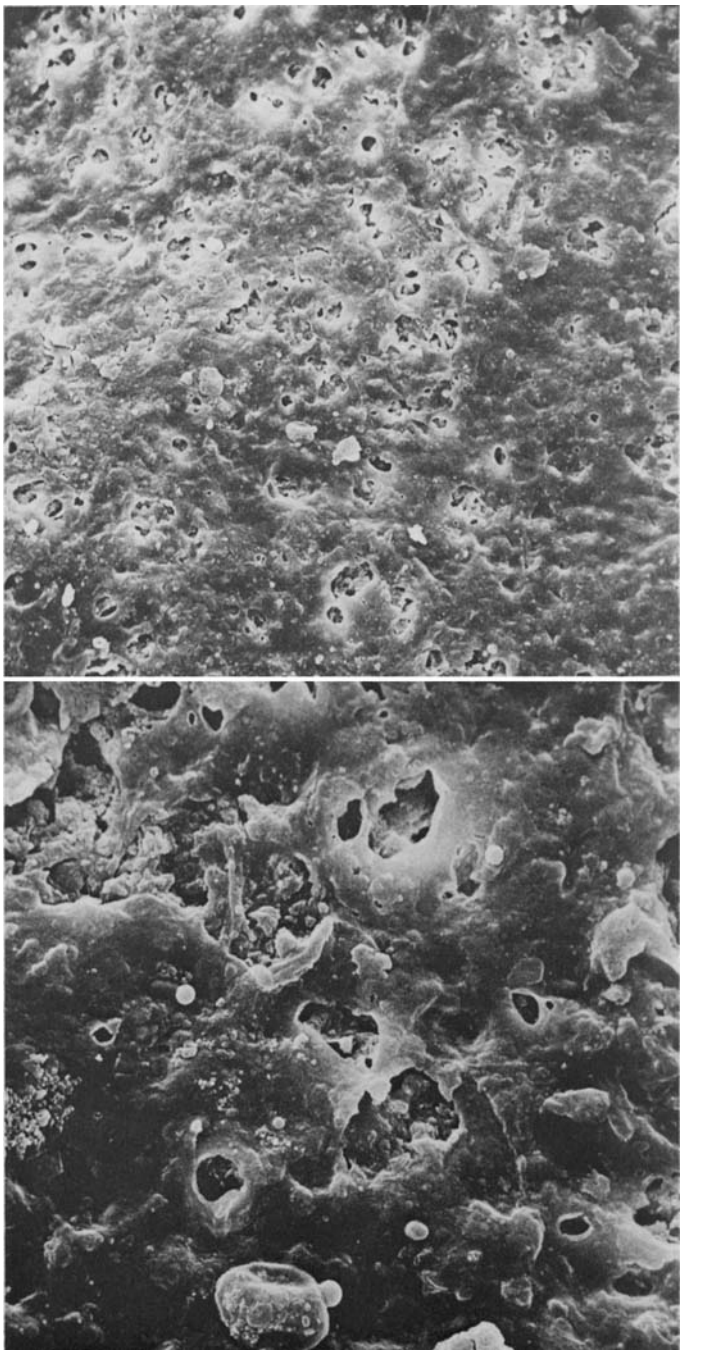

FIGURE 115.—*Parmelia livida* Taylor (*Hale* 15995, Virginia).

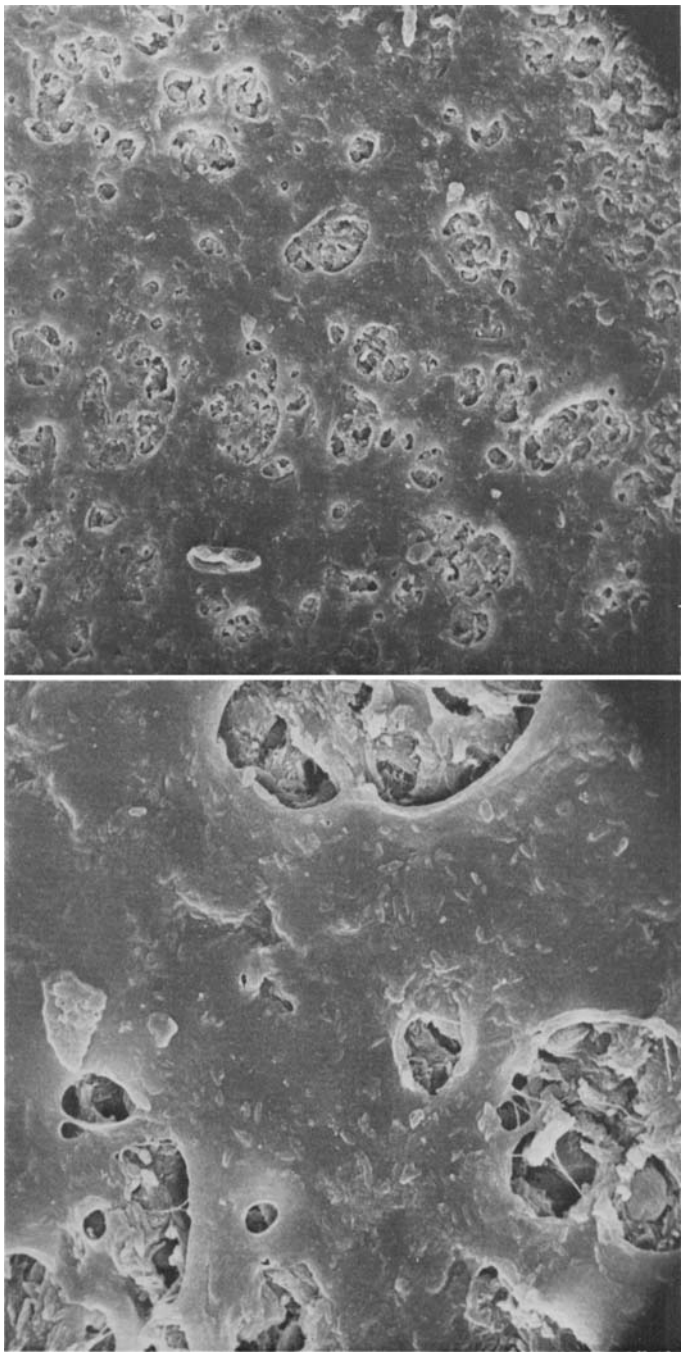

FIGURE 116.—*Parmelia neodissecta* Hale (*Santesson* 10597d, Guinea, holotype).

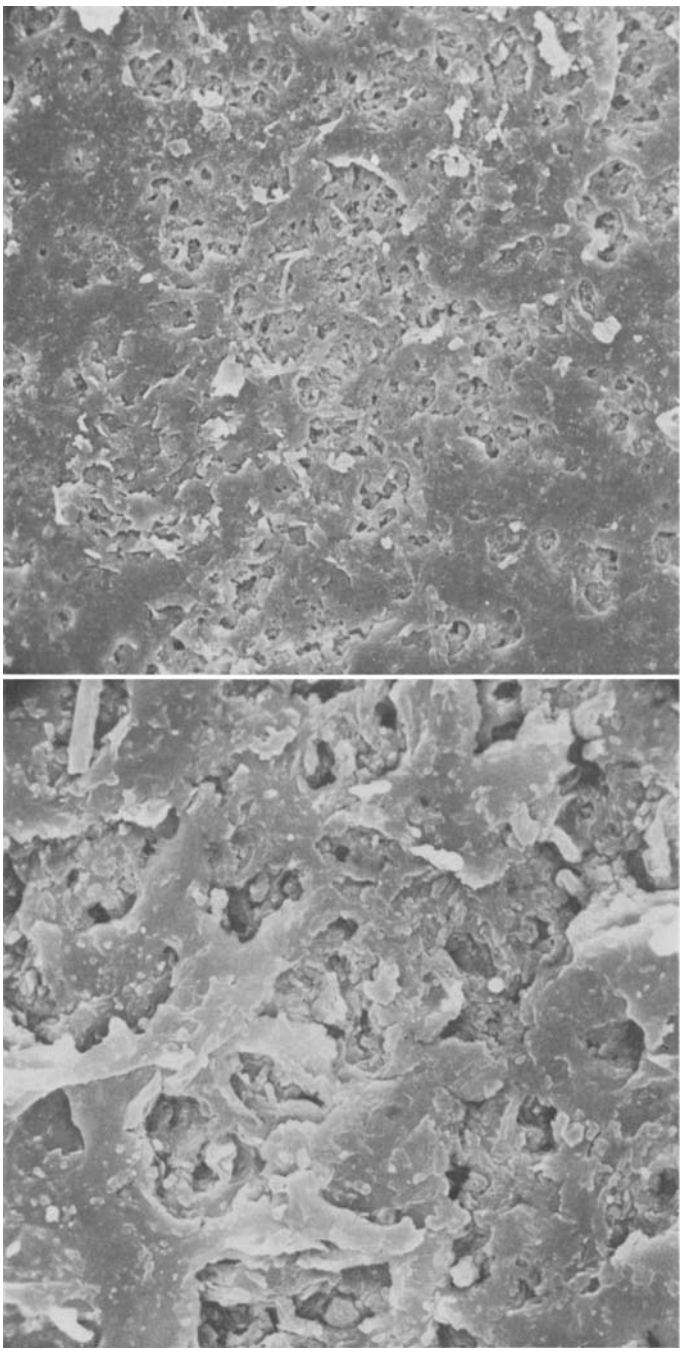

FIGURE 117.—*Parmelia orientalis* Hale (*Togashi* s.n., Nepal).

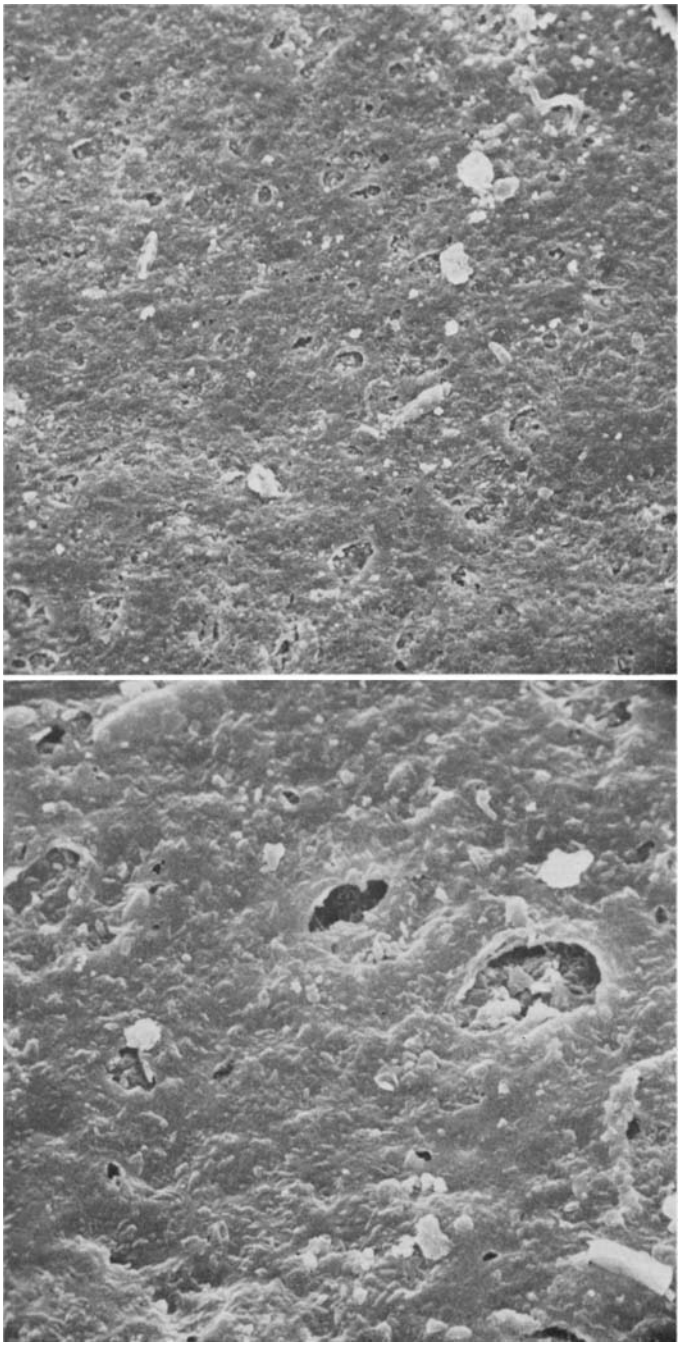

FIGURE 118.—*Parmelia physcioides* Nylander (*King* 472, Colombia).

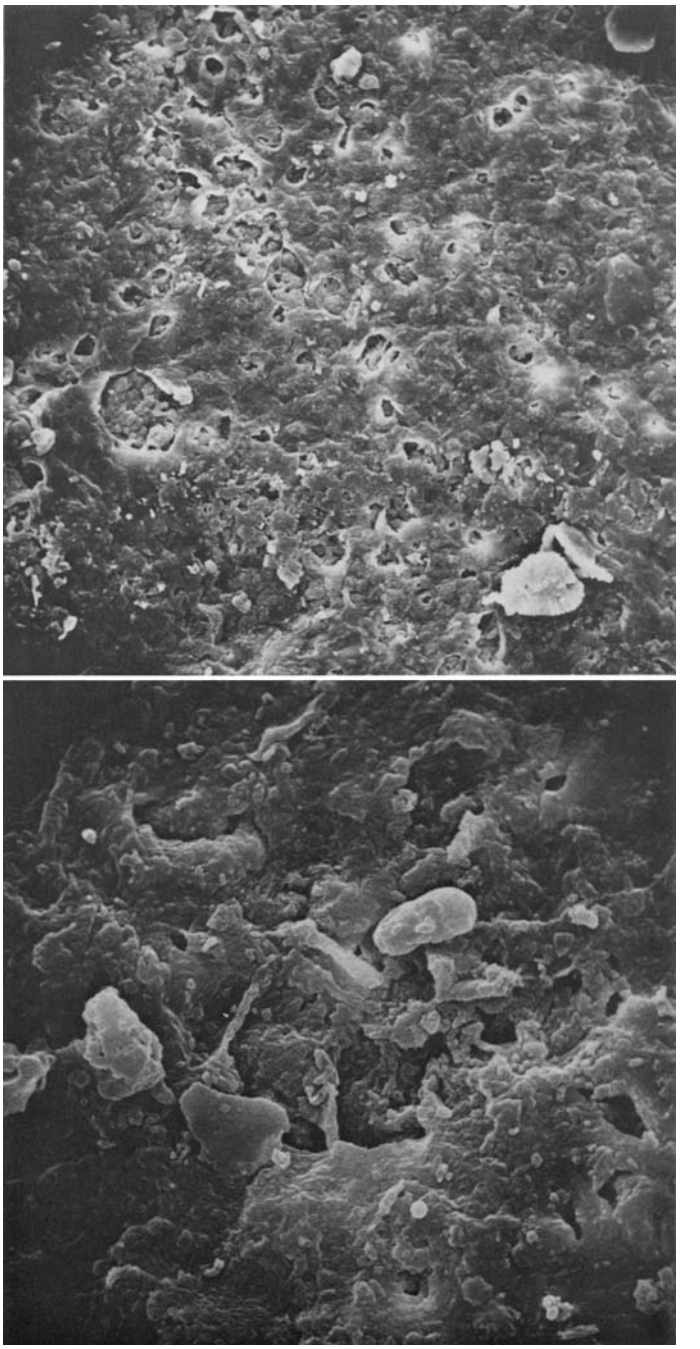

FIGURE 119.—*Parmelia pustulifera* Hale (*Hale* 30865, Georgia, holotype).

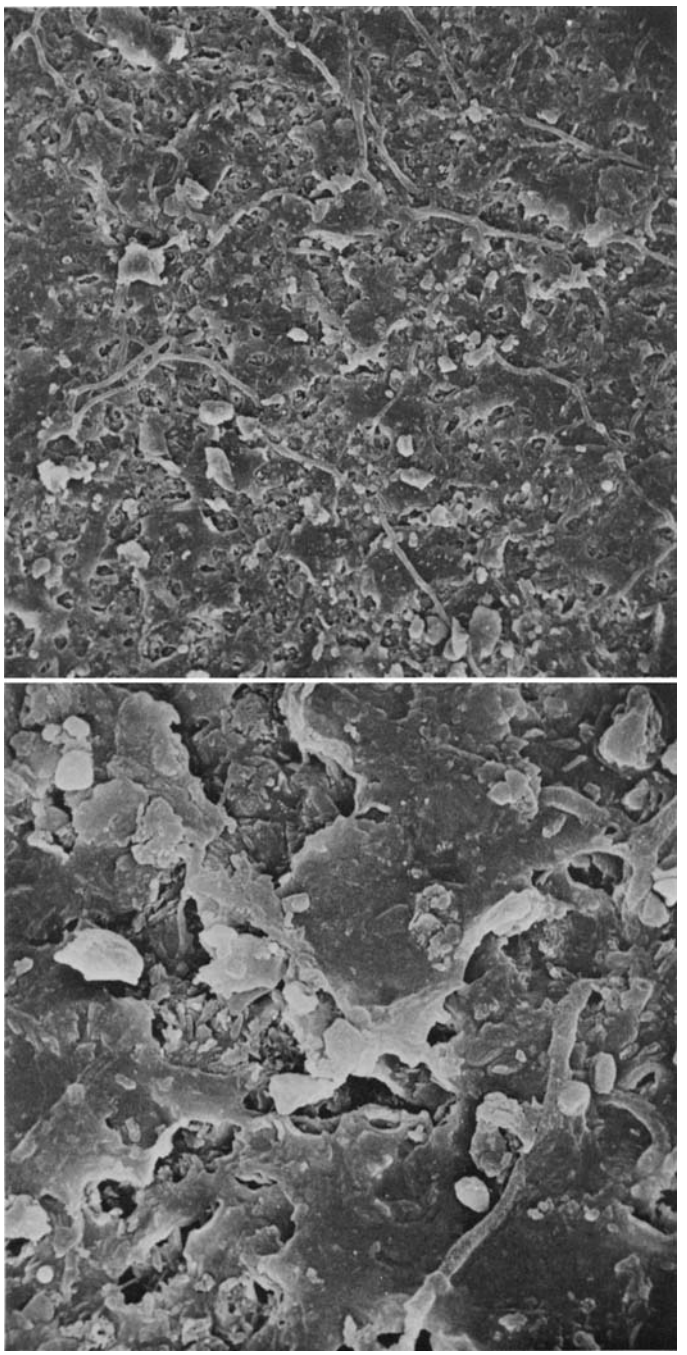

FIGURE 120.—*Parmelia scytodes* Kurokawa (*Togashi* s.n., India, isotype).

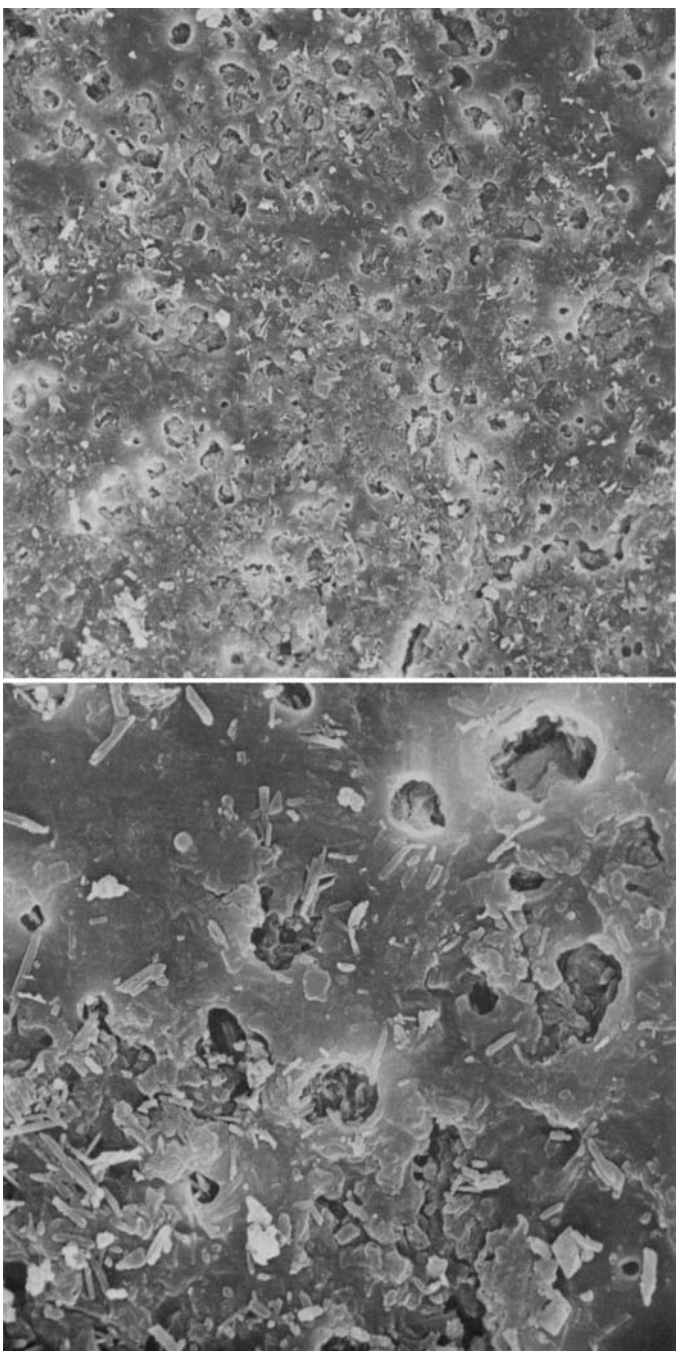

FIGURE 121.—*Parmelia sinuosa* (Smith) Acharius (*Steiner* 283 (Lichenes Selecti Exsiccati), Austria).

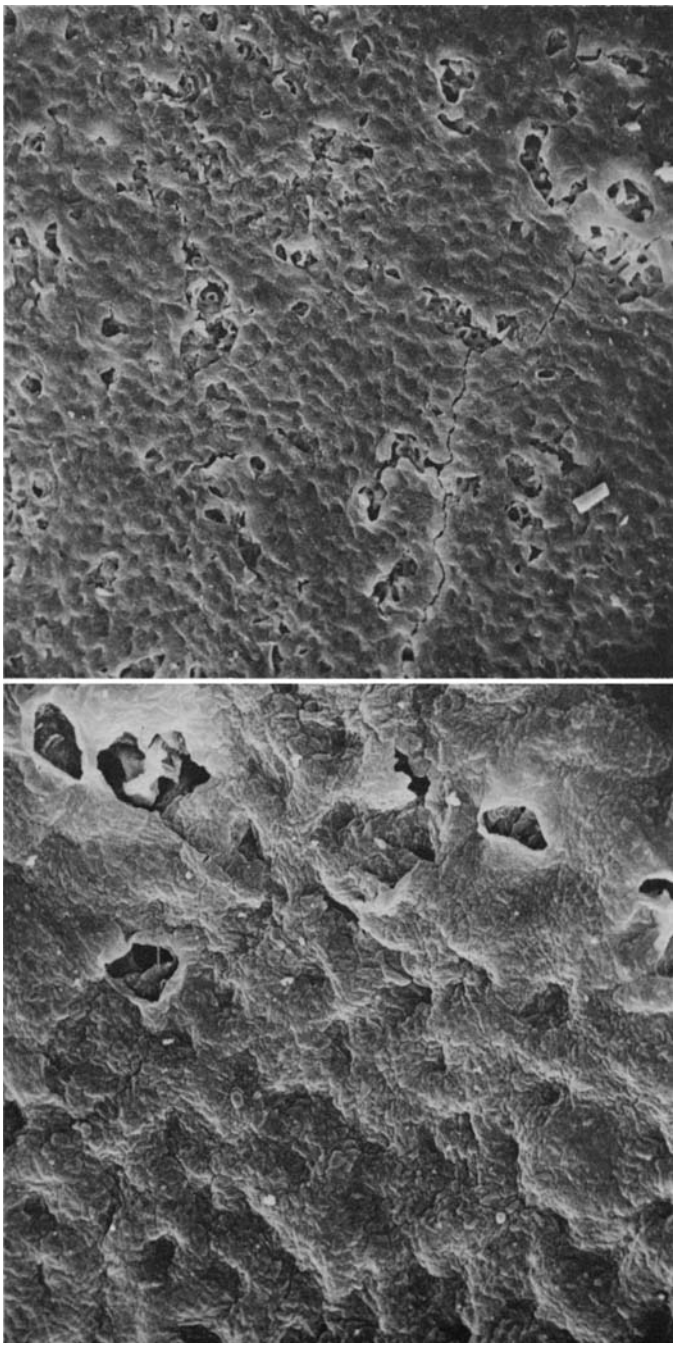

FIGURE 122.—*Parmelia americana* (Meyen and Flotow) Vainio (*Mahu* 2130, Chile).

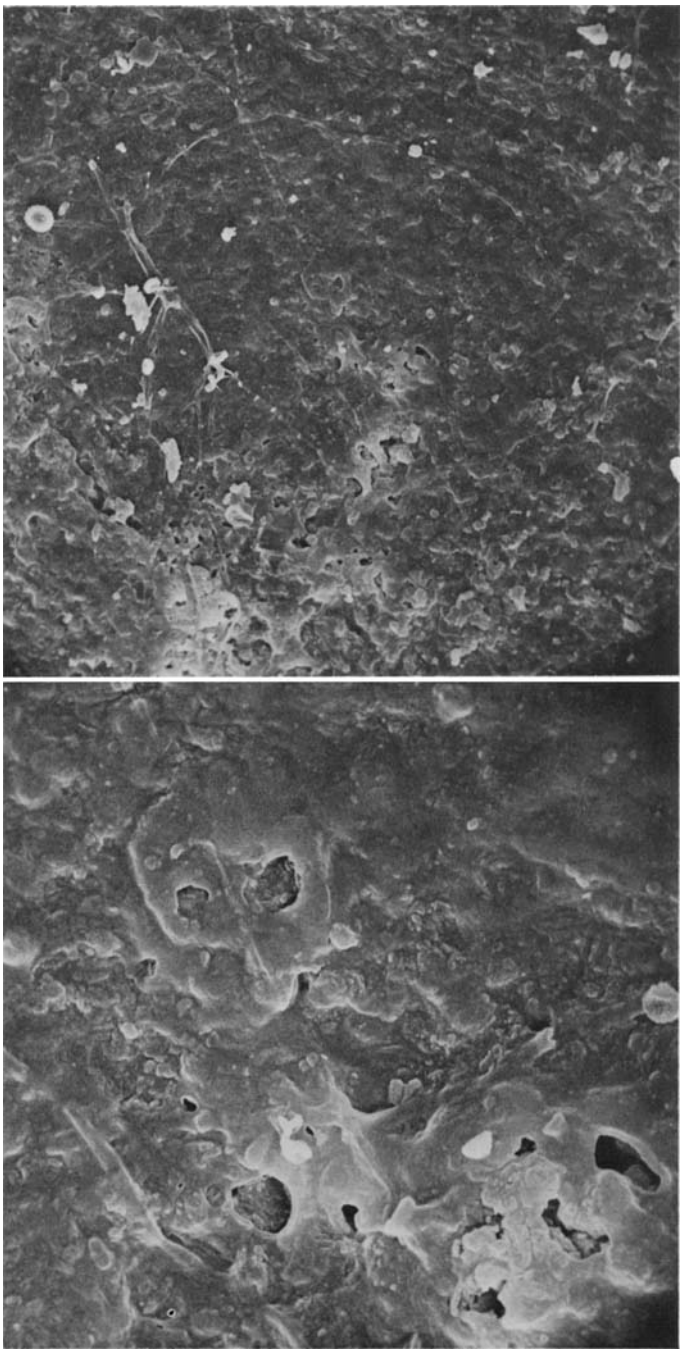

FIGURE 123.—*Parmelia neocirrhata* Hale (*Arsène* 3726, Mexico, holotype).

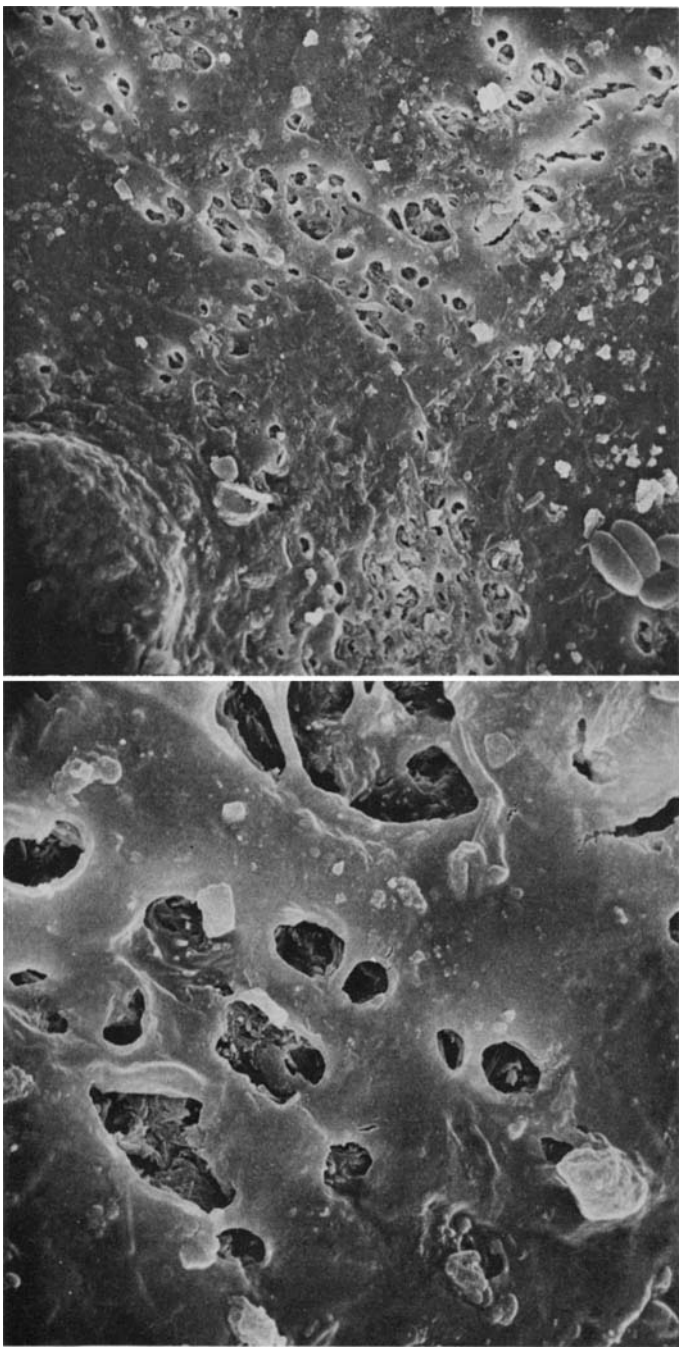

FIGURE 124.—*Parmelia pseudonepalensis* Hale (*Pringle* 10713, Mexico, holotype).

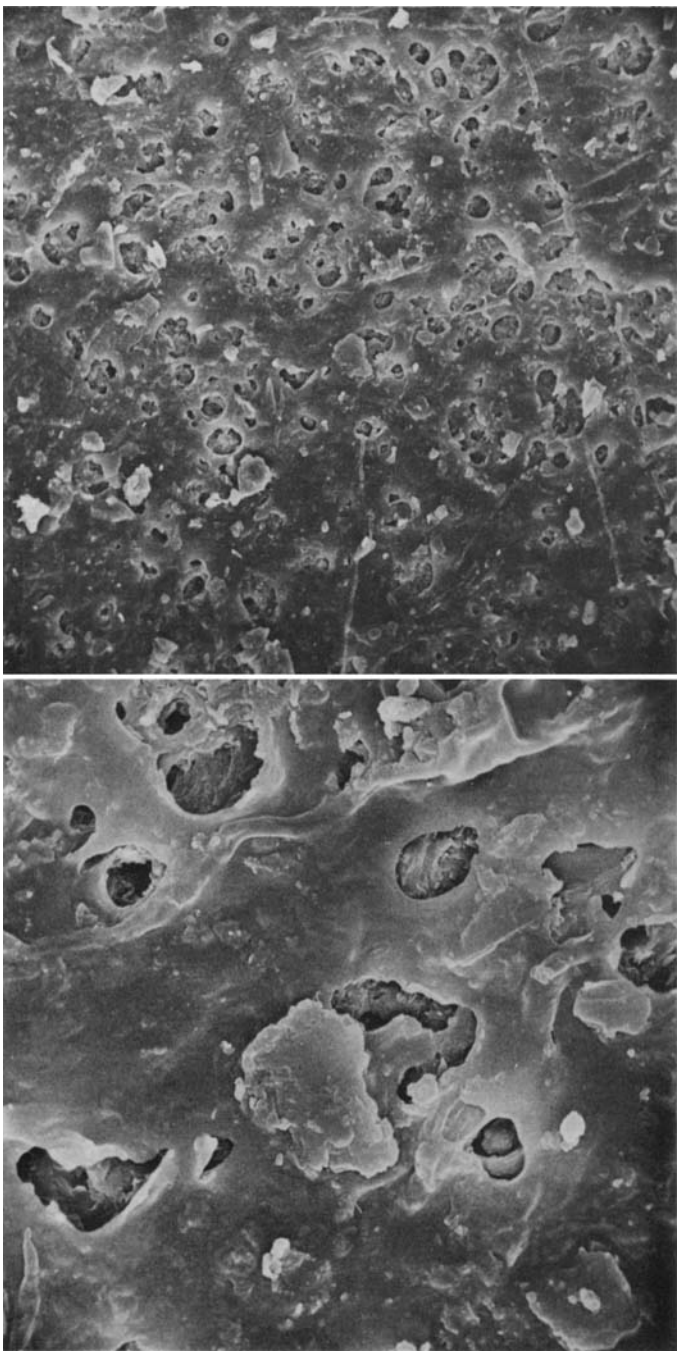

FIGURE 125.—*Parmelia vexans* Zahlbruckner (*Asahina* s.n., Taiwan, holotype in TNS).

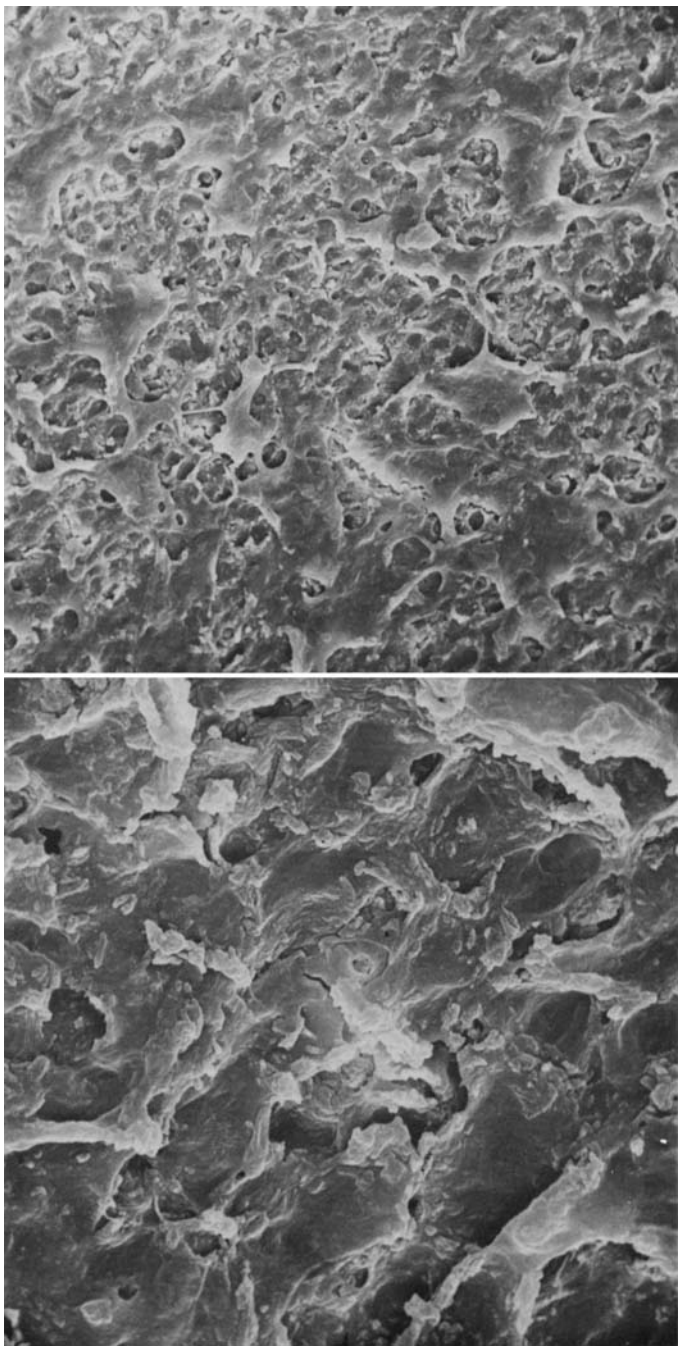

FIGURE 126.—*Parmelia cristifera* Taylor (*Hale* 35800, Dominica).

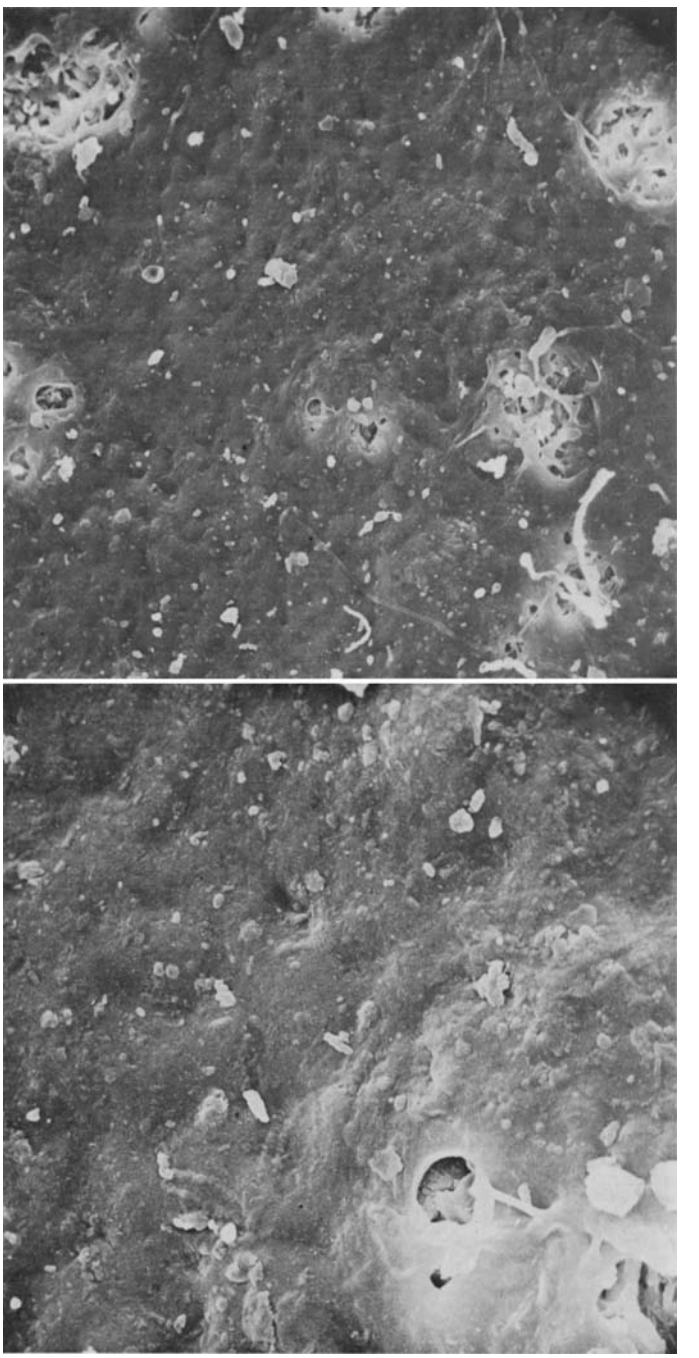

FIGURE 127.—*Parmelia haitiensis* Hale (*Orcutt* 2987, Jamaica, holotype).

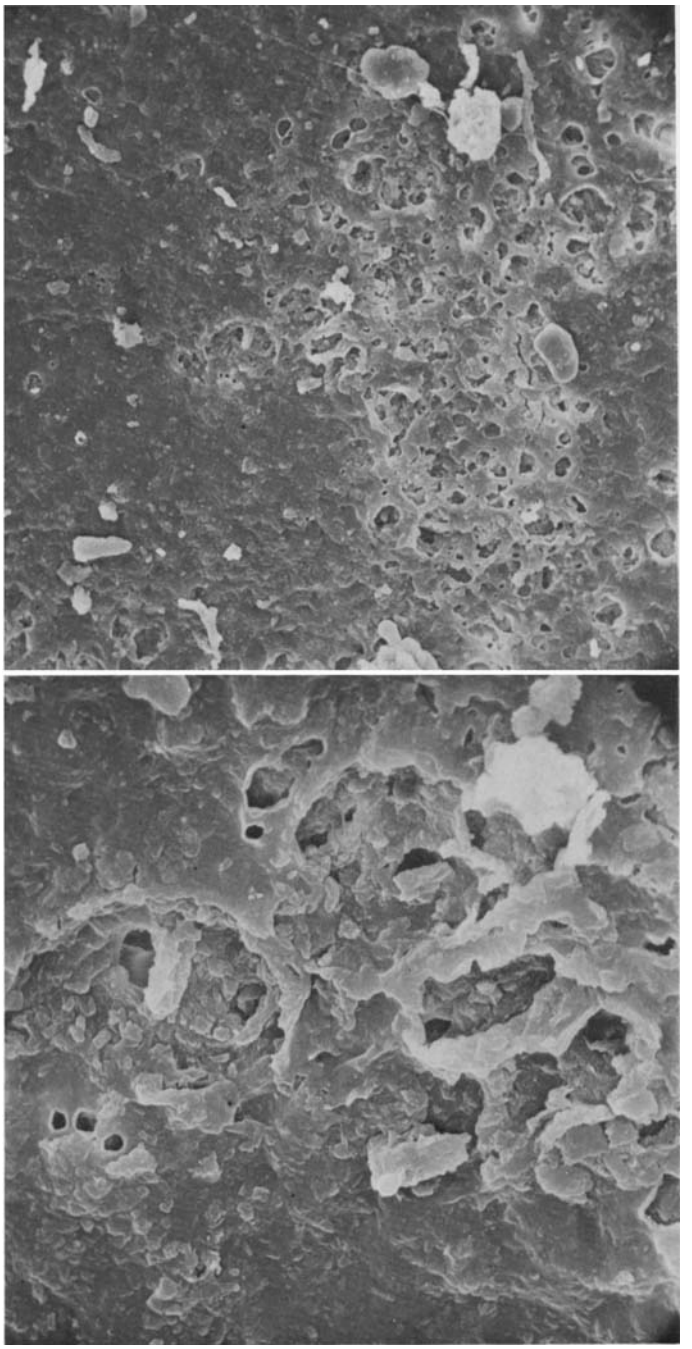

FIGURE 128.—*Parmelia hypoleucina* Steiner (*Rondon* 963 (Lichenes Selecti Exsiccati), France).

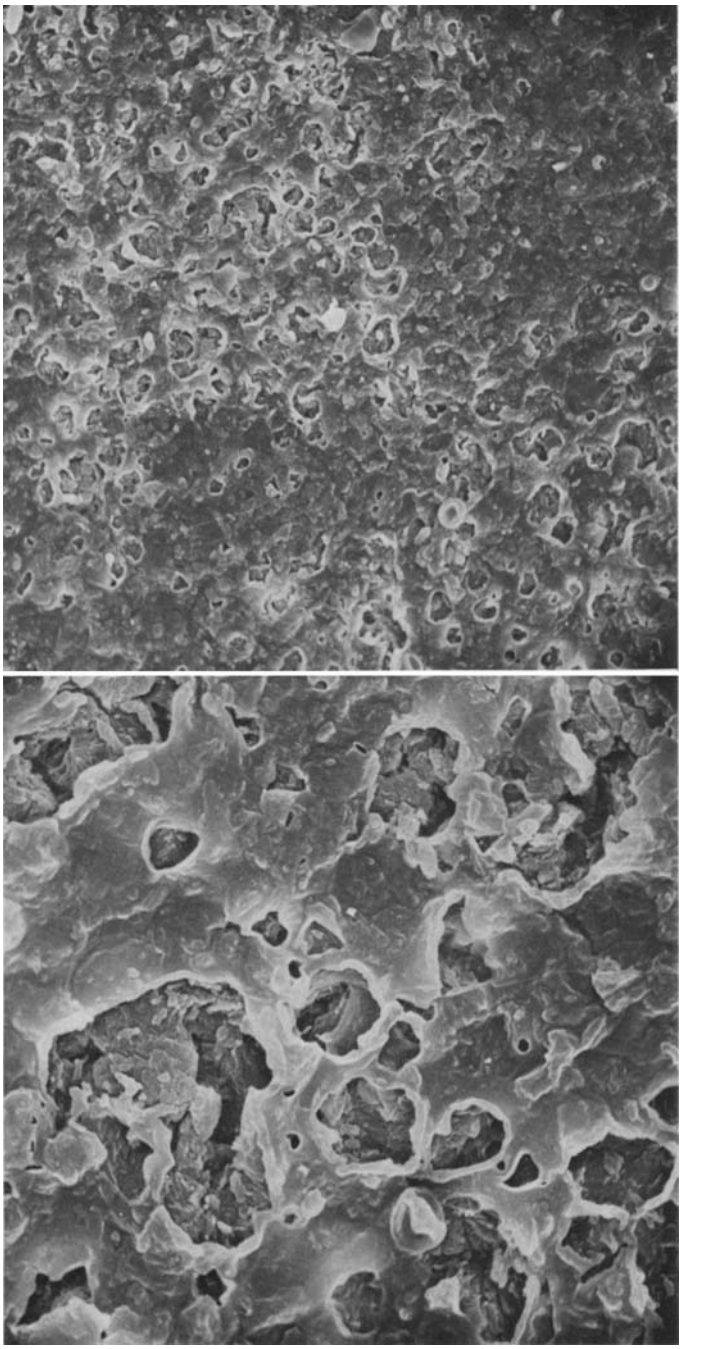

FIGURE 129.—*Parmelia hypotropa* Nylander (*Nakanishi* 72, Tennessee).

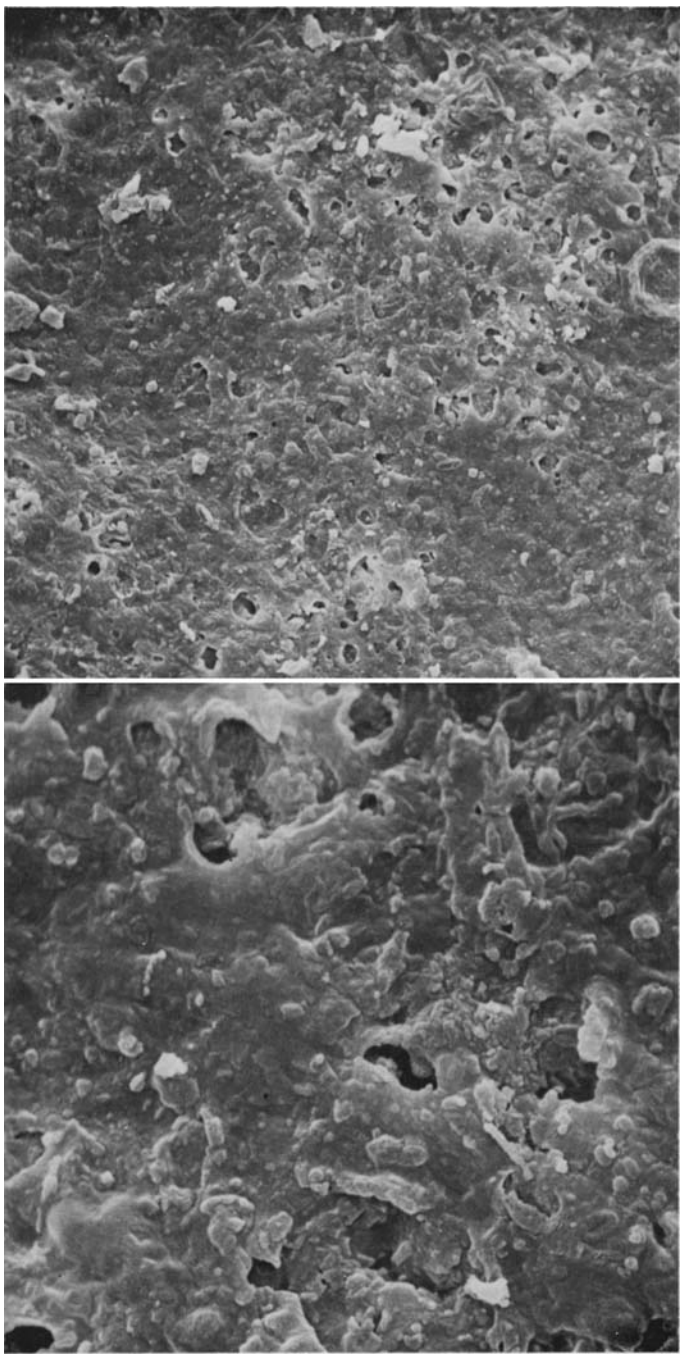

FIGURE 130.—*Parmelia louisianae* Hale (*Hale* 34013, Louisiana, holotype).

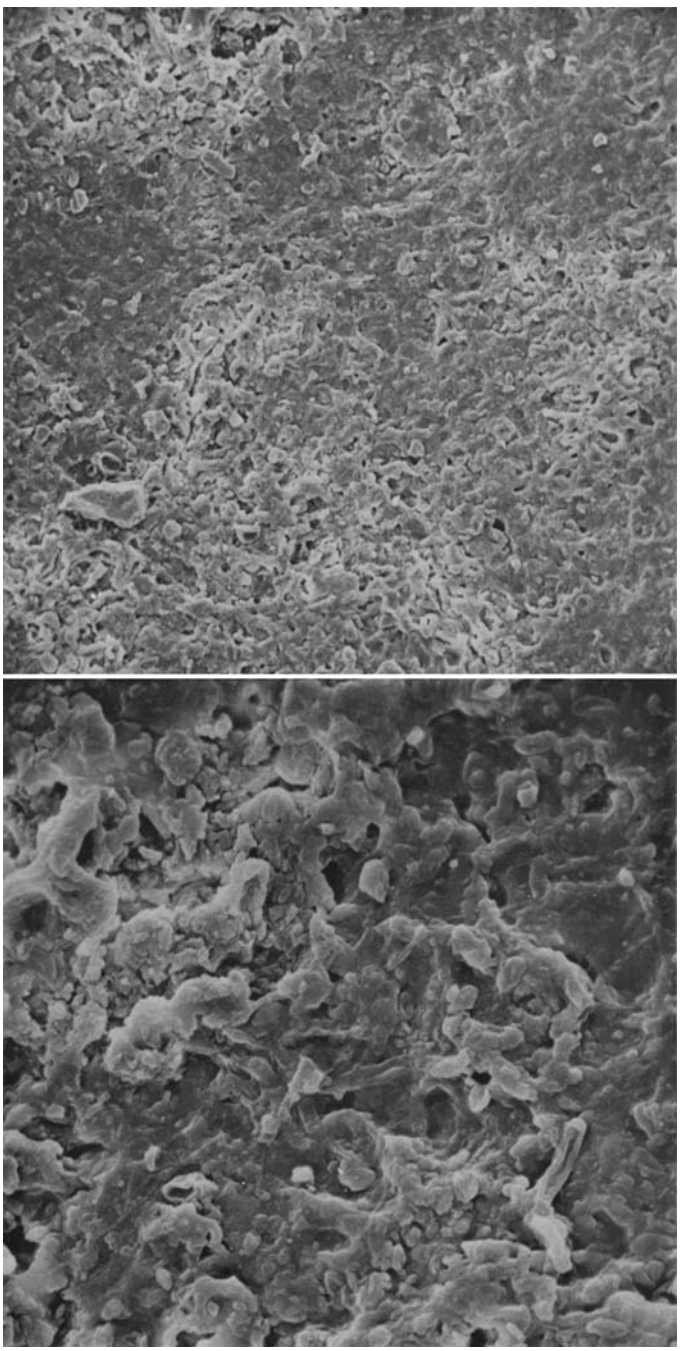

FIGURE 131.—*Parmelia perforata* (Jacquin) Acharius (*Reese* 6407, Louisiana).

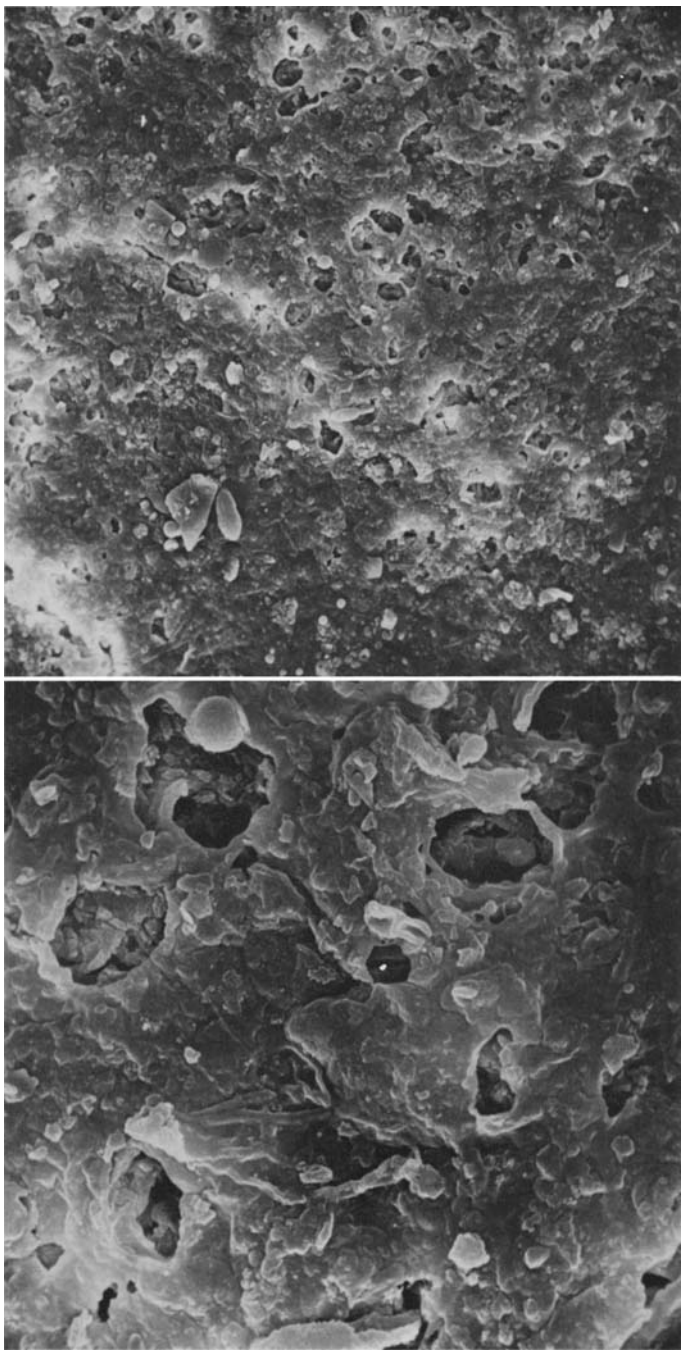

FIGURE 132.—*Parmelia rigida* Lynge (*Moore* 2456, Florida)

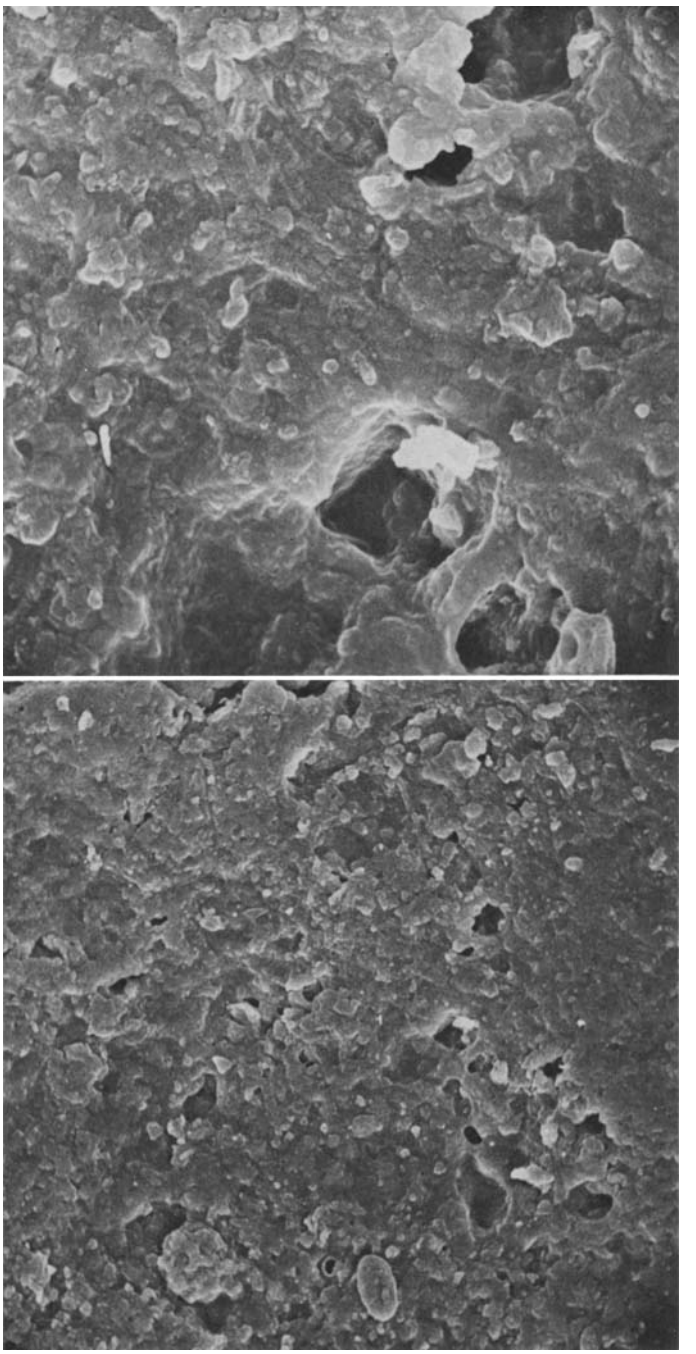

FIGURE 133.—*Parmelia rigida* Lynge (*Malme* 827B, Brazil, holotype in S).

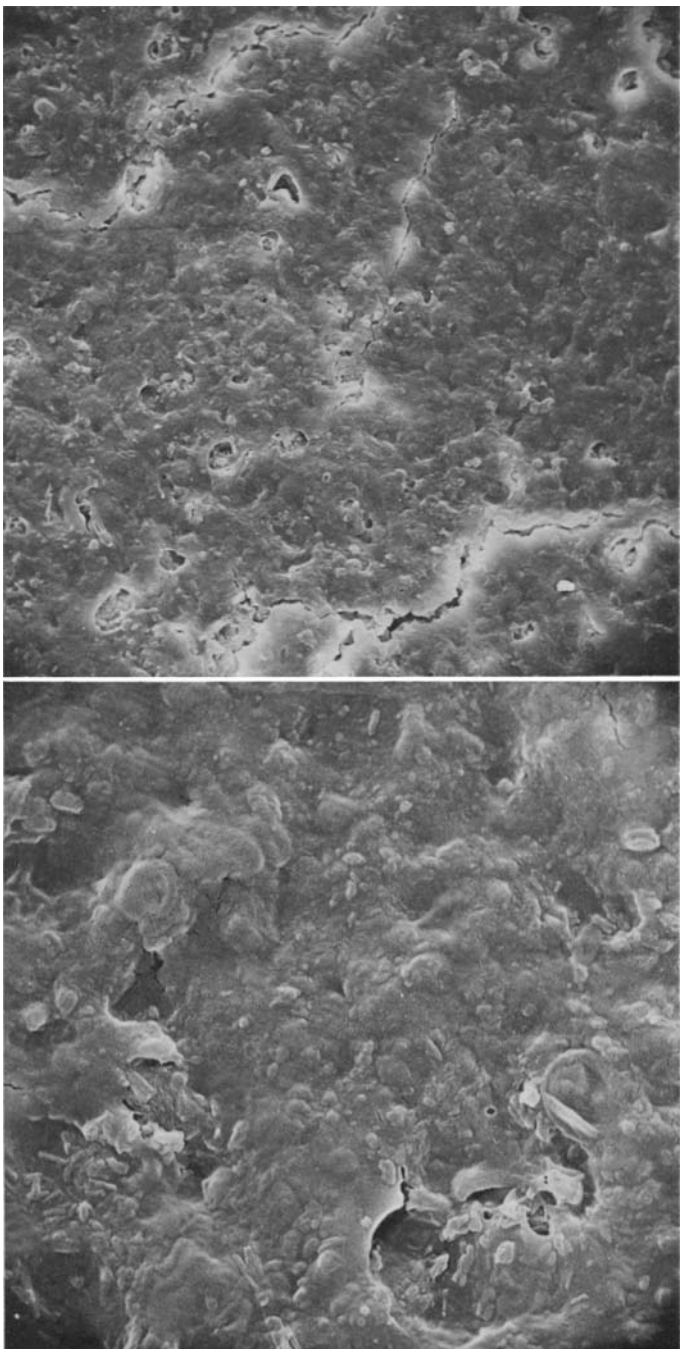

FIGURE 134.—*Parmelia tinctorum* Nylander (*Degelius* P–376, Fiji).

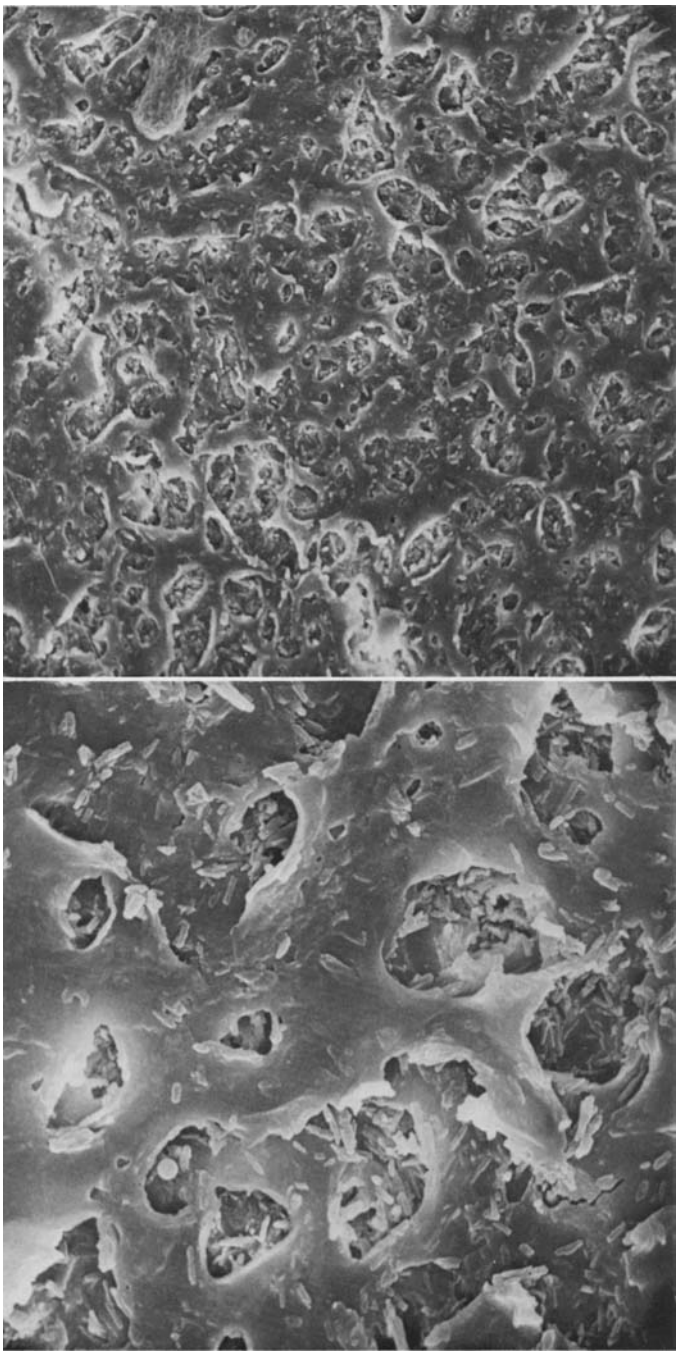

FIGURE 135.—*Parmelia xanthina* (Müller-Argau) Vainio (*Hale* 20594, Mexico).

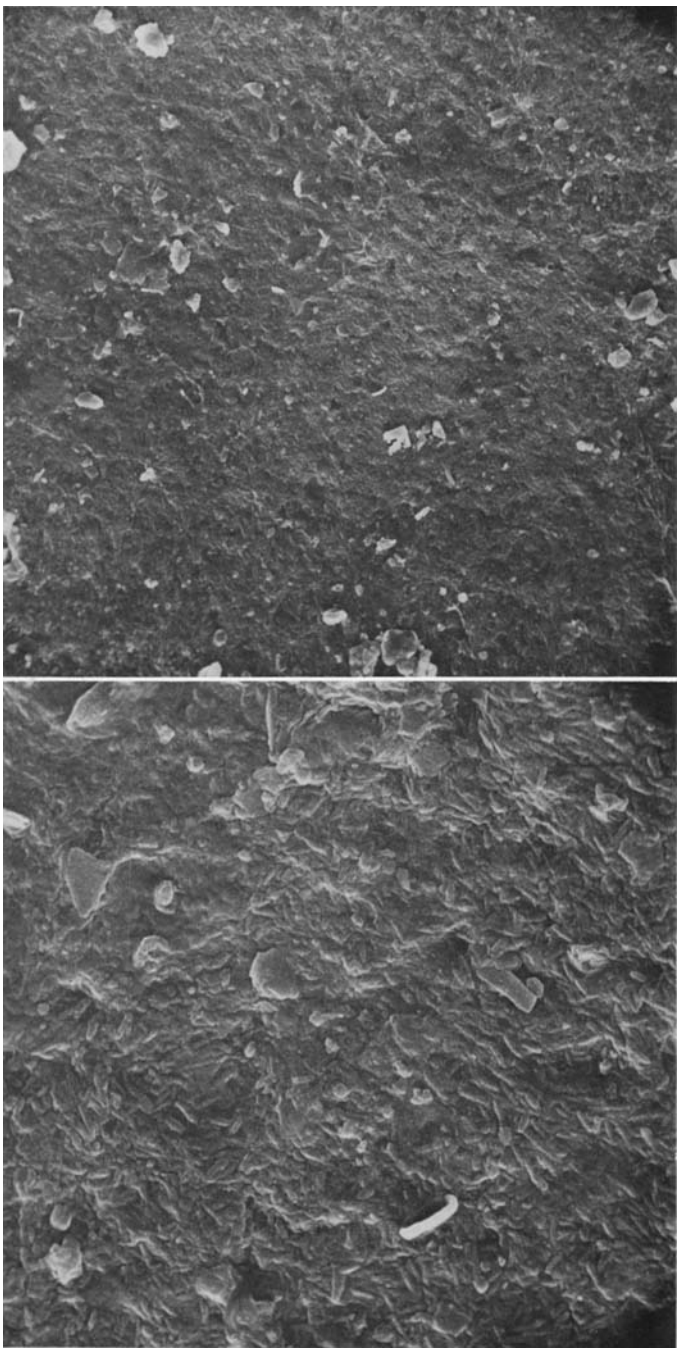

FIGURE 136.—*Parmelia flaventior* Stirton (*Follmann* 14875–H, Chile).

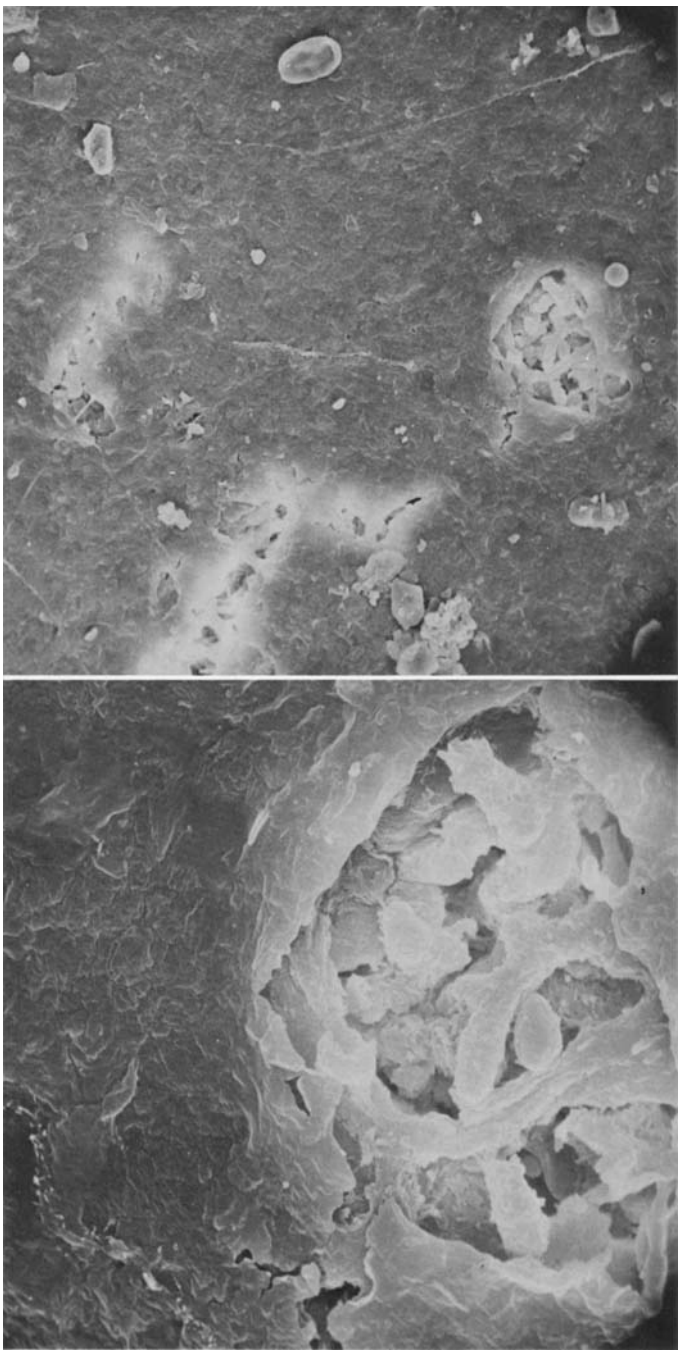

FIGURE 137.—*Parmelia meiophora* Nylander (*Delavay* s.n., China, isotype in US).

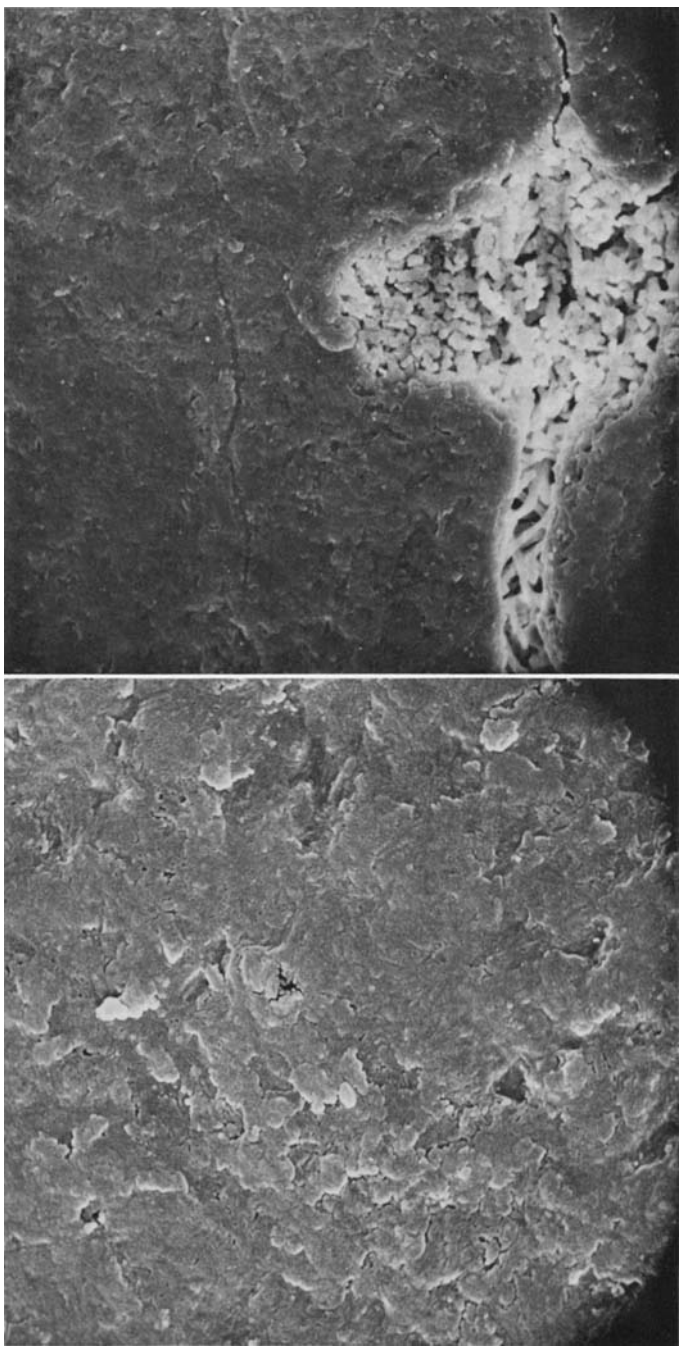

FIGURE 138.—*Parmelia praesignis* Nylander (*Bourgeau* s.n., Mexico, holotype in H).

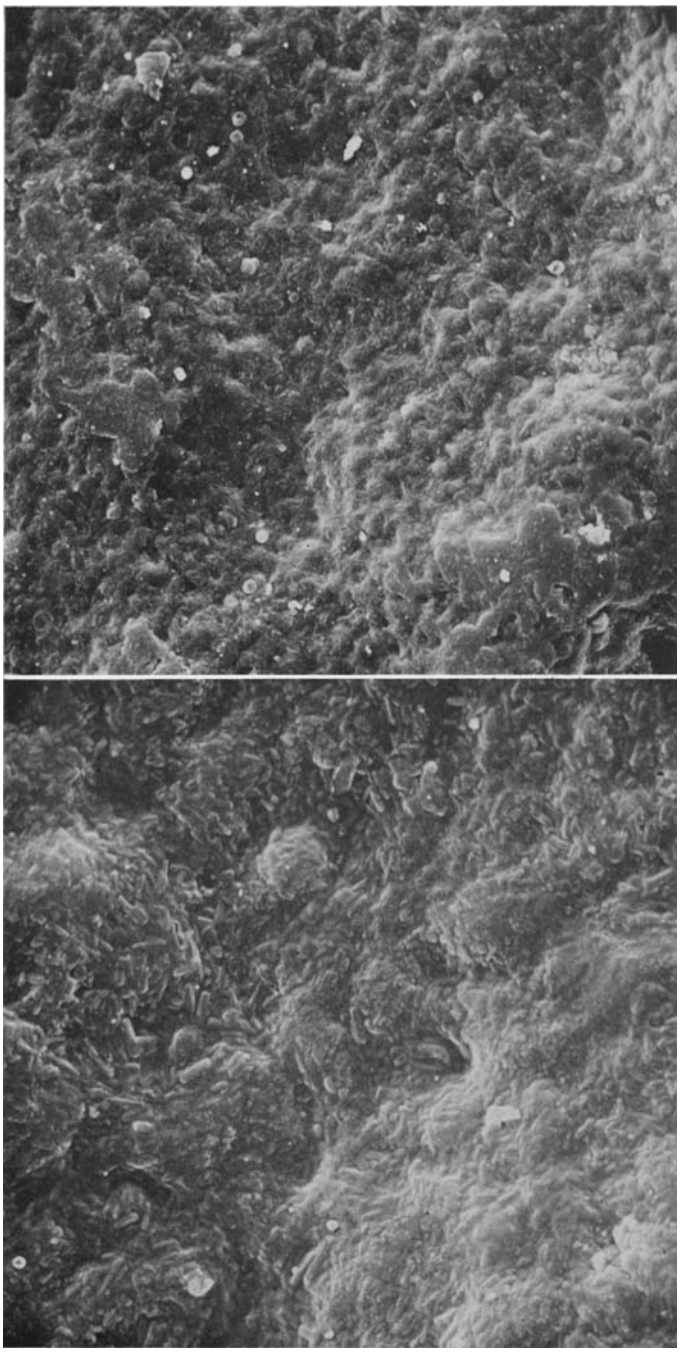

FIGURE 139.—*Parmelia sphaerosporella* Müller-Argau (*Imshaug* 379, Washington).

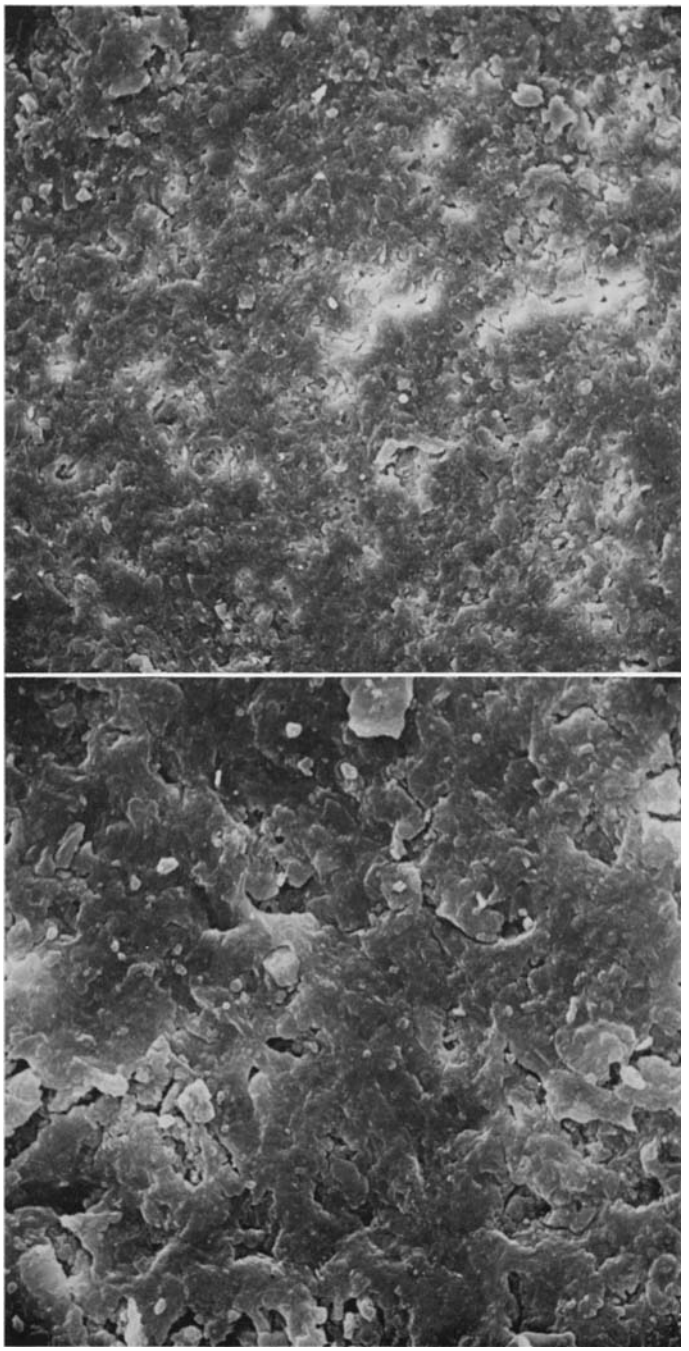

FIGURE 140.—*Parmelia thomsonii* (Stirton) Culberson (*Sarma* s.n., India).

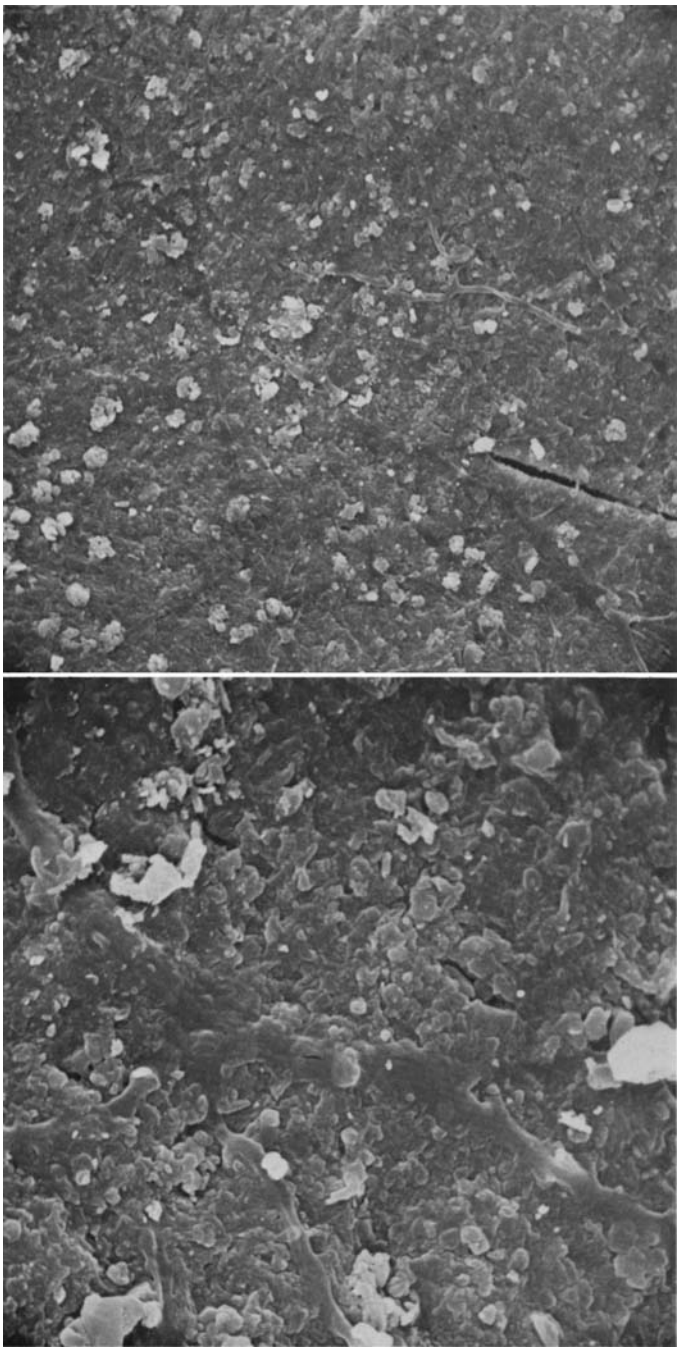

FIGURE 141.—*Parmelia ulophyllodes* (Vainio) Savicz (*Martianoff*, s.n., U.S.S.R., holotype in TUR).

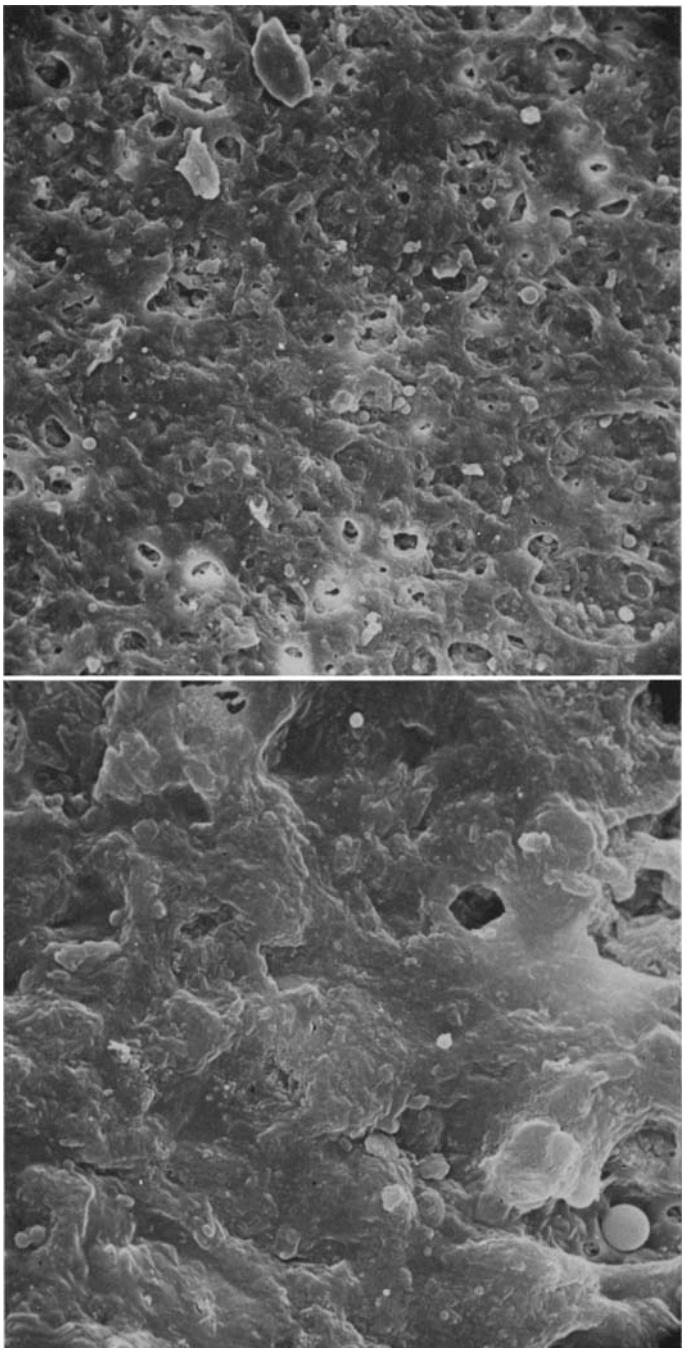

FIGURE 142.—*Parmeliopsis placorodia* (Acharius) Nylander (*Hale* 13051, Virginia).

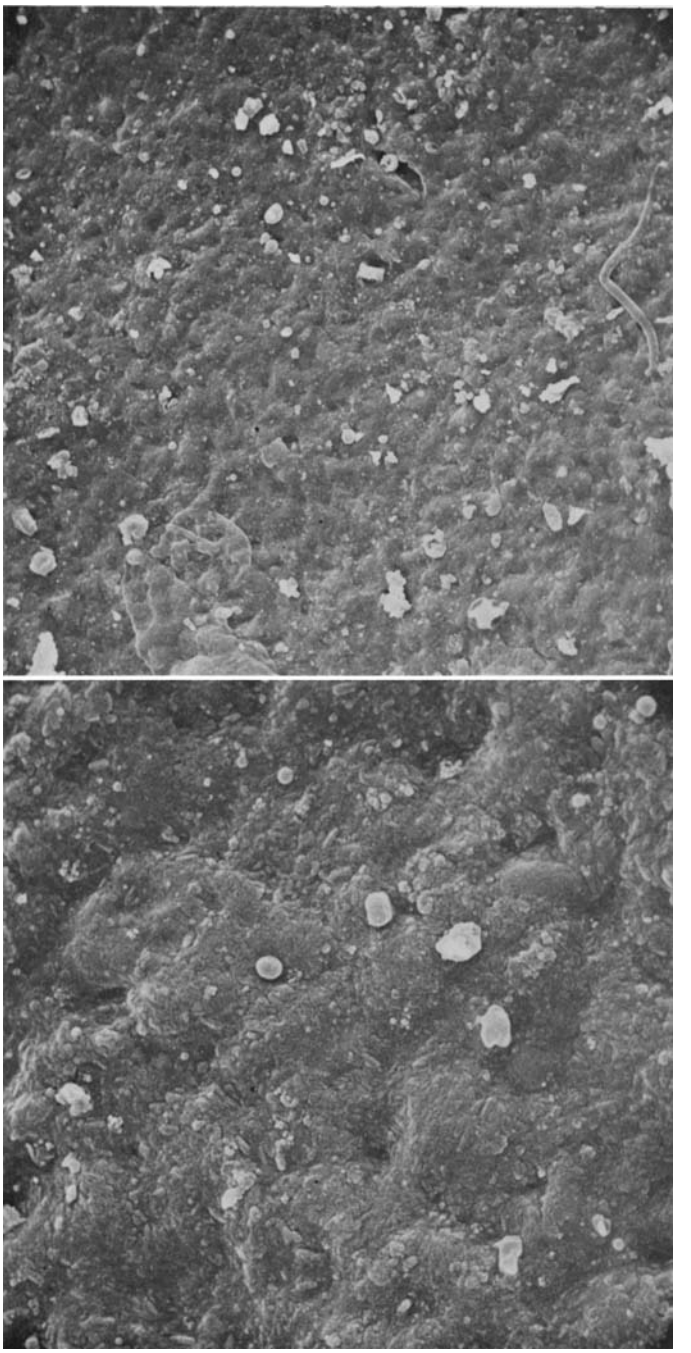

FIGURE 143.—*Platismatia glauca* (L.) Culberson and Culberson (*Hale* 33265, Sweden).

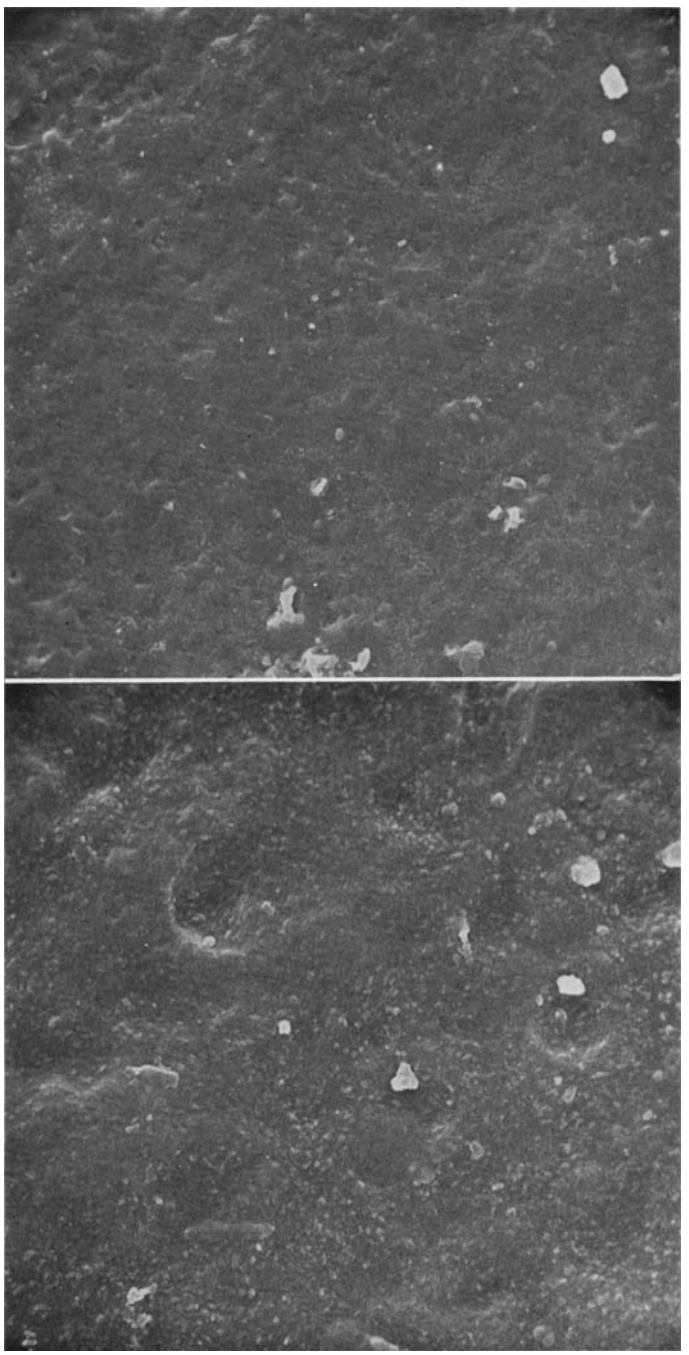

FIGURE 144.—*Platismatia stenophylla* (Tuckerman) Culberson and Culberson (*Shushan* 14737, California).

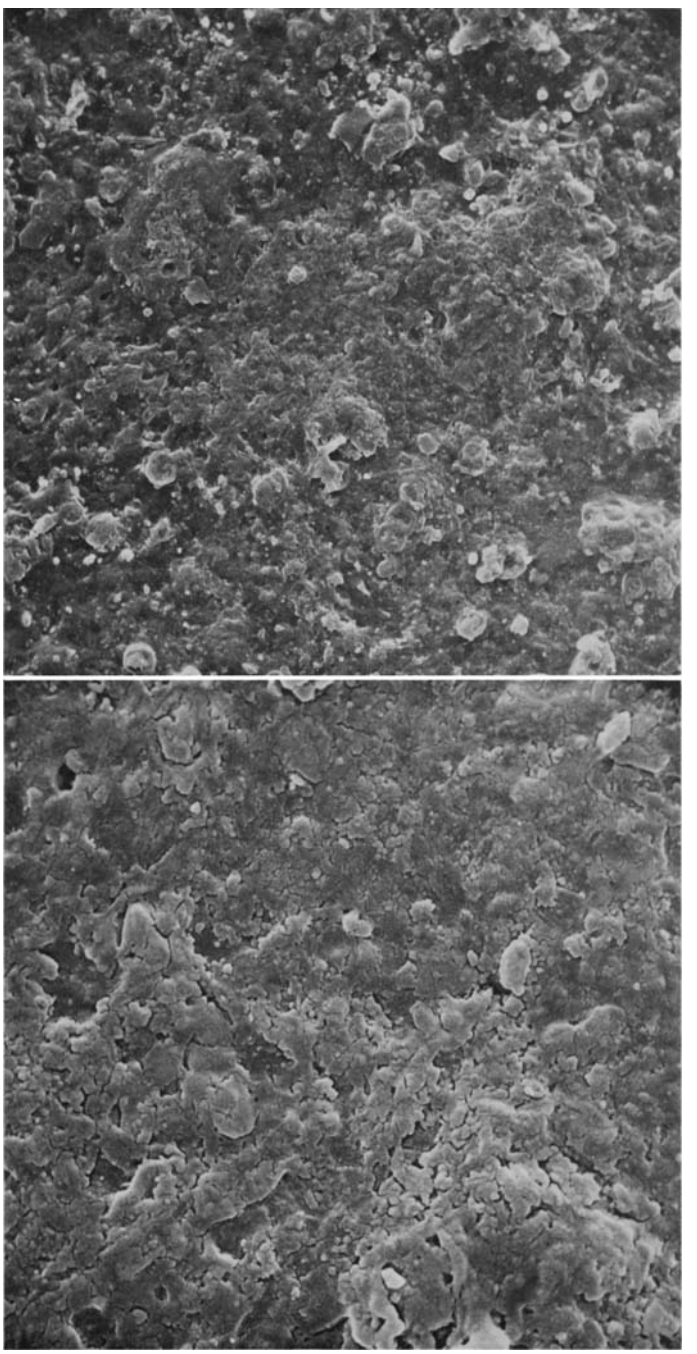

FIGURE 145.—*Platismatia tuckermanii* (Oakes) Culberson and Culberson (*Hale* 12634, Virginia).

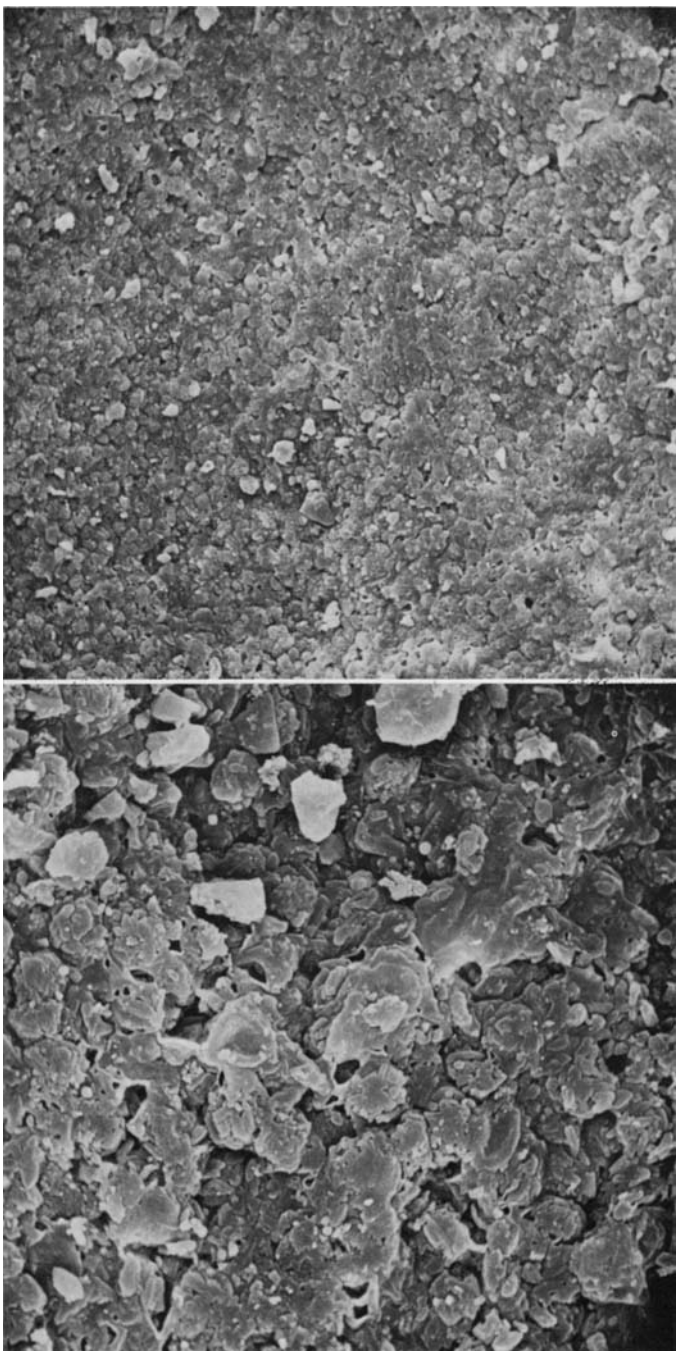

FIGURE 146.—*Pseudevernia cladonia* (Tuckerman) Hale and Culberson (*Merrill* 73, Vermont).

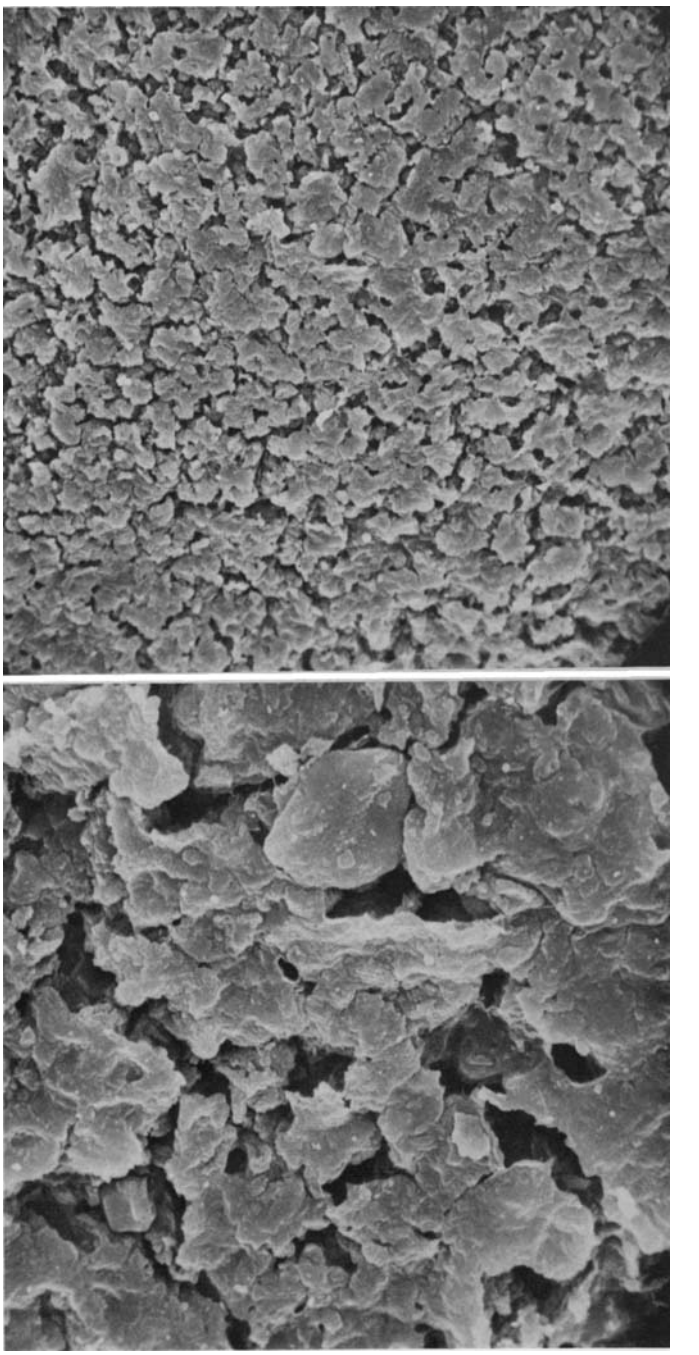

FIGURE 147.—*Pseudevernia consocians* (Vainio) Hale and Culberson (*Hale* 14294, West Virginia).

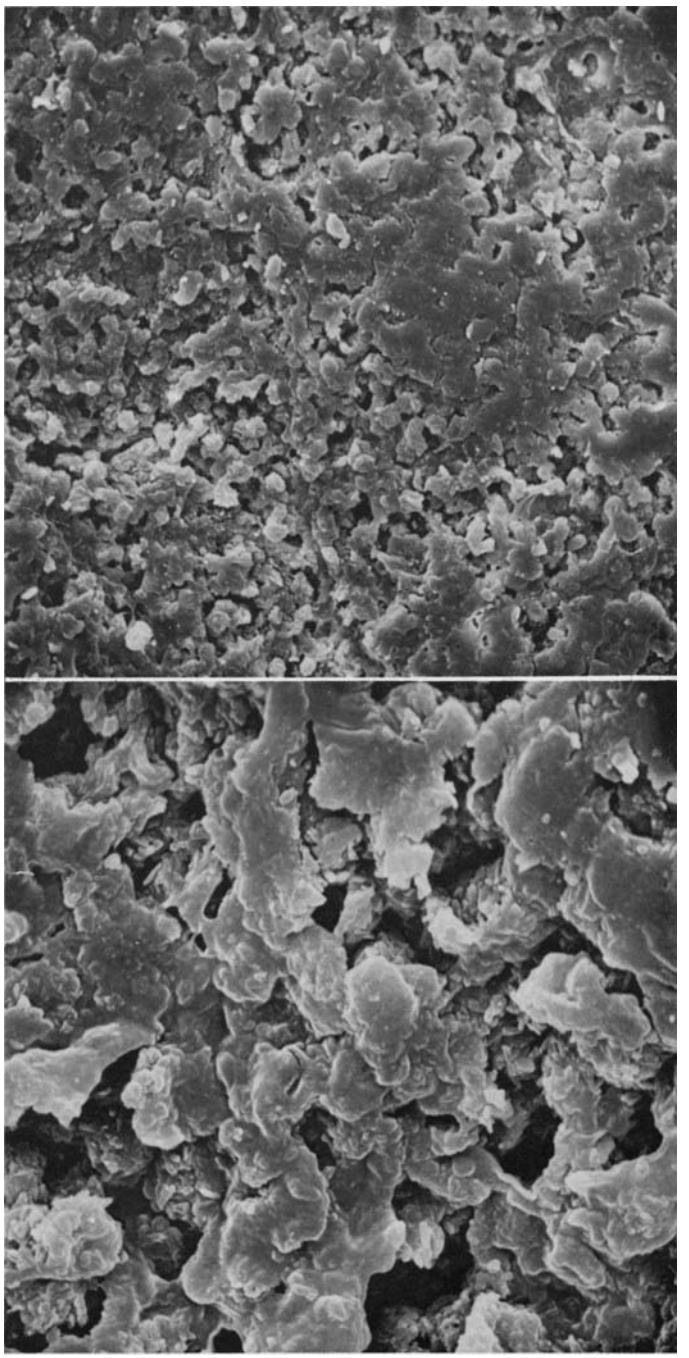

FIGURE 148.—*Pseudevernia furfuracea* (L.) Hale and Culberson (*Steiner* 4135 in Kryptogamae Vindobonensis, Austria).

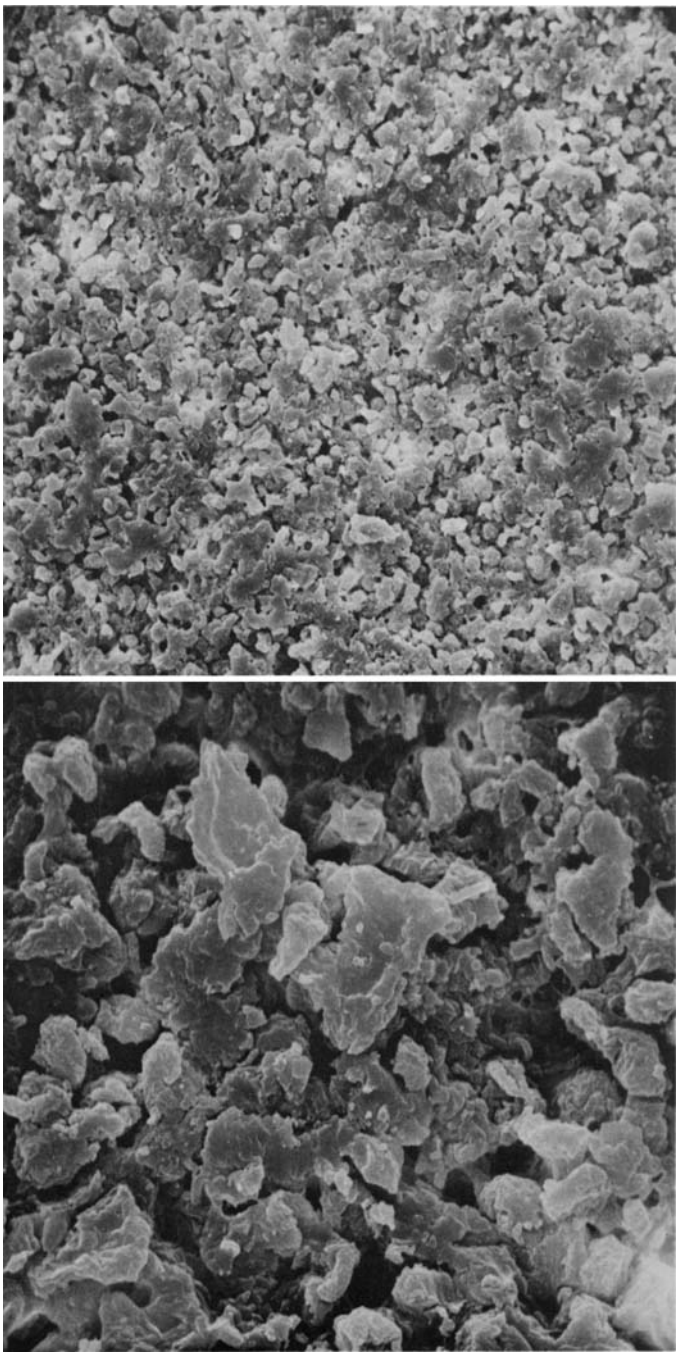

FIGURE 149.—*Pseudevernia olivetorina* (Zopf) Hale and Culberson (*Vrang* 6075, Sweden).

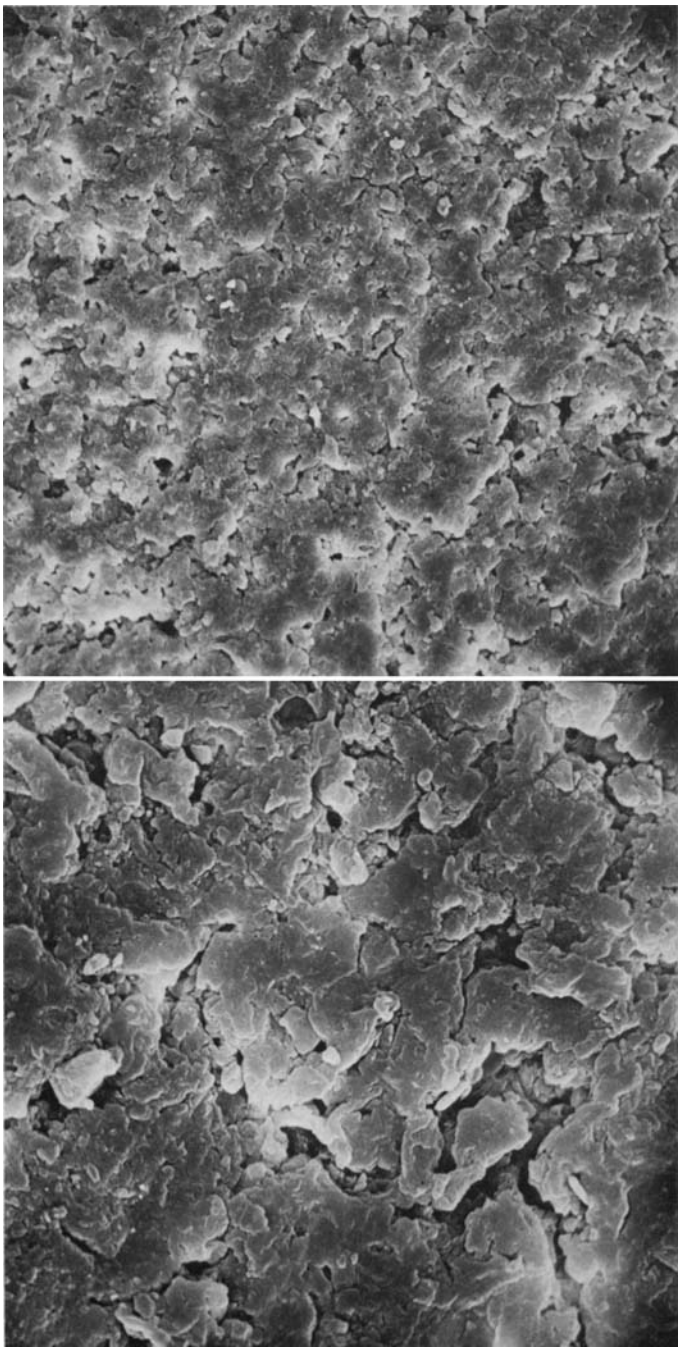

FIGURE 150.—*Pseudevernia intensa* (Nylander) Hale and Culberson (*Wetmore* 15182, New Mexico).

☆ U. S. GOVERNMENT PRINTING OFFICE: 1973— 484-322/37